The role of innate immune cells in ocular ageing and pathological neovascularisation

Scott J Robbie

A thesis submitted for the degree of

Doctor of Philosophy

2012

Department of Genetics

Institute of Ophthalmology

University College London

I, Scott Robbie, confirm that the work presented in this thesis is my own. Where information has been derived from other sources I confirm that this has been indicated in the thesis.

Abstract

Age-related macular degeneration (AMD) is the major cause of vision loss in the developed world. AMD is a chronic progressive disorder of the outer retina leading to vision loss from atrophy (geographic atrophy) and/or the development of choroidal neovascularisation (CNV). Mounting evidence indicates the importance of innate immunity in its pathogenesis. This thesis describes a programme of work conducted with the aim of further understanding the role of innate immune cells in AMD.

Analysis of mouse cell suspensions by flow cytometry demonstrated significantly greater densities of innate immune cell populations in the RPE-choroid than in the neurosensory retina. Dendritic cells accumulated in both tissues with increasing age, and this process was accelerated in mice deficient in a chemokine upregulated in the aged choroid - CCL2. Innate immune cells were recruited to CNV lesions in mouse models of laser-induced and spontaneous CNV. Increasing age was found to correlate with the extent of laser CNV lesion size but not with recruitment of innate immune cells. Impaired recruitment of innate immune cells in CCL2-deficient mice was associated with a smaller laser-CNV lesion size, which nonetheless increased with age. Attenuation of CNV lesion size by targeting key angiogenic pathways using the small molecule pazopanib or by direct targeting of innate immune cells by induction of alternative activation using a CD200R agonist was associated with subtle increases in the recruitment of innate immune cell subpopulations to CNV lesions.

Findings did not support the hypothesis that age-related vulnerability to laser CNV is a consequence of age-related changes in innate immune cell populations. However, the results indicated that CCL2 controls dendritic cell migration in the ageing retina and the recruitment of innate immune cells to CNV lesions. Further investigation of these pathways may lead to better treatments in the prevention and management of AMD.

Contents

Figures

11

Tables

Abbreviations

A2E	N-retinylidene-N-retinylethanolamine
AMD	age-related macular degeneration
APC	antigen presenting cell
BLamD	basal laminar deposit
BLinD	basal linear deposit
BM	Bruch's membrane
CD	cluster determinant
cDC	conventional dendritic cell
CFH	complement factor H
CNS	central nervous system
CNV	choroidal neovascularisation
CRP	C-reactive protein
CSF	colony stimulating factor
DC	dendritic cell
EAE	experimental autoimmune encephalitis
EAU	experimental autoimmune uveitis
FFA	fundus fluorescein angiogram
FGF	fibroblast growth factor
FSC-A	forward scatter area
GA	geographic atrophy
eGFP	enhanced green fluorescent protein
HLA	human leukocyte antigen
IFN	interferon
IL	interleukin
iNOS	inducible nitric oxide synthetase
LPS	lipopolysaccharide
MAC	membrane attack complex
M-CSF	macrophage colony stimulating factor
MDSC	myeloid-derived suppressor cell
MHC	major histocompatibility class

MMP	matrix metalloprotease
MPS	mononuclear phagocyte system
NK	natural killer cell
NKT	natural killer T cell
OIR	oxygen-induced retinopathy
PAMP	pathogen associated molecular patterns
PDGF	platelet-derived growth factor
PG	prostaglandin
PRP	pattern recognition receptors
RPE	retinal pigment epithelium
RTKI	receptor tyrosine kinase inhibitor
RT-PCR	reverse transcriptase polymerase chain reaction
SSC-A	side scatter area
TAM	tumour-associated macrophage
TEM	Tie-2 expressing macrophage
TGF	transforming growth factor
T_H	T helper type
Tip-DC	TNF-α/iNOS-producing dendritic cell
TLR	Toll-like receptor
TNF	tumour necrosis factor
VEGF	vascular endothelial growth factor

Publications arising from this work

The drusen-like phenotype in aging Ccl2-knockout mice is caused by accelerated accumulation of swollen autofluorescent subretinal macrophages. Ulrich F. O. Luhmann, <u>Scott Robbie</u>, Peter M. G. Munro, Susie E. Barker, Yanai Duran, Vy Luong, Frederick W. Fitzke, James W. B. Bainbridge, Robin R. Ali and Robert E. MacLaren. *Invest Ophthalmol. Vis. Sci.* **50**, 5934-5943 (2009).

Acknowledgements

I would like to thank my supervisors, Professors James Bainbridge and Robin Ali, for their unstinting support throughout the course of this work – I could not have asked for more inspirational mentors. I would also like to thank Professor Andrew Dick for both his encouragement and the many occasions on which he has made available his expertise and insight, particularly with regard to the work involving the CD200R agonist. Similarly, Professor David Shima and Eric Ng together with Peter Adamson at GSK deserve mention for their assistance with the work on receptor tyrosine kinase inhibition.

I owe a debt of gratitude to many at the Department of Genetics but Sander Smith and Ulrich Luhmann have been a constant source of support without which I might have foundered on many an occasion. Ulrich in particular must take credit for applying the rigours of scientific scrutiny to my more imaginative proposals and for his sterling work in managing the $CCL2^{-/-}$ mouse colony. Susie Barker has borne the task of sitting next to a man submerged in flow cytometry data with good humour for a few years now and has been a vital touchstone on all matters immunological. Kam Balaggan provided guidance on the application of the laser CNV model in the early phases of the study and has been a valued friend over the last few years, and Yanai Duran was regularly on hand to provide technical assistance. My thanks also to Ayad Eddaoudi and his team at the UCL Core Flow Cytometry Facility for all their help and support.

Finally, I would like to thank my parents, for instilling in me a love of learning, and my wife, who has had to live with the consequences. As if that wasn't enough, Katarina gifted me with a beautiful daughter in the middle of it all and so my thanks also to Eloise whose input, though indirect, in the end also proved essential.

Introduction

1.1   The challenge of age-related macular degeneration

1.1.1 The epidemiology of AMD

First described in 1874[1], age-related macular degeneration (AMD) is the commonest cause of blindness in persons aged ≥50 years old in the developed world[2-4]. AMD affects 1.75 million people in the United States and the prevalence is expected to increase by 50% in the United States and countries with similar demographics by the year 2020[5], posing a considerable burden in terms of the costs to affected individuals and society unless effective strategies aimed at prevention or treatment can be identified. The 'dry' form of the disease, also known as Geographic Atrophy (GA), is characterised by a gradual, irreversible loss of tissue and accounts for 90% of cases - there is no proven treatment for preventing or slowing it. The 'wet' form of AMD, characterised by choroidal neovascularisation (CNV), is less prevalent than GA but accounts for 90% of all cases of severe visual loss arising from the disease.

1.2 The pathology of AMD

1.2.1 The functions of the RPE-choroid complex

AMD is a clinical diagnosis based on fundoscopic findings at the macula - the area of the retina that allows us to read and recognise faces - in patients aged 50 or more. The tissues primarily involved are the retinal pigment epithelium (RPE), Bruch's membrane (BM) and the underlying choroid.

The RPE is a polarised monolayer of epithelium sited between the photoreceptors of the neurosensory retina and Bruch's membrane and has a multiplicity of functions in the eye (*Figure 1*), these include: daily phagocytosis

of outer segment tips shed from photoreceptors adjacent to apical microvilli; maintenance of the blood-retinal barrier via tight junctions between adjacent RPE cells; absorption of light energy by melanosomes in the RPE cytosol; enzymatic participation in the visual cycle; exchange of nutrients and metabolites with the blood and the secretion of a variety of factors which serve either to maintain the choriocapillaris and its fenestrated endothelium (through VEGF for example) or to regulate the local immune system[6]. The latter function has assumed greater prominence in recent years with growing evidence for the role of inflammation in AMD.

Bruch's membrane is a pentalaminar complex of extracellular matrix material comprising a thick elastin layer bounded on either side by layers of collagen IV with the basement membranes for the RPE and choroid outermost. Structural changes in this layer occur with ageing and in AMD.

The choroid is composed of a complex network of capillaries lying on a pigmented stroma and contains melanocytes, fibroblasts and an extensive and highly organised array of macrophages/dendritic cells and mast cells distributed throughout. Tissue macrophages are phagocytic immune cells of the myeloid lineage that serve to maintain tissue homeostasis through the clearance of senescent cells and the remodelling and repair of tissues after inflammation[7].

The choroid may be divided into layers according to blood vessel calibre with an outermost layer of larger blood vessels (Haller's layer), a middle layer of medium-sized vessels (Sattler's layer) and the innermost choriocapillaris layer. Its primary purpose is to supply oxygen and nutrients to the RPE and photoreceptors but, as with the RPE, the rise of inflammatory hypotheses for AMD has recently generated significant interest in its immunological profile.

Normal functioning of the RPE-choroid complex is essential to the health of the photoreceptor layer of the neurosensory retina. A breakdown in function
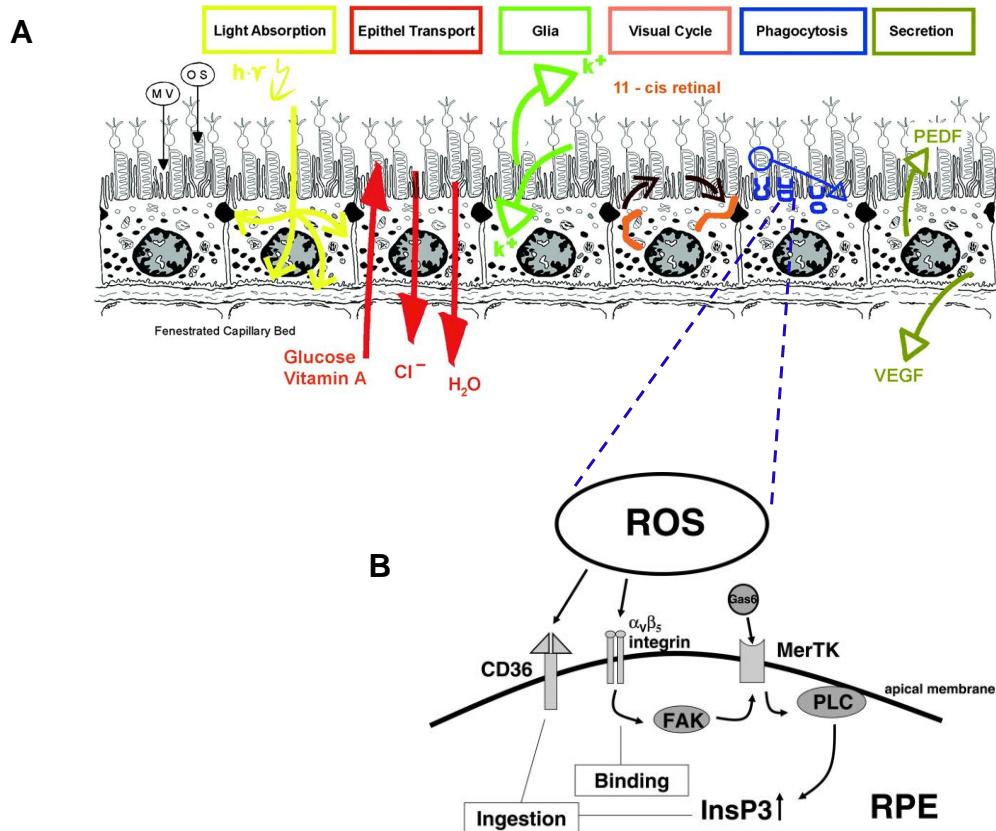
Figure 1. Summary of Retinal Pigment Epithelium functions (A) and the molecules involved in the initiation of photoreceptor outer segment phagocytosis (B).

a, The RPE is a monolayer of pigmented cells forming a part of the blood/retina barrier. The apical membrane of the RPE faces the photoreceptor outer segments. Long apical microvilli surround the light-sensitive outer segments establishing a complex of close structural interaction. With its basolateral membrane the RPE faces Bruch's membrane, which separates the RPE from fenestrated endothelium of the choriocapillaris. b, Phagcytosis of outer segments starts with binding of photoreceptor outer membranes. The event of binding is transduced into an intracellular signal, a rise in intracellular inositol 1,4,5-trisphosphate (InsP3), which in turn leads to ingestion of the bound photoreceptor outer segment membranes. Binding is likely mediated by integrins, and signal transduction occurs through the receptor tyrosine kinase MerTK. Ingestion involves the macrophage receptor CD36. Coordinate signal transduction occurs through integrin and MerTK interaction through the focal adhesion kinase. CD36, macrophage phagocytosis receptor; FAK, focal adhesion kinase; Gas6, growth-arrest-specific protein 6; MerTK, receptor tyrosine kinase c-mer; PLC, phospholipase C; POS, photoreceptor outer segment. The importance to RPE and photoreceptor health of normal processing of photoreceptor outer segments is highlighted in forms of autosomal retinal dystrophy that arise from mutations such as those in MerTK. Adapted from Strauss 2004.

often has serious implications for vision not just in the context of ageing but also in a number of retinal dystrophies of early onset. Mutations in genes such as *MerTK* (responsible for an autosomal recessive form of retinitis pigmentosa) and *ABCA4* (responsible for forms of Stargardt's disease – a degenerative condition affecting the macula) can result in a build-up of lipofuscin in RPE cells - a phenomenon not unlike that seen in early AMD. The accumulation of lipofuscin-containing, autofluorescent lysosomal storage bodies over time in post-mitotic cells is also a feature of normal ageing. In the RPE, lipofuscin is largely derived from phagocytosed photoreceptor outer segments and the level of oxidation of this material has some impact on the rate of lipofuscin deposition in cultured RPE cells. Lipofuscin itself is also a potent generator of reactive oxygen intermediates[8]. Whether the accumulation of lipofuscin occurs because once formed it is not possible for cells to eliminate it or whether the rate of its formation ultimately exceeds the rate of elimination is not known, however it is possible to reverse the build-up in experimental models and the age-dependent accumulation of lipofuscin in perivascular and subretinal microglia in mice suggests a role for these cells in lipofuscin turnover[9, 10].

1.2.2 Early AMD

Early AMD is characterised by the presence of drusen. These pale yellow deposits, which can be seen on clinical examination (*Figure 2*), consist of lipid and protein located in the space between the basal lamina of the RPE and the inner collagenous layer of Bruch's membrane. The aetiology of drusen is not fully understood, however their composition features a variety of proteins and lipids commonly found in a sub-population of morphologically abnormal RPE cells, these include: C-reactive protein (CRP), immunoglobulin G (IgG), vitronectin (Vn), Apolipoprotein E (ApoE), clusterin (Apolipoprotein J, Sp40, 40), fibroblast growth factor-2, and several terminal complement components. The identification of recognisable RPE organelles, melanin granules, lipofuscin and nuclear material in association with drusen suggests that their components may be derived from degenerated RPE cells and various inflammatory pathways (though the temporal relationship has yet to be determined).
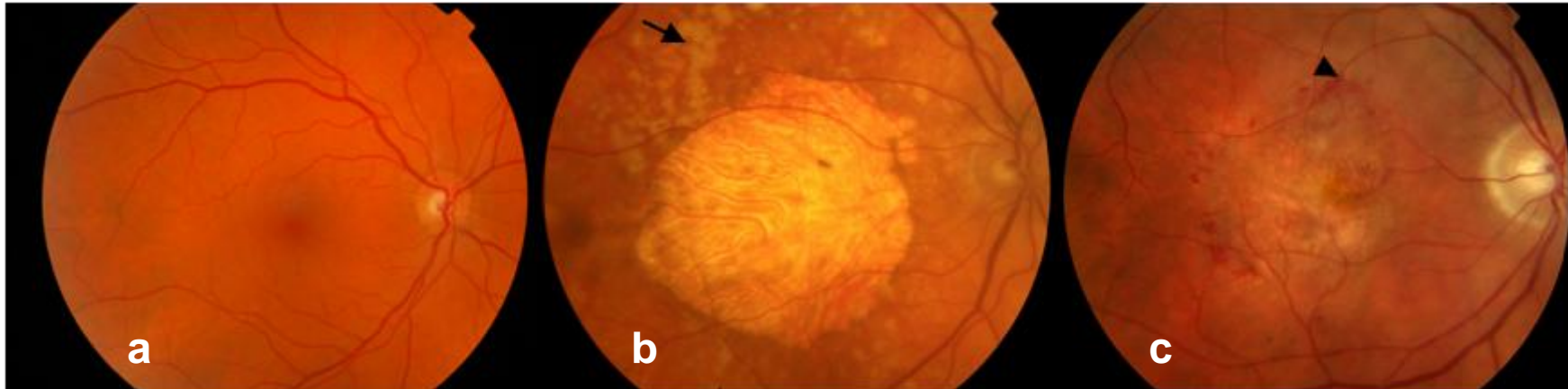
Figure 2. Colour photographs illustrating the fundal appearances in right eyes of normal ageing and AMD.

*a, normal >60 year old subject; **b**, a case of GA. **c**, a case of CNV. A normal clinical appearance in a subject >60 belies subclinical changes associated with aging: loss of neuronal cells (particularly rods), loss of RPE cells, accumulation of lipofuscin within the RPE as well as thickening of Bruch's membrane and alterations in its biophysical properties that may influence the development of RPE dysfunction. Note widespread soft drusen (arrow) bordering a large area of RPE atrophy in the subject with GA and intraretinal haemorrhage (arrowhead) and underlying RPE atrophy in the subject with CNV.*

Evidence also suggests a role for zinc in drusen biogenesis - high levels of zinc have been detected in the maculae of aged humans and high levels of bioavailable zinc in sub-RPE deposits.

Of the two clinical types, termed 'hard' and 'soft' drusen, the latter – characterised by irregular borders and a larger size – occurs in younger patients with better vision and is most strongly associated with progression to advanced AMD, in particular CNV[11, 12]. Drusen have also been classified according to the amount they autofluoresce – it has been demonstrated that drusen located in the equatorial region of the fundus will autofluoresce whilst those located centrally do not. Drusen located at the equator have been shown to be associated with the intercapillary pillars of the choriocapillaris and it has been suggested that impaired clearance of waste material by innate immune cells at such sites may be responsible for the development of drusen[13].

Various other by-products of RPE metabolism and precursors of drusen have been identified and attempts made to establish their significance with regards to AMD: the terms basal laminar deposit (BLamD) and basal linear deposit (BLinD) have been used to describe extracellular material found between the RPE basal plasma membrane and its basement membrane that is not visible on clinical examination but represents changes associated with sub-threshold AMD. In the case of BLinD this material may also involve the inner and outer collagenous zones of Bruch's membrane and its presence may form a cleavage plane in which new vessels can spread. Certain components of these deposits may also be chemotactic for macrophages[14]. Over time, morphological changes in the retinal pigment epithelium (RPE) may eventually become apparent, manifesting as areas of hyper- or hypopigmentation.

1.2.3 Late AMD

A proportion of patients with drusen and RPE changes will go on to develop severe visual loss as a result of GA and/or CNV. The appearance of GA arises from atrophy of the RPE at the macula, the affected area having a scalloped-border with choroidal vessels clearly visible beneath the retina (*Figure 2b*).

The mechanism of RPE loss in GA is unknown; however the aged RPE accumulates N-retinylidene-N-retinylethanolamine (A2E), a by-product of photoreceptor outer segment metabolism and the autofluorescent constituent of lipofuscin (and therefore drusen). A2E has been found to selectively inhibit phagolysosomal degradation of photoreceptor phospholipid by the retinal pigment epithelium *in vitro* and such effects could ultimately contribute to the accelerated loss of RPE and photoreceptor cells seen in AMD (failure to phagocytose outer segments has been demonstrated to result in retinal degeneration in animal models[15]). The accumulation of lipofuscin and drusenoid deposits in disorders such as Stargardt's disease indicates a role for lipofuscin in AMD - whether its presence consititutes a primary or secondary element of AMD pathology and whether its effects stem from direct cellular toxicity, disrupted metabolic exchange or ischaemia resulting from the increased thickness of Bruch's membrane is not known.

CNV typically results from a breach of Bruch's membrane and the rapid extension of fenestrated vessels from the choroidal circulation into the sub-RPE or subretinal space – again the precipitating factor is unknown. The vessels in CNV have an increased tendency to leak resulting in anatomical abnormalities such as retinal pigment epithelial detachment (and tears), fluid accumulation in the retina and the sequelae of toxic effects from blood on neuroretinal tissue. Leakage from CNV disrupts photoreceptor alignment in the short term and in the long term results in cell death and fibrosis at the macula (referred to clinically as a 'disciform macular scar').

1.3 Current treatments for AMD

Current treatments for AMD focus on the 'wet' form of the condition. There is, however, evidence to suggest that high doses of antioxidants and zinc slow down progression of the disease in individuals at high risk of developing both forms of advanced AMD[16].

Vascular endothelial growth factor (VEGF), of which there are a number of different isoforms, is a pivotal regulator of angiogenesis. Recent years have seen the advent of therapies targeted at blocking its effects in tumours and pathological neovascularisation in the eye. VEGF inhibitors such as ranibizumab (a humanised antibody that binds VEGF-A with high affinity) and pegaptanib (an aptamer that selectively binds the $VEGF_{165}$ isoform) have revolutionised the treatment of CNV with up to 95% of those undergoing treatment experiencing stabilised or improved levels of vision 1 year after commencement of therapy[17].

A key disadvantage of VEGF inhibitors is that they require delivery by intravitreal injection on a monthly basis (at least initially), which adds to their already considerable expense and contributes an added element of risk to patients' vision during therapy. VEGF inhibitors do not induce significant regression of the neovascular complex and instead act to reduce leakage from these vessels. In addition, the long-term efficacy and side effects of VEGF inhibitors have yet to be fully established[18, 19]. Evidence is mounting that VEGF has an important role in maintaining vascular homeostasis[20], that it has neuroprotective properties[21] and that alternative splicing gives rise to isoforms (such as $VEGF-A_{165}b$) that may affect the balance of angiogenic drivers both in disease and normal conditions with associated effects on the survival of non-endothelial cells important for blood vessel growth[22].

Crucially, the use of VEGF inhibitors is only indicated in <10% of cases and even then only at a late stage of AMD - these drugs therefore have no effect on the underlying causes of the disease. Evidence also suggests that the longterm loss of RPE cells and photoreceptors in wet AMD remains unchecked even

when leakage from CNV is controlled[23]. Since both 'wet' and 'dry' forms of AMD share a common aetiopathophysiology - with the potential for CNV and GA to develop together in the same eye, or CNV in one eye and GA in the other for any given patient – identification of the relevant pathways could potentially open new avenues in the prevention and treatment of both manifestations of the disease, possibly involving the use of viral vector-mediated gene transfer or cell-based and technologies.

1.4 Risk factors for AMD

1.4.1 Complement and AMD

Until relatively recently the only confirmed risk factors for the development of AMD, aside from the principle effects of aging, were smoking[24, 25] and to a lesser extent light exposure[26, 27]. These associations indicated a role for cumulative damage, most likely mediated by reactive oxygen species - a hypothesis supported by the evidence for reduced progression to advanced AMD in high-risk subjects administered high doses of antioxidants and/or zinc[16] and the increased metabolic and oxidative stress born by retinal and RPE cells as a normal part of the aging process. Familial associations were known of for many years but it was not until the presence of a number of complement system components, complement activators and complement regulatory proteins was established in the choroid and drusen[28, 29] (*Figure 3*) that genetic studies revealed significant associations with variants of several complement pathway-associated genes, namely: complement factor H (*CFH*)[30-33], complement factor H-related 1 and 3 (*CFHR1* and *CFHR3*)[34, 35], complement factor B (*CFB*), complement component 2 (*C2*) [36, 37] and complement component 3 (*C3*)[38-41].

Complement is central to the functioning of the body's innate (non-adaptive) immune system with roles in the opsonisation and lysis of microorganisms, removal of foreign particles and dead cells, recruitment and activation of inflammatory cells, regulation of antibody production and elimination of immune complexes[42]. It is a highly conserved system made up of inactive precursor proteins (rendered active through a series of proteolytic steps that also amplify

the response) and various membrane-bound regulators and receptors[43]. Components are found in the plasma, body fluids and on cells surfaces. The anaphylatoxin C5a has a particular role in the recruitment and activation of innate immune cells such as macrophages and both C3a and C5a have been implicated in the development of CNV[44]. Activation of complement ultimately results in formation of the membrane attack complex (MAC) - an aggregation of components C5b, C6, C7, C8 and C9 that generates a pore in the target cell's lipid bilayer resulting in cell lysis. The system is tightly regulated and there are four pathways of activation: The *classical* pathway is activated by the binding of C1q to immune complexes (antigen-antibody complexes), the *lectin* pathway by pattern-based recognition of molecules on pathogen surfaces, the *intrinisic* pathway (a recently discovered pathway as yet poorly defined) by direct cleavage of C3 and C5 by proteases and the *alternative* pathway by spontaneous hydrolysis of C3 to components C3a and C3b with subsequent steps mediated by complement factors B (CFB) and (CFD) in a process that turns over continuously at a low-level under normal conditions (*Figure 4*). Genetic studies have revealed that variants of *CFH* and *CFB/C2* alone may account for up to 75% of all AMD cases in European and North American populations[36] with *C3* variants estimated to account for up to 14.5% of cases[38]. Other variants, such as certain *CFH* haplotypes, may in fact be protective[35]. How such variants exert their effects is poorly understood but the process is likely to involve many decades of complement activity at interfaces between the choroid, Bruch's membrane and the basolateral RPE surface. The CFH_{402H} variant associated with AMD exhibits a strongly reduced affinity for C-reactive protein (CRP)[45-49] – a key component of drusen and a possible biochemical marker for AMD. The existence of two forms of CRP and this protein's pro- and anti-inflammatory potential complicate its relationship with complement[50, 51], however CFH_{402H} also exhibits reduced affinity for cultured endothelial and RPE cells[47].

Complement is primarily produced in the liver but certain tissues, such as the brain, are capable of production locally. Quantitative PCR (qPCR) analysis of
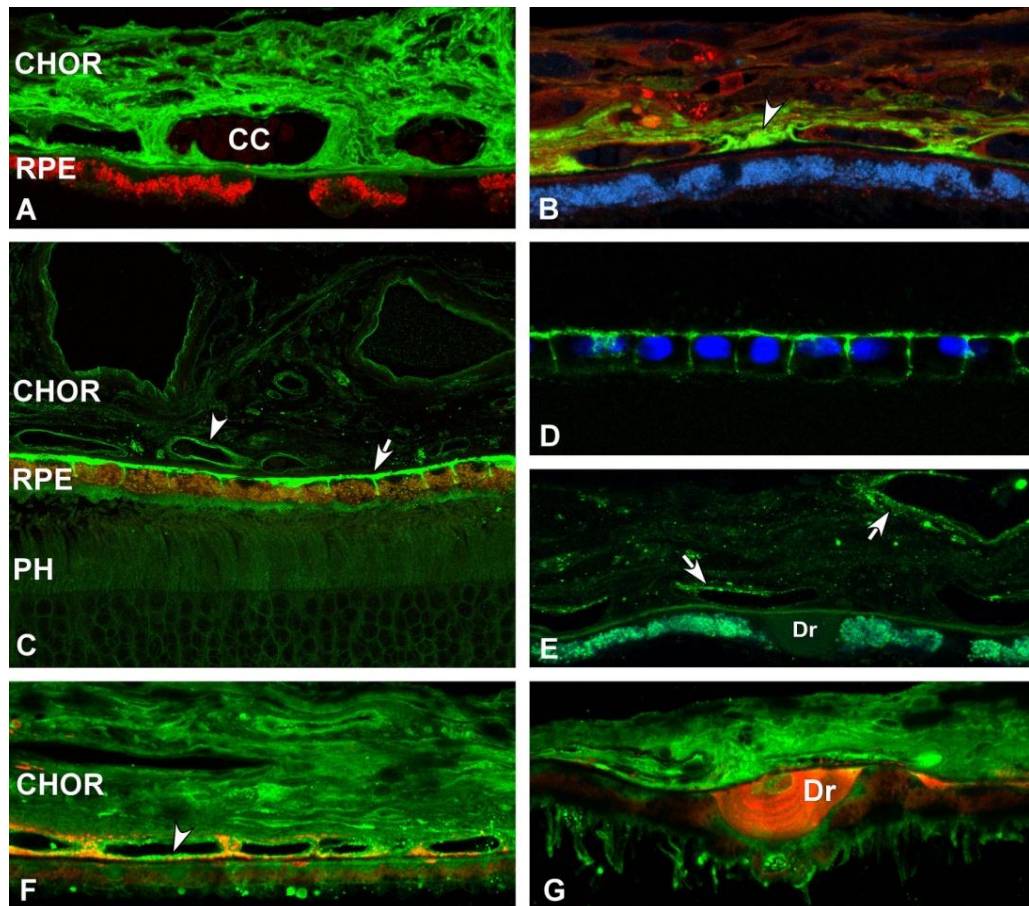
Figure 3. Localization of alternative pathway components and inhibitors in human RPE and choroid (CHOR) by confocal immunofluorescence microscopy.

a, Albumin immunoreactivity is distributed throughout the choroid (green). Lipofuscin autofluorescence is present in the RPE cytoplasm (red) b, Factor H is localized to choroidal capillaries and the intercapillary pillars (arrowhead) (green). Lipofuscin autofluorescence (blue), C-reactive protein (red). c and d, the complement regulator human membrane cofactor protein (MCP; CD46) is localized to choroidal vessel walls (arrowhead) and to the basolateral surface of the RPE (arrow). Photoreceptor layer of the retina (PH) (green). The polarized basolateral distribution of MCP is preserved in cultured human fetal RPE cells (shown in d) (green). RPE cell nuclei are stained by the DNA binding dye Hoechst 33258 (violet) (d). e, complement regulator, decay accerlerating factor (DAF; CD55) immunoreactivity is associated with choroidal vessel walls, but absent in the RPE and in drusen (arrows) (green). f and g, Factor B/C5b-9 co-localization [anti-Factor B (green); anti-C5b-9 (red)]. Diffuse anti-Factor B labeling is present throughout the choroid; choroidal capillary vessel walls are heavily labeled (arrowhead). Factor B immunofluorescence can be localized to the cores of some drusen (Dr). From Anderson et al. 2009.
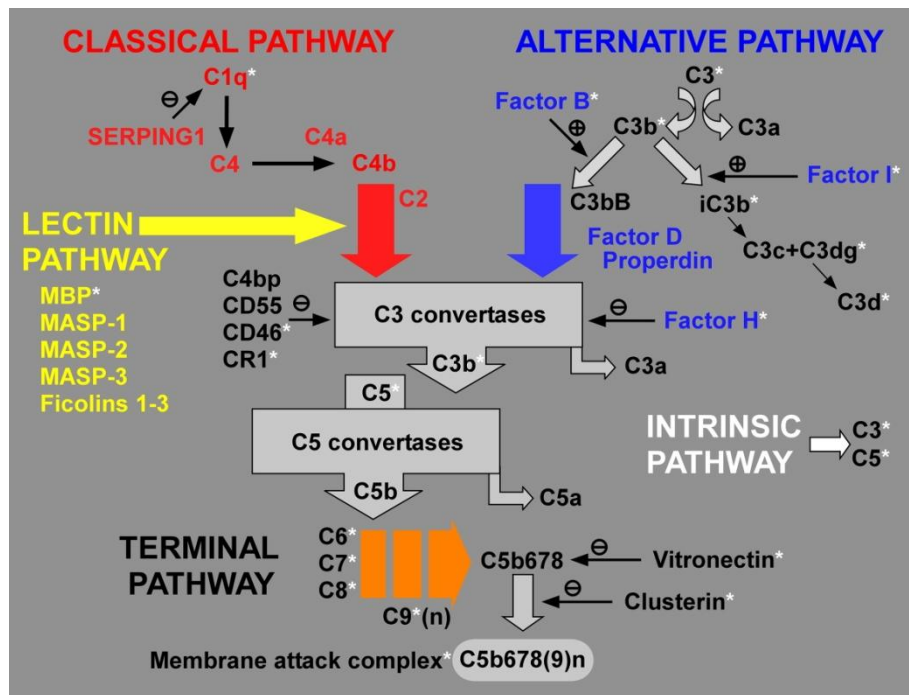
Figure 4. Schematic illustrating components and regulators of the complement system.

The complement cascade consists of 4 activation pathways, including the recently characterized intrinsic pathway, all of which converge upon a terminal pathway that results in the assembly of the membrane attack complex (MAC). Multiple complement regulatory proteins act at different levels to modulate the system. The complement components and regulatory molecules that are localized in drusen are highlighted by an asterisk. From Anderson et al. 2009.

complement gene expression in the human eye indicates that cells in the RPE-choroid complex express components and regulatory molecules of both the *classical* and *alternative* complement pathways with the choroid being the main source[52]. The specific cells responsible for complement production in the choroid have yet to be identified.

Whilst the choroid is a key source of complement in the eye, certain components such as the alternative pathway regulator MCP are also robustly expressed in the neural retina and RPE. MCP has been localised to RPE cells overlying drusen and at the basolateral surface of RPE *in vivo* and *in vitro* making it, together with CFH, one of the two main cell surface-associated alternative pathway inhibitors in the RPE-choroid[53-55]. The discovery of a local complement system in the RPE-choroid adds an extra layer of complexity in understanding the nature of ageing and AMD in the eye. Local expression of complement may serve to confer protection on tissues and organs more susceptible to the effects of aging and inflammation whereas 'risk' variants of CFH and C3 may effectively 'skew' the immune system in such a way that drives pathogenesis (the role played by systemic complement in this is unclear though evidence is emerging that circulating levels of several complement proteins and markers of activation are correlated with AMD[56, 57]). Such mechanisms are in evidence in other diseases with underlying inflammatory components such as Alzheimer's, rheumatoid arthritis and glomerulonephritis. It was in fact the recognition that a form of glomerulonephritis known as dense deposit disease (DDD also known as MPGN II) bears histological hallmarks not dissimilar to drusen that led to the identification of abnormalities in the *CFH* gene as a risk factor[58]. Patients with DDD develop subepithelial deposits containing C3 beneath the glomerular basement membrane and the condition is sometimes associated with the development of drusen in the eye clinically indistinguishable from those found in AMD.

The interactions between local and systemic complement systems, the by-products of RPE and photoreceptor metabolism and the innate immune cells of the chorio-retinal complex are likely to be finely balanced and critical to understanding the causes of AMD. Hypothesised imbalances in these

interactions constitute the 'inflammation' model for AMD pathogenesis and progression, in which drusen are regarded as the result of chronic inflammatory events at the level of Bruch's membrane (*Figure 5*).

1.4.2 The role of innate immune cells in AMD

As well as complement, the innate immune system comprises two principal cell types: granulocytes (neutrophils, basophils and eosinophils) and cells derived from the mononuclear-phagocyte system (MPS) (*Figure 6*). The MPS is composed of tissue-specific macrophages (termed microglia in the CNS and retina), dendritic cells (DCs) and monocytes. Monocytes share a common precursor with neutrophils in the bone marrow (as part of the myeloid lineage) and on infiltration of tissues from the circulation they are capable of differentiating into macophages (and DCs) of various phenotypes depending on cues taken from the local milieu of cytokines and chemokines.

Activated microglia may be found in the degenerating retina of patients with advanced AMD[59] (*Figure 7*) and the role of macrophages in pathological neovascularisation and vasculogenesis is well-documented. Direct evidence for involvement of these cells in early AMD, however, is relatively limited and comes from the presence of the Major Histocompatibility Class II (MHC II) molecule HLA-DR in drusen and evidence for the extension of processes from choroidal dendritic cells into drusen[60] (a feature reminiscent of gut DCs and their ability to extend their dendrites, penetrate epithelial tight junctions and sample bacteria in the intestinal lumen[61]). Analysis of cadaveric tissue from normal eyes, normal-aged eyes and eyes with early AMD has confirmed that choroidal macrophages in normal eyes, positive for the phagosomal marker CD68^{+}, do not express iNOS (an indicator of their activation status). Expression of iNOS by choroidal macrophages appears to be associated with the recruitment of macrophages to Bruch's membrane in eyes with early AMD, soft
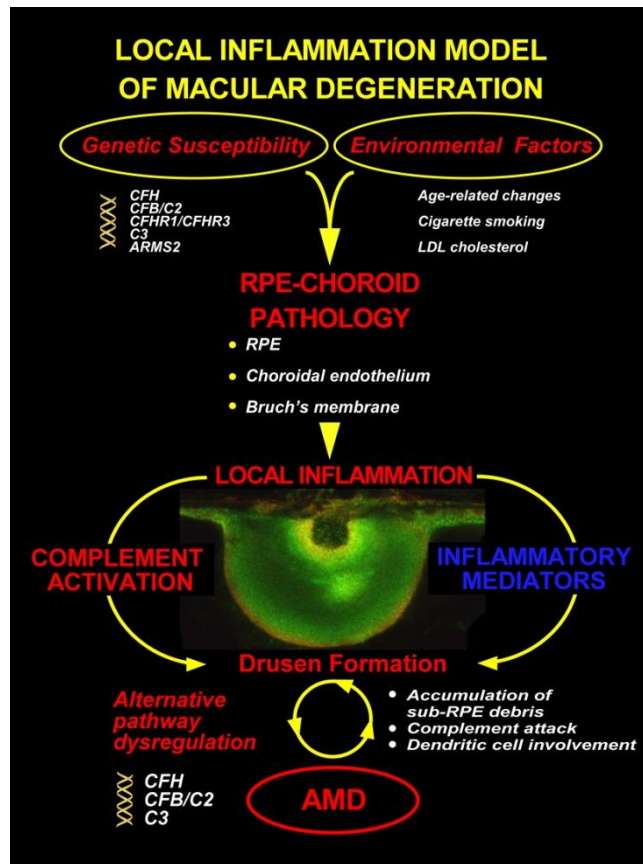
Figure 5. Inflammation model of macular degeneration.

According to the model, AMD may triggered by one or more environmental risk factors that occur against the background of a genetic susceptibility profile conferred by variants in the CFH, CFB/C2, and/or C3 gene triad. This confluence of environmental and genetic risk factors gives rise to pathological changes in the RPE–choroid late in life which generate a chronic, local inflammatory response that includes complement activation and other inflammation-mediated events characterized, in part, by alterations in Bruch's membrane, drusen formation and the accumulation of other sub-RPE deposits, bystander cell lysis, and dendritic cell involvement. Over time, these processes/events result in photoreceptor degeneration and the loss of central vision that defines the clinical entity of AMD. From Anderson et al. 2009
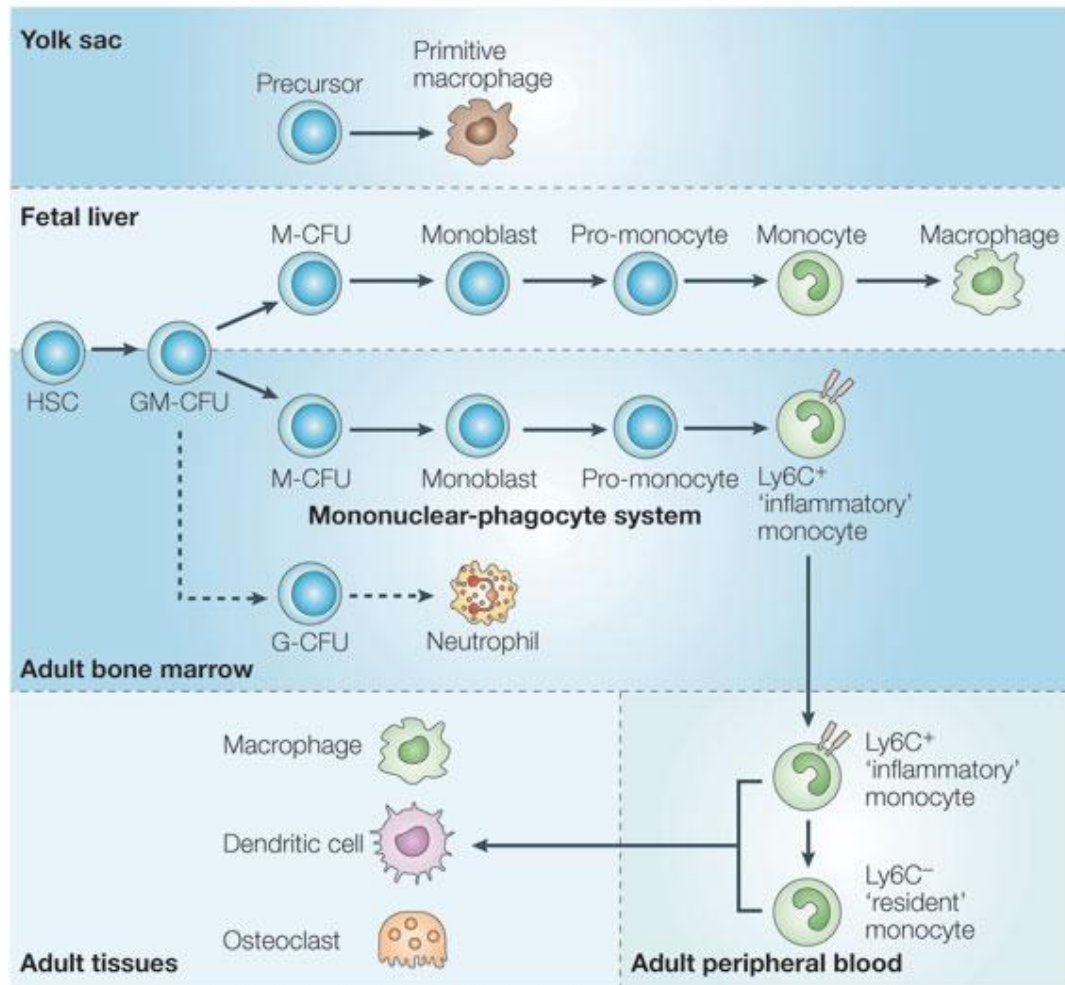
Figure 6. The Mononuclear Phagocyte System.

Developing macrophages are first found in the yolk sac, as identified by morphological characteristics, as well as by expression of macrophage markers such as CD11b. Later in development, haematopoiesis in the foetal liver becomes a source of macrophages that resemble those that are present in adults. Monocytes can be precursors for the replenishment of tissue-resident macrophage populations, however there is evidence to suggest that many of these macrophages may be derived from local proliferation in the adult rather than from recruited peripheral monocytes. When bone-marrow monocytes are released into the peripheral blood (having a Ly6C+ phenotype), they are thought to differentiate into a phenotypically distinct (Ly6C-) cell subset. From Gordon and Taylor 2005.

drusen or thick continuous BLamD and also with active disciform scarring. Expression of iNOS was found to be absent from macrophages associated with Bruch's membrane in the same study[62]. There is also limited evidence for patients with wet AMD being more likely to have circulating, activated monocytes that produce high amounts of pro-inflammatory TNF-α[63].

More compelling has been the identification of variants I249/M280 of the chemokine receptor CX3CR1 (expressed on neutrophils, monocytes, T cells and, in particular, all retinal microglia) as risk factors for AMD[64] and the subsequent confirmation of the accumulation of CX3CR1-positive microglia in the macular subretinal space of both human subjects with AMD (including those with CNV) and *CX3CR1*^{-/-} mice[65]. This has resulted in parallels being drawn between lipid laden subretinal microglia and the 'foam cells' found in atherosclerotic plaques. Similar changes are thought to occur in the ageing brain with evidence for increased numbers of activated microglia in the brains of those with Alzheimer's disease, the identification of age-related dystrophic changes in microglia and evidence indicating that the composition of extracellular debris found in AMD and diseases such as atherosclerosis and Alzheimer's shares similar characteristics[60, 66, 67] . Microglia have also been implicated in a number of other diseases of the CNS and retina including multiple sclerosis and diabetic retinopathy. The link between inflammation and AMD is further reinforced when one considers the well-known low-grade chronic inflammatory effects of smoking.

The significance of these findings is better appreciated with an understanding of inflammation, the changes in the immune system that occur with age, the various monocyte subsets, their markers and receptors, how myeloid cells traffic through the eye and how their phenotypes relate to key experimental models of AMD (including models of CNV).
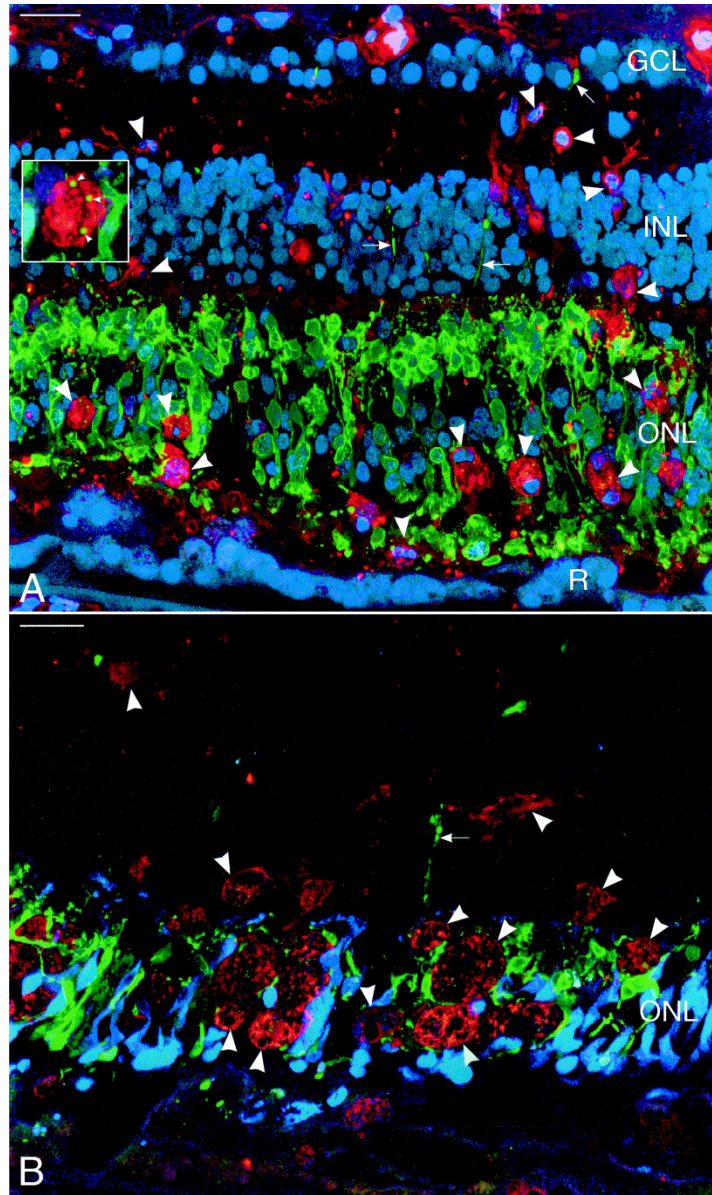
Figure 7. Confocal microscopy of a macula with AMD.

Rods are labelled with anti-rhodopsin (green). Microglia (MG) and blood vessel walls are positive with the lectin marker RCA-I (red). R, retinal pigment epithelium. Bars=100 µm. (A) In addition to stellate MG in the ganglion cell layer (GCL) and inner nuclear layer (INL), note large, RCA-I positive MG (arrowheads) among the degenerating rods and in the sub-retinal space. Most of these activated MG cells contain rhodopsin positive (green) cytoplasmic inclusions. Inset shows a MG cell at higher magnification (4X)-note rhodopsin positive (green, small arrowheads) inclusions in the cytoplasm. Nuclei are stained blue with TO-PRO-3. (B) Cones are positive (blue) with mAb 7G6 and rods, including a neurite (arrow), are labeled (green) with anti-rhodopsin. Large, RCA-I positive MG (red, arrowheads) in the outer nuclear layer contain rhodopsin positive cytoplasmic inclusions. From Gupta et al. 2003.

1.5 The innate immune system

1.5.1 The leukocyte adhesion cascade

Inflammation constitutes the body's response to tissue injury. Uncontrolled inflammation, however, can result in tissue damage and in itself be the cause of disease - making it of key importance in the pathology of a great many tissue-specific diseases. The process may be characterised as acute or chronic depending on the timecourse of the response and the predominating cell type. Acute inflammation, driven largely by neutrophil recruitment in the initial phase, may begin within seconds of onset of a stimulus and continue for hours or even days. Should a stimulus persist, chronic inflammation may ensue with macrophages the predominating cell type in a process of continual injury and healing that may last many years (*Table 1*).

Both acute and chronic inflammatory events rely on cells already present in the affected tissue to recruit circulating leukocytes to the site of injury. Activation of cells in the tissue triggers a cascade of events which, through the secretion of a range of cytokines and chemokines (small molecules involved in cell-cell signalling), leads to adhesion of circulating cells and their transmigration through blood vessel walls. This 'leukocyte adhesion cascade' classically consists of three steps: rolling, activation and firm adhesion, however recent refinements have been made to this model including the addition of slow-rolling, adhesion strengthening, intraluminal crawling and paracellular and transcellular migration (*Figure 8*). The rolling phase is mediated mainly by selectins, molecules expressed either on the activated endothelial luminal surface or by the leukocytes themselves, with subsequent rolling and firm adhesion established through the binding of β_1- and β_2-integrins. The myeloid-derived cell marker CD11b/CD18 (also known as complement receptor 3, Mac-1, $\alpha_M\beta_2$-integrin or simply CD11b) is one such example of an integrin - its rapid activation through G-protein-coupled receptor signalling leading to leukocyte arrest.

| Disease | Key effector cell | Proposed leukocyte receptors for endothelial traffic signals | | |
		L-selectin, ligand	GPCR	Integrin[a]
Acute inflammation				
Myocardial infarction	Neutrophil	PSGL-1	CXCR1, CXCR2, PAFR, BLT1	LFA-1, Mac-1
Stroke	Neutrophil	L-selectin, PSGL-1	CXCR1, CXCR2, PAFR, BLT1	LFA-1, Mac-1
Ishaemia reperfusion	Neutrophil	PSGL-1	CXCR1, CXCR2, PAFR, BLT1	LFA-1, Mac-1
TH1				
Atherosclerosis	Monocyte	PSGL-1	CCR1, CCR2, BLT1, CXCR2, CX3CR1	VLA-4
	TH1	PSGL-1	CXCR3, CCR5	VLA-4
Multiple sclerosis	TH1	PSGL-1 (?)	CXCR3, CXCR6	VLA-4, LFA-1
	Monocyte	PSGL-1 (?)	CCR2, CCR1	VLA-4, LFA-1
Rheumatoid arthritis	Monocyte	PSGL-1	CCR1, CCR2	VLA-1, VLA-2, VLA-4, LFA-1
	TH1	PSGL-1	CXCR3, CXCR6	VLA-1, VLA-2, VLA-4, LFA-1
	Neutrophil	L-selectin, PSGL-1	CXCR2, BLT1	LFA-1[b]
Psoriasis	Skin-homing TH1	CLA	CCR4, CCR10, CXCR3	VLA-4[c], LFA-1
Crohn disease	Gut-homing TH1	PSGL-1	CCR9, CXCR3	$\alpha_4\beta_7$, LFA-1
Type 1 diabetes	TH1	PSGL-1 (?)	CCR4, CCR5	VLA-4, LFA-1
	CD8	L-selectin (?), PSGL-1 (?)	CXCR3	VLA-4, LFA-1
Allograft rejection	CD8	PSGL-1	CXCR3, CX3CR1, BLT1	VLA-4, LFA-1
	B cell	L-selectin, PSGL-1	CXCR5, CXCR4	VLA-4, LFA-1
Hepatitis	CD8	PSGL-1	CXCR3, CCR5, CXCR6	VLA-4
Lupus	TH1	None	CXCR6	VLA-4[d]
	Plasmacytoid DC	L-selectin, CLA	CCR7, CXCR3, ChemR23	LFA-1, Mac-1
	B cell	CLA (?)	CXCR5, CXCR4	LFA-1
TH2				
Asthma	TH2	PSGL-1	CCR4, CCR8, BLT1	LFA-1
	Eosinophils	PSGL-1	CCR3, PAFR, BLT1	VLA-4, LFA-1
	Mast cells	PSGL-1	CCR2, CCR3, BLT1	VLA-4, LFA-1
Atopic dermatitis	Skin-homing TH2	CLA	CCR4, CCR10	VLA-4, LFA-1

Table 1. Trafficking molecules involved in inflammatory disease processes.

From Luster et al. 2005
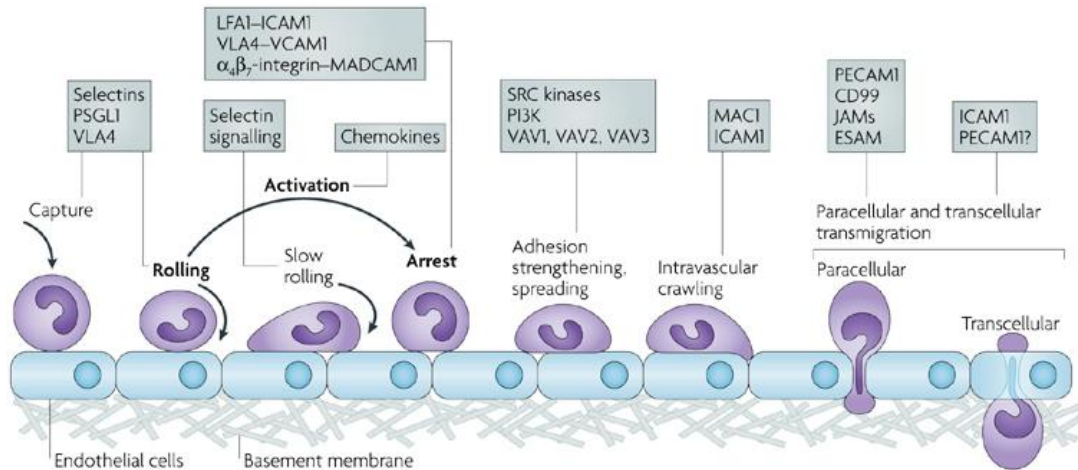
Figure 8. The Leukocyte Adhesion Cascade.

The original three steps are shown in bold: rolling, which is mediated by selectins, activation, which is mediated by chemokines, and arrest, which is mediated by integrins. Progress has been made in defining additional steps: capture (or tethering), slow rolling, adhesion strengthening and spreading, intravascular crawling, and paracellular and transcellular transmigration. Key molecules involved in each step are indicated in boxes. ESAM, endothelial cell-selective adhesion molecule; ICAM1, intercellular adhesion molecule 1; JAM, junctional adhesion molecule; LFA1, lymphocyte function-associated antigen 1 (also known as $\alpha_L\beta_2$-integrin); MAC1, macrophage antigen 1; MADCAM1, mucosal vascular addressin cell-adhesion molecule 1; PSGL1, P-selectin glycoprotein ligand 1; PECAM1, platelet/endothelial-cell adhesion molecule 1; PI3K, phosphoinositide 3-kinase; VCAM1, vascular cell-adhesion molecule 1; VLA4, very late antigen 4 (also known as $\alpha_4\beta_1$-integrin). From Ley et al. 2007.

In addition to mediating adhesion, integrins are capable of generating intracellular signals that regulate a variety of cellular functions. Binding of CD11b/CD18 to its ligand, Intercellular Cellular Adhesion Molecule 1 (ICAM-1), on the luminal side of the endothelium is a critical step in the transmigration of leukocytes through venular walls. Integrin activation drives the expression of other surface molecules on both immune cell and endothelium, reducing interendothelial contact and allowing penetration of the endothelial cell barrier and its pericyte sheath usually between cells (termed the 'paracellular' route). Certain cells, such as neutrophils infiltrating the CNS, have also been found to be capable of migration *through* cells (the *transcellular* route[68]). Subsequent penetration into the tissues is a dynamic process that begins during transmigration and involves the interaction of integrins and their ligands, the cadherins and, in some cells, the expression of matrix metalloproteases (MMPs).

During inflammation endothelial cells are triggered by cytokines not only to express adhesion molecules on their surfaces but to synthesise chemokines. They are also capable of actively transporting chemoattractants originating at the site of injury from their abluminal surface[69]. The recruitment of specific leukocyte populations depends not only on the differential expression of integrins and their ligands but also on the expression of chemokines and their receptors. Chemokines are powerful physiological activators of integrin-mediated adhesion and their effects are mediated via G-protein-coupled receptor signalling. They are small molecules which can be classified into C, CC, CXC and CX_3C categories depending on the arrangement of their N-terminal residues. A degree of pleiotropy and redundancy exists and chemokine receptors are expressed on a variety of cell types including immune cells, endothelial cells and neurones. The CCR2 receptor for example is expressed most highly on monocyte/macrophages and has an important role in their recruitment to non-lymphoid sites of inflammation,[70-72] however expression levels vary between monocyte subsets[73] and the receptor has also been demonstrated to be present on a number of other cell types including DCs at certain stages of maturation[74], neutrophils[75, 76], mast cells[76], ~15% circulating $CD4^+$ T cells[77] and even brain microvascular endothelial cells where it is thought

to be critical for macrophage transmigration[78]. CCR2 has multiple ligands that include CCL2 (which is specific for this receptor but expressed in a wide variety of tissues), CCL7, CCL8 and CCL13. It is not unusual for chemokine receptors to bind multiple ligands with varying degrees of affinity, some however, such as CCR8, are limited to only one.

Inflammatory cells are capable of expressing a range of chemokine receptors, only some of which are essential during the recruitment of a cell to a specific tissue - others may act to regulate the level of activation in a cell or influence the pattern of cytokine expression and cell-to-cell interactions. It has been demonstrated, for example that, despite strong CCL2 expression in the retina and CCR2 expression by recruited monocytes, CCR2 deletion does not lead to a reduction in disease severity in the experimental autoimmune uveitis model – suggesting that the effects of CCR2 deficiency are likely to be compensated for by other chemokine/chemokine receptor interactions[79]. Some chemokines may have more direct effects on inflammatory cell transmigration, for example the chemokine fractalkine (also known as CX3CL1 – a ligand for the CX3CR1 receptor expressed highly on specific monocyte subpopulations) exists in both soluble and membrane-bound forms and a role for this chemokine in cell adhesion has been proposed[80].

The importance of integrins and chemokines in regulating leukocyte activation and arrest has made and continues to make them prime targets for pharmacological intervention[81]. Chemokines and chemokine receptors are particularly attractive targets for cancer immunotherapy as they are involved in almost every step of tumourigenesis, including the growth and metastatic spread of malignant cells, neovascularisation and the recruitment of immunosuppressive cells – it is therefore conceivable that their manipulation might render similar benefits at different stages of AMD pathology. The results of clinical trials involving immunotherapy have been mixed however – a failure to demonstrate efficacy in trials designed to test CCR1, CCR2 and CXCR3 in various autoimmune diseases has been attributed to the nature of the drugs themselves, differences between the immune systems of animals and humans

and the fact that multiple receptors can be involved in driving the pathophysiology of disease.

1.5.2 The role of innate immune cells in inflammation

1.4.2.1 Interactions with the adaptive immune system

The innate immune system constitutes a phylogenetically ancient defence mechanism. As mentioned previously, innate immune cells may be broadly divided into two categories – the granulocytes and the cells of the MPS (Natural Killer cells forming a smaller subset). Components of either group may predominate during specific phases of the inflammatory process. However, despite these differences in their behaviour, innate immune cells are united in their expression of the myeloid cell marker CD11b.

For many years the innate immune system was considered separate to the adaptive immune system: Innate immune cells tend to be more responsive to inflammation-induced trafficking cues compared to naive lymphocytes of the adaptive immune system - this is largely because the former are capable of responding to less specific activation signals. These signals include Pathogen Associated Molecular Patterns, or 'PAMPS' (LPS being an example), which bind to 'PRPs' (Pattern Recognition Receptors) on the cells - examples of such receptors include Toll-like recepetors (TLRs). In contrast to innate immune cells, the migration of activated T and B cells is more dependent on the nature, quality and strength of an antigenic stimulus. Until recently the majority of immunological research focused on the intricacies of the adaptive immune system, with the role of the innate immune system regarded primarily as one of antigen presentation. However focus has shifted with growing recognition of the importance of the innate immune system in instigating, directing and regulating adaptive immune responses. Changes in the innate immune system associated with healthy (and morbidity-associated) ageing and pathological neovascularisation make them of particular interest in the study of AMD. The role of innate immune cells in antigen presentation and cytokine production

makes them key players in directing any subsequent lymphocyte responses, with particular cell types instigating particular patterns of inflammation. Broadly, patterns of inflammation can be divided into two categories mediated by the principal CD4$^+$ T lymphocyte populations (T lymphocytes being distinguishable from other cells of the adaptive immune system by their expression of a T cell receptor): T helper type 1 (T$_H$1) and T$_H$2 responses. Cytokines are small proteins which carry messages between cells in the immune system – the myriad interleukins (IL-), leukotrienes (LT-) and interferons (IFN-) are prominent examples. The cytokines interferon-γ (IFN-γ) and TNF-β (tumour necrosis factor-β) tend to predominate in T$_H$1 responses and as such drive a more pro-inflammatory and tissue-destructive environment. T$_H$2 responses may be regarded as more anti-inflammatory in nature, resulting in the production of IL-4, Il-5 and IL-13 (cytokines best known for their ability to modulate the behaviour of eosinophils in parasitic and atopic disease) and IL-10 a key 'suppressor' cytokine which can downregulate expression of IL-2 (a T cell activator), IFN-γ and IL-12.

A number of other T cell subsets may be influenced either directly or indirectly by myeloid cell activity in the retina, ciliary body and iris. These include cytotoxic CD8$^+$ T cells that have anti-viral and anti-tumour effects and also modulate transplant rejection, and regulatory CD4+ T cell (T$_{reg}$) populations. The latter, formerly known as suppressor T cells, may be identified by their expression of an intracellular protein known as Foxp3 and play a critical role in the induction of immune tolerance – this has been most extensively characterised in models of anterior chamber-associated immune deviation (ACAID). ACAID is a feature of ocular immunity whereby the usual responses to antigenic material are downregulated such that damage to the delicate structures of the 'immune priveleged' eye is limited. Inoculating an eye with antigen may therefore be seen to result in a form of systemic immunity characterised by T cells that eliminate pathogens and virulence factors in the absence of inflammation, an exclusion of effector CD4$^+$ T cells and the upregulation of regulatory T cells. A critical step in this process is the uptake of antigen by the resident F4/80$^+$ cells of the eye including (macrophages and DCs) and their migration to the spleen where T cell-mediated responses occur[82].

The role of the recently discovered T_H17 T cell population (thought to be involved in the aetiology of autoimmune diseases) in ocular pathology has yet to be determined but it has been established that certain myeloid cell populations have pivotal roles in modulating the balance of T_{Reg} and T_H17 populations with CD14+HLA-DR(-/low) myeloid-derived suppressor cells (MDSCs) inducing Foxp3+ regulatory T cells and $CD14^+HLA-DR^+$ monocytes promoting the generation of T_H17 cells[83].

1.4.2.2 Granulocytes

Granulocytes contain specialised granules released in the first phase of an immune response and comprise neutrophils, eosinophils and basophils. Neutrophils constitute the most abundant circulating leukocytes in healthy humans. Short-lived, they are recruited rapidly to sites of acute inflammation, particularly during bacterial and fungal infections, and have the potential to either cause tissue damage through the release of cytotoxic mediators such as TNFα (and hence may be said to drive T_H1-mediated responses) or implement a healing response, through the production of factors such as VEGF. Neutrophils express the chemokine receptor CCR2 (amongst others) and their response to the chemokine CCL2 has been found to be enhanced in the context of chronic inflammation[84]. Evidence suggests that neutrophils adopt a more complex profile of chemokine receptor expression (that includes CCR1, CCR2 and CCR3) compared to peripheral neutrophils in the context of chronically inflamed environments and that this affects their migratory capacity and function[85]. Eosinophils are much rarer in the circulation and are classically involved in modulating parasite-directed and allergic (T_H2-mediated) immune responses. Eosinophils share a number of surface markers with neutrophils, though expression of the chemokine receptor CCR3 is largely restricted to eosinophils and mast cells (mast cells are primarlily associated with allergic immune disorders and are derived from circulating basophils). CCR3 has recently been identified in choroidal neovascular endothelial cells in early AMD and antagonising this receptor has been demonstrated to result in inhibition of

CNV in experimental models (though this was appears not to be mediated by mast cells or eosinophils).[86].

1.4.2.3 Monocytes

Monocytes are much longer-lived cells than neutrophils and peripheral blood monocytes exhibit considerable morphological variability in terms of size, granularity and nuclear morphology. Identification of their differential expression of various antigenic markers has revealed them to be heterogeneous cells with varied physiological activities – these properties are largely conserved between mice and humans (*Table 2*). Until recently it was thought that monocytes circulated in the peripheral blood and patrolled vessels before differentiating into DCs or macrophages, however it has now been established that the spleen plays a significant role in the storage of undifferentiated monocytes and these may be deployed rapidly in response to inflammatory cues[87].

Monocytes have been implicated in many inflammatory diseases - they are recruited to atherosclerotic plaques, for example, where they ultimately become the lipid laden foam cells characteristic of the disease. They are also involved in combating chronic bacterial infections and responding to the presence of foreign material and injury. Certain subsets may also play critical roles in healing and immunological homeostasis - from clearing cell debris to directing angiogenesis. Monocytes are capable of producing large amounts of reactive oxygen species and cytokines such as TNF-α, IL-1β, IL-6 and IL-10 as well as VEGF and proteolytic enzymes. Most of these functions are carried out as macrophages in the tissues but monocytes also have the capacity to differentiate into DCs, cells that bridge the innate and adaptive immune systems through their capacity to trigger and regulate T-cell responses - essentially fine-
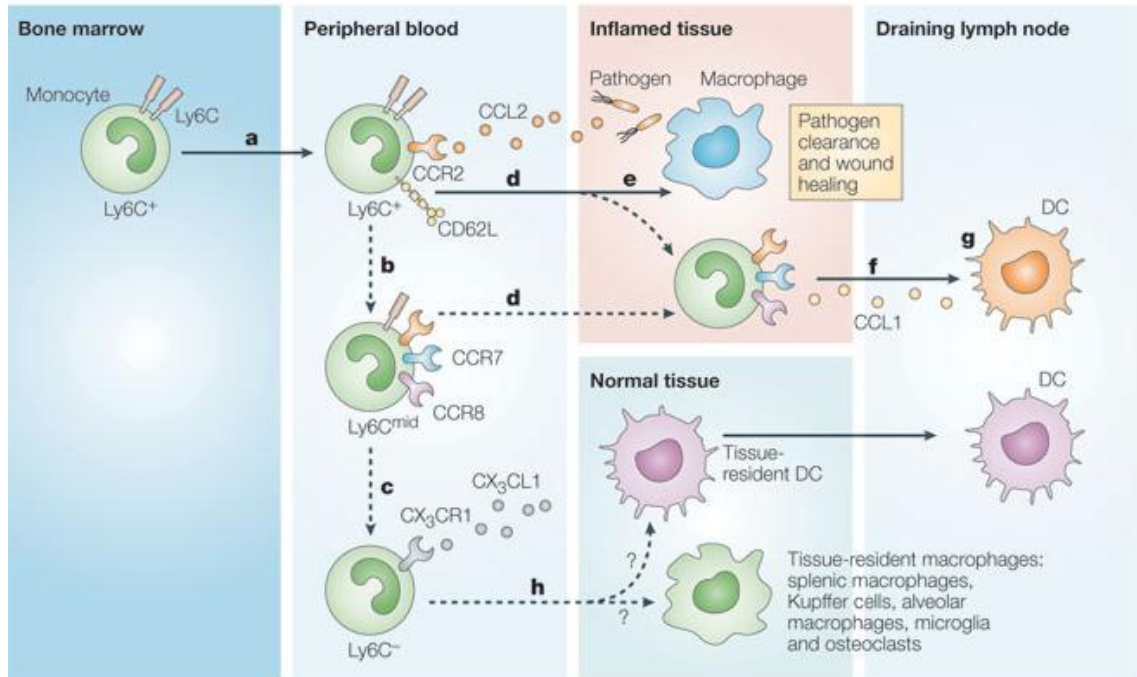
Figure 9. Cytokines produced by immune cells can give rise to macrophages with distinct physiologies.

*Ly6C+ bone-marrow monocytes are released into the peripheral blood, **a**, and are thought to adopt a Ly6C^mid phenotype **b**, which is associated with retention of CCR2, before (under steady-state conditions) they form CCR2⁻Ly6C⁻ monocytes, **c**, that are characterized by high CX_3CR1 expression. Both Ly6C+ and Ly6C^mid monocytes respond to pro-inflammatory cues, such as CCL2, and are recruited to inflammatory lesions, **d**. Of these, 'inflammatory' monocytes are thought to differentiate into macrophages, which are important for clearance of pathogens and for the resolution of inflammation, **e**. Some monocytes emigrate from the tissues to the draining lymph nodes, a process that uses CCR7 and CCR8 receptor–ligand interactions, **f**. CCR7+ CCR8+ monocytes that are present in the tissue must have been recruited directly from the peripheral blood to the inflammatory site or must have differentiated from Ly6C+ monocytes in situ. The expression of CCR7 and CCR8 by these cells makes them uniquely disposed to emigrate into the lymphatic vessels. In the draining lymph nodes, these monocytes acquire dendritic cell (DC)-like characteristics, **g**, which they do not obtain if they are retained in the tissue by selective chemokine-receptor deficiency. In the absence of inflammation, CX_3CR1^{High} Ly6C⁻ monocytes are thought to enter the tissues and replenish the tissue-resident macrophage and DC populations, **h**. Solid arrows represent pathways that are supported by established data, whereas dashed arrows represent pathways that are indicated from a compilation of more recent data and speculation. Adapted from Gordon & Taylor 2005.*

tuning the balance between inflammation and tolerance. Initially monocytes were considered the major antigen presenting cells of the immune system however the identification of discrete subsets of DCs suggests that these cells are in fact much more potent in this regard than the monocytes they are closely related to.

Monocytes in mice may be identified by their CD11b^{+} F4/80^{low} phenotype. F4/80 is a surface marker involved in T cell regulation that is restricted to the monocyte/macrophage pool and upregulated in states of activation[88, 89]. Monocytes can be further subdivided according to their differential expression of the chemokine receptors CCR2 and CX3CR1: one subset expresses CCR2, cluster determinant (CD) 62L (also known as L-selectin) and lower levels of the chemokine receptor CX3CR1 whereas the other expresses no CCR2 or CD62L but higher levels of CX3CR1[7, 90].

CCR2[+] monocytes migrate towards CCL2, a chemokine central to the recruitment of monocytes and other leukocytes such as basophils, natural killer (NK) cells, T cells, DCs and neutrophils to sites of inflammation[91]. This characteristic has led to CCR2^{+} monocytes being referred to as the 'inflammatory' subset. In keeping with this moniker these cells migrate to inflamed tissues and lymph nodes and produce high levels of the pro-inflammatory cytokines TNF-α and Il-1. The acquisition of an inflammatory monocyte phenotype has been demonstrated to be a time-limited property that is independent of external inflammatory signals – monocytes require a period of up to 48 hours in the circulation upon release from the bone marrow before they are capable of recruitment to inflamed tissues[92]. Inflammatory and TNF-α/iNOS-(inducible nitric oxide synthetase) producing DCs (Tip-DCs) can derive from CCR2^{+} monocytes – these cells either take up antigen in peripheral tissues and then migrate into lymphoid organs or, in the case of Tip-DCs, may

Table 2. Phenotype of the two best-characterized monocyte subsets in various mammals

Antigen	Human CD14^{hi} CD16^{-} 'inflammatory' monocytes	Human CD14^{+}CD16^{+} 'resident' monocytes	Mouse CCR2^{+} CX$_3$CR1^{low} 'inflammatory' monocytes	Mouse CCR2^{-} CX$_3$CR1^{hi} 'resident' monocytes
Chemokine receptors				
CCR1	+	-	ND	ND
CCR2‡	+	-	+	-
CCR4	+	-	ND	ND
CCR5	-	+	ND	ND
CCR7	+	-	ND	ND
CXCR1	+	-	ND	ND
CXCR2	+	-	ND	ND
CXCR4	+	++	ND	ND
CX$_3$CR1‡	+	++	+	++
Other receptors				
CD4	+	+	ND	ND
CD11a	ND	ND	+	++
CD11b	++	++	++	++
CD11c‡	++	+++	-	+
CD14	+++	+	ND	ND
CD31	+++	+++	++	+
CD32	+++	+	ND	ND
CD33	+++	+	ND	ND
CD43	ND	ND	-	+
CD49b	ND	ND	+	-
CD62L‡	++	-	+	-
CD80	ND	ND	ND	ND
CD86	+	++	ND	ND
CD115	++	++	++	++
CD116	++	++	++§	++§
CD200R	ND	ND	ND	ND

'Inflammatory' and 'resident' nomenclature is based on studies carried out in mice and extrapolated to other species. Data have been assigned arbitrary symbols that represent no expression (-), marginal expression (+/-) and increasing amounts of expression (+, ++, +++).

‡These receptors show good conservation of expression-pattern differences between the subsets of at least three species.

§There is no available commercial reagent that recognizes the extracellular domain of mouse CD116 (also known as granulocyte/macrophage colony-stimulating-factor receptor α-chain).

7/4, an unidentified mouse antigen recognized by monoclonal antibody 7/4; CCR, CC-chemokine receptor; CD200R, CD200 receptor; CXCR, CXC-chemokine receptor; CX$_3$CR1, CX$_3$C-chemokine receptor 1; EMR1, epidermal-growth-factor-module-containing mucin-like hormone receptor 1; F4/80, monoclonal antibody that recognizes the mouse homologue of the human protein EMR1; ND, either differences between the subsets have not been determined or, in some cases, there is no clear species conservation of the antigens.

(Adapted   from   Gordon   &   Taylor   2005)

migrate from the red pulp to the white pulp of the spleen. Additional markers for the 'inflammatory' population include Ly6-G (also known as Gr-1 – a granulocyte marker highly expressed on neutrophils, approximately 40% of NK cells and plasmacytoid DCs) and Ly6-C[73]. Gr-1 and Ly6C are epitopically distinct members of the same molecular family[93], though this is not always evident from the literature where the two markers are often referred to interchangeably, nevertheless CCR2$^+$ monocytes have been variously described as being Gr-1$^+$, Ly6-C$^+$ or Ly6-C^{High}.

CCR2$^-$ monocytes (Gr-1$^-$, Ly6-C$^-$ or Ly6-C^{Low}) are referred to as 'resident' monocytes because they are thought to migrate to tissues in the absence of inflammation and replenish tissue-resident macrophage and DC populations[7]. More recently, CCR2$^-$ Gr-1$^-$ monocytes have been found to exhibit a constitutive long-range crawling phenotype on the luminal side of the endothelium under steady state conditions that is CD11a/18 (β_2-integrin LFA-1) and CX3CR1 dependent[94]. This suggests that these monocytes patrol blood vessels and may play important functions in the scavenging of oxidised lipids, dead cells and pathogens[90].

The differential behaviour of CCR2$^+$ Gr-1$^+$ and CCR2$^-$ Gr-1$^-$ monocyte populations has been investigated using a number of different models. The CCR2$^-$ Gr-1$^-$ subpopulation appears to extravasate rapidly in response to peritoneal infection with *Listeria monocytogenes* for example and at 1h after infection is the major producer of the inflammatory cytokine TNF-α[90]. These cells continue to participate in the recruitment and activation of other effector cells such as granulocytes, NK cells and T-cells, before differentiating into macrophages of the so-called 'alternative' M2 phenotype. In contrast CCR2$^+$ Gr-1$^+$ monocytes, after becoming the main inflammatory cytokine producers later on in the inflammatory process (at an 8hr timepoint) go on to initiate a more DC-like differentiation programme (**Error! Reference source not found.**)[90]. Distinct patterns of recruitment and differentiation have also been identified in models of injury: sequential mobilisation of monocyte populations has been demonstrated in the healing mouse myocardium with CCR2$^+$ Gr-1$^+$ monocytes performing phagocytic, proteolytic and inflammatory functions before CCR2$^-$ Gr-1$^-$ cells with

attenuated inflammatory properties express VEGF and promote angiogenisis and healing of the tissue (**Error! Reference source not found.**)[95].

The effects of knocking-out the various monocyte chemokine receptors (CCR2 and CX3CR1 for example) and their cognate ligands have also been examined along with the effects of adoptive transfer of specific monocyte subsets and GFP-labelling of cells. This has proved useful, particularly in the field of atherosclerosis research but also in the investigation of inflammation in the brain and AMD in the eye, and will be discussed in more detail when the roles of these cells in the chorioretinal complex are considered.

1.4.2.4 Macrophages

Macrophages are a heterogeneous group cells capable of phagocytosing invading organisms, initiating inflammatory responses that drive the recruitment of neutrophils and NK cells and facilitating the maturation, differentiation and migration of DCs. They are also capable of secreting a wide array of cytokines, chemokines, growth factors and enzymes. Whilst the differential behaviour of monocyte populations gives some insight into the spectrum of macrophage activation, these populations were only discovered relatively recently and there remain many unanswered questions regarding whether specific *monocyte* populations give rise to specific *macrophage* populations and the contribution made by local proliferation to the pool of macrophages in the tissues (microglia are capable of proliferation in the CNS for example and this turnover may be enough to maintain their numbers throughout adult life except in defined conditions such as inflammation).

Macrophages may be classified as having an M1 or M2 phenotype, where M1 represents 'classically' activated macrophages and M2 'alternatively' activated macrophages. This model, though popular given its simplicity, has been largely superseded by other paradigms reflecting a broader spectrum of behavioural plasticity (**Error! Reference source not found.**). Classically activated macrophages are cells which respond to IFN-γ and TNF to produce inflammatory cytokines such as IL-1, IL-6

49

and IL-23; they are also associated with interactions with T_H17 cells that serve to recruit neutrophils which in turn contribute to inflammatory autoimmune pathologies – in short these macrophages fall neatly into a single category. *Alternatively* activated macrophages were initially defined according to the phenotype adopted by cells exposed to IL-4; however recent evidence suggests that this group can be further divided into macrophages with a wound-healing phenotype and macrophages with regulatory properties (**Error! Reference source not found.**). The IL-4 which drives development of wound-healing macrophages may arise either from a T_H2-mediated response or from an innate immune response promoted by granulocytes - the resulting cells, whilst less efficient at antigen presentation and killing pathogens, are able to secrete components of the extracellular matrix and interruption of IL-4 signalling therefore results in reduced fibrosis and reduced accumulation of wound-healing macrophages. Regulatory macrophages appear to require two signals for their activation - one may arise from immune complexes, prostaglandins, adenosine or apoptotic cells whilst a Toll-like receptor ligand may provide the other. These cells are prodigious producers of IL-10 (a potent inhibitor of the production and activity of a number of pro-inflammatory cytokines) they do not, however, contribute to the production of extracellular matrix. Interestingly, *IL-10⁻ᐟ⁻* mice which have an increased inflammatory response to diverse stimuli have been found to have reduced CNV following laser-induction compared to wild-type mice, a phenomenon associated with increased numbers of infiltrating macrophages[96].

1.4.2.5 Dendritic Cells

Dendritic Cells have been referred to as the 'quintessential professional antigen presenting cells' of the immune system - superior in this respect to macrophages. DCs in the peripheral tissues constantly monitor the local environment and in response to the appropriate maturation or 'danger' signals (usually upon ligation of a pattern recognising Toll-like receptor) migrate to lymphoid tissue where they may present processed antigen and trigger T cell

activation. DCs' functions straddle the innate and adaptive immune systems. They are capable of producing copious amounts of cytokines such as Il-12 and

52

interferons in mounting a host defence against microbes and have the capacity to activate not only T cells but regulatory T cells and NK cells. Most interestingly there is evidence to suggest that DCs capture antigen against which an immune response is usually avoided, including environmental proteins derived from the respiratory and digestive tracts and tissues where constitutive cell turnover is a feature – this suggests a role for DCs in maintaining homeostatic control over recognition of self and the local microenvironment. They are rare in peripheral blood but relatively common in lymphoid and various non-lymphoid tissues (such as the choroid) [90]. In the mouse circulating DCs can express the integrin CD11c (DCs are often said to be CD11c^{Hi}) and MHC class II antigen whereas monocytes do not.

The origins of DCs and the roles of the various subpopulations have yet to be fully determined – several subsets exist and there may be multiple precursors that include the so-called myeloid/DC progenitor, the common DC precursor and CCR2$^+$ Gr-1$^+$ monocyte populations (which have been demonstrated to be capable of replenishing DC resident cell compartments in the skin, lung and digestive tract as well as contributing to inflammatory/Tip-DC populations discussed earlier). Conventional 'non-myeloid' DCs (cDCs) represent those populations in lymphoid tissue originally identified as being responsible for 'mixed lymphocyte reaction activity' - these cells have a short half life and do not have a monocyte intermediate. Plasmacytoid DCs (that are also Ly6C$^+$ and Gr-1$^+$) represent a subset that is the most potent IFN-α-producing in response to viral infections[90] whereas it has been suggested that the Tip-DC subset is primarily responsible for killing bacteria rather than regulating T cell functions[90]. Interestingly, phagocytosis of apoptotic cells by immature DCs induces an anti-inflammatory response and promotes tolerance through production of TGF-β and IL-10 thereby reducing the ability of DCs to stimulate T cells directly. The impaired clearance of apoptotic cells that can result from complement deficiency, for example, potentiates secondary necrosis and the maturation of DCs (via their exposure to 'damage associated molecular patterns') - with pro-inflammatory consequences[42].

DCs have become a focus of atherosclerosis research in recent years since they have been demonstrated to have a role in atherosclerotic plaque destabilisation. CCL2 is thought to be involved in DC migration into vascular intimae and DC recruitment is impaired in mouse models of atherosclerosis that are deficient in the chemokine CX3CR1[97].

1.4.2.6 Natural Killer cells

Natural Killer cells (supporters of innate immunity) and Natural Killer T cells (a closely related population that bridges the innate and adaptive immune systems) are heterogeneous lymphocytes that have a critical role in the innate immune response to infections and tumours. NK cells do not require activation to kill cells missing 'self' markers such as MHC class I, consequently they have an important role in killing tumour and virus-infected cells which they do by releasing cytoplasmic proteins known as perforin and granzyme. NK cells express a number of cytokines and chemokine receptors that modulate their cytotoxic properties: NK cells migrate in response to CCL2, and both CCR2 and CCR5 on NK cells have been demonstrated to play a role their migration, target-binding and recruitment. The cytokines IL-2, IL-12, IL-15, IL-18 and IFN-α/β have been demonstrated to promote NK cell proliferation and activation and induce these cells to produce pro-inflammatory cytokines such as IFN-γ and TNF-α. In addition, models of infection suggest that neutrophils play a critical role in inducing NK cell IFN-γ production[98]. NK cells share a progenitor with T lineages but develop independently of the thymus and express neither the TCR (T cell receptor)/CD3 complex typical of T cells nor surface immunoglobulin. They do, however, exhibit a number of unusual markers including CD56 (in humans), CD16, CD57 and CD2 and are generally considered to be CD11b^{+}, Ly6C^{+} and Gr-1[+90]. Expression of the integrins CD11b and CD11c by NK cells has sometimes led them to be confused with macrophages. Both NK cells and macrophages also express Fc receptors that enable antibody-dependent cell cytotoxicity.

1.5.3 The innate immune system of the retina and choroid

The mammalian retina is of neuroectodermal origin and consists of two layers of neuronal cell bodies separated by two layers of synapses and an outer layer of photoreceptors the outer tips of which are enveloped by the apical processes of the RPE cells (with a ratio of approximately 30 photoreceptors to each RPE cell). In the uninflamed state the retina is invested with a repertoire of innate immune cells, the predominating cell type being microglia.

Microglia are the resident immune cells of the central nervous system (CNS) and in addition to the functional characteristics in keeping with their macrophage phenotype they have a range of other roles. These include: interacting with multiple CNS cell types (including the Muller glia, vessels and photoreceptors of the retina), participating in vasculogenesis[99] and synthesising and releasing neurotransmitters and neurotrophic factors that impact on the physiology and survival of neurones and photoreceptors[100]. In the resting state microglia adopt a dendritiform or 'ramified' appearance where primary processes emerge from the cell body and branch before ending in bulbous tips. In retinal explants these processes have been observed to exhibit highly dynamic properties consistent with their sampling of the extracellular space and an exchange of signals between neighbouring microglia. Following laser injury these movements increase in frequency, processes may be directed towards the site of injury and microglia are seen to migrate to the site of injury and may adopt a more 'amoeboid' phenotype[101].

Under physiological conditions there are two anatomically distinct populations of retinal microglia in the adult: a perivascular population located around the inner retinal vasculature and a parenchymal population arranged in a stratified configuration that is largely confined to the inner retinal layers and is mostly absent from a zone that extends from the outer nuclear layer to Bruch's membrane . Evidence derived from adoptive transfer experiments using eGFP-transgenic mice suggests that bone marrow-derived $CD11b^+$ $F4/80^-$ monocytes migrate across the blood-barrier and replace the retinal microglia with a turnover time of 6 months and that whilst the recruited cells are $CX3CR1^+$ the
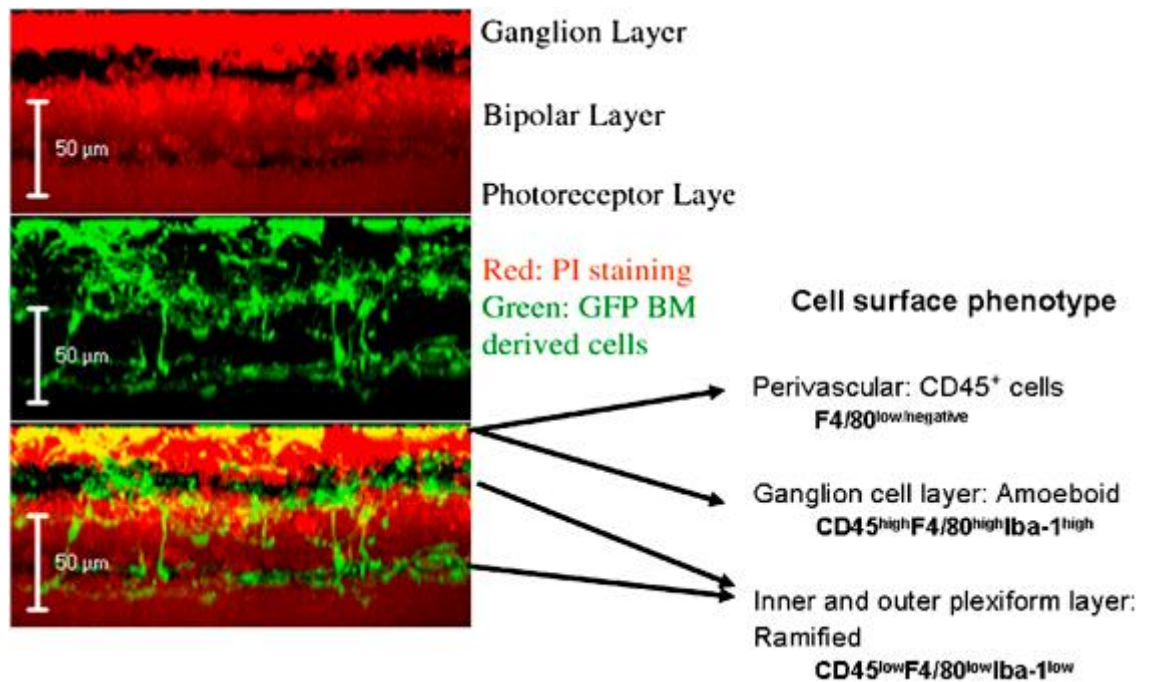
Figure 10 Phenotype of myeloid and microglial populations within mouse retina

Microglial populations in a chimaeric bone marrow EGFP-transgenic mouse model used to demonstrate microglial repopulation of the retina. Following reconstitution of the bone marrow in normal adult C57BL/6 mice with EGFP+ bone marrow, replacement of retinal microglia is observed over a 6-month period. Further immunohistochemical analysis permits the identification of a variety of microglial phenotypes that occupy different locations in the retina. F4/80 expression varies in the retina - amoeboid microglia present in the ganglion cell layer are F4/80high and ramified parenchymal microglia F4/80low. From AD Dick 2008.

receptor is not directly involved in the recruitment process[102, 103]. Whether the monocyte/macrophage population in the adult retina is CCR2⁻ Gr-1⁻ in phenotype has not yet been confirmed though microglia in *CX3CR1gfp* transgenic mice (in which one or both copies of the *CX3CR1* gene have been replaced with an eGPF reporter gene) appear to be CD45⁺, CD11b⁺, F4/80⁺, CD11c⁻ and MHC class II⁻[103]. Transferred cells are found initially at the peripheral and juxtapapillary retina and subsequently in the ganglion cell layer, the inner and outer plexiform layers and ultimately the photoreceptor layer. Cells in the ganglion layer assume an amoeboid shape and high levels of expression of the leukocyte-specific marker CD45, F4/80 and the microglia-specific Iba-1 whereas cells in the inner and outer retina are ramified and express low levels of the above markers (with perivascular macrophages expressing the least). The implications of changes in morphology and surface marker expression are unclear in the retina. In the brain there is evidence to suggest some regional differences in microglial marker expression although it should be noted that changes in microglial morphology and expression of a small number of markers cannot be used as simple guides to phenotype and function[104].

Both perivascular and parenchymal macrophage populations in the retina have limited antigen presenting potential and instead act to suppress T cell activation. The RPE appears to be actively involved in this process, maintaining the immune status of the 'resting' retina through the secretion of cytokines, such as TGF-β, that drive the retinal microglia to produce Il-10 and direct cells stimulated by TNF/IFN-γ towards an ant-inflammatory phenotype[105]. The CD200-CD200R system is also important in regulating retinal microglia under physiological conditions. CD200 is a type-1 membrane glycoprotein expressed on a variety of lymphoid and non-lymphoid cells including activated T cells, B cells, vascular endothelium and neurones[106-108]. CD200R is expressed predominantly on myeloid-derived cells, including microglia, macrophages, neutrophils and mast cells[108]. Ligation of CD200R has been demonstrated to dampen microglial activation and limit tissue damage in a variety of inflammatory models in the CNS, including experimental autoimmune uveitis

(EAU)[109] and experimental autoimmune encephalitis (EAE)[107]. Decreased neuronal expression of both ligand and receptor have been linked with the chronic inflammation of Alzheimer's disease and treatment of microglia and macrophages with the anti-inflammatory cytokines Il-4 and Il-13 (levels of which are reduced in human elderly brains) has been demonstrated to increase expression of CD200R[110].

In contrast to the microglia, dendritic cells account for a relatively small proportion of the innate immune cells of the retina. However a population of perivascular MHC class II$^+$ DCs that line the retinal vessels has been implicated in the induction of EAE in mice and another small population of MHC class II$^+$ 33D1$^+$ cells has been identified in the retinal periphery and around the optic nerve - sites where the first signs of autoimmune uveoretinitis are known to appear[111].

In common with the innate immune cell population of the uveal tract (the iris, ciliary body and choroid), the innate immune cell population in the choroid is composed primarily of macrophages and DCs that have been found to be extremely heterogeneous in terms of their morphology, immunophenotype and function. The macrophages of the mouse choroid have a perivascular arrangement that extends along the length of the medium and large vessels, and these cells have been described as being pleomorphic, dendriform or fusiform in shape[112]. In contrast an extensive network of DCs, defined as positive for MHC class II (Ia$^+$), were described in the same study as being less perivascular in distribution and more dendritiform in shape. Subsequent work using *CX3CR1^{gfp}* transgenic mice has confirmed the pattern of distribution and morphology described above and suggests that the majority of eGFP$^+$ cells in the choroid in this model are MHC Class II$^+$ (with high expression on the processes of dendriform cells) as well as being CD11b^{Low}, CD45$^+$ and CD68$^+$ (the latter being a marker for cytoplasmic granules in myeloid populations)[103]. Immunoelectron microscopic studies in the rat choroid suggest that macrophages and MHC Class II$^+$ DCs are located directly beneath Bruch's membrane and in the intercapillary pillars of the choroid where they lie in close apposition to the basal surface of the RPE and extend processes into a region

known to accumulate photoreceptor debris with age[113]. Uveal tract DCs have been further characterised as being CD8α^{-} CD11b^{+} CD11c^{+} ie. Cells of 'conventional' DC phenotype (other subsets have not been found) whilst uveal macrophages have been found to be predominantly CD11b^{+} F4/80^{+} cells, with few signs of activation under physiological conditions. Macrophage populations cultured from the choroid have been found to potentiate the antigen presenting function of certain dendritic cells[111].

1.6 Age-related changes in the eye and the role of the innate immune system

1.6.1 Parainflammation

The term 'parainflammation' has been used to describe levels of inflammation that lie between intermediate and basal. Parafinflammation reflects the innate immune response mounted by the body in various tissues to restore tissue homeostasis. It has been proposed that under basal conditions cells such as the perivascular macrophages and microglia of the retina may perform a house-keeping role that involves clearing the by-products of cell metabolism and maintaining neuronal integrity. In situations of more severe tissue damage, cells may need to be recruited from the circulation for the purpose of restoring tissue homeostasis. Should the response become uncontrolled - in the presence of persistent injury for example - chronic inflammation may ensue. Chronic inflammation is said to form the core of all age-related pathology and is a consequence of the exposure of tissues such as the brain and vasculature to free-radical-induced damage over the lifetime of the host beyond a point at which cells normally responsible for restoring homeostasis are able to cope without triggering further damage. Aside from AMD, diabetic retinopathy and glaucoma are the other two key age-related conditions affecting the eye[114].

1.6.2 Morphological changes associated with ageing in the retina and RPE-choroid

As a consequence of the cumulative damage described above (perhaps exaggerated in the retina because of the levels of light and oxygen exposure), the sensitivity of the retina declines with age. A reduction in the rate of dark adaptation is seen coupled by a loss of neuronal cells – particularly rods – and this is accompanied by a loss of RPE cells that primarily affects the macula and surrounding area[115]. The consequences of a failure to deal with apoptotic cells and their by-products (a process known as autophagy) by tissue resident macrophages have already been described: induction of a pro-inflammatory cascade of events and, in the CNS at least, neuronal cell death[116]. Additional changes with ageing include an accumulation of lipofuscin in RPE cells and an increased thickness of Bruch's membrane that is associated with the accumulation of drusen precursors described earlier. The changes in Bruch's membrane may have knock-on effects on RPE cell and photoreceptor function as a result of impaired hydraulic conductivity[117]. In AMD, Bruch's membrane may appear thinned with small defects in its structure. There is also a build up of complement and fibrinogen in the outer collagenous zone that may be the result of macrophage activation in the vicinity (macrophages have been found in close association with such changes[28]).

Ageing changes may also affect the blood-retinal barrier (BRB). The BRB is made up of tight junctions between the capillaries of the neuroretina and between individual RPE cells. Vascular endothelial cells have been demonstrated to increase production of pro-inflammatory cytokines (IL-6, TNF-α and CCL2) with ageing and this may account for the observed increase in leukocyte-endothelial interactions and the disruption of tight junctions. Disruption of tight junctions, either under the direct influence of cytokine signalling or as a result of leukocyte transmigration of endothelium, leads to the leakage of proteins and platelets into the neuroretinal tissue with injurious consequences that may occur acutely or over many years[114]. Aside from the critical effects of oxidative stress, the ageing retina is also exposed to other noxious stimuli that drive parainflammatory processes. These include: advanced glycation end products, oxidised lipoproteins and hyaluronan fragments – all of which are associated with the production of pro-inflammatory cytokines and the recruitment/activation of innate immune cells in the retina.

Changes associated with ageing in the choroid are perhaps less dramatic though probably no less significant than those seen in the retina. The thickness of the choroid increases with age in mice by a factor of three and this is associated with fibrosis in the outermost layer (Haller's layer) where fibroblasts and elongated melanocytes constitute a significant proportion of the cellular population[114]. The middle layer of the choroid (Sattler's layer – composed primarily of medium-sized blood vessels) is seen to accumulate round giant-melanocytes with age and these are also found occasionally in the subretinal space. In addition, the choriocapillaris becomes distended and, along with Bruch's membrane, is seen to accumulate fibrillar structures in samples of human tissue[118].

1.6.3 The immune response in the ageing retina

As in the rat brain, an increase in the numbers of innate immune cells (MHC class II[+]) has been found in the parenchyma of ageing rat retina compared with young animals. This phenomenon is associated, in the rat at least, with impaired blood-retinal-barrier function and a decline in cognitive function[119]. In the mouse, an accumulation of subretinal microglia (positive for the microglial marker Iba-1^{+}, CD68^{+} and MHC^{Low} but said to be negative for CD11c) has been observed with normal ageing[9, 120]. These cells, which have their origins in the inner retina, have a bloated, lipofuscin-filled appearance with the large cell body and short dendrites associated with microglial activation, and their proximity to the underlying RPE makes it likely that they influence RPE function. Lesions similar in appearance and with similar constituents to drusen (and therefore termed subretinal drusenoid deposits or pseudodrusen) have been demonstrated in the subretinal space of aged and AMD-affected humans (**Error! Reference source not found.**)[121, 122, 89]. Although the cellular nature of subretinal drusenoid deposits has yet to be confirmed in humans, their location on Spectral Domain Optical Coherence Tomography (SD-OCT) correlates with the location of the clinically diagnosed reticular drusen that have long been

associated with AMD. Parallels with the phenotype in aged mice therefore make this an area of intense interest (**Error! Reference source not found.**).

The migration of microglia to the subretinal space with age and a general increase in numbers of innate immune cells in the retina would require attendant changes in the pattern of cytokine and chemokine expression in the retinal microenvironment - this is indeed the case. Levels of the cytokine TNF-α and chemokines CCL2, CCL3, CCL8 and CCL12 have been found to be increased in the retinae of aged mice[114]. The source of this array of cytokines and chemokines has yet to be established but increases in the levels of pro-inflammatory cytokines associated with injured brain have been linked to astrocytes (the retinal equivalent being Muller glia)[123]. The reduced levels of expression of CD200 and CD200R in the brains of Alzheimer's patients suggest that a downregulation of regulatory proteins in the retina may also occur[110].

1.6.4 The immune response in the ageing RPE-choroid

Various changes consistent with a parainflammatory response have been noted in the ageing RPE-choroid. CD45$^+$ leukocytes have been found to be increased in number on examination of choroidal flatmounts in old mice compared to young and these cells appear to express CRIg, a receptor expressed on macrophage subsets that is involved in complement-mediated phagocytosis[114]. This hints at a possible role for these cells in scavenging cell debris from RPE/retina, aided by complement activation. Use of immunofluorescent techniques has demonstrated that CD45$^+$ leukocytes appear to be absent from Bruch's membrane in young mice whereas many appear to be attached in aged mice; some may also be seen to be attached to the surface of choroidal capillaries and some may be seen to be passing through Bruch's membrane[124].

Comprehensive work using microarray techniques and RT-PCR has demonstrated that as many as 16 pathways are upregulated in the

aged RPE-choroid the first 10, in order of significance, being those involved in: 1) leukocyte signalling; 2) complement cascades; 3) NK cell signalling; 4) IL-10 signalling; 5) B cell signalling; 6) T cell signalling; 7) IL-2 signalling; 8) granulocyte monocyte colony stimulating factor signalling; 9) Fc epsilon RI signalling; and 10) chemokine signalling. In contrast to the RPE-choroid, where immunological and inflammatory pathways are upregulated, those increased with age in the retina are largely related to stress responses and apoptosis[124].

Closer examination of those pathways upregulated in the RPE-choroid suggests that leukocyte extravasation activity is highly elevated. Genes responsible for leukocyte docking and rolling, including those coding for CD11b/CD18, αL-integrin and ICAM-1 are most prominent in terms of increased expression. Expression of MMPs (also integral to leukocyte extravasation and migration) also appears to be upregulated, principally MMP3 and MMP13. In keeping with the hypothesis that complement is integral to the clearance of cell debris by the choroidal innate immune system, levels of expression of C3 are increased by a factor of almost 10 in the aged choroid and immunohistochemistry has confirmed large, discontinuous clumps of C3 deposits on Bruch's membrane in aged mice[124].

Aside from those genes responsible for generalised leukocyte recruitment, a number of genes involved in NK cell signalling are expressed at increased levels in the aged RPE-choroid - these include genes encoding proteins that mediate the activation of NK cells[124]. Given that NK cells are generally thought to be involved in killing tumour and virus-infected cells it is interesting to speculate on their role in the ageing RPE-choroid.

Genes associated with the regulation of immune responses, most notably IL-10, are upregulated in the aged RPE-choroid. In contrast, production of pro-inflammatory cytokines such as IL-12, IL-6 and TNFα is reduced in the aged choroid – a pattern that may be linked to increased levels of prostaglandin E2 (PGE2). The macrophages thought to be responsible for secreting these cytokines have been demonstrated to be present in increased numbers in the choroid with age (**Error! Reference source not found.**). A range of techniques

has demonstrated that CCL2, a chemokine with a key role in leukocyte recruitment, is strongly upregulated in the aged RPE-choroid with immunofluorescent labelling demonstrating its presence in both RPE and endothelial cells[124]. Such changes would be consistent with alterations in the immune environment of the subretinal space – a low-grade chronic inflammatory response that involves the recruitment of innate immune cells not present in younger animals.

1.6.5 The ageing innate immune system

Immunosenescence, the deterioration of the immune response associated with ageing, is thought to underly the reduced ability of the elderly to combat infection and to mount effective immune responses following immunisation (particularly to influenza vaccines). It is also thought to be linked to the higher incidence of cancer in the elderly. Consequently, research has focused on the nature of immunity in successful ageing (those who reach extreme age with little or no associated morbidity) and the immune systems in those with increased morbidity and mortality at a relatively younger age. Significant differences have emerged regarding the behaviour of both the adaptive and the innate immune systems with age and evidence suggests that changes in the latter may to a certain extent explain those in the former. Evidence suggests that the antigen presenting function of DCs is well-retained in the elderly but that their numbers, and those of their precursors, are reduced. In addition it has been demonstrated that the chemotaxis and phagocytic capacity of both DCs and neutrophils is impaired with age – possibily as a result of changes in signal transduction pathways[125].

The numbers of circulating neutrophils and their precursors are not thought to be affected by ageing. However, evidence suggests that as well as exhibiting impaired chemotactic and phagocytic capacities, neutrophils in the elderly adopt a low-grade inflammatory status in the absence of stimulation that is characterised by CD62L shedding, altered signal transduction and constitutive production of reactive oxygen intermediates. Such changes suggest a role for

aged neutrophils in the pathogenesis of autoimmune diseases, Alzheimer's disease, cancer and atherosclerosis - the latter condition, for example, has been associated with higher numbers of circulating neutrophils and the decreased activity of NK cells. Stimulated neutrophils from elderly subjects have also been demonstrated to release more elastase than in younger subjects (which may have direct implications for ruptures in Bruch's membrane in the context of AMD) and higher levels of CD11b expression on neutrophils have been associated with Alzheimer's disease[126].

Ageing human and rodent macrophage populations have reduced levels of MHC Class II that may contribute to impaired T-cell responses and monocyte TLR-mediated induction is also compromised with ageing. Whilst there appears to be no difference in the numbers of peripheral blood monocytes between elderly and young subjects a slight decrease in macrophages and their precursors has been found in the bone marrow of elderly subjects (although the reverse appears true of bone marrow macrophage populations in rodents). An age-related decline in the ability of macrophages to adhere to surfaces, opsonise, kill tumour-infected cells and phagocytose has also been demonstrated, and although the affected pathways have yet to be fully elucidated, aberrant responses to chemotactic stimuli are likely to be involved. In keeping with these findings, macrophages from healthy elderly individuals have been shown to have an impaired response to complement-derived factors that may contribute to delayed pathogen clearance[127].

Increasingly evidence also suggests that microglial 'dystrophy', as opposed to activation, is linked to Alzheimer's disease. Microglia exhibit age-related changes such as telomere shortening and have been demonstrated to have neuroprotective properties that weaken with age and precede the neurofibrillary pathology of the disease. Such senescent changes have been demonstrated by focusing on morphological changes in the microglia instead of the more commonly used markers of activation such as MHC Class II expression that can also be upregulated on ramified cells. The principal feature of microglial dystrophy in the brain is cytoplasmic fragmentation (also known as cytorrehexis) – an appearance not unlike that which precedes apoptosis. The hypothesis that

age-related changes in microglia underly the development of Alzheimer's and similar neurodegenerative diseases is considered an attractive one because it places the effects of ageing, as the major risk factor, at the centre of the disease process[128].

The evidence for age-related changes in macrophage cytokine and chemokine secretion is mixed. This is partly the result of differences in the genetic heterogeneity and health of human cohorts and partly the result of differences between the responses elicited following *in vivo* and *in vitro* experimentation. There also appears to be interspecies variation: rodent studies suggest an age-related decline in the secretion of macrophage-derived pro-inflammatory cytokines such as IL-1, TNFα and IL-6 whereas the majority of human studies suggest the opposite. Macrophages from both aged mice and aged humans appear to produce more prostaglandin E2 (PGE2) than younger individuals however. PGE2 suppresses IL-12 secretion and decreases surface expression of MHC class II on APCs and also enhances IL-10 secretion – factors thought to contribute to a decline in T cell function with age[127]. Furthermore EGFP-expressing brain-derived microglia in rodents exhibit morphological changes with age such as the presence of lipofuscin granules, decreased complexity of processes, altered granularity and an increased expression of pro-inflammatory cytokines such as TNFα, IL-1β, IL-6 and IL-12 that appears to be counterbalanced by expression of IL-10 and TGFβ. Aged microglia also exhibit increased expression of pro-inflammatory cytokines compared to young microglia when challenged with lipopolysaccharide (LPS) accompanied by an enhanced Il-10 response and failure to downregulate TGFβ. These changes are proportional to the basal levels independent of age and this implies that ageing microglia function normally although their response to a challenge is adjusted in proportion to the level of basal activation[129].

Given that NK signalling is upregulated in the aged RPE-choroid the effects of ageing on the body's NK cell population may be relevant. In rodents, evidence suggests that NK cell activity peaks at 5-8 weeks of age before declining to nearly undetectable levels at 25 months of age. Similarly elderly subjects between 75 and 85 years have decreased NK cytotoxic function, a feature that

correlates with a history of severe infections or subsequent death due to infection. In contrast nonagenarians and centenarians exhibit similar NK cell cytotoxicity to subjects aged 60-65 years, indicating that preservation of NK cell cytotoxicity in an individual, along with a favourable ratio of subsets, may be associated with healthy ageing. In aged mice, NK cell cytotoxicity is preserved following stimulation with IL-2 but reduced on stimulation by IFN-γ. In humans, the response to Il-2 is also preserved but the cytoxic activity of cells stimulated with IL-12, IFN-α and IFN-γ is diminished with an associated age-related decline in perforin that affects men more than women. Production of IL-2, IL-12, IFN-α and IFN-γ by lymphocytes decreases with age (a shift towards a TH2 phenotype) with a consequent reduction in production of these cytokines by NK cells that impact on the adaptive immune system. Impaired cytotoxicity and IFN-γ production by NKT cells (which, in contrast to NK cells, tend to exert their cytotoxic effects through Fas/Fas ligand interactions) is also a feature of ageing in mice and humans – as with NK cells, a feature reversed in examples of extreme age in both cases. Decreased IL-4 production by certain immunoregulatory NKT subsets also appears to be associated with chronic age-related pathology.

A factor that unites the age-related changes in NK and NKT cell populations is their relationship to zinc ion bioavailability and metallothionein homeostasis. Zinc is a trace element essential for the efficient functioning of not only NK and NKT cells but also the efficient phagocytic functioning of monocytes, granulocytes and macrophages. It is also important in the recruitment of neutrophils and maintenance of their levels in the circulation, and the activation of mast cells. More recently, the maturation of DCs has been linked to a TLR-induced reduction in intracellular zinc[130]. Zinc is a component of over 300 enzymes and is also found at the core of sub-RPE deposits in AMD and deposits in neurodegenerative conditions such as Alzheimer's disease (its origin at these sites is unknown). Zinc bioavailability in cells is regulated by low molecular weight proteins known as metallothioneins – these serve as a store for zinc and are upregulated in response to high zinc concentrations. Metallothioneins have been found to be present at reduced levels in the peripheral RPE compared to the macular RPE - a difference that increases with

age[131]. Metallothionein expression is induced by pro-inflammatory cytokines, such as Il-6 and TNF-α, that have been demonstrated to be elevated in the plasma of the elderly. An abnormal increase in metallothionein expression may therefore be responsible for the progressive decrease in circulating levels of zinc seen with healthy ageing and this may explain changes in immune system functioning, at least systemically[132]. It is therefore possible that the effects of antioxidants and zinc supplementation in reducing progression of AMD[16] are mediated through immunomodulatory mechanisms.

1.7 Models for AMD

1.7.1 Animal models of AMD

The complexity of tissue and immune cell interactions in AMD means that the benefits of *in vitro* experimentation are limited. Currently, however, there is no single animal model that faithfully replicates what is seen in the human disease. There are a number of reasons for this: understanding of the underlying genotypic risk factors for AMD is incomplete; AMD is largely restricted to the macula (an anatomical feature of the human eye shared only with birds and non-human primates); AMD is a disease of ageing, and this places restrictions on the suitability of certain species for experimentation; and the relative contributions of established environmental risk factors have yet to be determined.

Rodents, in particular mice, are favoured as models of AMD for the ease with which transgenic animals may be developed and the lower cost of their maintenance compared to primates, rabbits and pigs. Diseases which might take years to manifest in humans also tend to progress at rates measured in weeks or months in mouse models. A disadvantage of their use, however, is that mice lack a macula and have a low cone-rod ratio (although they do have a higher concentration of photoreceptors centrally compared to the periphery and, of the total complement, it is rods that are lost earliest in AMD). In addition, the results obtained from mouse models with different backgrounds should be

interpreted with caution since immunological differences across strains have been identified[133].

Despite the development of a variety models relying on the controlled exposure of mice to dietary and environmental factors, progress towards reliable models of 'wet', 'dry' and 'mixed' AMD phenotypes has been slow. There are a number of models available that exhibit features of early AMD, these include: the 'senescence accelerated mouse' model, in which progressive abnormalities of the RPE and Bruch's membrane are seen (though the underlying genotype is unknown); a model in which D-galactose administered in the diet results in the advanced glycation end-product-induction of an ageing phenotype and a model in which immunisation of mice with carboxyethylpyrrole (a unique oxidation fragment of docasahexaenoic acid which is found in drusen) results in the formation of drusen and GA-like lesions in the fundus[134]. Increasingly, attention has focused on models that allow the effects of the innate immune system on ageing in mice and potential therapeutic options to be studied in more detail – such approaches have yielded valuable data not only in the field of AMD research but also in the study of other age-related pathology where chronic inflammation is a feature such as atherosclerosis and Alzheimer's disease.

1.7.2 The effects of chemokine deficiency in mice

1.7.2.1   The effects of *CCR2* or *CCL2* knockout

Deficiencies in either CCR2 or CCL2 result in impaired macrophage mobilisation and trafficking in mice[70] - deletion of *CCL2* results in reduced macrophage recruitment to atherosclerotic lesions and reduced lesion size in mice for example. Given that a failure of innate immune cells to effectively manage subretinal debris may be linked to the development of drusen and given that chemokines such as CCL2 are expressed at higher levels in the aged choroid[124], a number of studies have examined the effects of deleting chemokines or their receptors (sometimes in combination) using transgenic mice.

Initially it was thought that *CCL2*^{-/-} and *CCR2*^{-/-} animals exhibited all the key features of AMD. After 9 months of age these mice were thought to develop subretinal deposits with the pathological hallmarks of drusen (including complement and IgG deposition) together with thickening and disruption of Bruch's membrane and, in mice older than 18 months, spontaneous CNV[135]. A number of these assertions have since failed the test of replication - in particular it has not been possible to detect CNV in subsequent investigations of the model. Interestingly, however, it has recently been established that the lipofuscin-containing deposits claimed as drusen are in fact bloated lipofuscin-laden macrophages (positive for CD68 and F4/80 markers on immunostaining) akin to those seen in aged wild-types. In fact the principle difference between senescent wild-type and *CCL2*^{-/-} mice is that the accumulation of macrophages subretinally is accelerated in the knockout model and the cells have a more swollen appearance. It has also been observed that up to 50% of macrophages in wild-types and *CCL2*^{-/-} mice contain pigment suggestive of phagocytosed RPE cell debris. Other age-related changes such as thickening of Bruch's membrane and RPE damage appear to be unaffected by CCL2 deficiency[120]. Whilst it is most likely that the accelerated accumulation of subretinal macrophages in these models is the result of their dysregulated trafficking and recruitment, the possibility that their behaviour is part of a compensatory mechanism for another disrupted pathway (for example impaired RPE cell phagocytosis) cannot be discounted.

CCR2 has been demonstrated to have an important role in facilitating the release of Ly6C[Hi] monocytes from the bone marrow and their absence from the circulation (rather than a failure to traffic to sites of inflammation) has been postulated as the reason for the attenuated inflammation observed in a number of disease models employing the *CCR2*^{-/-} mouse[136].

Evidence therefore suggests a role for CCL2 in innate immune cell trafficking at the site of the RPE-choroid complex with deficiencies resulting in accelerated microglial dystrophic changes possibly in response to debris originating from the RPE. The exact nature of the affected microglia and why they appear to fail to process debris correctly (instead remaining static and lipofuscin-filled in the

subretinal space) is not known, but work on the recruitment of bone marrow derived cells to the brain using GFP-transgenic bone marrow chimeric mice suggests that Ly6C^{Hi} CCR2$^+$ monocytes are the principle cells involved in microglial turnover in the CNS – a process that appears to be at least partly dependent on CCR2 and CCL2, with double deletion of both receptor and ligand resulting in significant deficiencies of monocytic populations and bone marrow-derived parenchymal and perivascular microglia under physiological conditions[137, 138]. Manipulation of these populations may prove beneficial in delivering new therapies for AMD.

1.7.2.2   The effects of *CX3CR1* deletion

As with *CCL2$^{-/-}$* and *CCR2$^{-/-}$* mice, deletion of *CX3CR1* also results in the accelerated accumulation of bloated subretinal microglia with age (**Error! Reference source not found.**). CX3CR1 is expressed on a variety of innate immune cells, including NK cells, T cells and monocyte subpopulations. Its ligand, CX3CL1 (also known as fractalkine) exists in membrane-bound and soluble forms and, as well as being involved chemokine signalling, is a potent mediator of cell adhesion. CX3CL1 is abdundantly expressed in the CNS, the retina (particularly by Muller cells) and the choroid[139]. CX3CL1 deficiency attenuates the accumulation of foam cells in the vessel walls of *CCR2$^{-/-}$* mice, an effect thought to result from a failure to facilitate monocyte arrest[140].

Microglia in the normal retina have been identified as the sole cell type to express CX3CR1. Combadiere et al. identified that *CX3CR1$^{GFP/GFP}$* mice accumulated significant numbers subretinal microglia at 6 months compared to age-matched *CX3CR1$^{GFP/+}$* mice - a difference seen to increase with age. *CX3CR1$^{-/-}$* mice also exhibited a substantial degeneration of the outer retina at 18 months of age. In *CX3CR1$^{-/-}$* mice the drusen-like phenotype seen on fundoscopy has been confirmed as being the result of CD11b$^+$ microglia accumulating lipid droplets derived from partially digested photoreceptor outer segments. It has been suggested that such cells may form the origin of drusen since drusen contain deposits positive for CX3XCR1 as well as other debris

remarkably similar in composition to that found in degenerating microglia. It has also been suggested that the apparent migration of bloated microglia from the subretinal space to the sub-RPE space where drusen appear to develop may actually be the result of RPE cells mobilising to cover microglia.

Combadiere *et al.* undertook in vitro assays demonstrating the increased adhesion of monocytes expressing the M280 variant of the CX3CR1 receptor initially thought to account for a percentage of AMD cases (this has been found not to be the case with a subsequent study)[65, 141]. It was hypothesised that the accumulation of subretinal microglia was a result of increased adhesion of these cells in the subretinal space[65]. Given that CX3CR1 is also expressed on a variety of other innate immune cells and that genes involved in the signalling of, for example, NK cells are upregulated in the RPE-choroid with age, the possibility that subretinal microglial accumulation in CX3CR1$^{-/-}$ mice is a by-product of a failure to recruit other types of innate immune cell to the RPE-choroid cannot be excluded. For example, CX3CL1 has been implicated in the recruitment of CX3CR1^{+} NK cells in a model of experimental autoimmune encephalitis (EAE) and a failure to recruit these cells in CX3CR1-deficient mice results in increased EAE-related morbity and mortality[142].

Despite the apparent effects of CX3CR1 deficiency on the rate of subretinal microglia accumulation, a separate study of *CX3CR1$^{gfp/+}$* and *CX3CR1$^{gfp/gfp}$* mice suggested that this receptor is not essential for the normal turnover of resident macrophage and DC populations in retinal and choroidal tissue, indicating that CX3CR1 mediates *recruitment* of circulating cells that may have a role in clearing subretinal debris[103].
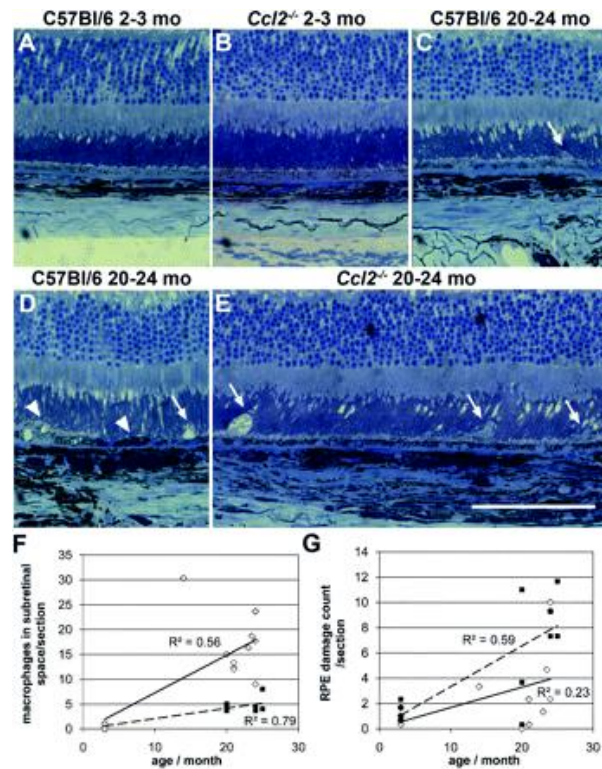
Figure 11. Ccl2-knockout (Ccl2^(−/−)) mice do not develop abnormal RPE changes with age, but show an accumulation of bloated macrophages in the subretinal space.

Toluidine blue-borax–stained semithin histologic sections of the outer retina, RPE, and choroid from young (2–3 months) and old (20–24 months) Ccl2^(−/−) and C57Bl/6 wild-type mice (A–E). No obvious histologic differences between young C57Bl/6 wild-type (A) and Ccl2^(−/−) (B) mice were observed. In old C57Bl/6 (C, D) and in old Ccl2^(−/−) (E) mice, photoreceptor morphology was also normal, but macrophage-like cells were observed in the subretinal space. These cells were swollen in Ccl2^(−/−) mice (C, D versus E, white arrows). Swelling/lysis of RPE cells and pyknosis (indicated by the darker staining) of RPE cells were observed in senescent animals of both genotypes, but are only shown as examples in C57Bl/6 wild-type mice (D, arrowheads). Note the higher pigmentation of the choroid in old C57Bl/6 and Ccl2^(−/−) mice compared with young mice (C, D, E versus A, B). Scale bar, 100 µm. Quantitative analysis of the number of macrophage-like cells in the subretinal space (F). The mean number of macrophages per individual animal is depicted [C57Bl/6, (■); Ccl2^(−/−) mice (◇)] and shows a significant positive correlation between age and number of macrophages in the subretinal space per section, which was much more pronounced in Ccl2^(−/−) mice. (G) Quantitative analysis of alterations in the RPE. The RPE damage count (Ccl2^(−/−), solid line; C57Bl/6, dashed line), revealing a similar accumulation of RPE alterations with age in both genotypes and an overall positive correlation of this accumulation with age (Pearson correlation r = 0.585, P = 0.001, n = 27).From Luhmann et al. 2009.

1.7.2.3   The effects of *CX3CR1* and *CCL2* double-deletion

The identification of AMD-like features in $CCL2^{-/-}$ mice and the description of loss-of-function single-nucleotide polymorphisms in *CX3CR1* associated with AMD have prompted exploration of the phenotype resulting from combined deficiency of both CCL2 and CX3CR1[143].

In comparison with $CCL2^{-/-}$ and $CX3CR1^{-/-}$ mice, double-knockout $CCL2^{-/-}$ $CX3CR1^{-/-}$ mice exhibit a focal, early onset, progressive retinal degeneration characterised by the development of lesions in the ONL as early as 1-4 months of age – a phenotype associated with the appearance of subretinal macrophages. Subsequent changes have been noted to include loss of all retinal layers, RPE damage (including accumulation of lipofuscin), increased RPE-retinal adhesion and vascular inflammation. The features of vascular inflammation and increased leakage in this model are supportive of a role for microglia/macrophages in maintaining a healthy vasculature in the eye[143, 144].

Double knockout of *CX3CR1* and *CCL2* would therefore appear to have an even greater effect on the rate of subretinal macrophage accumulation and associated damage in mice compared to single knockout of these genes. However, recent evidence has emerged to indicate that many of these double knockout animals have a third autosomal recessive gene – the *Crb1* gene – that is responsible for a well-characterised model of retinal degeneration. Consequently, it has been concluded that the phenotype of double knockout *CX3CR1*/*CCL2* mice described previously is in fact one of an inherited retinal degeneration - with vascular changes more in keeping with retinal telangiectasia then CNV - that is differentially modulated by CCL2-CCR2 and CX3CL1-CX3CR1 signalling (Luhmann *et al.*; in press).

1.7.2.4   The effects of light exposure on the migration of retinal microglia

Whilst light exposure is not a risk factor for AMD, ambient light exposure has nevertheless been demonstrated to influence the pattern of distribution of

microglia in mice. For example albino mice raised in a darkened environment retain microglia in the inner retinal layers but after exposure to light for as little as a week large numbers of cells positive for the microglial marker 5D4 may be seen to accumulate subretinally. Evidence suggests that the subretinal microglia originate from the inner retinal layers and that they assist RPE cells in the phagocytosis of photoreceptor-derived material - production of which is accelerated as a consequence of phototoxicity. Pigmentation appears protective for the effects of light exposure but differences in the levels of induced-migration between strains suggest other factors may also influence the process[145]. The effects of light exposure in the context of chemokine deficiency have yet to be fully explored, however it has been demonstrated that albino *CX3CR1$^{-/-}$* mice accumulate subretinal microglia at an accelerated rate compared to albino wild-type mice and this suggests a role for CX3CR1 signalling in the maintenance of a healthy retina and RPE-choroid.

1.7.3 Laser-induced choroidal neovascularisation

1.7.3.1 Background to laser-induction of CNV

Whilst not the only method of inducing CNV in animal models (others, including the use of Matrigel containing pro-angiogenic growth factors, have been described[146]), the use of a laser to rupture Bruch's membrane is perhaps the best characterised. Laser injury produces a wound composed of several concentric circular areas: a central area where the most energy is delivered and all cells are destroyed, a rim surrounding the centre that corresponds to an area where energy dissipates producing substantial cellular damage and an outer area where cell disruption is minimal and the healing process begins. Early morphological changes become visible at 3 days post- induction and precede neovascularisation which develops in the first week before becoming maximal at 2 weeks (persisting for several weeks thereafter).

First described in 1979, the laser-induced CNV model has a number of advantages in the study of wet AMD: principally the shared pathophysiological characteristics between disease and model. These features include the rapid

migration of choroidal endothelial cells and subsequent formation of fenestrated new vessels through defects in Bruch's membrane; the accumulation of subretinal fluid; the accumulation of leukocytes adjacent to developing new vessels; and fibrovascular scarring. The angiographic appearances of leakage following laser-induced CNV are also similar to those seen in the classic CNV of AMD. There is also a shared pattern of cytokine and growth factor expression - the presence of VEGF in RPE and leukocytes; VEGF receptors in RPE and endothelial cells; basic fibroblast growth factor in RPE cells, choriocapillaris and macrophages; TGF-β in RPE, choriocapillaris endothelium and fibroblasts; TNF-α expression in leukocytes; and the involvement of Fas and Fas-ligand interactions having been demonstrated in both laser-induced and wet AMD lesions[147].

Other advantages of this model include its suitability for use in mouse models, thereby permitting the study of genetic defects on pathological neovascularisation with relative ease, and its proven use in pre-clinical studies designed to test the effects of pharmaceutical compounds and novel therapeutic modalities in the treatment of CNV[148]. Individual lesions following laser delivery often vary in size, however, and this necessitates multiple areas of CNV-induction per fundus and occasionally many animals to demonstrate significant effects.

Laser induction of CNV departs from the natural course of CNV observed in AMD by its lack of chronicity. Whereas laser-induced CNV lesions involute spontaneously at 30 days (at least in young mice) lesions in subjects with AMD often persist for many years, requiring the administration of many treatments to control[23, 149]. In some ways the behaviour of laser-induced CNV is more akin to that of myopic CNV in young patients, which also tends to involute spontaneously, with much less in the way of functional consequences (although interestingly myopic CNV lesions are larger in older subjects)[150].

1.7.3.2 The complement system and CNV

Whilst several genes encoding complement pathway proteins have been implicated in the pathogenesis of AMD, evidence for the role of the complement system in the development of CNV is more circumstantial. The complement fragment C3 and C3a have been identified in surgically excised CNV lesions and elimination of C3 results in attenuation of laser-induced CNV. Similarly inhibition of the terminal complement complex C5b-9 using antibodies to C6 results in the inhibition of CNV formation in mouse models. It is thought that fragments C3a and C5a may contribute to the neovascular response by stimulating the recruitment of monocytes to the choroid[151].

The complement fragment C5 has been found to accumulate in the RPE and choroid of *CCL2*^{-/-} mice leading to the suggestion that a failure to recruit monocytes results in the accumulation of immune complexes and the chronic inflammation that drives AMD. C5a has also been linked to increased VEGF production and the propagation of laser-induced CNV. Whilst it has not been possible to demonstrate a clear association between genetic variants of C5 and AMD this complement fragment has nevertheless become a focus for pharmalological intervention and a number of C5-targetted pharmaceutical agents are currently being investigated in clinical trials for AMD[151].

1.7.3.3 Innate immune cell responses in laser-induced CNV

Evidence from multiple sources has confirmed a role for macrophages in the development of laser-induced CNV: *CCR2*^{-/-} mice have been found to have attenuated CNV following laser-induction as have mice depleted of both circulating and choroidal macrophage populations by clodronate liposomes[152].

Early work examining the kinetics of inflammatory cell recruitment suggested that recruitment of neutrophils and macrophages peaks at 48 hours post-laser-induction, with neutrophils the predominant cell type[153]. Attempts to attenuate macrophage, T cell, NK cell and neutrophil responses - all cell types purported to be involved in tumour angiogenesis - using antibodies to markers specific for these populations revealed a significant reduction in the neovascular response only upon targeting macrophages (antibodies were delivered intraperitoneally in the week preceding angiography performed 7 days post-induction of CNV). Use of chimeric GFP$^+$ bone marrow transplanted mice has also demonstrated that cells recruited from the circulation account for as much as 45% of the total F4/80$^+$ cells associated with CNV at 3 days post-laser (a figure that rises to 70% at 2 weeks when lesion size is maximal). Further evidence for the role of recruited monocytes is provided by the concurrent upregulation of adhesion molecules in CNV such as Vascular Cell Adhesion Molecule (VCAM) that also coincides with increased size of the lesion (**Error! Reference source not found.**). That recruited monocytes should appear to have a role in laser-induced CNV is significant given their pro-inflammatory potential exceeds that of the microglial population and their close association with activated Muller cells (a population which in the quiescent state releases neurotrophic factors essential for retinal homeostasis)[154]. The appearance of monocytes in CNV lesions at 3 days post- laser coincides with the proliferation of RPE and endothelial cells in this model - at day 4 post-laser isolectin-positive cells forming vascular tubes may be visualised and the size of the lesion then increases exponentially in the 3 days that follow[155].

The role of monocyte subsets in CNV has yet to be fully explored. Work on the *CCR2$^{-/-}$* mouse confirmed only that recruitment of F4/80$^+$ cells was reduced in association with a reduction in lesion size with subsequent experiments demonstrating a role for neutrophils in laser-induced CNV[153, 156]. Conversely,

CX3CR1$^{GFP/GFP}$ mice, deficient in CX3CR1, exhibit an enhanced responsed to laser-induction of CNV (double that of controls) with many more cells seen to accumulate at the site of injury compared to CX3CR1$^{GFP/-}$ mice at 7 days post-injury. The latter study involved use of 12 month old animals that have already accumulated significant numbers of subretinal microglia – it is unclear to what extent this may have contributed to the increased levels of neovascularisation or whether the effect is mediated by a failure to recruit specific monocyte subsets from the blood (particularly as both CCR2$^+$ and CCR2$^-$ subsets may be affected by CX3CR1 knockout). Nevertheless, as part of the work it was demonstrated that VEGF was produced by F4/80$^+$ subretinal microglia following laser-induction of CNV[65].

A considerable amount of research has focused on the role of monocyte subsets in tumour angiogenesis (innate immune cells in general, from neutrophils to mast cells, are thought to make a significant contribution to tumour angiogenesis). In particular, parallels have been drawn between the activities of so-called TEMs (Tie-2-expressing monocytes) and CCR2$^-$ Gr-1$^-$ monocytes; and TAMs (tumour-associated macrophages) and CCR2$^+$ Gr-1$^+$ monocytes. Tie-2 is a receptor for angiogenic growth factors known as angiopoietins. Both subsets share gene expression profiles, with TEMs appearing to have enhanced proangiogenic and tissue remodelling activity and lower proinflammatory activity - much like the CCR2$^-$ Gr-1$^-$ monocyte subset that is thought to promote angiogenesis in the post-ischaemic myocardium. Consequently, TEMs have become novel targets for anti-cancer therapy. Tumours grown in *CCR2$^{-/-}$* mice recruit few TAMs and it has been suggested this population is derived from the 'inflammatory' monocyte subset[157-159].

The roles of CCR2$^+$ Gr-1$^+$ and CCR2$^-$ Gr-1$^-$ monocytes have also been explored using models of alkali-induced corneal angiogensis. Lu et al. found that, in keeping with the results of laser-induced CNV experiments, *CCR2$^{-/-}$* mice exhibit a reduced corneal neovascular response whereas *CX3CR1$^{-/-}$* mice exhibit an increased corneal neovascular reponse. Reduced levels of infiltrating F4/80$^+$ cells, but not neutrophils, were noted in *CX3CR1$^{-/-}$* animals. Selective depletion of macrophages results in reduced corneal infiltration by macrophages but no

change in the neovascular response compared with controls. CX3CR1$^+$ cells were found to express the antiangiogenic molecules ADAMTS-1 and thrombospondin-1, and topical application of CX3CL1 was found to inhibit neovascularisation in this model. The role of CX3CL1 in mediating ocular angiogenesis remains unclear, however, since the results of other groups have suggested a role for this chemokine in the promotion of ocular angiogenesis in other models of corneal neovascularisation, the OIR model and in vitro assays.

The use of *CXC3CR1*$^{GFP/+}$ mice has yielded data that largely concerns the behaviour of the resident microglial population following laser-induction of CNV in mice. Eter et al. subjected *CXC3CR1*$^{GFP/+}$ mice to laser-induction of CNV (**Error! Reference source not found.**) and, using flow cytometric techniques, established the accumulation of macrophages and DCs in both retina and choroid 2 days after injury, with evidence of further increases in the numbers of microglia in the retina at subsequent timepoints up to 35 days post-laser (in contrast Combadiere et al. found numbers of F4/80$^+$ GFP$^+$ cells peaked at 7 days in *CX3CR1*$^{GFP/+}$ mice before a decline was noted at 14 days). Eter et al. also found that numbers of innate immune cells remain increased in the choroid up to 35 days post-injury. Attempts to distinguish between CX3CR1^{High} and CX3CR1^{Low} monocytes did not feature in the study however and the possibility that the *CX3CR1*$^{GFP/+}$ genotype interferes with CX3CR1-mediated cell recruitment cannot be excluded. Findings were in keeping with other work suggesting that DCs may have a role in pathological neovascularisation in the eye – Nakai et al. having already established that immature DCs (CD11c$^+$ MHC class II^{Low} cells) expressing VEGFR2 peak between 2 and 4 days post-induction of CNV by laser, appear closely involved with the developing neovascular complex and when transplanted intravenously are capable of augmenting CNV growth[160]. Other studies have also confirmed a role for immature DCs in the angiogenesis associated with tumour growth[161].

In contrast to findings that a failure of macrophage recruitment results in *reduced* choroidal neovascularisation, Apte et al. identified that the *increased* recruitment of CD11b$^+$ F4/80$^+$ cells to CNV lesions was associated with a reduction in lesion size at 1 week post-laser-induction in *Il-10*$^{-/-}$ mice and that

intravitreal injection of CD11b$^+$ cells (obtained from bone marrow cultures) at the time of CNV induction also resulted in an attenuated response. Restoration of Il-10 to the eye resulted in a comparative increase in lesion size and overall their results indicated a role for both Il-10 (driving pro-angiogenic pathways) and macrophages (exerting anti-angiogenic effects - possibly via Fas and FasL interactions) in modifying the neovascular reponse[96].

Finally, age has been found to be an independent risk factor for severity of laser-induced choroidal neovascularisation. Lesions in 16 month old wild-type mice are significantly larger than those in 2 month old mice (being thicker and more cellular) though no significant difference has been established in terms of the amount of leakage from induced-CNV between young and old animals. No mechanism for the increased severity of CNV in older animals has been established though age-related systemic changes resulting in altered vascular biology have been proposed as a cause independent of local changes in the retina and RPE-choroid[162].

1.8 Aims of the thesis

Age-related macular degeneration is a complex disease, for which ageing is the main pathogenic driver. The clinical endpoints in AMD are tissue loss in the majority of cases (particularly in geographic atrophy) and choroidal neovacularisation, resulting in scarring, in the remainder. The identification of age-related macular degeneration as a chronic inflammatory disease in which dysregulation and dysfunction of the immune system (the complement system in particular) features prominently was a major milestone[31]. However, there remain several unresolved questions regarded as being of critical importance to our understanding of the pathogenesis of this blinding disease:

● What cellular events lead to complement activation at the RPE–choroid interface? It is not known whether complement activation occurs at a systemic, or local level.

● What are the respective roles of acute phase proteins and pro-inflammatory cytokines in RPE-choroidal pathology, and when do they come into play?

● What is the temporal relationship between local inflammation, complement activation, dendritic cell involvement, and drusen biogenesis at the RPE–choroid interface?

● Does the presence of HLA-DR in drusen, and the invasion of drusen by dendritic cells, signify an ongoing process of antigen presentation to the immune system? If so, what are the antigens involved?

The interplay between innate immune cell populations as tissues age and the reasons for a divergence into the two phenotypes described above have yet to be fully determined. This thesis focuses on questions surrounding the role of innate immune cells in AMD pathology. The aims of this thesis are therefore:

1) To define the innate immune cell populations in the retina and RPE-choroids of young adult wild-type mice.

2) To determine the effects of ageing on innate immune populations in wild-type mice and the effects of a deficiency in CCL2 (a chemokine central to innate immune cell recruitment and expressed at higher levels in aged tissues).

3) To determine the effects of ageing and CCL2-deficiency on lesion size using experimental models of CNV.

4) To determine the key innate immune cell populations involved in the the development of CNV.

5) To determine whether any changes in innate immune cell populations in the retina, RPE-choroid and periphery correlate with the observed effects of ageing on CNV lesion size.

6) To explore the effects of experimental therapeutics, both intended and unintended, on innate immune cell populations in the context of choroidal neovascuarisation. Does targeting members of the receptor tyrosine kinase family, such as VEGF receptors and PDGF receptors, in the treatment of CNV affect innate immune cell populations that also express these receptors? Does targeting the activation pathways of innate immune cells confer benefit in the context of CNV and what is the effect on cells' phenotypes?

This is a broad set of aims that reflects the cellular complexity of AMD and makes best use of the models currently available. The approach encompasses an analysis of the innate immune cell populations present in young, healthy tissue and how these change with normal ageing before examining the effects of chemokine deficiency and CNV induction. Finally, the effects of compounds targeting angiogenic pathways and innate immune cell activation in the context of experimental CNV are determined. The identification of any positive and negative effects of these approaches on innate immune cell populations may help in informing future therapeutic strategies. This thesis does not address the role of complement or the role of cytokines in the pathogenesis of AMD but does aim to contribute to understanding of the cells involved. Further work may seek to determine how complement and cytokines interact with innate immune cells to engender disease.

Materials and Methods

2.1 Reagents

Laboratory supplies and powdered reagents were sourced from established suppliers.

2.2 In vivo experiments

2.2.1 Animals

CCL2-knockout (*CCL2$^{-/-}$*) mice on a C57Bl/6 background were kept as a homozygous line (a kind gift from Kath Else at the University of Manchester from the original stock maintained by Barrett Rollins) [163]. Age-matched control animals (C57Bl/6 6JOla Hsd; Harlan UK Ltd., Blackthorn, UK) were kept in the same animal room. The animal experiments were performed in accordance with the ARVO Statement for the Use of Animals in Ophthalmic and Vision Research and under the UK Home Office project licence (PPL 70/2045).

2.2.2 Anaesthesia

For in vivo procedures, the mice were anesthetized by a single intraperitoneal (IP) injection of a mixture of medetomidine hydrochloride (1 mg/ kg body weight; Domitor; Pfizer Animal Health, New York, NY), and ketamine (60 mg/kg body weight) in water for injection. Whenever necessary, the pupils were dilated with 1 drop of 1% tropicamide (Bausch and Lomb, UK). The animal experiments were performed in accordance with the ARVO Statement for the Use of Animals in Ophthalmic and Vision Research.

2.2.3 Laser induction of choroidal neovascularisation

A slit-lamp-mounted diode laser system (wavelength 680 nm; Keeler, UK) was used to injure Bruch's membrane in each eye (laser settings: 210 mW power, 100 ms duration, 100 μm spot diameter). These settings consistently generate a subretinal gas bubble which strongly correlates with adequate laser-induced

rupture of Bruch's membrane and successful induction of CNV. Only eyes in which laser-induced subretinal vapourisation bubble formation occurred were included in the analysis. Eyes were also excluded if there was significant cataract or keratopathy formation which could affect laser energy delivery or angiography. For subsequent assessment of CNV lesion size energy was targeted at 3 areas approximately 3-4 disc diameters from the optic nerve head at the 10 o'clock, 2 o'clock and 6 o'clock positions and avoiding any vessels. For subsequent flow cytometric analysis, lesions were induced in 10 locations equally spaced throughout the fundus.

2.2.4 Image quantification of choroidal neovascularisation

In vivo FFA was performed at 1 and 2 weeks after induction of CNV by diode laser. Images from the early (90 seconds after fluorescein injection) and late (7 minutes) phases were obtained using a small animal fundus camera with appropriate filters (Kowa Genesis, Tokyo, Japan). The pixel area of CNV-associated hyperfluorescence was quantified for each lesion using image-analysis software (Image Pro Plus; Media Cybernetics, Silver Spring, MD). Where comparison of two eyes in the same animal was required the sequence of imaging from right to left was alternated to avoid any bias.

2.3 Intraocular delivery of bioactive compounds

Surgery was performed under direct retinoscopy through an operating microscope. Pupils were dilated with topically administered 1% Tropicamide (Bausch and Lomb, UK). The eye was gently prolapsed by exerting pressure adjacent to the globe. A fundal view was obtained by applying a coupling solution (Viscotears, Novartis Pharmaceuticals, UK) and glass cover slip. Counter-traction was applied to the globe using toothed forceps to grasp the conjunctiva and rectus muscle of the eye. The tip of a 1.5cm, 34G hypodermic needle mounted on a 5µl Hamilton syringe (Hamilton, Switzerland) was then passed into the posterior vitreous via a sclerotomy made just posterior to the limbus and 5ul of either CD200R agonist antibody or isotype control antibody

(courtesy of Andrew Dick/DNAX Schering Plough Inc.) slowly injected. The cornea was allowed to clear completely before withdrawal of the needle so as to minimise reflux.

2.4 Oral delivery of bioactive compounds

0.2mls of suspension containing pazopanib or vehicle (GSK, UK) was delivered by oral gavage using a 22G curved, ball-tipped needle (Braintree Scientific).

2.5 Blood collection and plasma preparation

Mice were culled by exposure to CO_2 and bled immediately by cardiac puncture (27G needle on a 1µl syringe). Blood was transferred to EDTA vacutainers (BD, Europe) and kept on ice. Samples were centrifuged at 2000RPM for separation of plasma and the resulting supernatant transferred to polypropylene tubes and stored at $-20^{o}C$ prior to shipping on dry ice for pharmacokinetic analysis. Plasma samples were analysed for pazopanib by an analytical method based on protein precipitation followed by analysis with high-performance liquid chromatography and two stages of mass spectrometry (GSK, UK).

2.6 Flow cytometry

2.6.1 Basis of surface marker selection

Surface markers were selected with the aim of defining monocyte/macrophage subsets in the eye and periphery and establishing the role of dendritic cells in the ageing process as well as the key cell populations involved in the response to laser-induced choroidal neovascularisation, including granulocytes. The markers CD11b, F4/80, Gr-1, Ly6C and CD11c were selected for the panel. The inclusion of other markers (such as those for NK cells) was limited by the availability of suitable fluorophores for conjugation at the time of experimental design – analysis of over 16 channels is theoretically possible using the BD LSRII flow cytometer and the appropriate fluorophores, however the repertoire of quantum dot-conjugated antibodies is restrictive and the use of standard fluorophores increases the risk of spectral overlap during analyses.

Consideration also had to be given to the likelihood of identifying rarer cell populations in retina and RPE-choroid using additional markers when the cell yield would in any case be much lower than in the spleen, bone marrow or blood. Where possible conjugated antibodies were employed so that handling of suspensions and loss of cells was minimised.

2.6.2 Fluorochrome-conjugated antibodies and flow cytometer configuration

Monoclonal antibodies directly-conjugated to fluorochromes were selected to minimise the risk of non-specific binding and to improve experimental efficiency. The PE fluorochrome was reserved for F4/80 staining as F4/80 antigen was known to be weakly expressed in the retina and PE has a high quantum yield. Cells suspensions were incubated with rat anti-mouse CD16/32 Fc block (2.4G2; BD Biosciences) prior to immunostaining to minimise non-specific binding of antibodies to innate immune cell Fc receptors. The following antibodies were used for staining (*Table 3*; rat anti-mouse unless stated otherwise): anti CD11b PerCP 5.5 (M1/70; eBioscience), hamster anti CD11c PE-Cy7 (N418; eBioscience), anti Ly6G AlexaFluor 488 (RB6 8C5; eBioscience), anti F4/80 PE (CI: A3-1; Serotec), anti Ly6C AlexaFluor 647 (ER-MP20; Serotec).

Three lasers on the BD LSR II were employed to excite the above fluorochromes: the 488nm laser was used to excite all except DAPI (355nm laser) and AlexaFluor 647 (633nm laser). Filters were configured in such a way as to minimise spectral overlap. The BD LSR II cytometer octagon and trigon arrays use dichroic long-pass mirrors on their inner rings and band-pass filters on their outer rings - these were configured to minimise spectral overlap when using the above antibody panel (*Figure 12*). The band pass filter performance with this arrangement was estimated using the BD Multicolour Spectrum Viewer (http://www.bdbiosciences.com/research/multicolor/spectrum_viewer/index.jsp).

a

Band pass filtre (BP)   **Long pass filtre (LP)**

b

BLUE LASER (488nm)
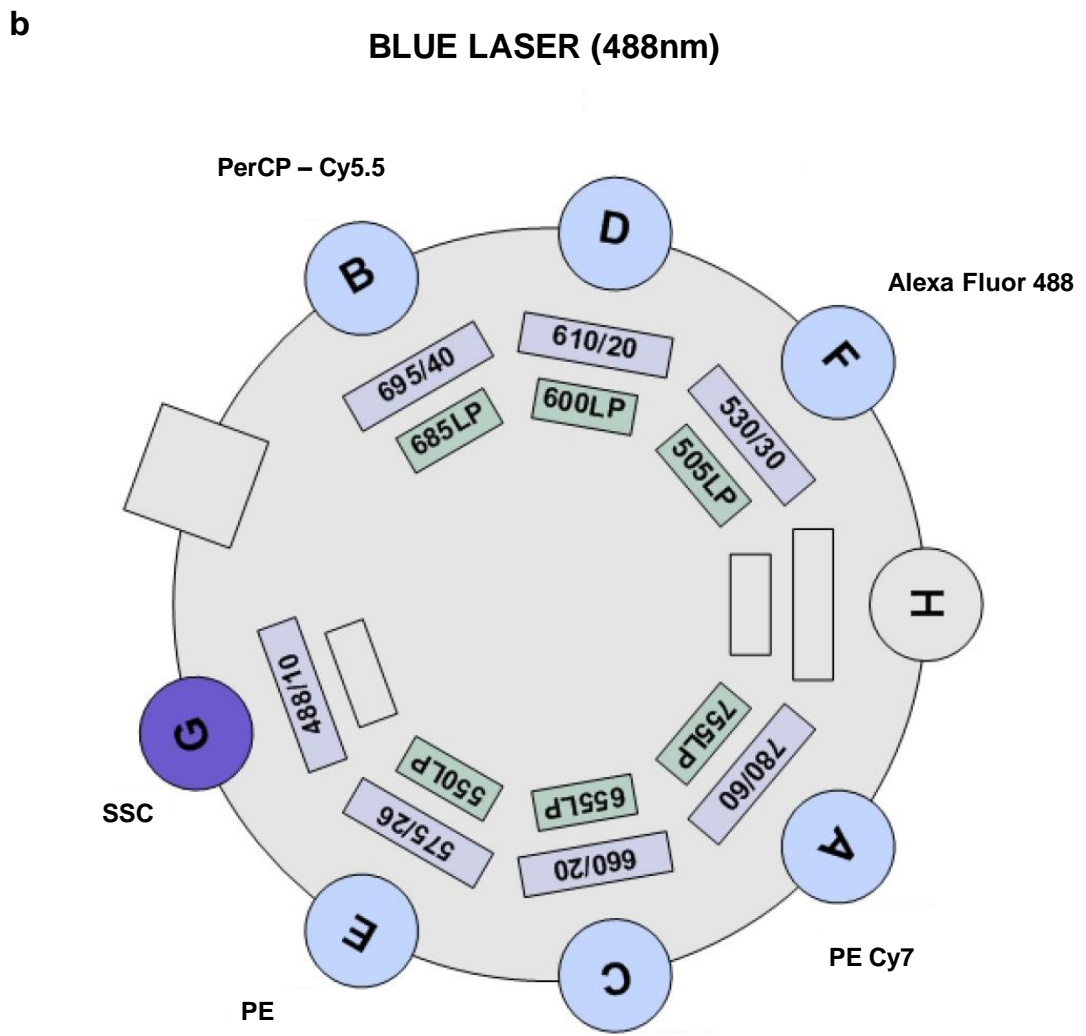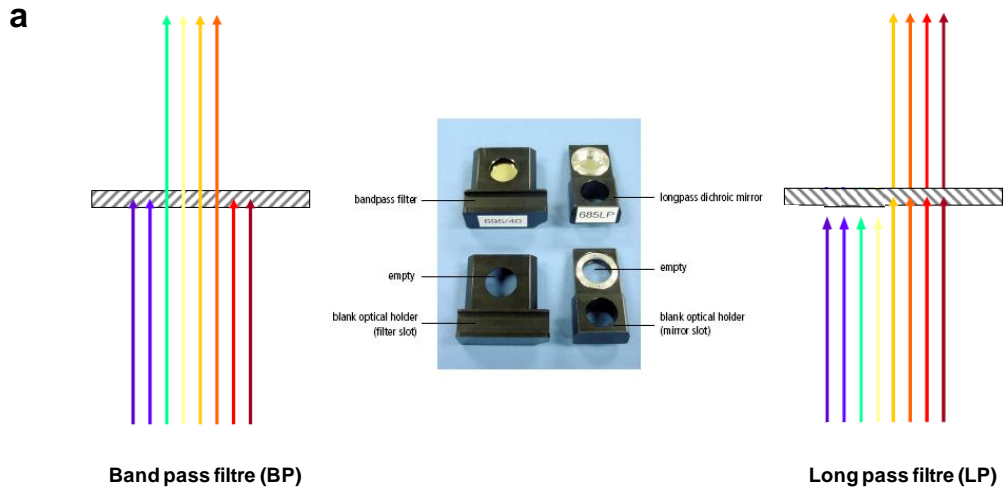
355 UV LASER (355nm)   RED LASER (633nm)

Alexa Fluor 647

DAPI
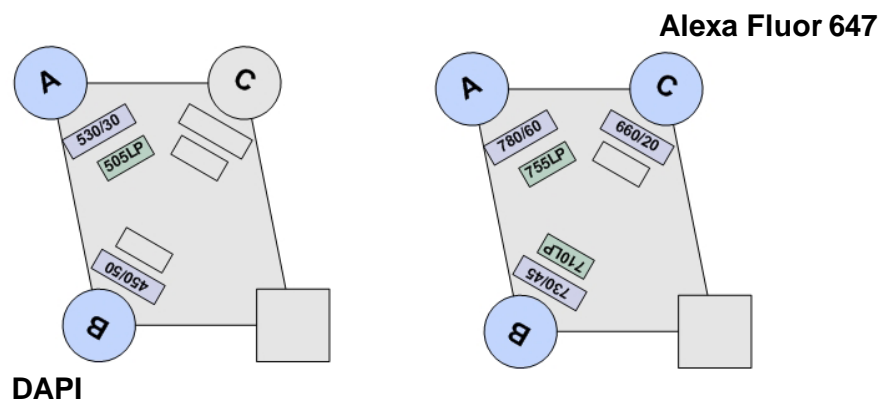
Figure 12 Configuration of BD LSR II flow cytometer

Optical filters attenuate light or help direct it to the appropriate detector. Dichroic filters transmit light of a specific wavelength while reflecting other wavelengths. Long pass filters transmit wavelengths that are longer than the specified value and band pass filters pass a narrow spectral band of light (a). Filters were configured in such a way as to minimise spectral overlap - BD LSR II cytometer octagon and trigon arrays use dichroic longpass mirrors on their inner rings (blue) and band pass filters on their outer rings (green); the arrangement for each laser used in this work is shown above (b).

Epitope	Fluorochrome	Host	Clone	Source
CD11b	PerCP Cy5.5	Rat	M1/70	eBioscience
Gr-1	AlexaFluor 488	Rat	RB6 8C5	eBioscience
CD11c	PE Cy7	Hamster	N418	eBioscience
F4/80	PE	Rat	CI: A3-1	Serotec
Ly6C	AlexaFluor 647	Rat	ER-MP20	Serotec

Table 3 Primary conjugated monoclonal anti-mouse antibodies used in flow cytometry of splenocyte, choroidal and retinal cell suspensions

Monoclonal antibodies directly-conjugated to fluorochromes were selected to minimise the risk of non-specific binding and to improve experimental efficiency. Cells suspensions were incubated with rat anti-mouse CD16/32 Fc block (2.4G2; BD Biosciences) prior to immunostaining to minimise non-specific binding of antibodies to innate immune cell Fc receptors.

b
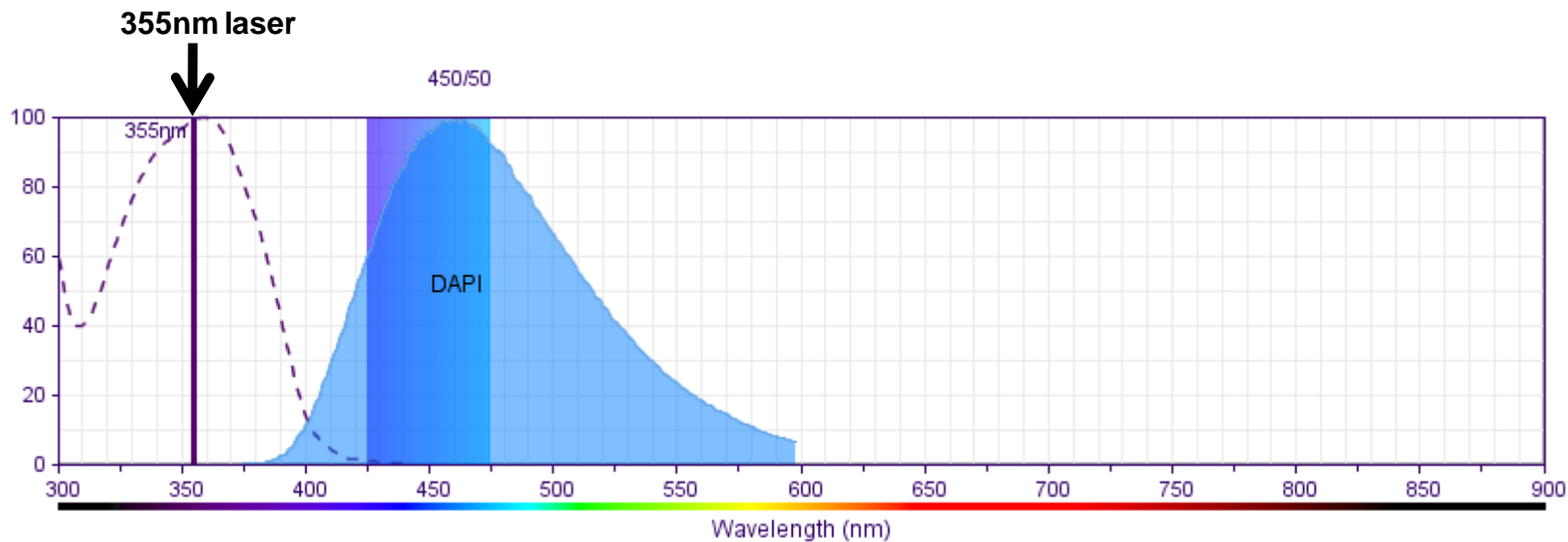
Fluorochrome	%	☑ Ex	☑ Em	☑ Filters	Alexa Flu...	PE	PerCP-C...	PE-Cy7	Alexa Flu...	DAPI
Alexa Fluor® 488 ▼	75	☑	☑	530/30 ▼ ☑	(48.6 %)	0.7 %	--	2.9 % *	--	25.5 %
PE ▼	62	☑	☑	575/26 ▼ ☑	20.2 %	(55.9 %)	--	20.8 % *	--	7.5 %
PerCP-Cy5.5 ▼	98	☑	☑	695/40 ▼ ☑	--	3.5 %	(68.1 %) *	2.3 % *	97.7 %	--
PE-Cy7 ▼	62	☑	☑	780/60 ▼ ☑	--	--	8.2 % *	(60.5 %) *	4.2 %	--
Alexa Fluor® 647 ▼	0	■	■	660/20 ▼ ☐	0.7 %	4.5 %	6.6 % *	2.1 % *	(38.3 %)	--
DAPI ▼	0	■	■	450/50 ▼ ☐	0.0 %	--	--	--	--	(44.7 %)

Figure 13 Filter performance estimates for selected fluorophores using the BD LSR II

Estimations of filter performance (filters configured as described in Figure 12). Charts show summated emission signals (normalised to the degree of excitation at the indicated laser line wavelength) that fall within a filter specification by wavelength. Estimated filter performances when using 355nm laser (a); 488nm laser (b) and 633nm laser (c) are shown. For any given filter/fluorophore combination the efficiency for the primary detector filter (shown with light gray background within parentheses) is displayed along with spillage into other detectors. The spill estimate is expressed as a percentage of that measured in the primary detector (varies with primary filter).Band pass filters are rendered as rectangles. (Estimates obtained using BD Fluorescence Spectrum Viewer - http://www.bdbiosciences.com/research/multicolor/spectrum_viewer/index.jsp)

2.6.3 Tissue sample preparation

Samples were kept on ice unless stated otherwise.

2.6.3.1 Retinal/RPE-choroidal tissue

Eyes were dissected microsurgically in 1ml ice-cold RPMI 1640 (Invitrogen) containing 5% FCS, 2.38g/L HEPES and 1.5g/L sodium hydrogen carbonate (Sigma). The lens was removed and discarded and the retina was removed by careful dissection including the ciliary marginal zone but not retinal pigment epithelium or choroid. Retina and RPE-choroid were then processed separately as follows. Tissue from each eye was diced into approximately 20 pieces with Westcott scissors, transferred to 14ml Falcon tubes (BD Falcon) in a total of 5mls of buffer and centrifuged for 5 mins at 1200RPM. Buffer was decanted and tissue re-suspended in 50µl pre-warmed buffer containing 0.5mg collagenase D (Roche, Lewes, UK) and 750 U/ml DNase I (Sigma) for 15 min at 37 °C. The treated tissue was homogenised and washed through a 70 µm filter (BD Biosciences) to obtain a single cell suspension. Suspensions were centrifuged at 1200RPM and re-suspended in 100µl of ice-cold buffer. Suspensions were incubated with 1µl rat anti-mouse CD1b/CD32 Fc block for 5 mins (BD Biosciences) prior to immunostaining.

2.6.3.2 Splenocytes

Spleen was dissected from surrounding connective tissue and homogenised and washed with ice-cold RPMI 1640 (Invitrogen) (containing 5% FCS, 2.38g/L HEPES and 1.5g/L sodium hydrogen carbonate) through a 70 µm filter (BD Biosciences) to obtain a single cell suspension. Suspensions were centrifuged at 1200RPM for 5 mins and re-suspended in 1 ml of red blood cell lysing buffer Hybri-Max (Sigma Aldrich) for 5mins. Buffer was then added up to 50mls and suspensions centrifuged at 1200RPM for 5 mins. Supernatant was decanted and cells re-suspended in 50mls of buffer prior to centrifuging for a further 5 mins at 1200RPM. Cells were re-suspended in 500µl buffer. 10µl of the cell suspension was mixed with an equal volume of trypan blue (Sigma Aldrich) and

cell counts performed using a haemocytometer (Marienfield, Germany) to obtain a suspension of approximately 1×10^6 cells/100µl. Suspensions were incubated with 1µl rat anti-mouse CD1b/CD32 Fc block for 5 mins (BD Biosciences) prior to immunostaining.

2.6.4 Flow cytometry

2.6.4.1 Compensations

Optimisation of fluorescence compensation settings for multicolour flow cytometric analysis was performed using anti-rat and anti-hamster Ig κ negative control particles set (BD^{TM} CompBeads; BD Biosciences) and further refined using splenocyte suspensions.

BD CompBeads were vortexed thoroughly before use and separate sample tubes labelled for each fluorochrome-conjugated mouse Ig, κ antibody. 100µl buffer, RPMI 1640 (Invitrogen) containing 5% FCS, 2.38g/L HEPES and 1.5g/L sodium hydrogen carbonate, was added to each tube and 1 drop (approximately 60µl) of the BD CompBead negative control and 1 drop of the CompBead anti-rat/hamster Ig, κ beads added to each tube. Tubes were vortexed and 1µl of the fluorochrome-conjugated antibody to be tested added to each (including one tube containing a mixture of all 5 antibodies). Samples were incubated for 60mins at room temperature and protected from direct light. Following incubation, 2mls of buffer were added to each tube and samples centrifuged at 1200RPM for 5 mins. Supernatant was discarded and each pellet resuspended in 0.5ml of buffer before vortexing. BD LSR II photomultiplier tube voltage settings were adjusted using BD CompBeads Negative Control and samples run through the BD LSR II flow cytometer at 200-300 events per second. Gating was performed on singlet bead populations based on FSC (forward-light scatter) and SSC (sidelight scatter) characteristics and median fluorescence intensities adjusted as appropriate to achieve suitable compensations.

Compensations were then optimised using splenocyte suspensions. Briefly, tubes for unstained cells and single-colour controls together with one mixture of all 5 antibodies were prepared as for beads (except antibody was added to a volume of 100µl cell suspension and samples were kept on ice). Samples were made up to 5mls with buffer after incubation for 60mins and centrifuged at 1200RPM for 5mins before repeating. Cells were resuspended in 300µl buffer and run at a 'Hi' flow rate through the BD LSR II flow cytometer. Compensations values were then determined (*Figure 23*).

2.6.4.2 Data acquisition and gating

Multiparameter flow cytometry was carried out following Fc block and staining with the panel of fluorochrome-conjugated monoclonal antibodies as described above. Cell suspensions were incubated with fluorochrome-conjugated mAbs against cell surface markers (1µl antibody per 100µl of suspension) for 60 minutes whilst avoiding direct light exposure. Cells were washed twice in RPMI 1640 (containing 5% FCS, 2.38g/L HEPES and 1.5g/L sodium hydrogen carbonate) and resuspended in 300µl of buffer in Falcon FACS tubes (BD Biosciences). 10 µl DAPI was added to each cell suspension and samples analysed using the BD LSR II flow cytometer at a 'Hi' flow rate. Dead cells were excluded from the analysis by gating on the DAPI⁻ cells. As a guide for applying gates to key innate immune cell populations, fluorescence-minus-one controls were performed on samples of the relevant tissues – that is, cell samples were incubated with all but one of each fluorochrome-conjugated antibody (*Figure 15* and *Figure 26*). All flow cytometric analyses were performed using FlowJo software (Tree Star). Flow-cytometrical classification of immune cells was done in accordance with established criteria[73, 95, 164].

2.7 Histological methods

2.7.1 Cryo-sectioning

Animals were sacrificed by exposure to carbon dioxide and perfused by cardiac intraventricular puncture with ice-cold PFA 4%. Eyes and spleens were then removed and immersed in ice-cold PFA 4% for 1 hour before being embedded

in Optimal Cutting Temperature compound (OCT; RA Lamb, East Sussex, UK). Embedded tissue was frozen in isopentane which had been pre-cooled in liquid nitrogen and stored at -20°C. Sagittal sections were cut at a thickness of 18µm onto poly-lysine coated slides using a a Bright cryostat and then stored at -20°C.

2.7.2 Immunohistology

2.7.2.1 Immunostaining for mouse F4/80

Sections were air dried for at least 1 hour before rehydration of the sections with PBS. For mouse F4/80 antigen immunohistochemistry, components of a catalysed signal amplification kit (CSA kit; K1500; Dako Ltd., UK) were used. Reagents were as supplied by Dako Ltd. unless specified otherwise. Sections were blocked with avidin blocking solution for 10 minutes followed by biotin block for 10 minutes before being washed in PBS-T (2 x 5 mins). Sections were then exposed to protein block for 10 minutes. Protein block was tapped off the slide and primary antibody (rat anti-mouse F4/80:Biotin; clone CI:A3-1; Serotec, UK) added at a dilution of 1/500 in antibody diluent and incubated at room temperature for 1 hour. Directly conjugated antibody against Ly6C (1/50; rat anti-mouse Ly6C AlexaFluor 647; clone ER-MP20; eBioscience, UK) or Gr-1 (1/50; rat anti-mouse Gr-1 AlexaFluor 488; clone RB6 8C5; eBiosciences, UK) was included at this stage where staining for multiple antigens was undertaken. Samples were washed in PBS-T (2 x 10 mins) and streptavidin-biotin complex applied for 5 mins (prepared 15 minutes prior to use by adding 1 drop of reagent A and 1 drop of reagent B to streptavidin buffer). Slides were then washed in PBS-T (4 x 10 mins) and amplification reagent added to sections for 5 mins before washing again in PBS-T (4 x 10 mins). Slides were incubated with streptavidin-AlexaFluor 546 (1:250, S11225; Invitrogen-Molecular) before washing in PBS-T (4 x 10mins) and mounting in and mounted with fluorescence mounting medium containing Hoechst 33342 (Dako, Cambridgeshire, UK). Images were obtained with a laser scanning microscope (LSM 510; Carl Zeiss Microimaging, Jena, Germany).

2.7.2.2 Immunostaining for mouse Gr-1 and Ly6C

Sections were air dried for at least 1 hour before rehydration of the sections with PBS-T. Non-specific binding sites on the sections were blocked for 1 hour with PBS/1%BSA (Sigma Aldrich, Steinheim, Germany)/5% non-specific goat serum (AbD Serotec, Kidlington, UK). Directly conjugated antibodies against Ly6C (1/50; rat anti-mouse Ly6C AlexaFluor 647; clone ER-MP20; eBioscience, UK) and Gr-1 (1/50; rat anti-mouse Gr-1 AlexaFluor 488; clone RB6 8C5; eBiosciences, UK) were diluted in blocking solution and added to sections for 1 hour at room temperature before washing in PBS-T (4 x 10 mins). Slides were mounted in fluorescence mounting medium containing Hoechst 33342 (Dako, Cambridgeshire, UK). Images were obtained with a laser scanning microscope (LSM 510; Carl Zeiss Microimaging, Jena, Germany).

2.7.2.3 Immunostaining for collagen IV

Sections were air dried for at least 1 hour before rehydration of the sections with PBS-T. Non-specific binding sites on the sections were blocked for 1 hour with PBS/1%BSA (Sigma Aldrich, Steinheim, Germany)/5% non-specific goat serum (AbD Serotec, Kidlington, UK). Slides were incubated with rabbit anti-mouse collagen type IV antibody (1/300 in block; AbD Serotec; 2159-1470) for 1 hour at room temperature before washing in PBS-T (4 x 10mins). Slides were then incubated with goat anti-rabbit AlexaFluor 488-conjugated antibody (1/500 in block; AbD Serotec) for 4 hours at room temperature before washing in PBS-T (4 x 5 mins). Slides were mounted in fluorescence mounting medium containing Hoechst 33342 (Dako, Cambridgeshire, UK). Images were obtained with a laser scanning microscope (LSM 510; Carl Zeiss Microimaging, Jena, Germany).

2.8 Buffers and solutions

Distilled water (dH$_2$O) was used to prepare all solutions.

Phosphate Buffered Saline (PBS 1x) was prepared using tablets from Oxoid Ltd. (10 tablets per litre of dH$_2$O)

2.9 Statistical analysis

Power calculations for experiments conducted with the aim of determining CNV lesion size between genotypes/age-groups, were based on published data (approximately 12 animals per study group)[148]. N numbers were sometimes limited by the availability of mice for study (for aged study groups for example). For experiments designed to test the effects of pharmaceutical agents on lesion size, smaller N numbers were considered acceptable given that multiple dosages were often tested.

The identification of populations derived from the retina and RPE-choroid is limited by the relatively small numbers of cells present in the eye[87, 138, 165, 166]. This has implications for interpreting flow cytometry data. The protocols and presentation of data in this thesis adhered, as far as possible, to the available guidelines[167]. Where a target population constitutes less than 5% of total events, as is the case with many innate immune cell subpopulations in the eye, these are referred to in the guidelines as 'rare' events. The analysis of rare events therefore required particular attention to the reliability and precision of data acquired from each sample. Use of the 'coefficient of variance' (CV) gives some indication of the total number of cells required for reliable identification of a change in a target population (CV = $100/\sqrt{r}$; where r = the number of positive events). For a CV of 5%, 400 positive events need to be acquired. Where a rare subset is present at a value of 5% of total events, a total of 8000 events should be collected for a CV of 5%; if present at 0.5% of total events then 80 000 cells should be collected to achieve an equivalent CV. The smallest population examined as part of this work was the Gr-1$^+$ macrophage population in young wild-type retinae – this constituted 0.01% of total live cells and consequently to achieve a CV of 5% it would be necessary to collect a total of 400 positive cells ultimately derived from a total of 4 million live cells (depending on how the live cell subset is gated). The live cell yield from two pooled retinae using the published protocol employed in this study is generally no more than 2 million - this exposes the limitations of working with tissue where the viable cell yield is so small[168]. Establishing the viable cell population is essential since dead cells can bind or take up antibodies and fluorescent dyes non-specifically.

Consequently, it was necessary to accept a CV of 10% and increase n numbers to 10 or more to achieve significance in certain experiments. Analysis of continuous, non-parametric data between two groups was undertaken using a Student t-test.

Chapter 3: The effects of ageing on innate immune cell populations in mouse retina and choroid

3.1 Introduction

This chapter describes the changes in innate immune cell populations that occur with age in the retina, the RPE-choroid and systemically in both wild-type and $CCL2^{-/-}$ animals. Identification of the innate cell populations and pathways involved in normal and abnormal ageing in the eye is important because their manipulation may prove essential in furthering understanding of the pathology of AMD and aid in the development of better treatments for the disease.

Ageing results in the accumulation of subretinal microglia in the retina and leukocytes in the choroid. The exact nature of these cells is unknown though evidence suggests that they originate from parenchymal microglia in the retina. Similarly, how these cells interact with the complement system to maintain homeostasis or drive pathology in the eye is also unknown. Ageing in the retina and RPE-choroid is associated with the upregulation of a number of cytokine and chemokine pathways yet, somewhat paradoxically, subretinal microglia have been demonstrated to accumulate more rapidly in mice deficient in both chemokines and their receptors (examples of these include $CCL2^{-/-}$, $CX3CR1^{-/-}$ and $CCL2^{-/-}$ $CX3CR1^{-/-}$ double-knockout mice)[120, 169]. This suggests that the recruitment or trafficking of particular innate immune cell populations is important for the maintenance of retinal and RPE-choroidal homeostasis with ageing. The effect of chemokine deficiency on these populations in the context of ageing was examined using a $CCL2^{-/-}$ mouse model and compared with wild-type animals. CCL2 is upregulated in the aged wild-type mouse RPE-choroid and it was hypothesised that a failure to recruit certain innate immune cell populations might underlie the accumulation of subretinal microglia in $CCL2^{-/-}$ mice[124].

Multicolour flow cytometry was used to characterise cell populations in the retina and RPE-choroid. Cell numbers are relatively low in these tissues compared to brain or spleen and the inherent variability of immunohistochemical staining combined with high levels of autofluorescence would have necessitated the sacrifice of many more animals to achieve equivalent results. Multicolour flow cytometry has previously been employed to determine innate immune cell responses, particularly those involving monocyte subsets, in models of myocardial infarction and atherosclerosis (*Table 4*)[95, 170]. Patterns of surface marker expression were used to define key innate immune cell populations. Analyses were performed on live cells so that autofluorescent dead cells might be excluded.

Two colour flow cytometry has previously been used in ophthalmic research to establish that infiltrating macrophages are critical for the development of laser-induced choroidal neovascularisation in mice (macrophages being defined as CD45$^+$ F4/80$^+$ cells in this instance) [156]. Using three colour flow cytometry it has been suggested that retinal microglia are CD45^{Low} CD11b/c$^+$ CD4^{Low} and largely MHC class II$^-$ (except for a small ED2$^+$ population) in rats[171]. More recently a five colour approach was used to confirm that *CX4CR1$^{GFP/+}$* retinal microglia are CD45$^+$ CD11b$^+$ F4/80$^+$ CD11c$^-$ MHC class II$^-$[103] and other work has employed the technique to define the retinal cellular infiltrate in experimental autoimmune uveitis using markers including Gr-1 and Ly6C[168].

It was hypothesised that ageing and CCL2 deficiency would primarily result in altered numbers of specific innate immune cell populations either locally or in the periphery. The proportions of innate immune cells in the relevant tissues using specific cell surface markers was established using gating strategies successfully employed in the identification of monocytic populations in models of other diseases where macrophage accumulation and chronic inflammation is a feature[95].

Innate immune cell population	Markers expressed	Comments/Reference
Granulocytes	CD11b$^+$ Gr-1^{Hi} SCC^{Hi}	[172]
	CD11b$^+$ Gr-1$^+$ F4/80^{VAR}	In a mouse model of intraperitoneal foreign body inflammation[173]
	CD11b$^+$ Ly6C$^+$ F4/80$^-$	[173]
Macrophages	CD11b$^+$ F4/80$^+$ Ly6C$^-$	[173]
	CD11b^{Hi} F4/80^{Hi} CD11c^{Lo} SCC^{Med}	[172]
	CD11c$^+$ F4/80$^+$	[174]
	CD11c^{Hi} F4/80^{Hi} I-Ab^{Hi}	[175]
Conventional DCs	CD11c$^+$ MHCII$^+$	[160]
	CD11c^{Hi} F4/80^{Hi} I-Ab^{Hi}	[175]
Plasmacytoid DCs	CD11c$^+$ MHCII$^+$ Ly6C$^+$	[164]
Myeloid-derived suppressor cells	CD11b$^+$ Gr-1$^+$ (F4/80^{VAR} Ly6C^{VAR})	Mixture of immature monocytes and granulocytes but also including mature neutrophils and inflammatory monocytes)[173, 176, 177]
Monocytes	CD11b$^+$ F4/80^{INT}	[178]
	CD11b^{Hi} SCC^{Lo} Gr-1$^-$	[172]
Monocytes CCR2$^+$; classical 'inflammatory'	CD11b$^+$ F4/80^{INT} CD11c$^-$ Ly6C$^+$	[178]
	CD11b$^+$ F4/80$^+$ Gr-1$^+$ Ly6C$^+$	[90]
	CD11b^{Hi} Gr-1^{Lo} Ly6C^{Hi}	[175]
	CD11b$^+$ Gr-1$^-$ Ly6C^{Hi}	[179]

Monocytes CCR2^{-}; non-classical 'resident'	CD11b^{+} F4/80[INT] CD11c[INT/+] Ly6C[Lo]	178
	CD11b^{+} F4/80^{+} Gr-1^{-} Ly6C^{-}	90
	CD11b[Hi] Gr-1[Lo] Ly6C[Lo]	Equivalent subset in tumour models is Tie-2 expressing monocytes (TEMs)[175, 180]
	CD11b^{+} Gr-1^{-} Ly6C[Lo]	179
Microglia	CD11c^{+} CD45[Lo] F4/80[Lo]	181

Table 4 The key innate immune cell subsets and various definitions for them based on surface marker expression in mice

Table summarising the key myeloid cell populations as defined by mainly using the cell surface markers CD11b, F4/80, Gr-1 and Ly6C (VAR=variable; INT=intermediate; MED=medium; Hi=high; Lo=Low; SCC=side scatter). Additional markers described in the publications referred to may have been omitted for clarity. Overlap of marker expression between different populations reflects the high levels of heterogeneity and plasticity in innate immune cell populations – this is at least partly dependent on a variation in activation states that is dependent on the local inflammatory environment and the tissue being analysed. Variations in marker expression within the same population may reflect differences between experimental models, protocols and gate definitions, and occasionally differences of opinion on the exact nature of a cell population (dendritic cells for example).

3.2 Establishing the phenotype of innate immune cell populations in young wild-type retina and choroid

3.2.1 Innate immune cell populations in young wild-type retina

Using directly conjugated antibodies for CD11b, F4/80, Gr-1, Ly6C and CD11c, compensations for flow cytometry were set using single-stained splenocyte suspensions and gates set using fluorescence-minus-one controls for each tissue as a guide (*Figure 23 and Figure 15*).

Despite use of the brightest fluorochrome, the signal from F4/80$^+$ cells was relatively low indicating that F4/80 is expressed at low levels in microglia - a finding confirmed on immunohistochemistry of *CCL2$^{-/-}$* mouse eye sections where signal amplification was necessary to enable visual detection (*Figure 16*). Retinal microglia were identified as being largely CD11b$^+$ F4/80$^+$ Gr-1$^-$ in young (<4m) wild-types. An example of the gating strategy employed in the identification of the CD11b$^+$ F4/80$^+$ Gr-1$^-$ population is shown (*Figure 17*). Microglia constituted approximately 0.07% (mean; n=9) of live cells in a retinal suspension and are henceforth referred to as Gr-1$^-$ macrophages. CD11b$^+$ F4/80$^+$ Gr-1$^+$ cells (henceforth referred to as Gr-1$^+$ macrophages) were by comparison very few in number in uninflamed tissue and staining may represent non-specific antibody binding (*Figure 18*).

The granulocyte population in the retina was identified as CD11b$^+$ Gr-1$^+$ F4/80$^-$ (*Figure 18*, main plot ungated cells). Previous studies[153] have identified neutrophils (which constitute the majority of granulocytes) as CD45$^+$ Gr-1$^+$ or CD11b$^+$ Gr-1$^+$. Given that Gr-1 is expressed on a number of other myeloid cell types (including F4/80$^+$ monocyte/macrophage subsets and NK cells) granulocytes were further distinguished as being F4/80$^-$. It was not possible to separate eosinophils and basophils from the neutrophil population using the panel of markers available so the population was collectively referred to as the granulocyte population. As a general rule the levels of expression of Gr-1 in this population mirrored those of Ly6C. Gating for double-positive or negative

populations for these markers was performed but more consistent results were obtained if either Gr-1 or Ly6C was used (probably because a further reduction in numbers in the final gate was avoided). Granulocytes constituted 0.13% of live cells in the retina (mean; n=9).

Dendritic cells were defined as CD11b$^+$ CD11c$^+$ Gr-1$^-$ (*Figure 19*). It was noted that whilst most CD11b$^+$ CD11c$^+$ cells were Gr-1$^-$ a small number were Gr-1$^+$ (most likely plasmacytoid DCs). CD11b$^+$ CD11c$^+$ Gr-1$^-$ cells were largely negative for F4/80. DCs exhibited the most consistent changes in response to ageing or laser-induction of CNV and constituted 0.05% of live cells (mean; n=9).

A total of 42 permutations of marker expression on CD11b$^+$ cells were analysed across experiments with the aim of identifying any small but significant shifts in sub-populations. CD11b$^+$ cells constituted 1.2% of live cells in the retina (mean; n=9), in keeping with the findings of other groups[168], interestingly however most retinal CD11b$^+$ cells were completely negative for all other markers in the panel (*Figure 20*), that is they were CD11b$^+$ F4/80$^-$ Gr-1$^-$ Ly6C$^-$ CD11c$^-$. The reasons for this are unclear since this was not found in choroidal tissue or spleen and cannot be explained by the inadvertent inclusion of CD11b$^-$ cells in a CD11b$^+$ gate alone. It is possible that F4/80 is expressed at such low levels in retina that a significant number of microglia are excluded when gating for F4/80$^+$ cells, alternatively other populations such as NK cells and pericytes may be CD11b$^+$ yet negative for the other markers.

Of the four principle populations identified, granulocytes formed the largest group followed by roughly equal proportions of Gr-1$^-$ macrophages and DCs, Gr-1$^+$ macrophages formed the smallest subset.
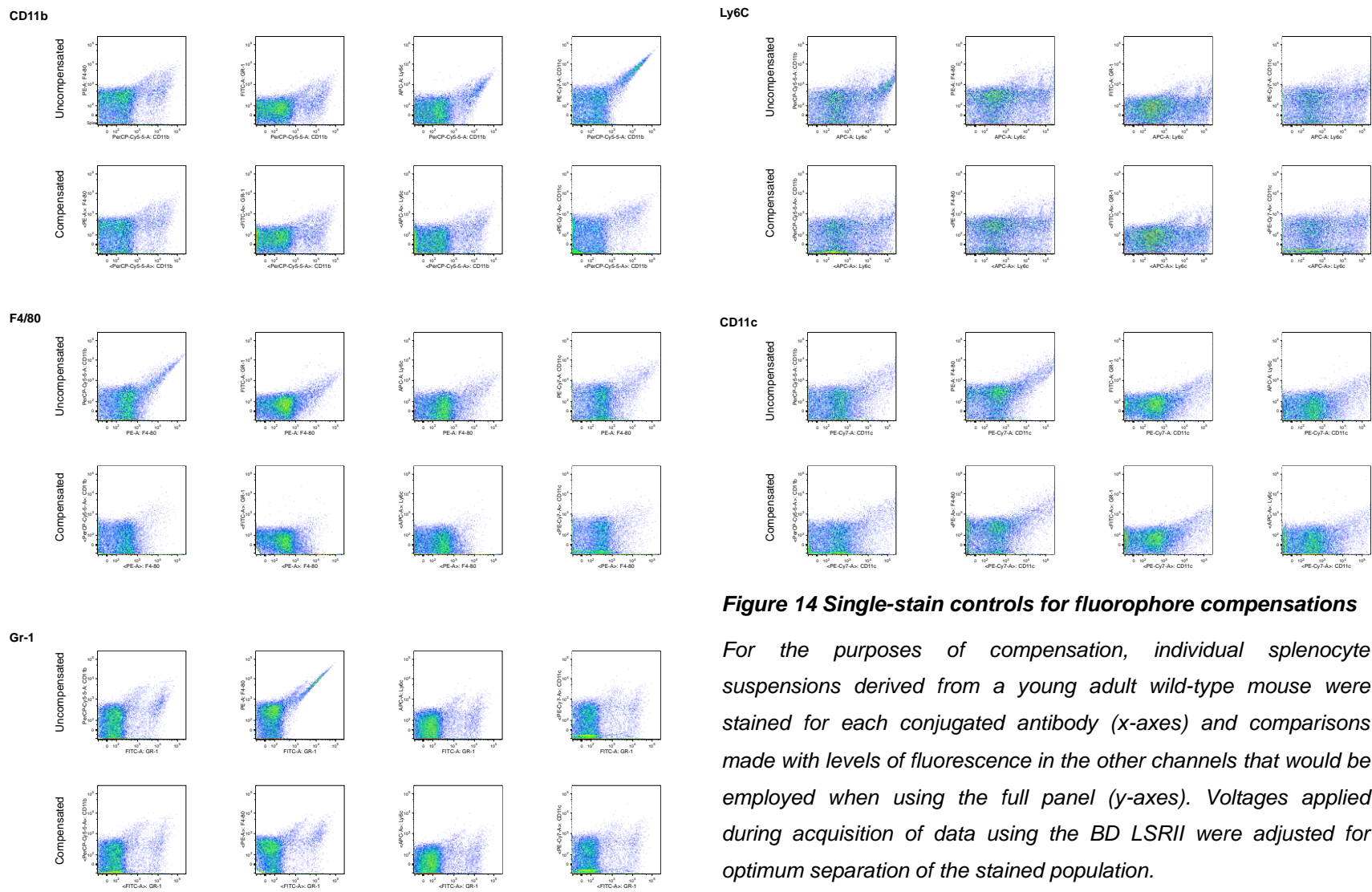
Figure 14 Single-stain controls for fluorophore compensations

For the purposes of compensation, individual splenocyte suspensions derived from a young adult wild-type mouse were stained for each conjugated antibody (x-axes) and comparisons made with levels of fluorescence in the other channels that would be employed when using the full panel (y-axes). Voltages applied during acquisition of data using the BD LSRII were adjusted for optimum separation of the stained population.

114
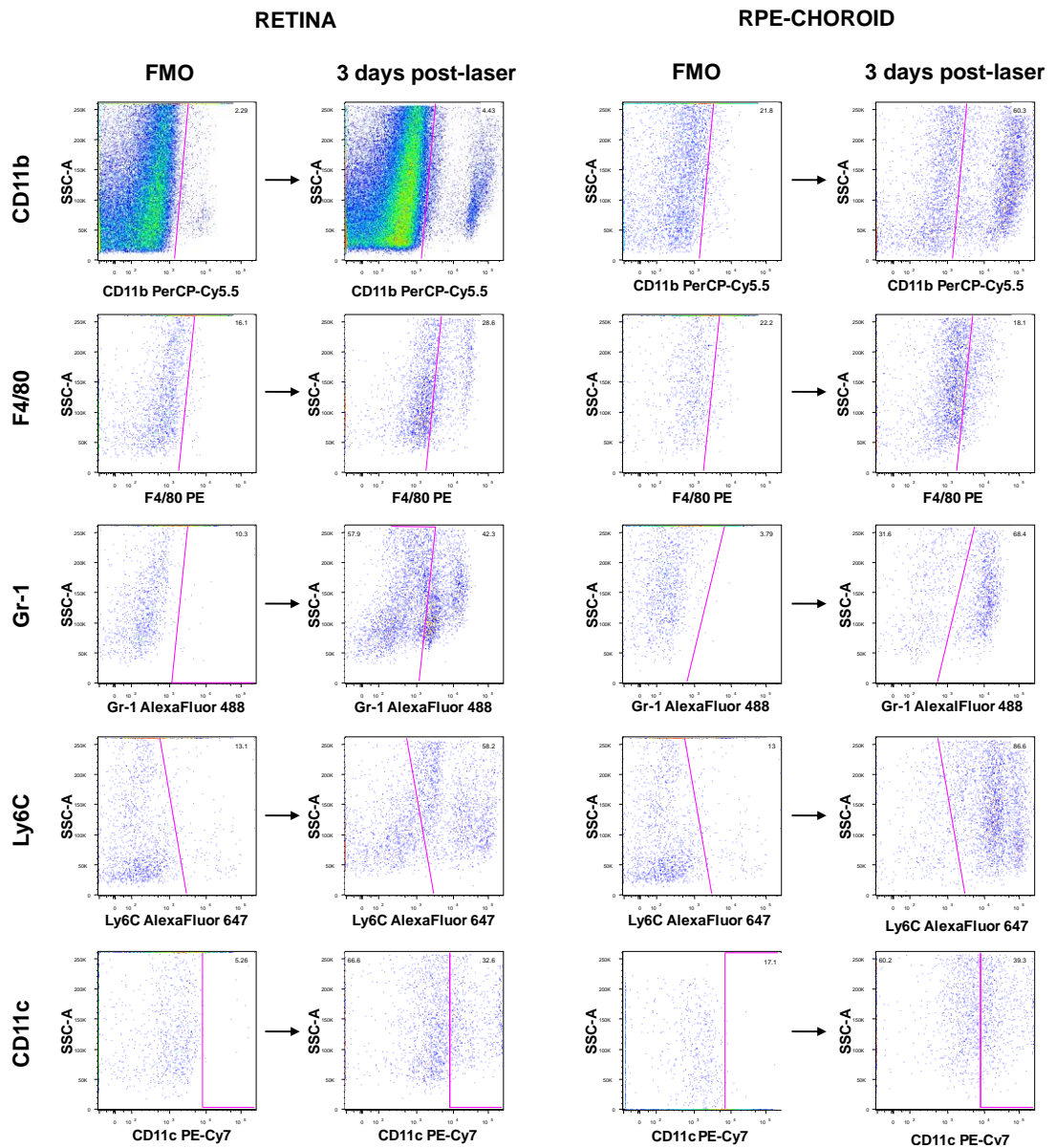
Figure 15 Fluorescence-minus-one controls for retinal and RPE-choroidal cell suspensions

Fluorescence minus one controls for retinal (first column) and RPE-choroidal (third column from the left) cell suspensions. Representative plots obtained by staining for all markers in tissue 3 days post-induction of CNV by diode laser are shown in adjacent columns for comparison. DAPI was used to stain for and exclude dead cells from the analyses and data is fully compensated. Plots show gating for the marker excluded from panel as part of FMO (x-axis) against side-scatter area (y-axis) for clarity – other gating strategies (see following Figures for examples) based on FMO controls were employed to identify specific cell populations.
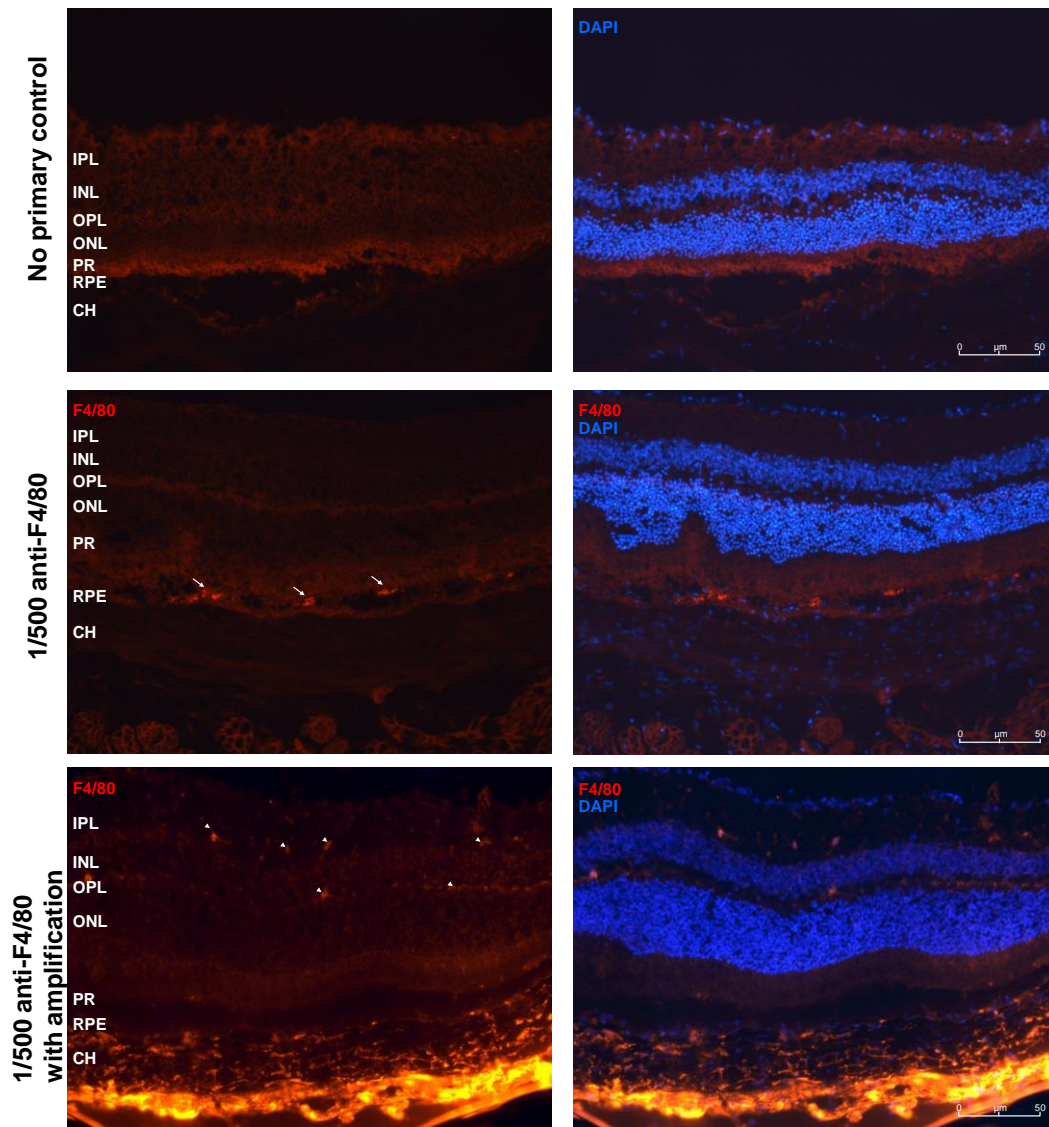
Figure 16 The macrophage-specific marker F4/80 is expressed at low levels in the retina and choroid of CCL2$^{-/-}$ mice

Immunohistochemistry staining for the microglia/macrophage marker F4/80 in sections taken from >18m CCL2$^{-/-}$ mouse eyes (40x magnification using fluorescent microscopy). A protocol involving signal amplification was required to demonstrate F4/80$^+$ cells in mouse retina and RPE-choroid (wild-type and CCL2$^{-/-}$ mice). No primary control - 1/250 streptavidin-Alexa546 conjugated secondary following signal amplification (top panels); 1/500 anti-F4/80 with no signal amplification (middle panels), arrows indicate location of autofluorescent material in the subretinal space; 1/500 anti-F4/80 staining with signal amplification (bottom panels), arrowheads indicate position of F4/80$^+$ ramified microglia in the inner and outer plexiform layers of the retina, F4/80$^+$ cells were also seen throughout the choroid where levels of expression were considerably higher. IPL=inner plexiform layer; INL=inner nuclear layer; OPL=outer plexiform layer; ONL=outer nuclear layer; PR=photoreceptor layer; RPE=retinal pigment epithelium;CH=choroid.

116
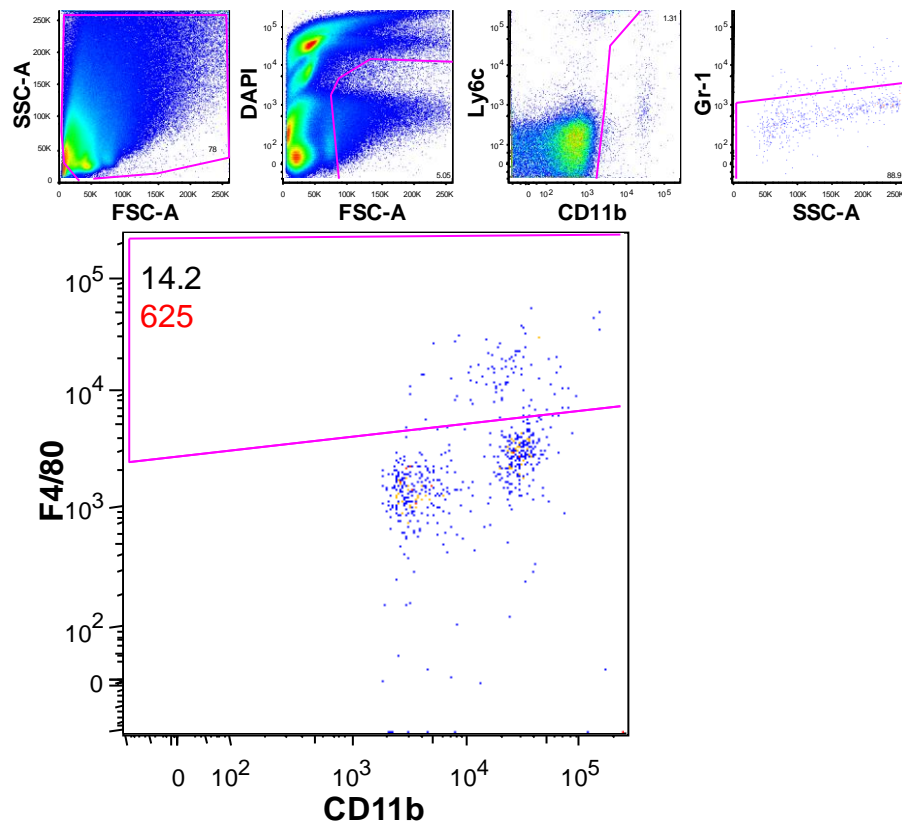
Figure 17. Representative flow cytometry scatter plot of a _Gr-1_ F4/80⁺ macrophage population derived from the pooled retinae of a young (<4m) wild-type mouse

Smaller plots illustrate the ancestry of the F4/80⁺ population. Gates (from left to right) show: all events; live cells (dead cells DAPI positive); CD11b⁺ cells; CD11b⁺ Gr-1⁻ cells; with main plot demonstrating the final live CD11b⁺ Gr-1⁻ F4/80⁺ population. F4/80 was expressed at low levels in the retina (confirmed by immunohistochemistry analysis, fluorescence minus one controls and analysis of splenocyte suspensions). The number of cells in each gate expressed as a percentage of all events on the plot is shown in black with the total number of events plotted shown in red. Fluorophores conjugated to antibodies against the respective markers are listed in the Methods section. Gates were set according to fluorescence-minus-one controls performed on retinal cell suspensions. Side scatter area (SSC-A); forward scatter area (FSC-A); numbers in gates indicate gated cells as a percentage of all events on plot.
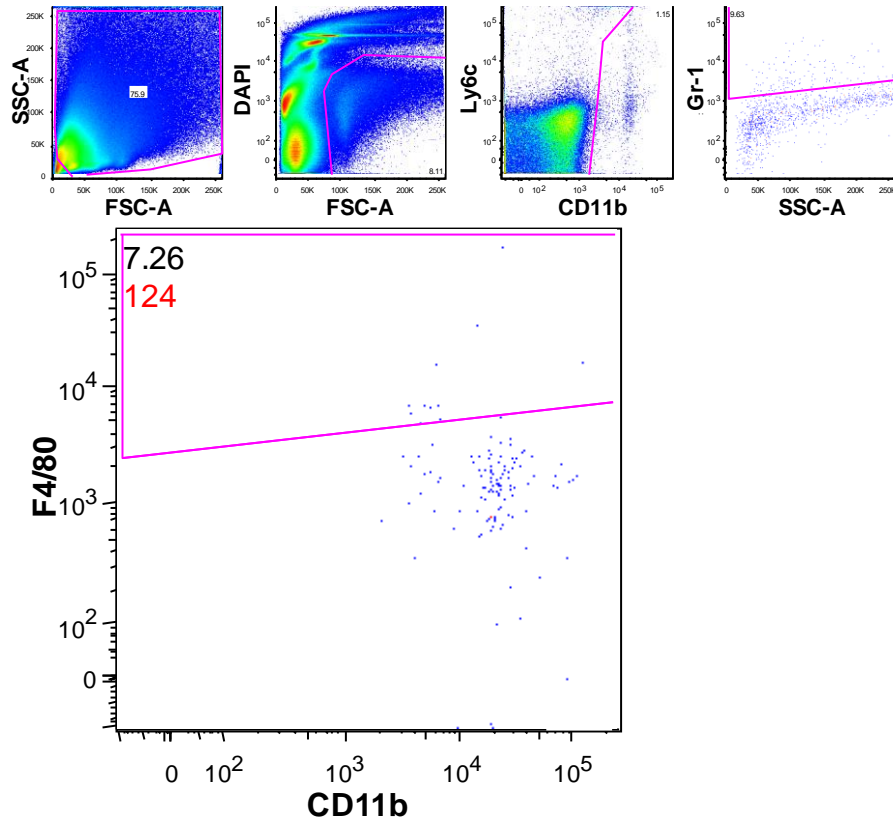
Figure 18. Representative flow cytometry scatter plot of a <u>Gr-1⁺</u> F4/80⁺ macrophage population derived from the pooled retinae of a young (<4m) wild-type mouse

Smaller plots illustrate the ancestry of the F4/80⁺ population. Gates (from left to right) show: all events; live cells (dead cells DAPI positive); CD11b⁺ cells; CD11b⁺ Gr-1⁺ cells; with main plot demonstrating the final live CD11b⁺ Gr-1⁺ F4/80⁺ population. Numbers of Gr-1⁺ macrophages in retina from unprocedured eyes were extremely low and most likely the result of non-specific staining or gated granulocytes. F4/80⁻ population in the main plot constitutes a Gr-1⁺ subset of high scatter these were considered to be granulocytes (predominantly neutrophils). The number of cells in each gate expressed as a percentage of all events on the plot is shown in black with the total number of events plotted shown in red. Fluorophores conjugated to antibodies against the respective markers are listed in the Methods section. Gates were set according to fluorescence-minus-one controls performed on retinal cell suspensions. Side scatter area (SSC-A); forward scatter area (FSC-A).
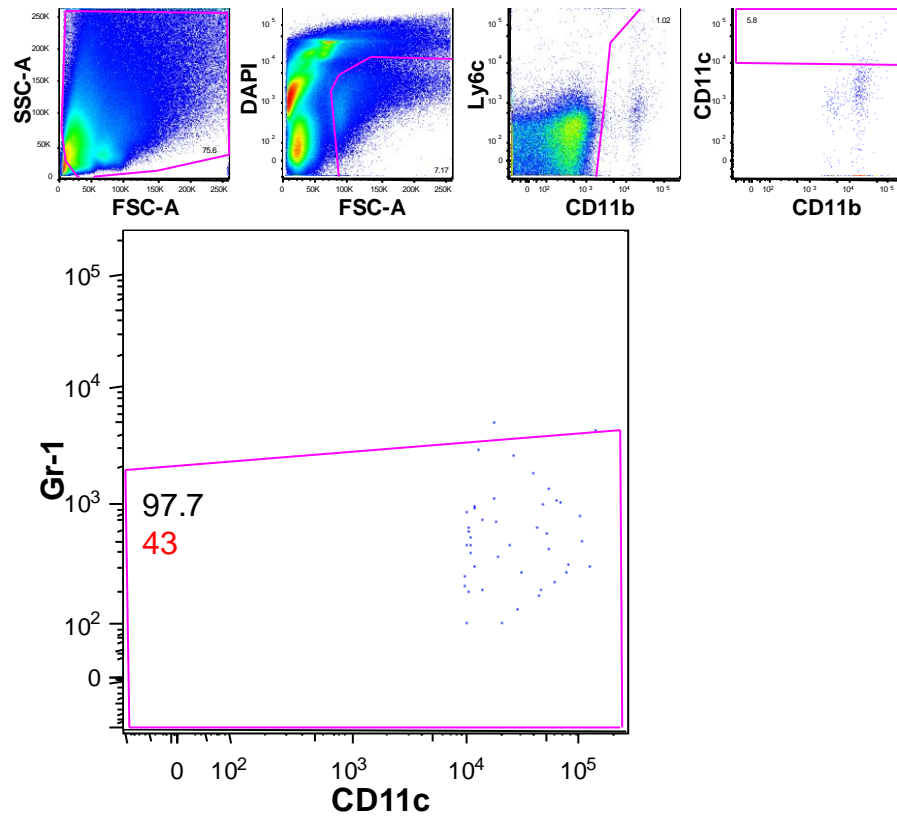
Figure 19 Representative flow cytometry scatter plot of a CD11c$^+$ innate immune cell population (DCs) derived from the pooled retinae of a young (<4m) wild-type mouse

Smaller plots illustrate the ancestry of the CD11c$^+$ population. Gates (from left to right) show: all events; live cells (dead cells DAPI positive); CD11b$^+$ cells; CD11b$^+$ CD11c$^+$ cells; with main plot demonstrating the final live CD11b$^+$ Gr-1$^-$ CD11c$^+$ population. CD11c$^+$ cells were consistently Gr-1$^-$ but expressed varying levels of F4/80 (data not shown). The number of cells in each gate expressed as a percentage of all events on the plot is shown in black with the total number of events plotted shown in red. Fluorophores conjugated to antibodies against the respective markers are listed in the Methods section. Gates were set according to fluorescence-minus-one controls performed on retinal cell suspensions. Side scatter area (SSC-A); forward scatter area (FSC-A).
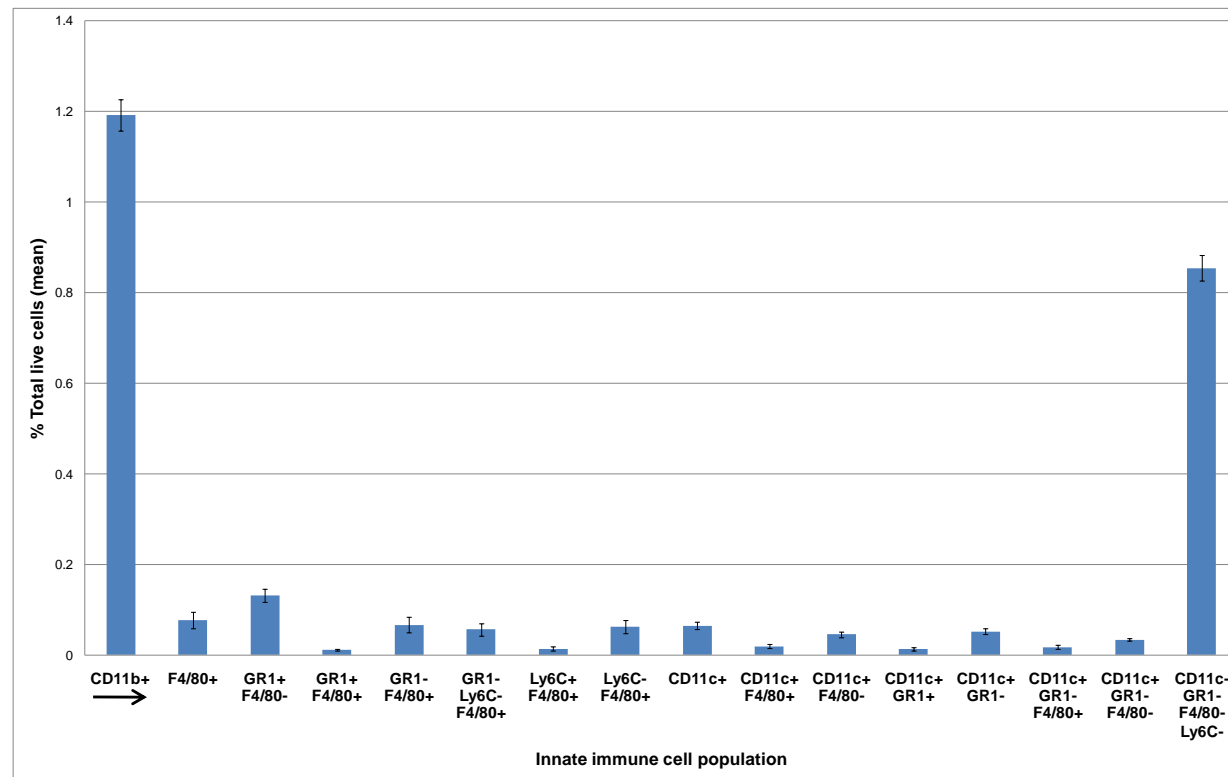
Figure 20. Permutations of marker expression on retinal cells from young (<4 month old) wild-type mice.

A total of 42 permutations of marker expression on CD11b^{+} cells were analysed in order to establish populations of interest. Some of these permutations are shown above. Four permutations were useful in identifying distinct CD11b^{+} populations that might change with age or in pathological neovascularisation (n=9; mean number of live cells=73996; error bars=SEM; all populations are CD11b^{+}). Gating strategies for these key subsets are shown in Figure 17,Figure 18 and Figure 19. Most cells gated for CD11b were negative for CD11c, Gr-1, Ly6C and F4/80 (see final column) and may include pericytes, natural killer cells and a number of CD11b^{-} cells.

3.2.2 Innate immune cell populations in young wild-type choroid

Using fluorescence-minus-one controls as a guide it was possible to establish that gates drawn for retinal cell suspensions could also be used for RPE-choroid - thereby allowing direct comparison of the two tissues.

CD11b$^+$ cells constituted 16.6% of live cells in young (<4m) wild-type RPE-choroid (mean; n=6), a finding that gives some indication as to the highly immunologically active nature of this tissue. The gating strategies employed were as for retinal cell suspensions (*Figure 21*, *Figure 22* and *Figure 23*), as were the permutations of marker expression examined (*Figure 24*). Key populations were as defined for retina, with Gr-1$^-$ macrophages consitituting 1.4% of live cells; Gr-1$^+$ macrophages 0.29%; granulocytes 5.4% and DCs 3.5% of live cells (mean; n=6).

Of the 4 principle populations identified, relative proportions were as in young wild-type retina except for DCs which constituted a larger population than Gr-1$^-$ macrophages (*Figure 25*).
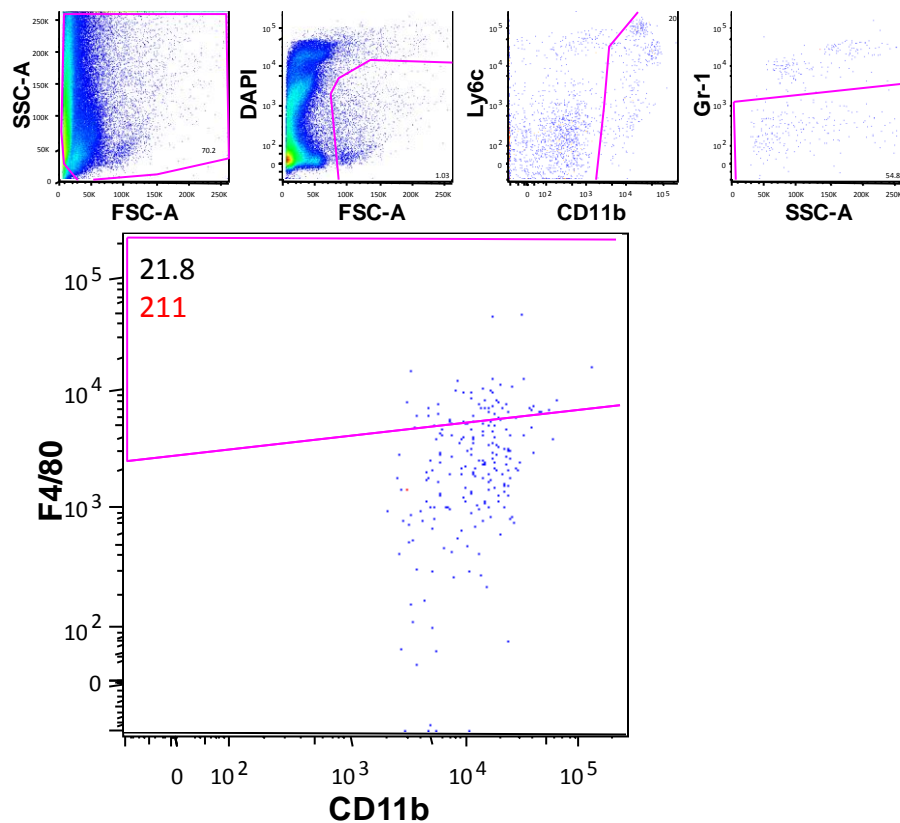
Figure 21. Representative flow cytometry scatter plot of a <u>Gr-1</u>⁻ F4/80⁺ innate immune cell population (Gr-1⁻ macrophages) derived from the pooled RPE-choroids of a young (<4m) wild-type mouse.

Smaller plots illustrate the ancestry of the F4/80⁺ population. Gates (from left to right) show: all events; live cells (dead cells DAPI positive); CD11b⁺ cells; CD11b⁺ Gr-1⁻ cells; with main plot demonstrating the final live CD11b⁺ Gr-1⁻ F4/80⁺ population. As in the retina, F4/80 was expressed at low levels in the choroid (confirmed by immunohistochemistry analysis, fluorescence minus one controls and analysis of splenocyte suspensions). The number of cells in each gate expressed as a percentage of all events on the plot is shown in black with the total number of events plotted shown in red. Fluorophores conjugated to antibodies against the respective markers are listed in the Methods section. Gates were set according to fluorescence-minus-one controls performed on retinal cell suspensions. Side scatter area (SSC-A); forward scatter area (FSC-A).
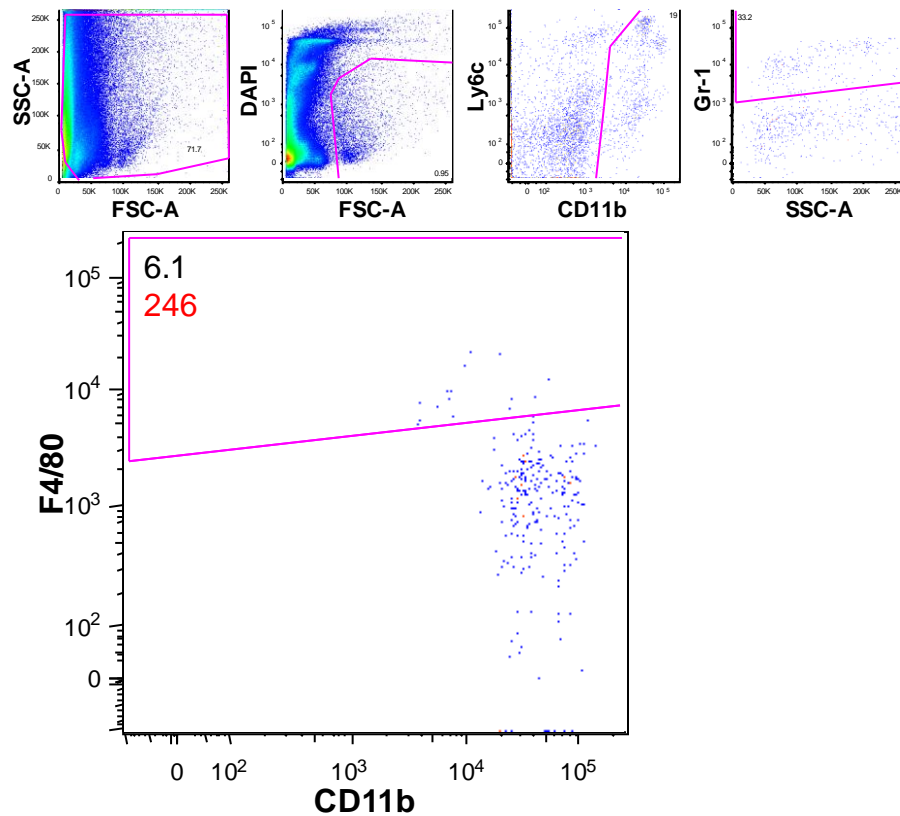
Figure 22. Representative flow cytometry scatter plot of a _Gr-1_⁺ F4/80⁺ innate immune cell population (Gr-1⁺ macrophages) derived from the pooled RPE-choroids of a young (<4m) wild-type mouse.

Smaller plots illustrate the ancestry of the F4/80⁺ population. Gates (from left to right) show: all events; live cells (dead cells DAPI positive); CD11b⁺ cells; CD11b⁺ Gr-1⁺ cells; with main plot demonstrating the final live CD11b⁺ Gr-1⁺ F4/80⁺ population. Gr-1⁺ macrophages constituted a small proportion of total macrophages in the RPE-choroid. F4/80⁻ population in the main plot constitutes a Gr-1⁺ subset of high scatter that were considered to be granulocytes (predominantly neutrophils). The number of cells in each gate expressed as a percentage of all events on the plot is shown in black with the total number of events plotted shown in red. Fluorophores conjugated to antibodies against the respective markers are listed in the Methods section. Gates were set according to fluorescence-minus-one controls performed on retinal cell suspensions. Side scatter area (SSC-A); forward scatter area (FSC-A).
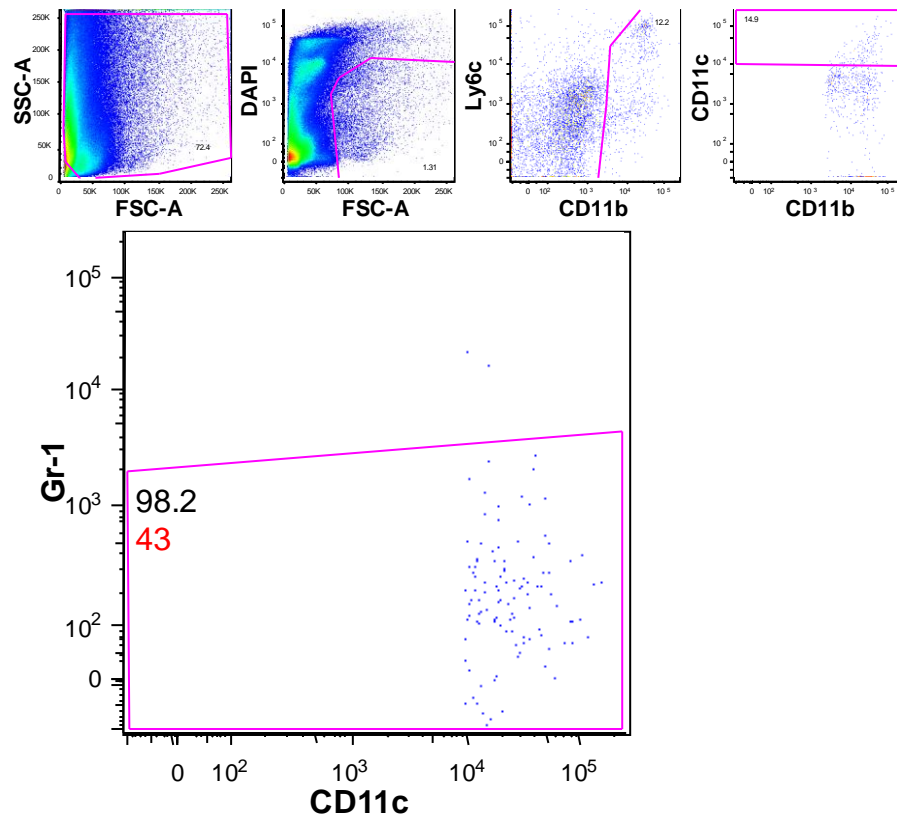
Figure 23 Representative flow cytometry scatter plot of a CD11c⁺ innate immune cell population (DCs) derived from the pooled RPE-choroids of a young (<4m) wild-type mouse

Smaller plots illustrate the ancestry of the CD11c⁺ population. Gates (from left to right) show: all events; live cells (dead cells DAPI positive); CD11b⁺ cells; CD11b⁺ CD11c⁺ cells; with main plot demonstrating the final live CD11b⁺ Gr-1⁻ CD11c⁺. Fluorophores conjugated to antibodies against the respective markers are listed in the Methods section. Gates were set according to fluorescence-minus-one controls performed on retinal cell suspensions.
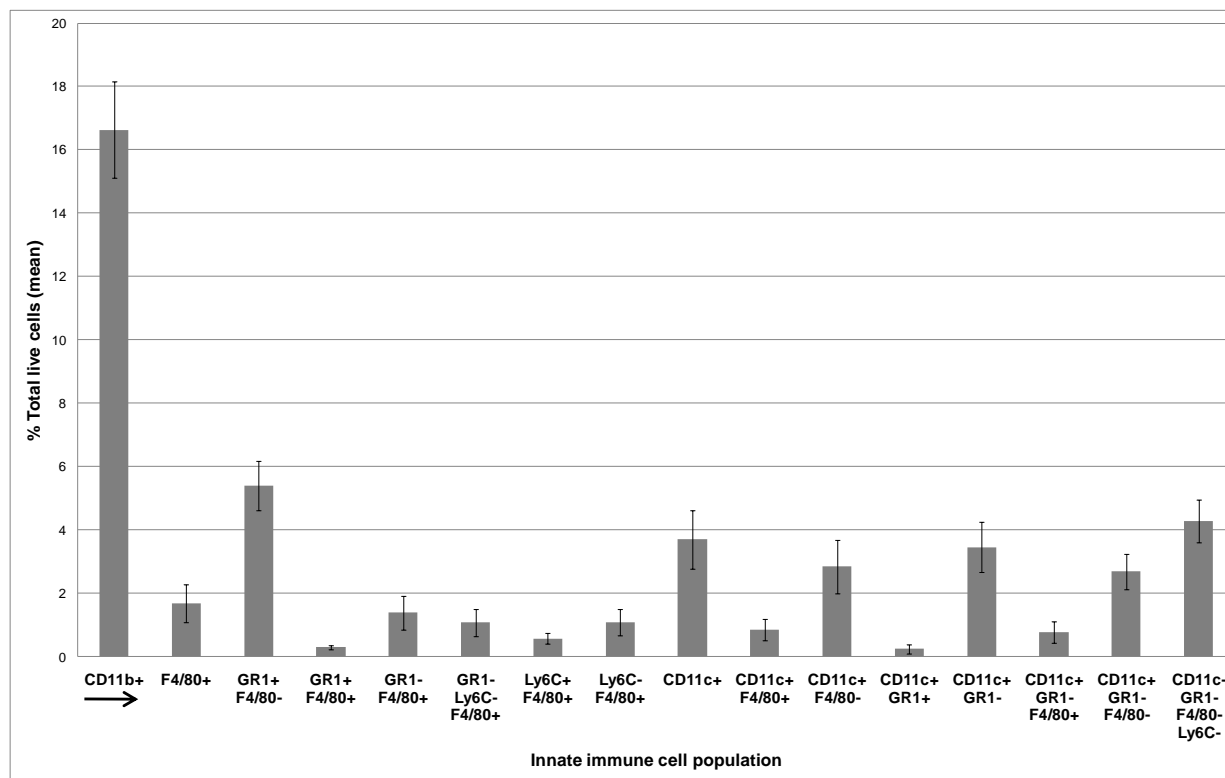
Figure 24. Permutations of marker expression on RPE-choroid cells from young (<4 month old) wild-type mice

As with retina, a total of 42 permutations of marker expression on CD11b$^+$ cells were analysed in order to establish populations of interest and four permutations were useful in identifying distinct CD11b$^+$ populations that might change with age or in pathological neovascularisation (n=6; mean number of live cells=3348; error bars=SEM; all populations are CD11b$^+$). Gating strategies for these key subsets are shown in Figure 21, Figure 22 and Figure 23. Overall, CD11b$^+$ cells were found to constitute a much higher proportion of the cell population in the RPE-choroid (over 16% of live cells compared to 1.2% in retina). In contrast to retina, CD11c$^-$ Gr-1$^-$ Ly6C$^-$ F4/80$^-$ cells formed a smaller proportion of total CD11b$^+$ cells.

3.3 The effects of ageing on innate immune cell populations in the retina and choroid

Having determined the proportions of innate immune cell populations in the retinae and RPE-choroids of young wild-type mice, the effects of ageing on the same populations were established by analysing tissue obtained from 12 month old and >18 month old wild-type animals (*Figure 25*).

A significant increase in the proportion of DCs was observed in both retina and RPE-choroid between <4 and 12 months of age (mean % live cells; t-test p<0.01 for both tissues) with no significant increase thereafter. Comparison of >18m old and <4m old tissues revealed that the proportion DCs was almost 4 times greater in aged retina (t-test p<0.01) and more than double in aged RPE-choroid (t-test p<0.05).

An increase in the proportion of Gr-1⁻ macrophages was also seen in the retina with age – mainly in >18m animals where, as a percentage of live cells, the proportion of Gr-1⁻ macrophages was more than double that observed in <4m mice (t-test p<0.05).

No significant difference between young and old age groups was observed in any of the other key populations.
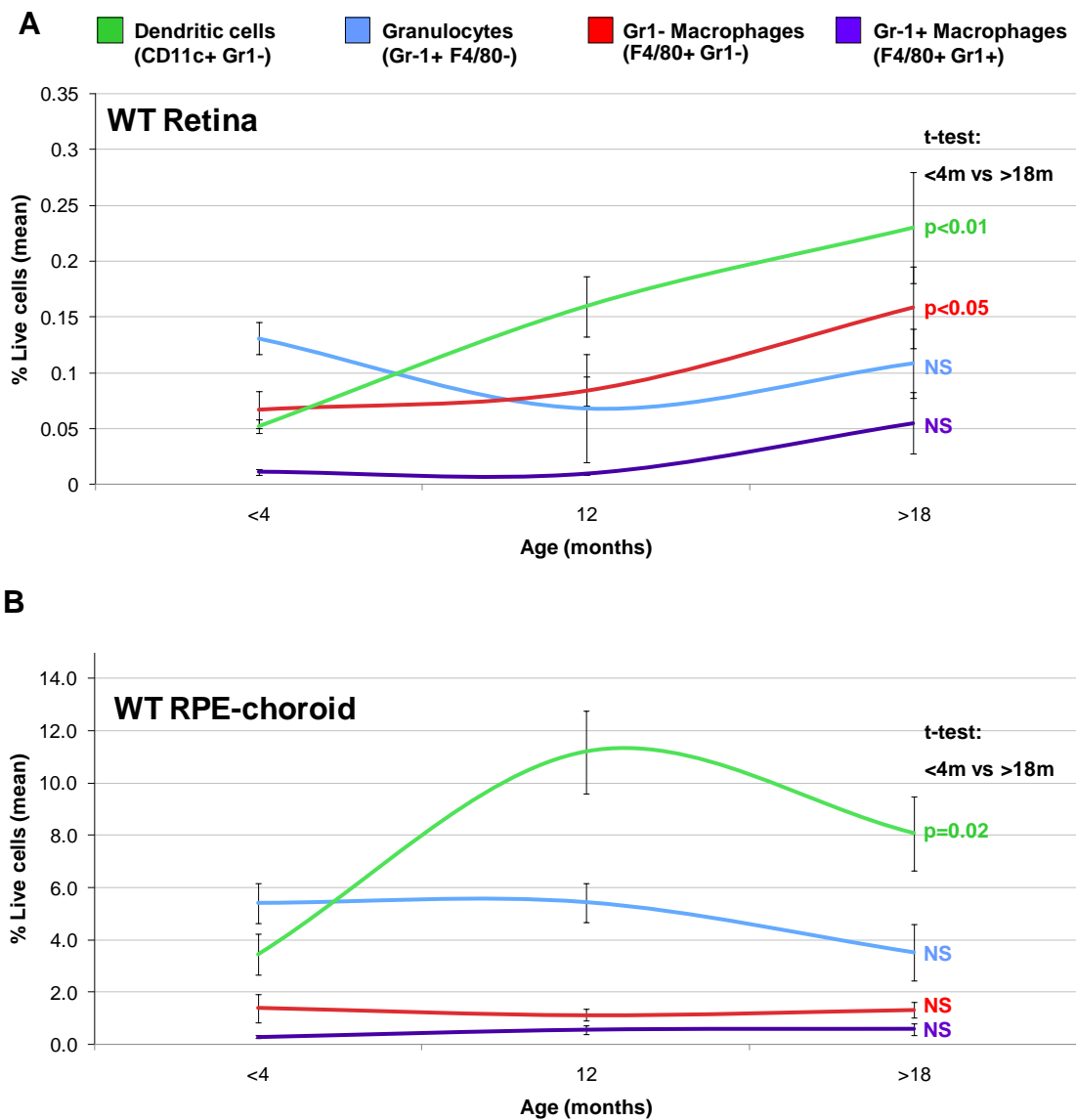
Figure 25. Age-related changes in the innate immune cell populations of wild-type retina (A) and RPE-choroid (B)

Graphic representations of changes in key innate immune cell populations (CD11b^{+}) in unprocedured wild-type retina and RPE-choroid expressed as a proportion of total live cells. Tissue pooled from each animal and mean % of live cells calculated for each population (n=9, 5 and 9 for retina and n=6, 5 and 9 for choroid - for age groups <4, 12 months and >18 months respectively; error bars=SEM). Dendritic cells (CD11c^{+} Gr-1^{-}) and Gr-1^{-} macrophages (F4/80^{+} Gr-1^{-}) accumulate with age in the retinae of wild-type mice with a significant increase in the proportion of DCs as early as 12 months of age (A). DCs also accumulate with age as early as 12 months in the RPE-choroid, there were no significant changes in any other RPE-choroidal innate immune cell populations with age (B).

127

3.4 Peripheral effects of ageing on innate immune cell populations

To determine whether changes observed with ageing in innate immune cell populations were restricted to the eye or associated with changes in the periphery, splenocyte suspensions from wild-types aged <4m and >18m were analysed.

Fluorescence-minus-one controls used as a guide for gating are shown (*Figure 26*). Gating for DCs, Gr-1$^-$ macrophages, Gr-1$^+$ macrophages and granulocytes in spleen revealed significant changes in the proportions of DC and Gr-1$^-$ macrophage populations with age with an approximately 3-fold increase in their sizes (*Figure 27A*). These findings correlated with data obtained from the retinae and RPE-choroids of wild-type mice (*Figure 25*).

The greater cell numbers in this tissue permitted an additional strategy for identifying CCR2$^+$ and CCR2$^-$ monocytes. This involved gating CD11b$^+$ F4/80^{Low} cells (monocytes) for Ly6C^{High} (CCR2$^+$), Ly6C^{Mid} and Ly6C^{Low} (CCR2$^-$ monocytes) populations (*Figure 28B* and *Figure 28*). Comparison of these populations between <4m and >18m animals revealed a significant increase in the proportion of the Ly6C^{Low} (CCR2$^-$) monocyte population with age. Again this finding was in keeping with changes in the CCR2$^-$ monocyte populations as determined using the Gr-1 marker and suggests that, in spleen, F4/80$^+$ Gr-1$^-$ cells may equate to F4/80$^+$ Ly6C^{Low} populations.

Analysis of other subgroups revealed a significantly higher proportion of CD11b$^+$ CD11c$^-$ F4/80$^-$ Gr-1$^-$ Ly6C$^-$ cells in aged spleen compared to young (*Figure 27B*). It was noted that, as in RPE-choroid and retinal tissue, monocyte/macrophages in wild-type spleen were largely CCR2$^-$ (as defined using Gr-1 or Ly6C).

SPLEEN
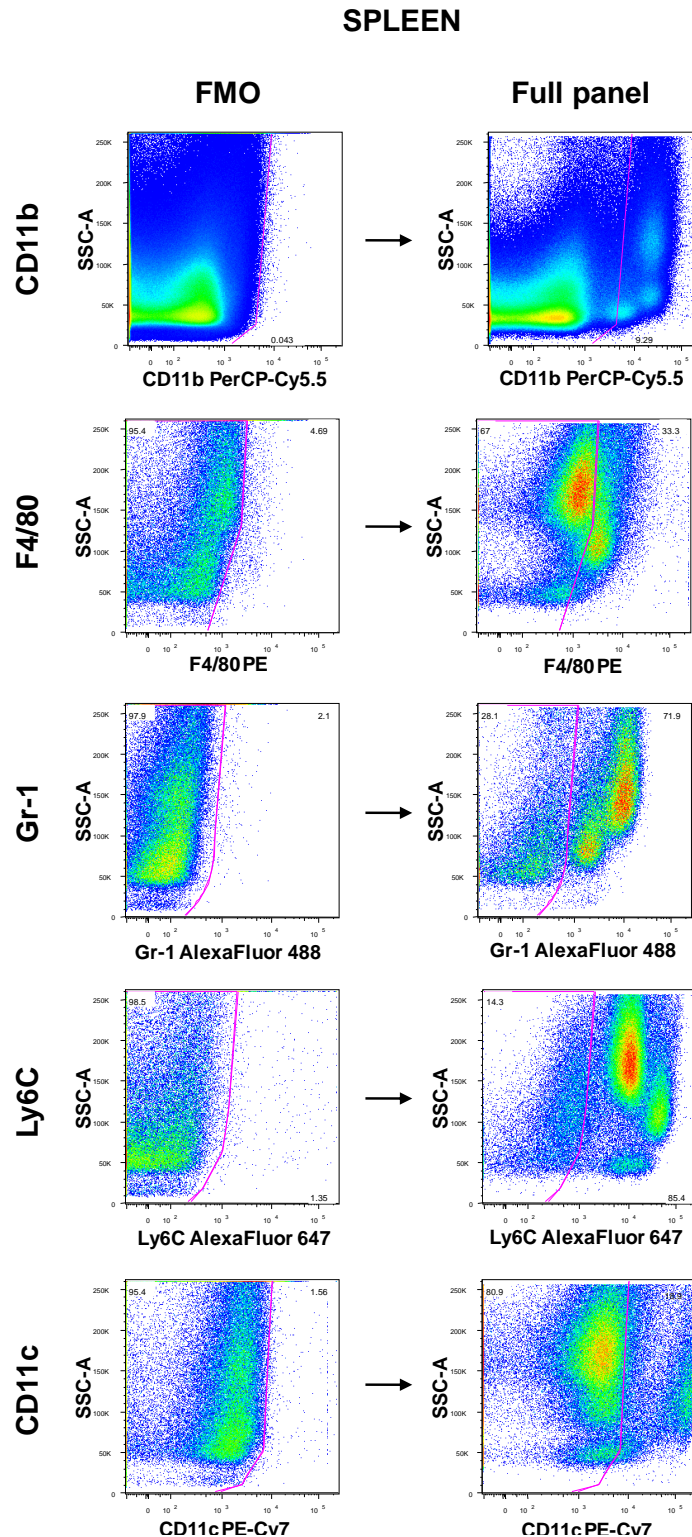
Figure 26 Fluorescence-minus-one controls for splenocyte suspensions

Fluorescence-minus-one controls for splenocyte suspensions derived from young wild-type mice. DAPI was used to stain for and exclude dead cells from the analyses and data fully compensated. Plots show gatin for the excluded marker as part of the FMO (x axis) against side-scatter (y axis). Gating strategies based on FMO controls were used as the basis for identifying specific cell populations.

130
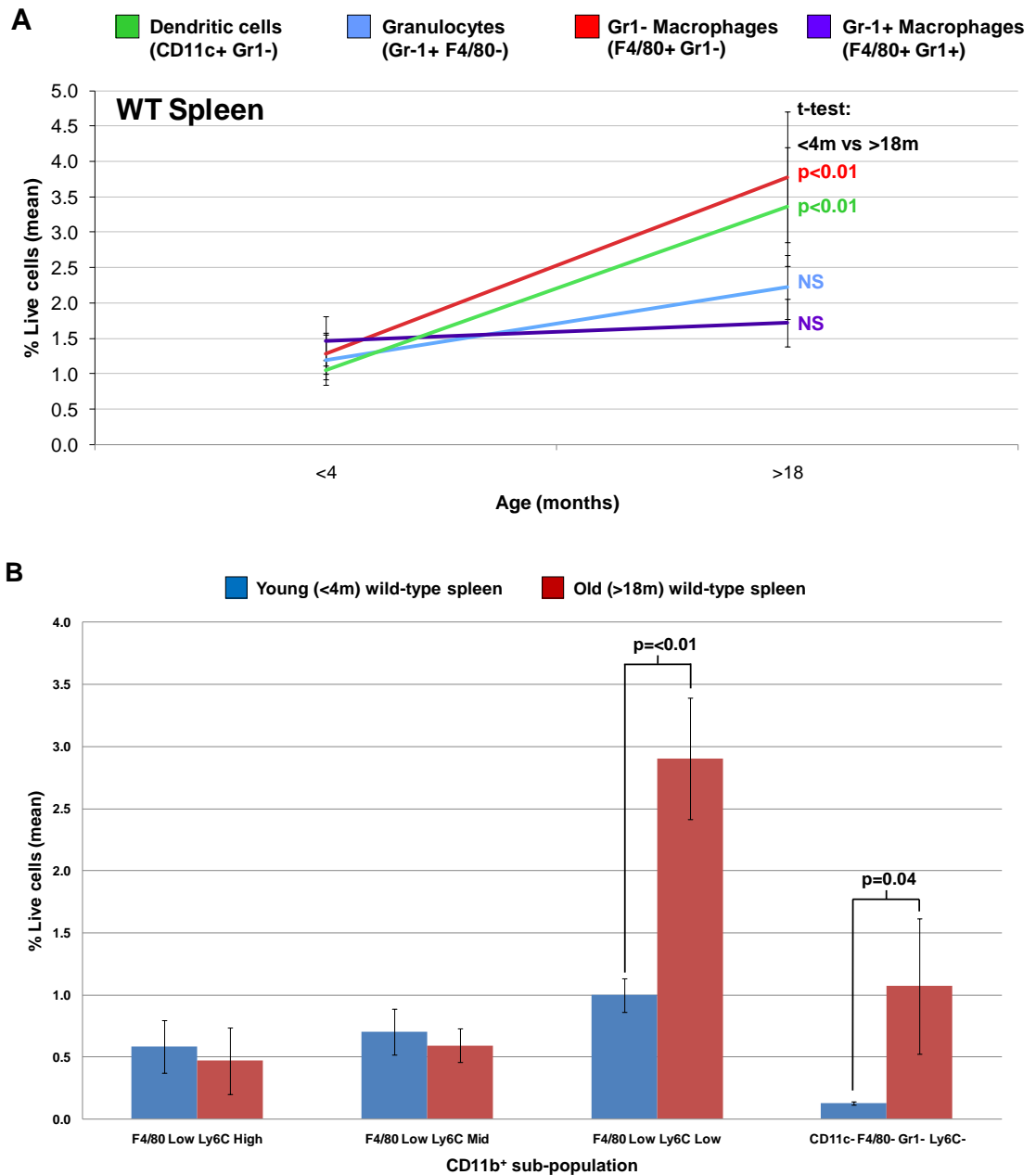
Figure 27. Changes with age in spleen innate immune cell populations of wild-type mice

Key innate immune cell populations derived from wild-type spleen. Mean % of live cells calculated for each population (n=12 for <4m group and n=7 for >18 month group; error bars=SEM). Dendritic cells and Gr-1⁻ macrophages accumulate with age in the retinae and RPE-choroids of wild-type mice – this was also found to be the case in the spleen where an approximately 3-fold increase in these populations was observed (A). In addition, the identification of subpopulations of CD11b⁺ F4/80^Low Ly6C^High, Ly6C^Mid and Ly6C^Low cells was also possible in spleen and a significant increase in the proportion of Ly6C^Low (CCR2⁻) monocytes was observed with age (B). A significant increase in the proportion of CD11b⁺ CD11c⁻ F4/80⁻ Gr-1⁻ Ly6C⁻ cells (possibly NK cells) was also observed.
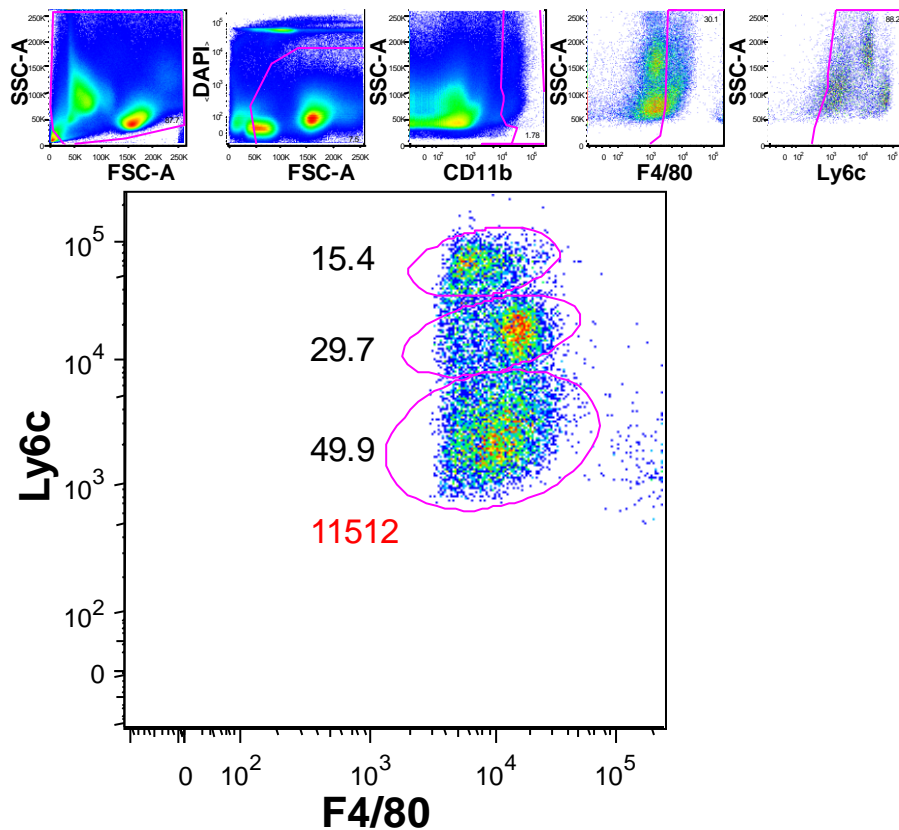
Figure 28. F4/80^Low population in the spleen may divided into Ly6C^High, Ly6C^Mid and Ly6C^Low subgroups

Whereas the limited number of cells derived from retina and RPE-choroid did not permit analysis of F4/80⁺ Gr-1⁺ or F4/80⁺ Ly6C⁺ subpopulations in these tissues it was possible to determine such groups with more confidence, particularly using Ly6C, in splenocyte suspensions. Smaller plots illustrate the ancestry of CD11b⁺ F480^Low Ly6C⁺ populations derived from young (<4 month old) wild-type spleen. Gates (from left to right) show: all events; live cells (dead cells DAPI positive); CD11b⁺ cells; CD11b⁺ F4/80⁺ cells and CD11b⁺ F4/80⁺ Ly6C⁺ cells; with main plot demonstrating the final live CD11b⁺ F4/80^Low Ly6C^High, Ly6C^Mid and Ly6C^Low subsets. Gating strategies were otherwise as applied to retinal and RPE-choroid cell suspensions. F4/80^Low population represents monocytes whilst F4/80^High cells (outside gates in main plot) represent mature macrophages.

3.5 Effects of CCL2 deficiency on the profile of innate immune cells in retina and choroid

Deficiencies in certain chemokines, such as CCL2, and their receptors have been demonstrated to result in the accelerated accumulation of subretinal macrophages with age[120, 169]. Levels of the chemokine CCL2 are significantly elevated in the retinae and RPE-choroids of aged wild-type mice and the receptor for CCL2 (CCR2) is expressed on a range of innate immune cells including CCR2$^+$ monocytes[124]. It was hypothesised that CCL2 deficiency results in the subretinal accumulation of macrophages through altered trafficking or maturation of specific innate immune cell populations and that it might be possible to confirm such effects by identifying changes in the proportions of these cells in the retinae and RPE-choroids of *CCL2$^{-/-}$* mice over time.

In comparison with age-matched wild-type retina, the proportion of DCs was found to be significantly higher in <4m *CCL2$^{-/-}$* mouse retina by a factor of more than 4 (t-test p<0.02) – making it the dominant innate immune cell population in the retinae of CCL2-deficient mice (*Figure 29*). There was a trend, though not significant, towards a slight increase in the proportion of DCs in the retinae of *CCL2$^{-/-}$* mice with ageing (<4m *CCL2$^{-/-}$* mice vs. >18m *CCL2$^{-/-}$* mice) suggesting a ceiling was reached earlier in these animals. A concomitant rise in the proportion of DCs in the retinae of wild-type mice with age meant there was ultimately no significant difference in the levels of DCs between aged *CCL2$^{-/-}$* mice and aged wild-types. Gr-1$^+$ macrophages were also found to be 4 times higher in the retinae of *CCL2$^{-/-}$* mice (t-test p<0.02), though again no change was observed with ageing.

Most striking, aside from the elevated levels of DCs, was the rapid increase in the proportion of Gr-1$^-$ macrophages observed around 12 months of age in *CCL2$^{-/-}$* mouse retina. Similar changes were observed in wild-types (in which numbers almost doubled), however in *CCL2$^{-/-}$* mice the proportion of Gr-1$^-$ macrophages more than doubled after 12 months of age (t test 12m *CCL2$^{-/-}$*
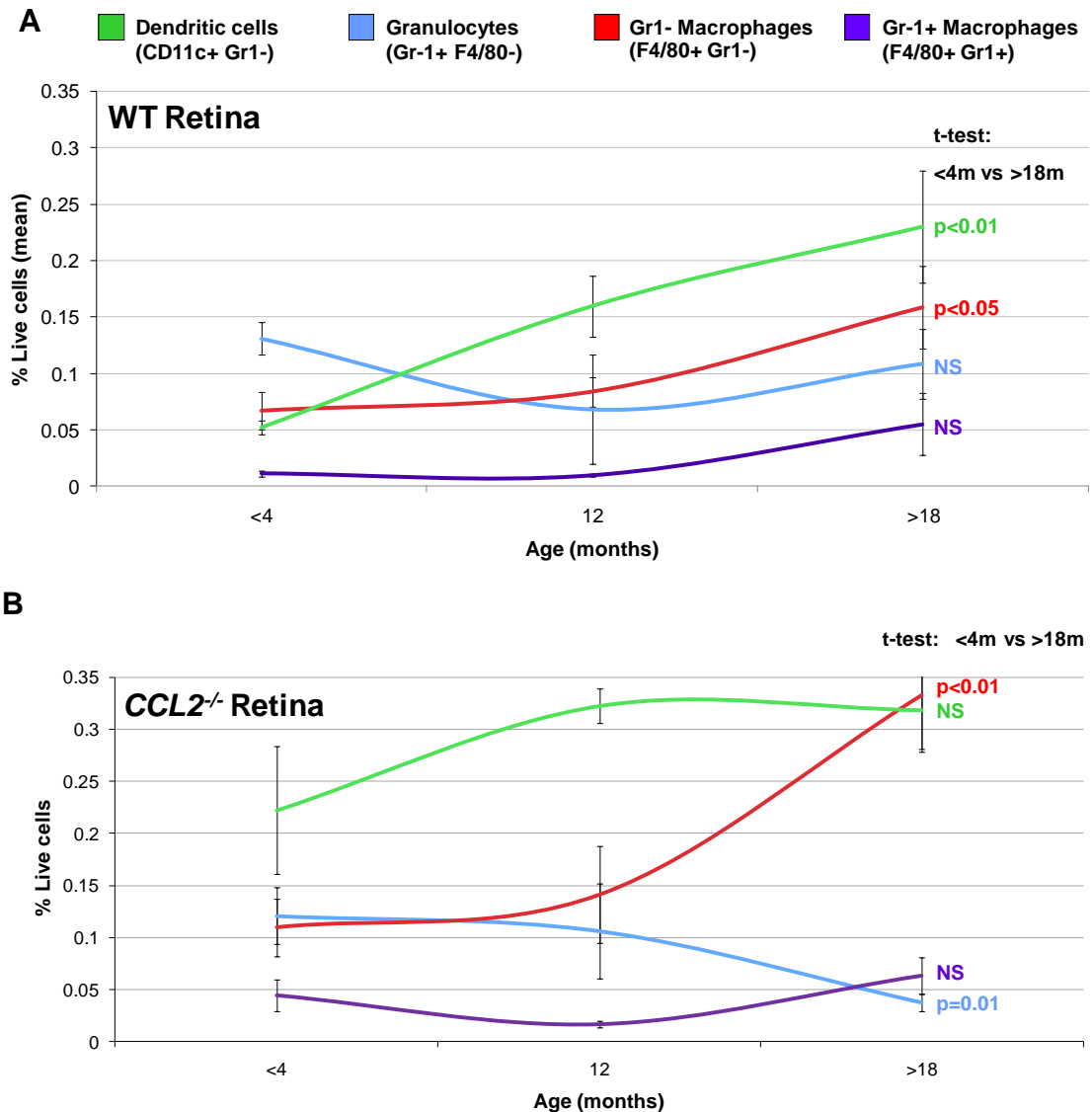
Figure 29. The effect of CCL2 deficiency on innate immune cell populations in the retina and how they change with age

Proportions of innate immune cell populations in the retina of CCL2^-/- mice (B) with analysis for wild-type mice provided above for comparison (A – as for Figure 25A). The proportion of DCs in young (<4m) CCL2^-/- retina is higher than age-matched wild-type retina by a factor of more than 4 (p=0.02). The proportion of Gr-1+ macrophages is also significantly higher in young CCL2^-/- retinae (p=0.02). With increasing age it can be seen that the proportion of DCs plateaus such that there is no significant difference between wild-type and CCL2^-/- retina at >18m; however the proportion of Gr-1^- macrophages rises rapidly after 12m in CCL2^-/- retina such that levels are equivalent to those of DCs and more than double that seen in age-matched wild-types (p=0.01). The rise in the proportion of Gr-1^- macrophages coincides with a decline in granulocytes in CCL2^-/- retina. Tissue pooled from each animal and mean % of live cells calculated for each population; n=8, 4 and 7 for age groups <4, 12 months and >18 months respectively (B); error bars=SEM.

134

mice vs. >18m $CCL2^{-/-}$ mice; p=0.03) ultimately matching levels of DCs in the retinae of >18m. The rise in Gr-1⁻macrophages coincided with a decline in the proportion of granulocytes in $CCL2^{-/-}$ mouse retina with levels significantly lower in >18m animals compared with <4m mice (t-test; p=0.02), no such decline was observed in wild-type mice.

In contrast to findings in the retina, no significant difference in the proportion of DCs in $CCL2^{-/-}$ RPE-choroid was observed at any timepoint compared with age-matched wild-type tissue (*Figure 30*). Even so, the DC population in $CCL2^{-/-}$ RPE-choroid appeared to behave in a similar manner to that in $CCL2^{-/-}$ retina, with a suggestion of higher numbers in younger animals that approached a ceiling by 12 months of age.

3.6 Effects of CCL2 deficiency on the profile of innate immune cells in the spleen

It was hypothesised that changes in the balance of CCR2⁺ and CCR2⁻ monocyte populations in the periphery might explain the effects of CCL2 deficiency on local innate immune cell populations in retina and RPE-choroid. Certain DC subsets are derived from CCR2⁺ monocyte populations and resident microglia are thought originate from CCR2⁻ monocyte populations. Having previously established that the proportions of DCs and CCR2⁻ monocytes appeared significantly elevated in aged wild-type spleen - with a trend towards decreased Ly6C^{High} (CCR2⁺) monocytes - the spleens of $CCL2^{-/-}$ mice were analysed.

Splenocyte suspensions from <4m and >18m $CCL^{-/-}$ mice were analysed and compared with those obtained from age-matched wild-type animals (*Figure 31*). Proportions of Gr-1⁻ macrophages and DCs were significantly lower in young $CCL2^{-/-}$ spleen compared with young wild-types (t-test; p=0.02 for both populations). The proportion of granulocytes and Gr-1⁺ macrophages was not significantly different in young $CCL2^{-/-}$ spleen compared with age-matched wild-type tissue.
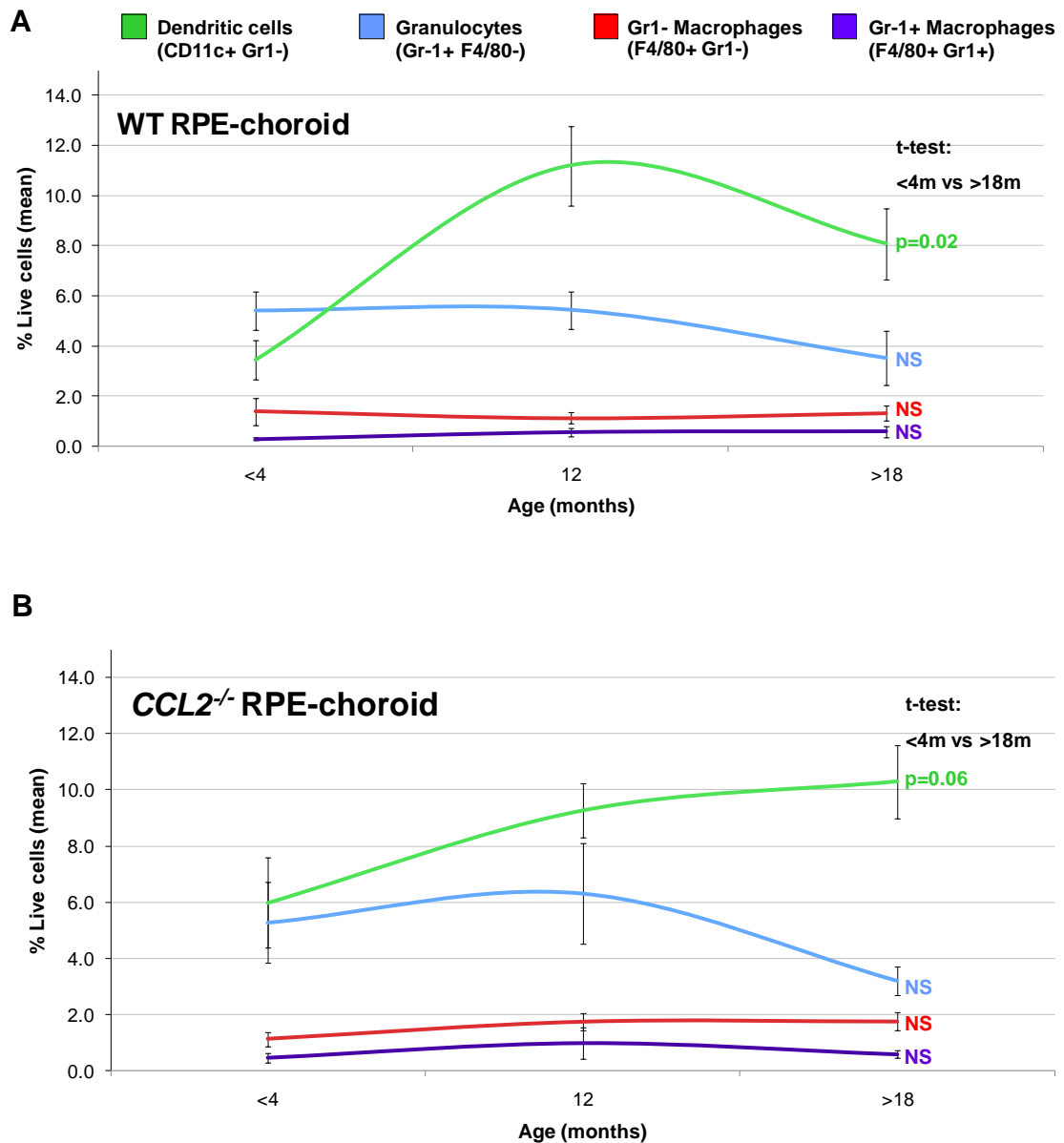
Figure 30. The effect of CCL2 deficiency on innate immune cell populations in the RPE-choroid and how they change with age

Proportions of innate immune cell populations in the choroid of CCL2^{-/-} mice (B) with analysis for wild-type mice provided above for comparison (A – as for Figure 25B). In contrast to findings in retina, there was no significant difference in the proportion of DCs in CCL2^{-/-} choroid at any timepoint compared with age-matched wild-type choroid, although the trend was for this population to be higher at the extremes of age in CCL2^{-/-} mice and DCs appeared to increase with age without quite achieving significance. There was no significant change in the proportions of any other innate immune cell population with age in CCL2^{-/-} mouse choroid although there was a trend towards a decrease in the levels of granulocytes (as in wild-types). Tissue pooled from each animal and mean % of live cells calculated for each population; n=7, 4 and 6 for age groups <4, 12 months and >18 months respectively (B); error bars=SEM.
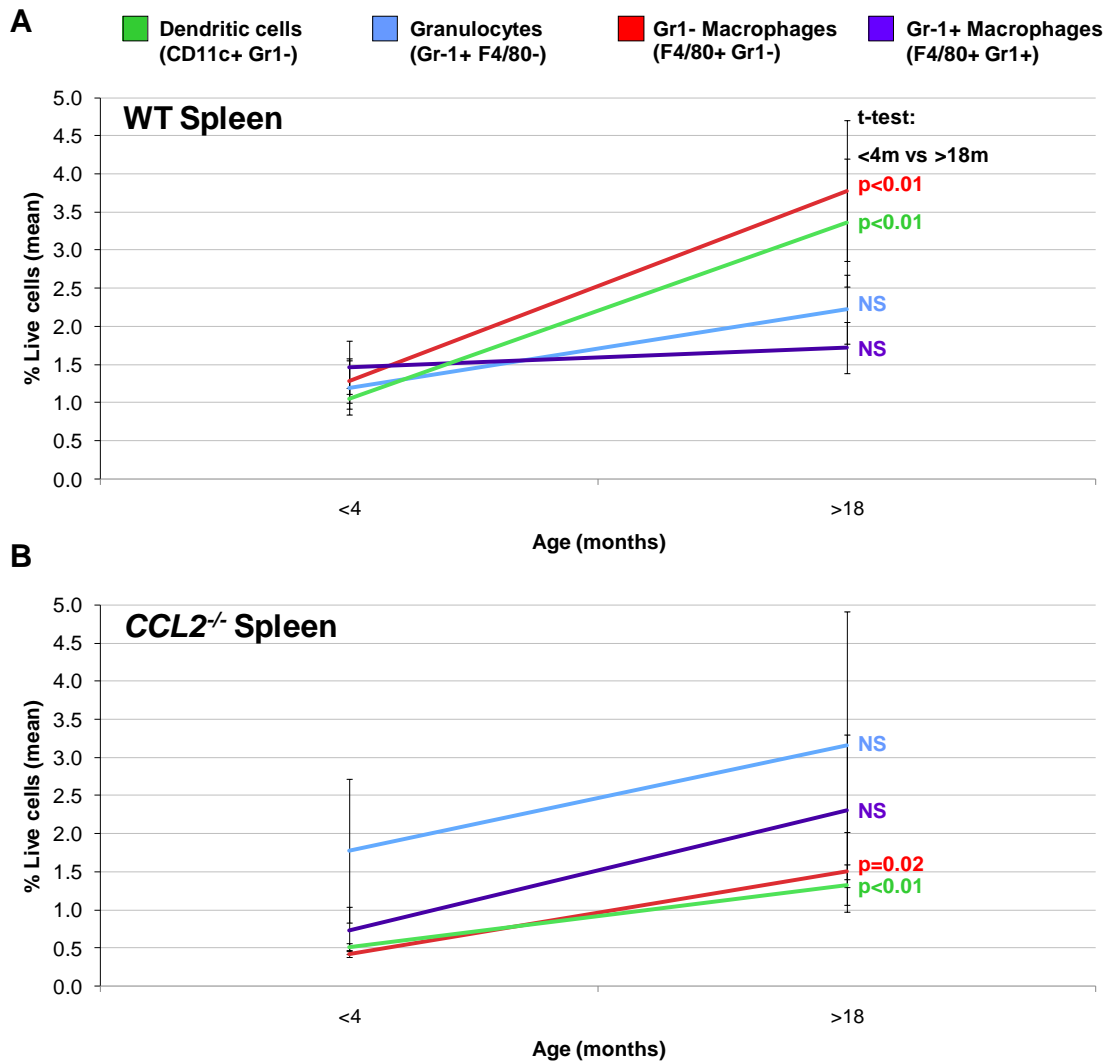
Figure 31. The effect of CCL2 deficiency on innate immune cell populations in the spleen and how they change with age

Proportions of innate immune cell populations in the spleen of CCL2$^{-/-}$ mice (B) with analysis for wild-type mice provided above for comparison (A - as for Figure 27A). The proportion of Gr-1$^-$ macrophages was 3 times smaller, and that of DCs 2 times smaller, in young (<4m) CCL2$^{-/-}$ spleen compared with age-matched wild-type spleen (t-test; p=0.02 for both populations). The proportion of granulocytes and Gr-1$^+$ macrophages was not significantly different in young CCL2$^{-/-}$ spleen compared with age-matched wild-type tissue. Increasing age was associated with significant increases in the proportions of Gr-1$^-$ macrophages and DCs in CCL2$^{-/-}$ spleen (approximately 3-fold – as in wild-types). Levels of these populations appeared to still be below those seen in >18m wild-types (t-test; p=0.06 for Gr-1$^-$ macrophages and p=0.05 for DCs). Comparison of the other populations in aged CCL2$^{-/-}$ mice with those in age-matched wild-types revealed no significant difference between them. Tissue pooled from each animal and mean % of live cells calculated for each population; n=9 and 6 for CCL2$^{-/-}$ age groups <4 and >18 months respectively (B); error bars=SEM.

137

Significant increases in the proportions of Gr-1⁻ macrophages and DCs were observed in spleens of >18m *CCL2⁻/⁻* mice compared with <4m animals (t-test; p=0.06 for Gr-1⁻ macrophages and p=0.05 for DCs). Levels of DCs were seen to double with age (t-test; p<0.01) and Gr-1⁻ macrophages seen to treble (t-test; p<0.02), although levels of these populations appeared to remain below those seen in >18m wild-type spleen (t-test; p=0.06 for Gr-1⁻ macrophages and p=0.05 for DCs). Comparison of the other populations in aged CCL2⁻/⁻ mice with those in age-matched wild-types revealed no significant difference between them.

Application of the gating strategy designed to establish monocyte subsets according to levels of Ly6C expression revealed changes consistent with those obtained using the Gr-1 marker. Ly6C^{Low} (CCR2⁻) monocytes were found to be significantly lower in young *CCL2⁻/⁻* mice, however the size of this group was seen to increase 5-fold with age (t-test <4m *CCL2⁻/⁻* vs. >18m *CCL2⁻/⁻* mice; p=0.02) and levels at >18m were observed to be the equivalent of those seen in >18m wild-types. No significant change was observed with age in the other monocyte populations of *CCL2⁻/⁻* mice though in general the trend was for the Ly6C^{High} (CCR2⁺) population to be smaller. Unlike wild-types, no increase in the proportion of CD11b⁺ CD11c⁻ F4/80⁻ Gr-1⁻ Ly6C⁻ cells was seen with age in *CCL2⁻/⁻* mice (*Figure 32*).

Overall, results suggest that ageing is associated with increased levels of CCR2⁻ monocytes and DCs in the spleens of wild-type animals. The effect of CCL2 deficiency is to significantly reduce the levels of these populations in the spleens of young *CC2L⁻/⁻* mice. The effects of ageing on spleen monocyte/macrophage populations and DCs appeared broadly similar in wild-type and *CCL2⁻/⁻* mice though the trend was for levels of these populations to be lower in CCL2-deficient animals.
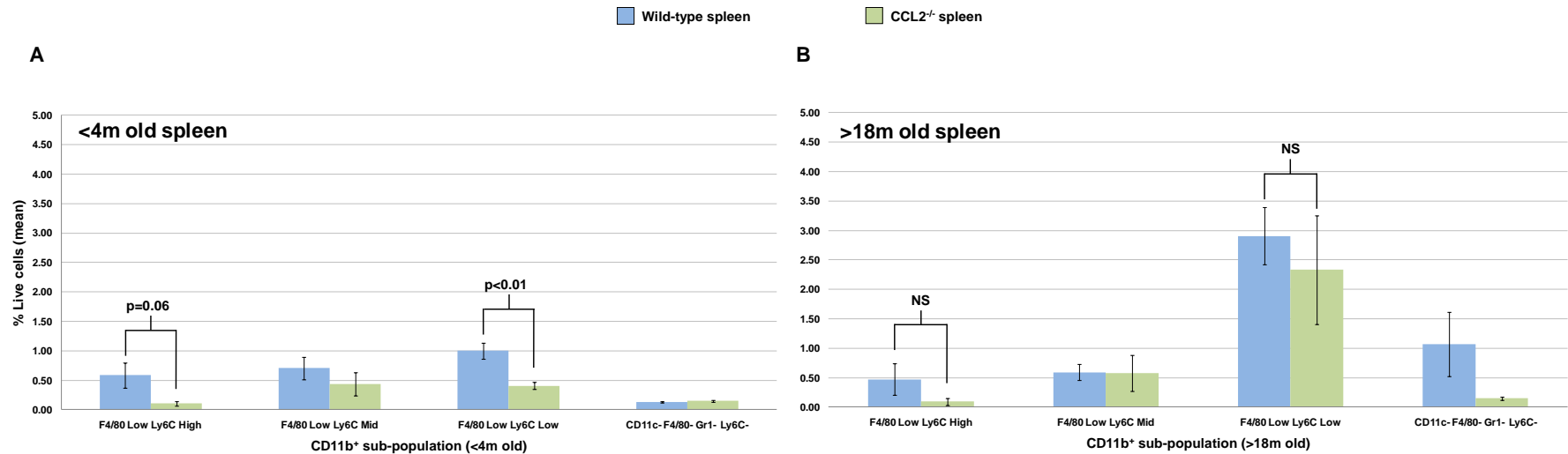
Figure 32. The effect of CCL2 deficiency on CD11b⁺ F4/80^Low Ly6C⁺ subpopulations and CD11b⁺ CD11c⁻ F4/80⁻ Gr-1⁻ Ly6C⁻ cells in the spleen.

Proportions of Ly6C^High, Ly6C^Mid and Ly6C^Low monocyte subpopulations and CD11b⁺ F4/80⁻ Gr-1⁻ Ly6C⁻ populations in the spleen of wild-type and CCL2⁻/⁻ mice aged <4m (A) and >18m (B). Data for wild-type spleens as for Figure 27B – shown here for comparison. The proportion of Ly6C^Low (CCR2⁻) monocytes in the spleens of <4m CCL2⁻/⁻ mice was less than half that in age-matched wild-types (t-test; p<0.01). The proportion of Ly6C^High (CCR2⁺) monocytes also appeared lower in young CCL2⁻/⁻ mice however this was of borderline significance. With ageing, levels of Ly6C^Low monocytes were seen to increase 5-fold in CCL2⁻/⁻ mice (t-test <4m CCL2⁻/⁻ vs. >18m CCL2⁻/⁻ mice; p=0.02) with no significant difference in this population between >18m CCL2⁻/⁻ animals and age-matched wild-types. Unlike wild-type mice, CCL2⁻/⁻ mice showed no significant increase in the proportion of CD11b⁺ F4/80⁻ Gr-1⁻ Ly6C⁻ cells in the spleen with age. For CCL2⁻/⁻ mice, n=9 and 6 for age groups <4 and >18 months respectively; for wild-type mice, n=12 and n=7 for each of age groups <4 and >18 months respectively; error bars=SEM.

3.7 Discussion

Ageing results in changes in innate immune cell populations in the retina, RPE-choroid and spleen.

The proportions of CCR2$^+$ and CCR2$^-$ monocytes have been demonstrated previously to be the same in the spleen as in peripheral blood, consequently it may be inferred that changes in the spleen, in wild type animals at least, reflect those in circulating innate immune cell populations[95]. Evidence suggests a role for Ly6C^{Low} (CCR2$^-$) monocytes in the maintenance of tissue resident macrophage populations[7]. In support of this, flow cytometric analysis of splenocyte populations revealed an increase in the proportion of CCR2$^-$ monocytes with age that correlates with a significant age-related increase in the levels of Gr-1$^-$ macrophages (most likely microglia) in wild-type retina. Similarly, a significant increase in the DC population of wild-type spleen with age was associated with significant increases in the DC populations of both retina and RPE-choroid. Levels of Gr-1$^-$ macrophages remained unchanged in the RPE-choroid with age.

Proportions of CCR2$^-$ monocytes and DCs were significantly lower in the spleens of young CCL2-deficient mice compared with young wild-types and this difference was largely preserved with ageing. Given the above findings one might have expected to observe lower levels of these populations in the retinae of young $CCL2^{-/-}$ mice compared with young wild-types (and possibly even in the older age-groups). In the case of DCs the opposite was the case, with four times as many observed in the retinae of young $CCL2^{-/-}$ mice. In contrast, there was no significant difference in the proportions of the Gr-1$^-$ macrophage population in the retinae between the two genotypes before 12m of age. These findings suggest, not surprisingly, that recruitment of CCR2$^-$ monocyte populations for the purpose of forming resident microglial populations is not CCL2 dependent. They also suggest that CCL2 is in some way important for either the maturation or trafficking of DCs in the retina and that a failure of the appropriate signalling leads to an accumulation of these cells locally with a

diminution of their numbers in the periphery (where migration to lymph nodes and spleen would normally occur).

The changes with age in the spleens and retinae of $CCL2^{-/-}$ mice appear to support a role for CCL2 in DC trafficking. Increases in DC populations with age in wild-type retina were matched by similar increases in the proportions of this population in the wild-type spleen. In contrast, the increase in the proportion of DCs in the spleens of $CCL2^{-/-}$ mice with age was much smaller compared with the highly elevated levels in the retina - this raises the possibility that a system-wide failure of DC trafficking from the tissues might be responsible for reduced numbers of these cells in the spleen. Evidence of increased numbers of DCs in other non-lymphoid tissues from $CCL2^{-/-}$ mice would be needed to confirm this.

DC levels, though greatly elevated, were seen to plateau in the retinae of $CCL2^{-/-}$ mice after 12 months of age. This was associated with a sharp rise in the proportion of Gr-1$^-$ macrophages in the retina – much higher than that observed in wild-types. Given that levels of CCR2$^-$ monocytes in the spleens of aged $CCL2^{-/-}$ mice are certainly not higher than those in age-matched wild-types it is interesting to speculate on the mechanism behind the increased levels of Gr-1$^-$ macrophages in the retinae of CCL2-deficient animals. Their accumulation appears to be a reaction to chronic failure of DC maturation/trafficking and not driven by age-related changes in 'resident' phenotype monocyte populations in the periphery.

No subretinal macrophages have been demonstrated on histological sections before the age of 18 months in either wild-type or $CCL2^{-/-}$ mice[120]. Since the DC population is elevated in the retinae of $CCL2^{-/-}$ mice at an early age it is the behaviour of Gr-1$^-$ macrophage populations that fits better with the histological data (data that also suggest subretinal macrophages accumulate more rapidly in the $CCL2^{-/-}$ mouse retina than the wild-type). The differential behaviour of DC populations in these models has not been noted previously - it is possible that a focus on subretinal cells and the use of microglial - rather than DC-specific markers has led to DCs escaping inclusion in any counts of innate immune cells in histological sections.

CCL2 deficiency (unlike CCR2 deficiency) has been demonstrated not to affect directly the egress of monocytes and other innate immune cells from the bone marrow[170]. This suggests that the changes observed in the spleens of $CCL2^{-/-}$ mice arise from altered maturation pathways for monocytes in the peripheral blood – unless, that is, CCL2 somehow plays a role in the recruitment of monocytes that do not express its receptor. The changes in monocyte subpopulations and DCs observed with age were not significantly different between wild-types and $CCL2^{-/-}$ mice suggesting that CCL2 does not have a direct role in innate immunosenescence in this tissue. An exception to this was the observation that an undefined population of CD11b$^+$ CD11c$^-$ F4/80$^-$ Gr-1$^-$ Ly6C$^-$ cells (possibly NK cells) increased with age in wild-type but not CCL2-deficient mice (no such change was observed in retinal or RPE-choroidal tissue).

Findings in the RPE-choroid were broadly similar to those in the retina, though not statistically significant – this may be because the yield of live cells from two pooled RPE-choroids was approximately 20 times smaller than from retinae. Nevertheless, DCs appeared to constitute a larger population in young $CCL2^{-/-}$ RPE-choroid compared with age-matched wild-type tissue and, similarly to the retina, the size of the DC population appeared to increase in the first 12 months of life. Whereas significant increases in Gr-1$^-$ macrophage populations were observed in the retina with age in both wild-type and $CCL2^{-/-}$ mice, this was not the case in the choroid where macrophage populations remained low relative to DCs and granulocytes.

It could be argued that the observed effects of ageing in wild-type and $CCL2^{-/-}$ mice arise from selection for animals of advanced age with a specific immune phenotype (potentially certain phenotypes may be associated with a higher risk of death at younger age thereby skewing the cohort of aged animals). It would be difficult to control for this. In this study there was a natural loss of animals from both CCL2$^{-/-}$ and wild-type cohorts as the animals aged but this was not felt to be at levels which might bias results. Regardless, the use of inbred

strains, which are more-or-less genetically identical, greatly minimises the risk of selection for animals with a specific immunophenotype.

Overall these results suggest that age-related changes in the peripheral innate immune cell compartment may modulate inflammatory effects at a local level in the retina and RPE-choroid of the eye in wild type mice. CCL2 appears not to play a direct role in changes observed with age systemically but deficiency of this chemokine does result in a shift towards lower levels of CCR2$^-$ monocytes and DCs in the spleen for the lifespan of the animal. Normal maturation and/or trafficking of DCs appears to be CCL2-dependent and a failure of normal signalling results in increased levels of DCs, and subsequently microglia, in the retina - an effect that may explain some of the changes in innate immune cell populations in the spleens of *CCL2$^{-/-}$* mice.

Chapter 4: The characterisation of innate immune cell populations involved in CNV

4.1 Introduction

This chapter documents work aimed at identifying whether the changes observed in innate immune cell populations in the retina, RPE-choroid and spleen might explain the increase in CNV severity observed with ageing, and the role of the chemokine CCL2 in this process.

AMD is associated with CNV in approximately 10% of cases. CNV is also a feature of eye diseases other than AMD. The extent of CNV and its sequelae appear strongly related to the nature of the eye disorder and the age of an affected individual. For example, the type of CNV that most commonly affects young subjects (CNV associated with myopia or presumed ocular histoplasmosis) tends to be smaller, leaks and haemorrhages less, and tends not to result in the disciform scar so frequently seen in long-standing AMD[150].

It has been demonstrated previously that age is an independent risk factor for the severity of CNV induced by laser-mediated rupture of Bruch's membrane in wild-type mice[162]. CNV in older mice are larger, thicker, more cellular and probably more vascularised than in younger animals. Increased neovascular responses have been found in older animals using other models of vascular injury and a number of mechanisms have been proposed for this including the loss of soluble growth factor inhibitors from the blood, increased soluble growth stimulants, changes in immune function and changes in vascular progenitor cells. However, the picture is further complicated by the finding of impaired angiogenesis in aged animals in other models such as those for hind limb ischaemia and wound healing models[182].

There is contradictory evidence for the role of macrophages in laser-induced CNV that might be explained by a bias towards the recruitment of one type of F4/80$^+$ cell over another[96, 154, 156]. Apte et al. suggested a role for macrophages in the inhibition of laser-induced CNV after demonstrating that increased macrophage recruitment is associated with smaller CNV size in *IL-10$^{-/-}$* mice and anti-CD11b and anti-F4/80 antibody-mediated depletion of monocyte/macrophage populations is associated with increased lesion size. Espinosa-Heidmann et al. used clodronate liposomes to deplete circulating and choroidal monocyte/macrophage populations and demonstrated a correlation with reduced lesion size[96, 152]. Pro-angiogenic properties have been ascribed to CCR2$^-$ monocytes and their counterparts in tumour biology, the tie-2 expressing monocytes (TEMS). In contrast, CCR2$^+$ monocytes have been described as having a more 'inflammatory' phenotype[95]. It was therefore hypothesised that the observed changes in innate immune cell populations locally and in the periphery with age might explain the increased severity of CNV seen in aged wild-type mice. This was tested by subjecting young (<4m), 12m and >18m wild-type and *CCL2$^{-/-}$* mice to laser-induction of CNV. The size of the CNV and the local innate immune cell reponse to laser induction to CNV were both determined. Analysis of the CNV response in *CCL2$^{-/-}$* mice was considered to be of particular interest given the increase in the CCR2$^-$ (Gr-1$^-$/ Ly6C^{Low}) monocyte population in the periphery with age.

To determine whether findings might be conserved across models of choroidal neovascularisation, the innate immune cell populations in the retinae, RPE-choroids and spleens of a strain of mouse in which CNV occurs spontaneously were examined (*Figure 33*). The JR5558 mouse develops multiple areas of CNV in the posterior fundus around 10-12 days post-natally before developing a lethal leukaemia at 3 months of age. CNV in the JR5558 mouse has been demonstrated to be associated with an infiltration of F4/80$^+$ cells on immunohistochemistry. Whilst the genotype corresponding with the above phenotype is unknown, this model was felt to be more in keeping with the pathological neovascularisation seen in AMD than alternatives such as the oxygen-induced retinopathy model where retinal neovascularisation arises primarily   as   a   result   of   dysregulated   vasculogenesis.

No primary control   **6wk old JR5558**
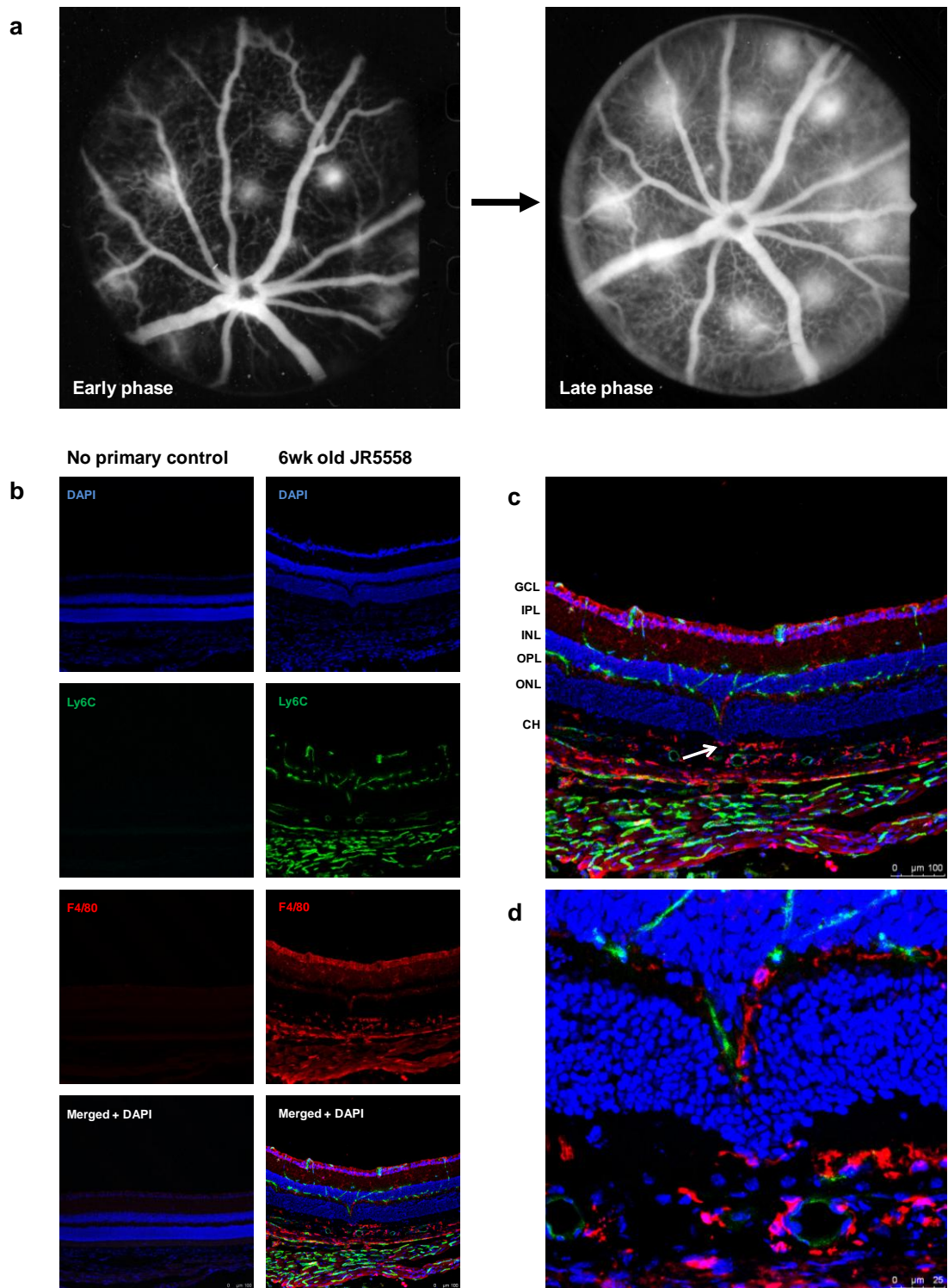
Figure 33 F4/80 and Ly6C immunostaining of a retinal and RPE-choroidal section taken from a 6 week old JR5558 mouse

Fundus fluorescein angiographic images demonstrating multiple areas of choroidal neovascularisation in the posterior pole of a 6wk old JR5558 mouse eye with leakage evident in the late phase of the angiogram (a); confocal microscopic images of 16µm sagittal sections stained for the monocyte/macrophage marker F4/80 and Ly6C - a marker expressed on

granulocytes, CCR2$^+$ monocyte subsets and retinal/choroidal vascular endothelium (b); merged images show F4/80$^+$ cells associated with neovascular changes in the subretinal space at x20 magnification (arrow; c) and x40 magnification (d).

4.2 Effects of ageing and CCL2 deficiency on the severity of laser-induced CNV

Three separate experiments were conducted with the aim of better understanding the effects of ageing and CCL2 deficiency on the extent of CNV. Each experiment involved the induction of CNV by diode laser in wild-type and $CCL2^{-/-}$ mice aged <4 months, 12 months and >18months with comparison of the mean size of CNV between the two genotypes in each age group (as determined by analysis of the early phase of fundus fluorescein angiography performed at 2 weeks post-laser).

The mean size of CNV lesions in <4m $CCL2^{-/-}$ mice was found to be 42% smaller (t-test; p<0.01) than in age-matched wild-type mice (*Figure 34*). This difference in lesion size between the two genotypes remained consistent and statistically significant with ageing.

Lesion size was seen to increase significantly with age in both wild-type and $CCL2^{-/-}$ mice. Lesions in >18m wild-type mice were larger, on average, by a factor of 2.6 compared with <4m wild-type mice (p<0.01) and, in the case of >18m $CCL2^{-/-}$, 2.7 times larger compared with <4m $CCL2^{-/-}$ animals (p<0.01). Findings in wild-type mice were in keeping with those published in the literature[162].

Linear regression analysis indicated that CCL2 deficiency reduces the effects of ageing on CNV size. These results suggest a role for CCL2 in modulating the neovascular response in CNV and that CCL2 may play a role in the age-dependent increase in CNV severity. They also suggest that the subretinal microglia, observed to accumulate more rapidly with age in $CCL2^{-/-}$ mice, do not exert a significant pro-angiogenic effect – if they did then the effect of CCL2 deficiency on lesion size would be attenuated with age compared with wild-type mice.
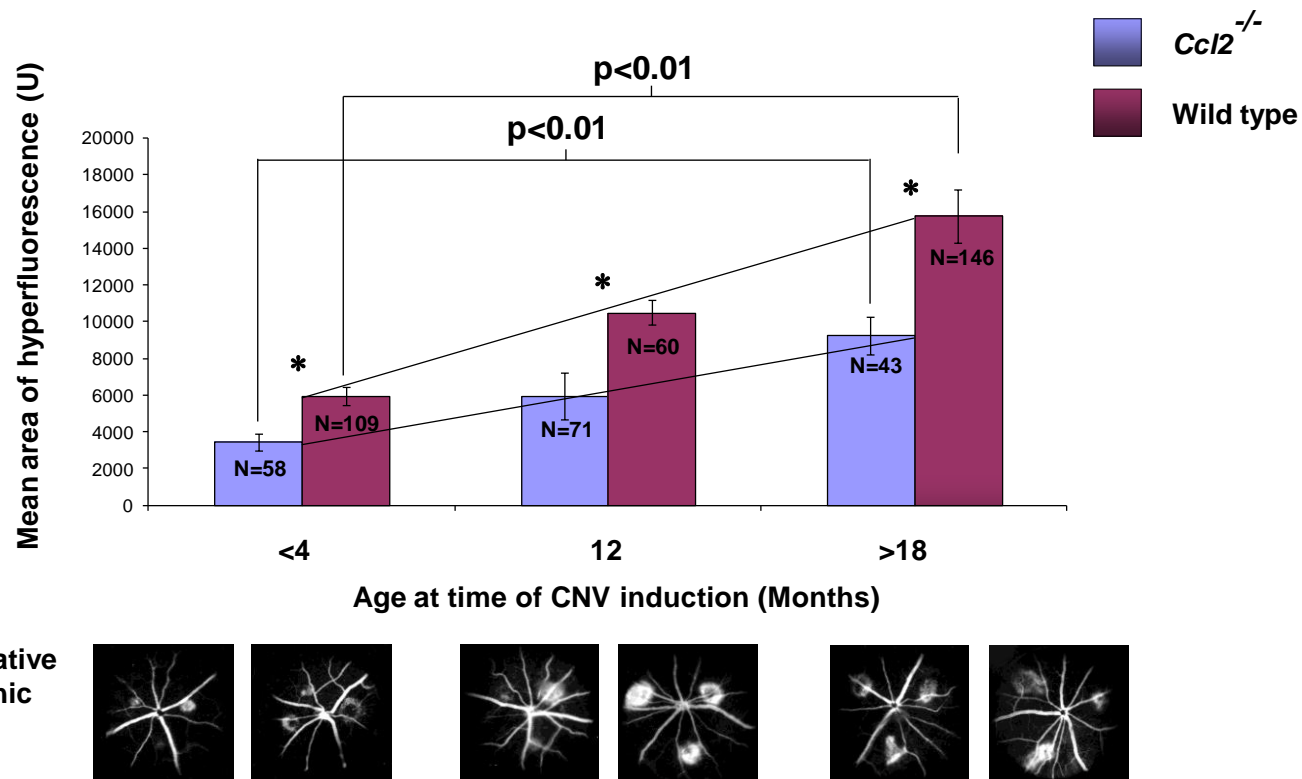
Figure 34. The effects of ageing and CCL2 deficiency on laser-induced choroidal neovascularisation

Mean lesion size following laser-induced CNV in WT and Ccl2$^{-/-}$ mice and the changes with age. Results are shown from the early phase of fluorescein angiograms at 2 weeks post-laser (mean area of hyperfluorescence +/- SEM; N refers to number of lesions) with representative images from angiograms shown below. Significant differences between age-matched groups are indicated with an asterisk (student t-test; p<0.05).Mean lesion size was significantly reduced in young Ccl2$^{-/-}$ mice compared to age–matched wild-types with the effect preserved in 12m and >18m mice. Both wild-type

and Ccl2$^{-/-}$ mice exhibited significant linear increases in lesion size with age however the trend lines suggest that the effects of ageing on CNV severity were attenuated in CCL2 deficient mice (linear regression; p=0.059).

4.4 Titration of a dose response to laser-induced CNV

Laser-induced CNV has been used in conjunction with flow cytometric assays to establish a role for macrophages, DCs and neutrophils in CNV and to determine the kinetics of cell recruitment[153, 156, 160]. The protocols adopted by these studies have employed standardised laser settings to induce CNV in multiple locations in the mouse fundus using observation of a cavitation bubble as evidence of successful Bruch's membrane rupture – the most critical aspect of laser delivery in this model.

It is highly unlikely that the cell infiltrate associated with 3-4 lesions (the numbers used in the assessment of effects on CNV size) would be sufficient to allow for the analysis of small populations, or even be detectable using flow cytometry. Consequently, previous studies have delivered as many as 30-50 burns per fundus before harvesting tissue[153, 156, 160]. Given the size of mature CNV lesions relative to the mouse fundus, the dimensions of the mouse eye and the degree of acute inflammation associated with CNV induction, these numbers were considered excessive – even after taking into account variations in equipment and laser settings. The number of CNV lesions per fundus was therefore optimised for the purpose of accurately determining the pro-angiogenic inflammatory response in the retinae and RPE-choroids of young and old mice of different genotypes. The decision was made to harvest tissue at 3 days post-CNV induction for the following reasons: previous studies have indicated that peak macrophage infiltration at the site of CNV takes place 2-3 days post-induction of CNV[153, 155]; the start of RPE and endothelial cell proliferation is a feature of the day 3 timepoint and this immediately precedes the exponential growth of CNV. The 3 day post-induction timepoint was considered sufficiently removed from the initial phase of inflammation (which would most likely be directed at removal of apoptotic cells and necrotic tissue) for any pro-angiogenic infiltrate to be identified.

Having decided on the timepoint of interest, two cohorts of young (<4m) wild-type mice were subjected to laser-induction of CNV – one group receiving 10

burns per fundus and the other 20 burns per fundus. Retinae and RPE-choroids were harvested at 3 days post-laser and tissue pooled for flow cytometric analysis. Induction of 10 CNV lesions per fundus was found to result in a significant increase in the proportion of CD11b$^+$ cells in retinal tissue without the significant reduction in live cell numbers observed following the induction of 20 lesions per fundus (*Figure 35*). CNV induction resulted in significant increases in the proportion of CD11b$^+$ cells in the RPE-choroid but without a significant difference between groups receiving either 10 burns or 20 burns and with no significant reduction in the live cell population (*Figure 36*).

4.5 The innate immune response to laser-induced CNV

Induction of CNV by laser is a well-established animal model that has proved a reliable method for investigating the pathology of human CNV and developing therapeutic modalities[183]. The model was therefore employed to determine whether the effects of CCL2 deficiency in reducing CNV size and attenuating the effects of ageing on CNV severity were modulated by specific innate immune cell populations. It was hypothesised that a failure to recruit CCR2$^+$ monocytes to CNV lesions might be responsible for these effects.

To determine the effects of CCL2 deficiency and age on the innate immune response to CNV, cohorts of wild-type and *CCL2$^{-/-}$* mice were divided into 3 age groups (<4m, 12m and >18m - as for unlasered animals) and CNV induced at 10 locations in each fundus of each animal. Retinal and RPE-choroidal tissue was then harvested 3 days after CNV-induction for flow cytometric analysis and the results compared across age groups and between age-matched lasered and unlasered animals.
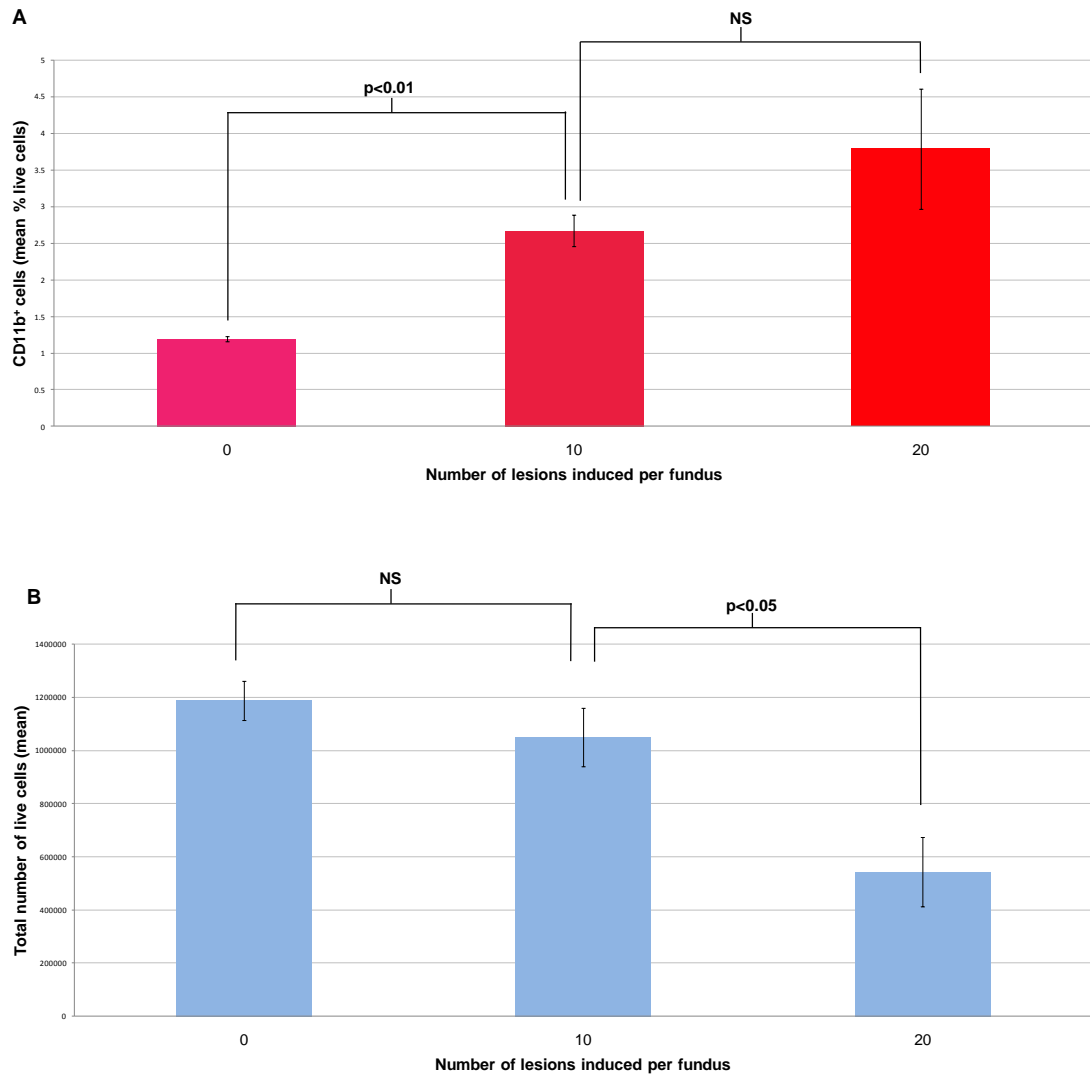
Figure 35. Induction of CNV by diode laser at 10 separate locations in each fundus results in significant inflammatory infiltrate without excessive tissue destruction in the retina of <4m wild-type mice

The percentage of CD11b^{+} cells in the retina increased at 3 days post-induction of CNV following delivery of either 10 or 20 burns to the fundi compared with unlasered tissue. There was no significant difference between groups receiving 10 or 20 burns in terms of CD11b^{+} cell infiltrate although data acquired following delivery of 20 burns was more variable (A). Delivery of 20 burns to each fundus resulted in significant tissue loss in the retina with half the number of live cells acquired for analysis compared with fundi receiving 20 burns each. There was no significant difference in live cell counts between the unlasered group and that receiving 10 burns per fundus. Retinae pooled for each animal and mean % of live cells calculated for CD11b^{+} population (n=9, 8 and 7 for unlasered, 10 and 20 lesions per fundus groups respectively); error bars=SEM.

A
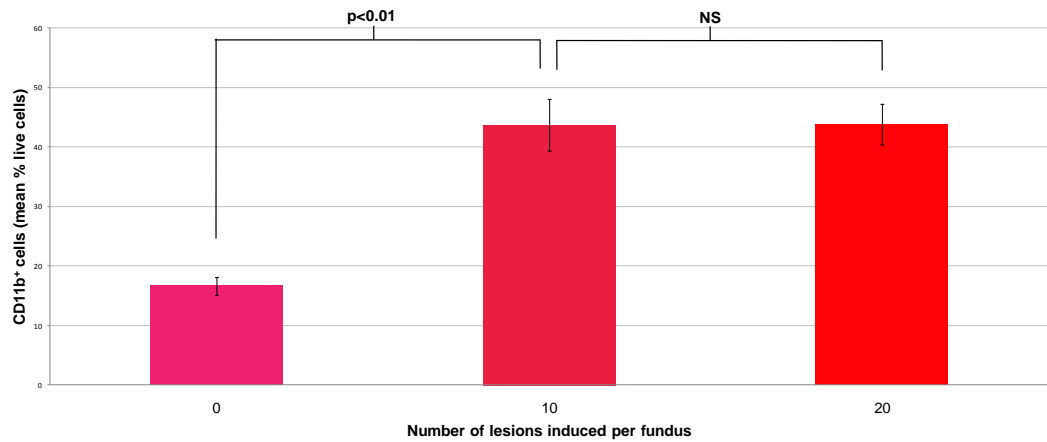
B
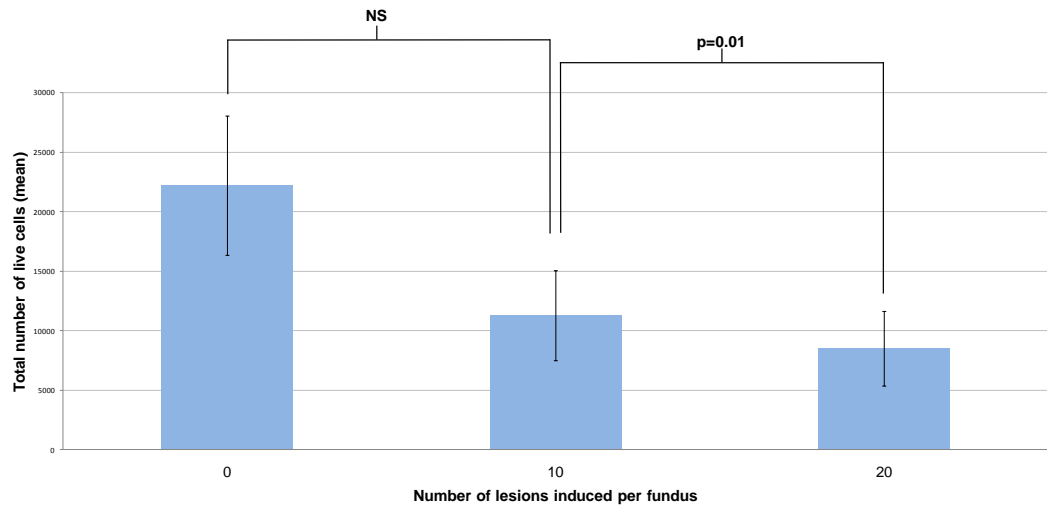
Figure 36 Induction of CNV by diode laser at 10 separate locations in each fundus results in significant inflammatory infiltrate without excessive tissue destruction in the choroid of <4m wild-type mice

The percentage of CD11b+ cells in the choroid increased at 3 days post-induction of CNV following delivery of either 10 or 20 burns to the fundi compared with unlasered tissue. There was no significant difference between groups receiving 10 or 20 burns in terms of CD11b+ cell infiltrate (A). Delivery of 20 burns to each fundus resulted in significant tissue loss in the choroid with less than half the number of live cells acquired for analysis compared with fundi receiving 10 burns each. There was no significant difference in live cell counts between the unlasered group and that receiving 10 burns per fundus. Delivery of 10 or 20 burns per fundus resulted in significant increases in the proportion of CD11b+ cells in the choroid. Choroids pooled for each animal and mean % of live cells calculated for CD11b+ population (n=9, 8 and 7 for unlasered, 10 and 20 lesions per fundus groups respectively); error bars=SEM.

4.5.1 The innate immune response to laser-induced CNV in wild-type mice

4.5.1.1 The innate immune response to laser-induced CNV in wild-type mouse retina

Laser-induction of CNV at 10 separate locations in the fundi of <4m wild-type mice resulted in significant increases in the key innate immune cell populations compared to age-matched unlasered tissue (t-test; $p<0.05$). As a proportion of live cells, CD11b$^+$ cells increased significantly, suggesting recruitment of cells from the periphery. The sub-population found to undergo the greatest rise were DCs which increased more than 10-fold, with granulocytes increasing more than 4-fold. A 3-fold increase in Gr-1$^-$ macrophages and 7-fold increase in Gr-1$^+$ macrophages was also noted – these constituted a much smaller proportion of live cells in lasered retina.

Comparison of lasered >18m wild-types with age-matched unlasered wild-type tissue suggested that only an increase in DC and granulocyte populations was reproduced post-laser in aged animals ($p<0.01$). Comparison of lasered and unlasered age-matched tissue should be viewed in the context of significant increases in the proportion of Gr-1$^-$ macrophages and DCs in unlasered tissue with age – this may account for significant increases post-laser in young groups for macrophage subpopulations but not in older animals. Subtraction of values obtained for age-matched *unlasered* tissue from those obtained for *lasered* tissue suggested no difference in the proportions of cells recruited to lasered retina between young and old wild-type animals. Statistical analysis of results obtained for young lasered and old lasered tissue revealed no significant difference in the proportions of any of the key populations with age (*Figure 37A*).

The data obtained from young and old lasered wild-type retina suggest the increase in CNV severity with age, in wild-types, is not due to differences in innate immune cell recruitment in the retina.

4.5.1.2 The innate immune response to laser-induced CNV in wild-type mouse RPE-choroid

Significant increases in the proportion of granulocytes and DCs were seen post-laser in <4m wild-type choroid (t-test unlasered vs lasered age-matched tissue; p<0.01) with a small, borderline significant increase in the Gr-1$^+$ macrophage population. The granulocyte population increased 4-fold in young animals after lasering (*Figure 38*A).

Only the proportion of granulocytes was significantly elevated in >18m wild-type RPE-choroid post-CNV induction with a 9-fold increase observed (p<0.01. Comparison of <4m, 12m and >18m lasered groups suggested a trend (of borderline significance) towards an increase in granulocyte recruitment to the lasered RPE-choroid (t-test <4m vs >18m lasered wild-types; p=0.06).

Values obtained for age-matched *unlasered* tissue were subtracted from those obtained for *lasered* tissue. Findings supported the evidence for enhanced granulocyte recruitment to choroidal CNV with age. DC recruitment appeared primarily to be a characteristic of young animals with recruitment appearing to decline with age.

The increase in granulocyte recruitment to lasered RPE-choroid may explain the observed increase in CNV lesion size with age in wild-types.

4.5.2 The innate immune response to laser-induced CNV in *CCL2$^{-/-}$* mice

4.5.2.1 The innate immune response to laser-induced CNV in *CCL2$^{-/-}$* mouse retina

Comparisons were made between genotypes and as well as within genotypes. Comparisons were also made between lasered and unlasered tissue within these two groups (*Figure 37B*).

Laser-induction of CNV at 10 separate locations in the fundi of <4m $CCL2^{-/-}$ mice resulted only in a significant increase in the granulocyte population in the retina (t-test unlasered vs lasered <4m wild-type tissue; p<0.01). This was in contrast to wild-type retina where all populations – in particular the DC population – were observed to increase significantly. This suggests that CCL2 is not as important for the recruitment of granulocytes (most likely neutrophils) as it is for other innate immune cell populations in the laser CNV model.

However, comparison of data obtained from lasered >18m $CCL2^{-/-}$ retinae with those obtained from unlasered >18m $CCL2^{-/-}$ mice revealed a borderline significant increase in the proportion of DCs in lasered $CCL2^{-/-}$ retina with age (t-test; p<0.06). Comparison across age groups in lasered $CCL2^{-/-}$ animals suggested that suppression of DC recruitment to lasered retinae was limited to animals <4m old with some recovery of recruitment by 12 months of age. As with wild-type animals, however, comparison of data obtained from lasered and unlasered age-matched tissue should be viewed in the context of significant increases in the proportion of Gr-1⁻ macrophages and DCs in unlasered tissue with age. Compensating for these changes, however, did not alter the trend for an increase in DC recruitment to lasered $CCL2^{-/-}$ retina with age.

The proportion of Gr-1⁻ macrophages was significantly reduced in the lasered <4m $CCL2^{-/-}$ mice in comparisons made between both unlasered and lasered tissue in young $CCL2^{-/-}$ mice and comparison of young lasered tissue between genotypes, and was seen to increase with age whilst remaining significantly lower than that in >18m unlasered tissue (t-test >18m unlasered vs >18m lasered tissue; p=0.05). Compensating for the increase observed in unlasered tissue with age suggested a possible emigration of Gr-1⁻ macrophages from the retina following laser in aged mice.

The granulocyte response to laser-induced CNV in the retina of $CCL2^{-/-}$ mice was maintained in >18m animals but found not to be significantly different to that seen in the <4m age group – reinforcing the conclusion that CCL2 is not vital to the recruitment of granulocytes to retina in this model.

4.5.2.2 The innate immune response to laser-induced CNV in *CCL2*^{-/-} mouse RPE-choroid

Comparisons were made between genotypes and as well as within genotypes. Comparisons were also made between lasered and unlasered tissue within these two groups (*Figure 38B).*

DC and macrophage recruitment recruitment in lasered <4m *CCL2*^{-/-} RPE-choroid was impaired (t-test <4m unlasered tissue vs. <4m lasered tissue). There was a doubling of the granulocyte population after lasering young animals that was of borderline significance (t-test <4m unlasered tissue vs. <4m lasered tissue; p=0.08). This pattern was largely maintained in aged animals - comparison of >18m unlasered mice with >18m lasered mice revealed that DC and macrophage recruitment remained impaired whilst a 5-fold rise in the proportion of granulocytes was observed (t-test >18m unlasered tissue vs. >18m lasered tissue; p<0.01*).*

As in retina, proportions of $Gr\text{-}1^+$ and $Gr\text{-}1^-$ macrophages were seen to increase significantly in lasered RPE-choroid with age (t-test <4m lasered vs. >18m lasered tissue; p<0.01 for both populations). Numbers were small, however, and taking into account populations in unlasered tissue revealed that recruitment remained unaltered with age.
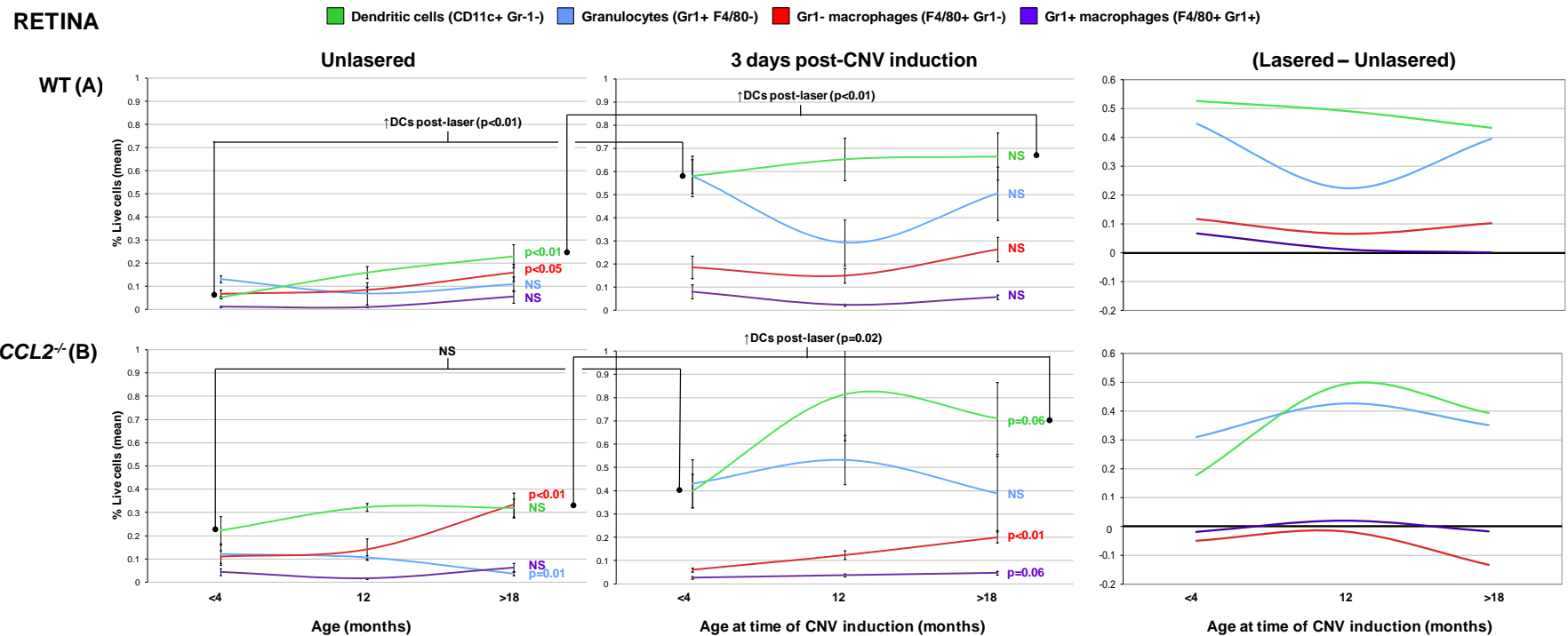
Figure 37 Gr-1⁻ monocyte/macrophages and DC recruitment to the retina following laser-induced CNV is impaired in young CCL2⁻/⁻ mice but DC recruitment appears to increase with ageing

Charts illustrating the key innate immune cell populations in wild-type (A) and CCL2⁻/⁻ mouse retina (B). Changes with age in unprocedured eyes are shown on the left and the changes with age in eyes 3 days after induction of 10 CNV lesions by diode laser are shown in the middle panels. Charts with corrections for the levels of innate immune cell populations present in the retina prior to lasering are shown on the right (percentages of cells in age-matched unlasered tissue subtracted from percentages of cells in lasered tissue). Comparison of age-matched unlasered and lasered tissue revealed a significant increase in all populations in young wild-type retina post-laser but only granulocytes and DCs in aged animals. Only the proportion of

granulocytes was increased post-laser in young CCL2$^{-/-}$ mice suggesting that granulocyte recruitment is not as dependent on CCL2 as other innate immune cell populations. Some recovery of DC recruitment to 12m and >18m lasered retina in CCL2$^{-/-}$ animals was noted in comparisons with age-matched unlasered tissue. Significant increases in Gr-1$^-$ macrophage populations with age in lasered CCL2$^{-/-}$ retina (t-test <4m vs >18m) most likely reflect underlying increases in these populations with age in unlasered tissue – correction for this suggested that laser induction of CNV resulted in net emigration of this population from the retina in the aged mice. Tissue pooled from each animal and mean % of live cells calculated for each population. N numbers for unlasered tissue as for Figure 29A and B. For lasered tissue: n=8, 4 and 7 for wild-type mice aged <4, 12m and >18m respectively and n=10, 5 and 6 for CCL2$^{-/-}$ mice aged <4m, 12m and >18m respectively. P values to the right of each plot are for t-tests comparing data obtained for <4m and >18m tissue. Error bars=SEM.
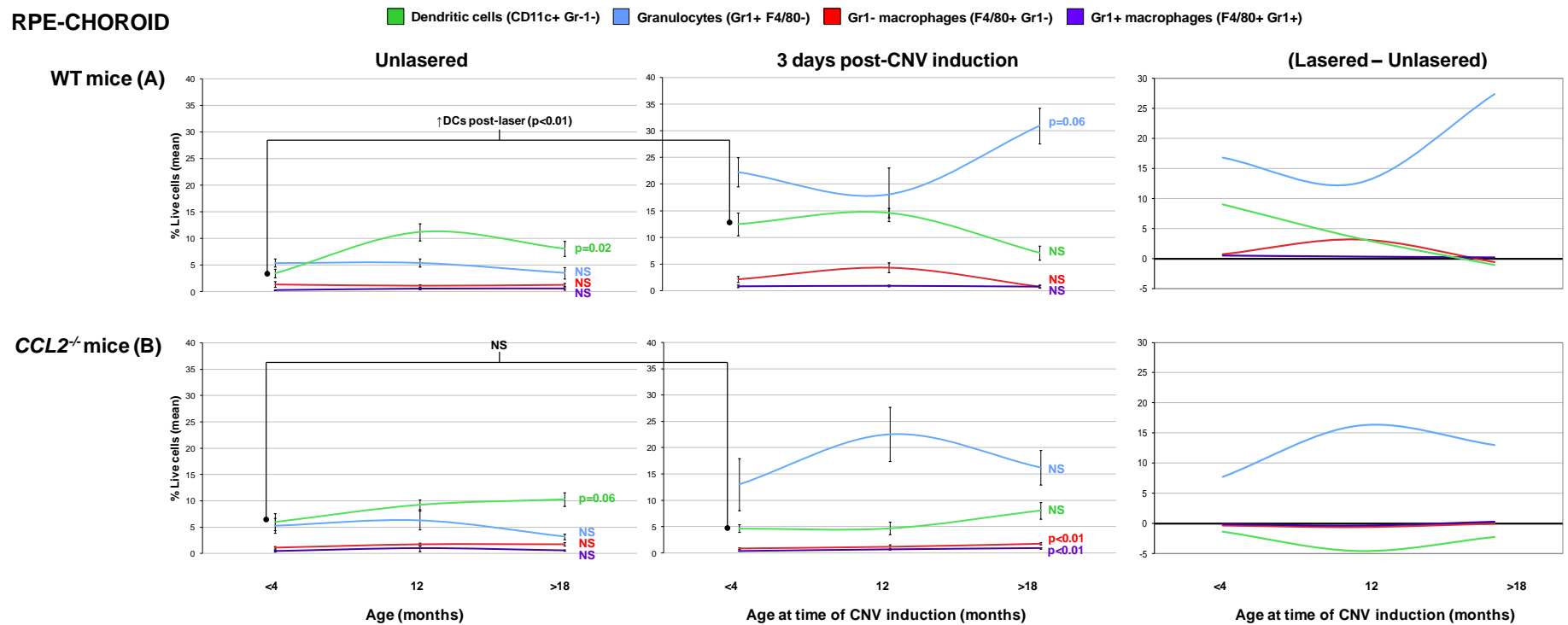
Figure 38. DC recruitment/maturation in the RPE-choroid following laser-induced CNV is impaired in young CCL2$^{-/-}$ mice and enhanced granulocyte recruitment may account for increased lesion size with age in both wild-type and CCL2-deficient animals.

Charts illustrating the key innate immune cell populations in wild-type (A) and CCL2$^{-/-}$ mouse RPE-choroid (B). Changes with age in unprocedured eyes are shown on the left and the changes with age in eyes 3 days after induction of 10 CNV lesions by diode laser are shown in the middle panels. Charts with corrections for the levels of innate immune cell populations present in the RPE-choroid prior to lasering are shown on the right (percentages of cells in age-matched unlasered tissue subtracted from percentages of cells in lasered tissue). Comparison of age-matched unlasered and lasered tissue

revealed a significant increase in granulocytes and DCs in young wild-type RPE-choroid post-laser (p<0.01) but only granulocytes in aged animals (p<0.01).The granulocyte population was seen to increase 4-fold in young WT mice and to increase 9-fold in aged WT mice post-laser. No significant difference in DC and macrophage/monocyte populations was observed post-laser in young CCL2$^{-/-}$ mice in comparison with age-matched unlasered tissue; a borderline significant doubling of the granulocyte population was observed, however (p=0.08). A significant increase in the proportion of granulocytes only was observed in aged CCL2$^{-/-}$ mice post-laser (5-fold increase; p<0.01). Tissue pooled from each animal and mean % of live cells calculated for each population. N numbers for unlasered tissue as for Figure 30A and B. For lasered tissue: n=9, 4 and 6 for wild-type mice aged <4, 12m and >18m respectively and n=8, 5 and 6 for CCL2$^{-/-}$ mice aged <4m, 12m and >18m respectively. P values to the right of each plot are for t-tests comparing data obtained for <4m and >18m tissue. Error bars=SEM.

4.6 The immunophenotype of a model of spontaneous choroidal neovascularisation

Confirmation of the involvement of specific immune cell populations in choroidal neovascularisation was sought through analysis of the innate immune cell populations present in the spleen, retina and RPE-choroid of <4m JR5558 mice. These animals develop CNV at multiple locations in the posterior fundus at p10-12 before expiring from leukaemia at approximately 3 months of age[184]. Retinal neovascularisation, though not choroidal neovascularisation, has been described in cases of acute myeloid leukaemia (in the absence of radiotherapy), chronic myelocytic leukaemia and acute lymphocytic leukaemia[185]. The underlying genetic defect in JR5558 mice is unknown. Given the significant increases in DCs and granulocytes associated with CNV at the 3 day timepoint in the laser model it was hypothesised that these cells might be implicated in CNV in JR5558 mice.

Flow cytometric analysis of splenocytes obtained from 2m old JR5558 mice revealed significant increases in the proportions of Gr-1$^+$ and Ly6C^{High} (CCR2$^+$) F4/80$^+$ cells compared with young adult wild-type mice – these populations were increased by as much as 14-fold (t-test $p<0.01$). A small, borderline significant increase in the proportion of Gr-1$^-$ macrophages was also observed but aside from this no other changes in the patterns of innate immune cell distribution in JR5558 mouse spleen were found.

In keeping with the above findings in the periphery, the levels of Gr-1$^+$ macrophages in JR5558 RPE-choroid were double that in young wild-types (t-test; $p<0.01$), however no changes were observed in any of the other key populations in this tissue. In JR5558 mouse retina, the granulocyte population was found to be significantly reduced whilst the proportion of DCs was more than double that observed in wild-type tissue (t-test; $p<0.01$). Macrophage/monocyte populations in retina were unchanged.

163

The above findings support evidence derived from application of the laser model in young wild-type and $CCL2^{-/-}$ animals for a role for DCs in pathological neovascularisation in the eye. The absence of any increase in this population in the RPE-choroid was unexpected, however, and it is possible that the Gr-1$^+$ macrophage population in the RPE-choroid, which is greatly elevated, is the main driver of choroidal neovascularisation in this model.

The dominance of the Ly6C^{High} (CCR2$^+$) monocyte population in JR5558 spleen (quite the reverse of findings in wild-type tissue) may explain the increase in Gr-1$^+$ macrophages in the RPE-choroid in these mice. The high levels of Ly6C^{High} (CCR2$^+$) monocytes in JR5558 spleen may also explain the increased levels of DCs in their retinae. Given that CCR2$^+$ monocytes are known precursors of inflammatory DCs one might hypothesise that a higher ratio of CCR2$^+$ monocytes to CCR2$^-$ monocytes in the periphery (as occurs in younger wild-type and CCL2$^{-/-}$ mice as well as JR5558 mice) favours higher levels of DCs in the tissues. An alternative explanation for the elevated proportion of DCs in the retinae of these mice is that this is a reactive phenomenon to choroidal neovascularisation and inflammation in much the same way that levels of DCs in the retina rise with age. In any case it is unlikely that retinal DCs play a minor role in the neovascular response in this model – whether a pro- or anti-angiogenic one remains to be confirmed.

The nature of the choroidal neovascularisation observed in JR5558 mice and that following laser-induced rupture of Bruch's membrane are clearly not directly comparable – the acute inflammation associated with neovascularisation in the laser model is typified by an increase in granulocytes in the retina whereas the opposite is seen in JR5558 mice. Equally, higher levels of DCs are seen in the retinae of aged wild-type and $CCL2^{-/-}$ mice yet this is not associated with the spontaneous neovascularisation observed in the JR5558 model. This suggests that the DCs recruited following laser-induction of CNV have a markedly different phenotype to those seen to accumulate with age in the retina and RPE-choroids of wild-type and $CCL2^{-/-}$ animals. Analysis of the innate immune cell populations in JR5558 mice is nevertheless relevant since the results support the involvement of DCs and Gr-1$^+$ macrophages in pathological

neovascularisation and indicate a role for changes in peripheral innate immune cell populations in driving this process.

A Spleen
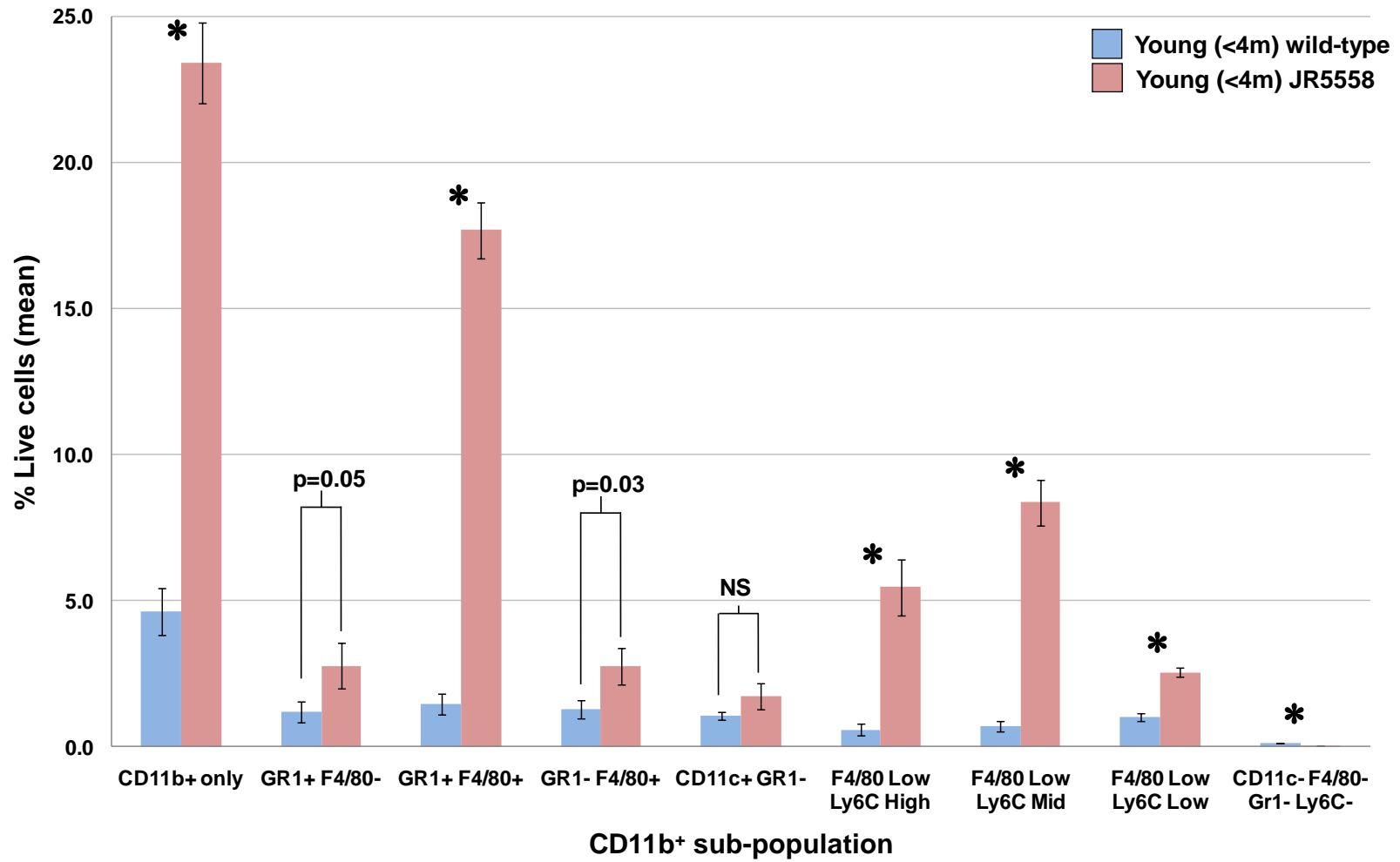
B Retina
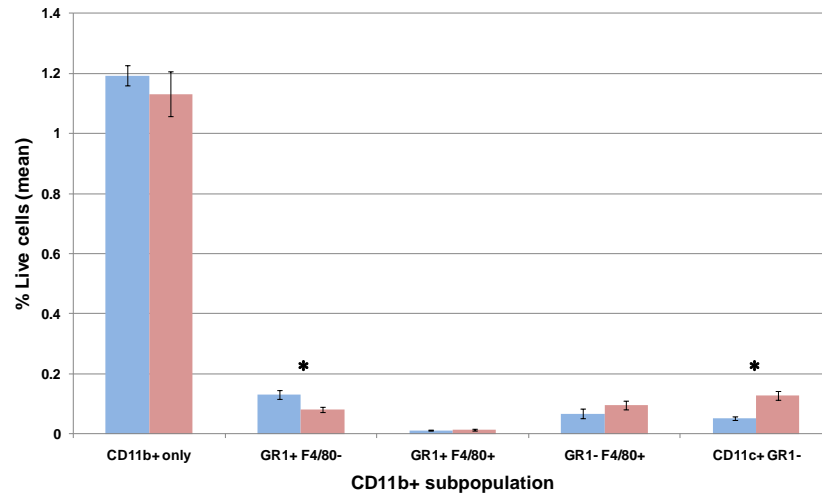
C RPE-choroid
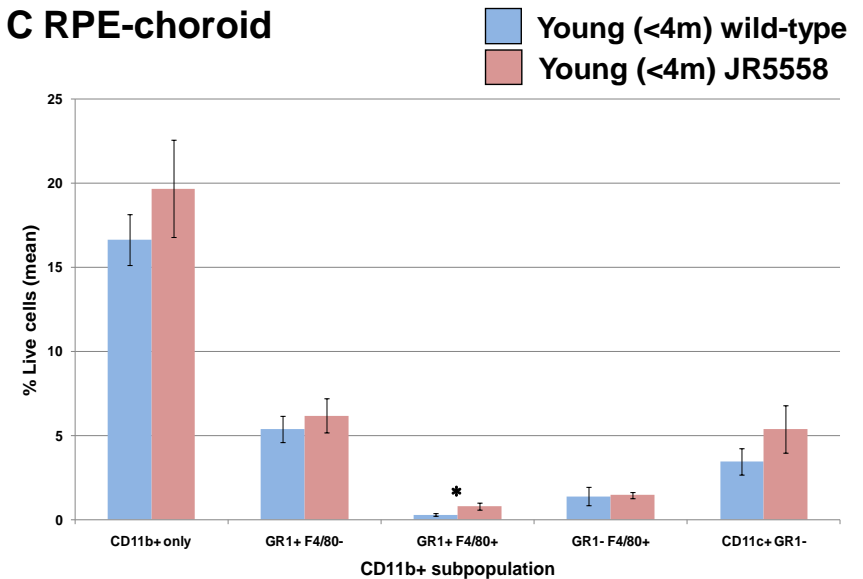
Figure 39 The pattern of innate immune cell distribution in the spleen, retina and RPE-choroid of JR5558 mice

The proportion of CD11b^{+}cells in young JR5558 spleen was significantly increased (A). Most of these cells were Gr-1^{+} macrophages/monocytes. Separation of monocyte subsets based on levels of Ly6C expression revealed a predominance of Ly6C[High] (CCR2^{+}) cells - whilst increases in all monocyte populations were observed, the Ly6C[High] (CCR2^{+}) population was found to be 9-fold greater in size than in young wild-type spleen (t-test; $p<0.01$). The pattern of monocyte distribution in the spleen was associated with changes in innate immune cell populations in both the RPE-choroids and retinae of JR5558 mice compared to wild-type age-matched animals. The proportion of DCs in JR5558 retina was more than double that in wild-type tissue (t-test; $p<0.01$) and the granulocyte population significantly reduced (B). In RPE-choroid levels of Gr-1^{+} macrophages were more than double in JR5558 mice, in keeping with findings in the spleen (t-test; $p<0.01$). Asterisks indicate significance of $p<0.01$.

4.7 Discussion

The purpose of the work described in this chapter was to identify whether changes in innate immune cell populations associated with CNV lesions, or in the periphery, might explain the increased severity of CNV with age and whether CCL2 has a role in this process.

To identify the key innate immune cell populations recruited to choroidal neovascular lesions in the mouse eye, CNV was induced in young adult wild-type eyes and the innate immune cell populations in retina and RPE-choroid analysed 3 days later (at the time of peak recruitment of these populations). All populations in the retina were seen to increase significantly after CNV induction – in particular those of granulocytes and DCs (*Figure 37*). Granulocytes and DC populations were also increased in the choroid post-laser (*Figure 38*). Interpreting these data required that age-related changes in unlasered tissue be taken into account. Findings were in keeping with published work suggesting that DCs and granulocytes have a role in pathological neovascularisation in the eye. It has previously been demonstrated that immature DCs (CD11c^{+} MHC class II[Low] cells) expressing VEGFR2 peak between 2 and 4 days post-induction of CNV by laser. Immature DCs have been shown to be closely involved with the developing neovascular complex and when transplanted intravenously are capable of augmenting CNV growth[160]. Other work has demonstrated that neutrophil recruitment peaks at 48 hours post-laser-induction, with neutrophils the predominant cell type at this timepoint[153]. In this thesis, granulocytes were found to be recruited in equal numbers to DCs at the 3 day timepoint, a finding which would be in keeping with the expected kinetics of innate immune cell recruitment.

The chemokine CCL2 is upregulated in the aged retina and choroid and is central to innate immune cell recruitment[124]. It was hypothesised that a deficiency in CCL2 might impair recruitment of innate immune cell populations expressing CCR2 and attenuate the neovascular response in young mice. It was also hypothesised that CCL2 deficiency would limit the increase in CNV lesion size observed with ageing in wild-types. To test the first of these

hypotheses, young adult wild-type and $CCL2^{-/-}$ mice were subjected to induction of CNV by laser and the mean lesion size in each group determined by fluorescein angiography 2 weeks later. The mean CNV lesion in <4m $CCL2^{-/-}$ mice was found to be 42% smaller (t-test; p<0.01) than that in age-matched wild-type mice (*Figure 34*). The innate immune cell populations recruited to lesions in <4m $CCL2^{-/-}$ mice were then determined as they had been for young adult wild-type mice using flow cytometry. The smaller mean CNV lesion size in CCL2-deficient mice was found to be associated with an impaired recruitment of DCs and macrophages to both retina and RPE-choroid. A two-fold increase in the granulocyte population in the RPE-choroids <4m $CCL2^{-/-}$ mice post-induction of CNV was identified - this was of borderline significance (unlasered vs. lasered tissue; p=0.08). The preservation of granuloctyte recruitment in $CCL2^{-/-}$ mice suggests that CCL2 is important for the recruitment of DCs and monocyte/macrophages to CNV lesions. It also suggests that the level of granulocyte recruitment in CCL2-deficient mice, though half that seen in wild-types, is still sufficient to drive a reduced neovascular response and that these cells are important in CNV development. The maintenance of granulocyte recruitment in the absence of CCL2 has also been demonstrated in $CCR2^{-/-}$ mice[70, 72].

The possibility that CCL2 deficiency in $CCL2^{-/-}$ mice would result in a failure to recruit CCR2+ monocytes – thereby confirming the pro-angiogenic or anti-angiogenic nature of this population - was investigated. Neither the CCR2+ nor the CCR2- monocyte populations (as determined using the Gr-1 marker) was increased in lasered RPE-choroids derived from either wild-type or CCL2-deficient mice. This suggests that these monocyte populations do not have an important role in CNV development, at least at the 3 day timepoint. However, a failure to increase the proportion of not only Gr-1+ macrophages but also Gr-1- macrophages did appear to be a feature of the retinal microenvironment 3 days post-laser induction of CNV in young $CCL2^{-/-}$ mice (reductions in the former population did not quite achieve significance however; t-test of lasered wild-type vs lasered $CCL2^{-/-}$ mouse retinae; p=0.065). On this evidence, CCL2 deficiency would in some way appear to affect not only the recruitment of CCR2+ monocytes but also, rather unexpectedly, CCR2- monocytes to the retina and

consequently it cannot be said with confidence whether one subset is more pro-angiogenic than the other. One possible explanation for this is that monocyte subpopulations were sequentially recruited, as has been described in other models. In the healing mouse myocardium post-infarction, for example, recruitment of CCR2$^+$ monocytes with phagocytic, pro-inflammatory capacities precedes the arrival of CCR2$^-$ monocytes with more pro-angiogenic, 'healing' properties[95]. It is therefore possible that failure to recruit CCR2$^+$ monocytes in young $CCL2^{-/-}$ mice at 1 or 2 days post-laser resulted in a subsequent failure of CCR2$^-$ monocyte recruitment at 3 days post-laser – analysis of these populations at these timepoints would be necessary to confirm this. It should be noted that use of the F4/80 marker did not allow for a distinction between proliferating microglia and recruited monocytes. Microglial proliferation and migration in response to CNV induction by laser has been demonstrated in a number of studies previously but the extent to which this behaviour influences CNV development has yet to be determined[186]. A further caveat to those data derived from use of the laser model was the observation that raised levels of CCR2$^+$ monocytes (Gr-1$^+$ or Ly6C^{High} F4/80$^+$ cells) in the spleens of JR5558 mice, together with raised levels of CCR2$^+$ monocytes in the choroid and DCs in the retina, were associated with spontaneous CNV. The model is not directly comparable with the laser-induced CNV model, however, and the cell populations involved in acute and chronic neovascular responses are likely to be very different. Nevertheless, results from analysis of JR5558 tissue do suggest an important role for CCR2$^+$ monocytes in the development of CNV.

To determine whether CCL2 deficiency attenuates the effects of ageing on CNV lesion size, wild-type and $CCL2^{-/-}$ mice aged 12 months and >18 months were subjected to laser induction of CNV and lesion sizes determined at 2 weeks post-laser. Results were compared with those obtained from <4 month old animals. A linear increase in mean lesion sizes in both groups was observed with age. Lesion sizes in aged animals were more than double those observed in young animals, regardless of genotype. The effect of CCL2 deficiency in attenuating CNV was preserved with ageing and linear regression analysis indicated that the protective effect of CCL2 deficiency was increased with age. Flow cytometry of retinal and RPE-choroidal cell suspensions derived from

lasered 12m and >18m mice was performed to determine whether changes in recruited innate immune cell populations might account for the differences in lesion sizes. Recruitment of key populations to lasered retina appeared to be unchanged in wild-type mice with age. DC recruitment to lasered $CCL2^{-/-}$ retinae increased with age whilst an emigration of Gr-1$^-$ macrophages also appeared to occur in older animals. Analysis of RPE-choroid, perhaps of more relevance given the inclusion of CNV lesions, suggested that recruitment of granulocytes to lasered choroid more than doubled with age in both wild-type and $CCL2^{-/-}$ mice. The possibility that enhanced granulocyte recruitment with age might explain the increases in lesion size with age for each genotype was considered, however flow cytometry results obtained from 12m wild-type mice were not entirely in keeping with the linear changes in lesion size. Granulocyte recruitment to wild-type choroid was seen to increase 4-fold in young wild-types, 3-fold in 12m mice, and 9-fold in >18m mice. Granulocyte recruitment to the choroids of $CCL2^{-/-}$ mice increased by 2-fold in young animals post-laser, over 3-fold in 12m mice and 5-fold in aged mice. The numbers of circulating neutrophils and their precursors are not thought to be affected by ageing in humans (this would fit with unchanged numbers found in the spleens of wild-type and $CCL2^{-/-}$ mice). However, evidence suggests that neutrophils derived from aged humans exhibit impaired chemotactic capacities - this would appear not be the case in mice in the laser-induced CNV model. Infiltrated neutrophils from patients with chronic inflammatory lung diseases and rheumatoid arthritis highly express chemokine receptors such as CCR2 on their surfaces that are absent or only marginally expressed on circulating neutrophils[85]. Similarly *in vivo* work in models of vasculitis has demonstrated that neutrophils express CCR2 in adjuvant-immunised but not naive rats and constitute the dominant population recruited by CCL2. This raises the possibility that neutrophil recruitment to aged or chronically inflamed retina and choroid may also be enhanced. Neutrophils in the elderly also adopt a low-grade inflammatory status in the absence of stimulation and release more elastase on activation. The release of more elastase by neutrophils recruited to Bruch's membrane could potentiate a choroidal neovascular response in the aged[126].

The possibility that increased DC populations observed in unlasered tissue with age might correlate with increased CNV lesion size was considered. This theory is not supported by the observation that the size of DC populations in the retina and RPE-choroid of young $CCL2^{-/-}$ mice is significantly higher than in young wild-types yet CNV size is significantly smaller. However, overall, innate immune cell numbers are increased in the unlasered tissue of both genotypes with age and this suggests underlying damage that renders the eye more susceptible to laser-induction of CNV. An untested observation was that cavitation bubbles arising from delivery of diode laser in older animals were consistently much larger than in younger ones suggesting that Bruch's membrane is more susceptible to rupture and that CNV might spread in the subretinal plane with more ease in aged eyes. This may be because the accumulation of subretinal microglia with age disrupts the interaction between RPE and neuroretina. It is likely that the DCs which accumulate with age in retina and RPE-choroid exhibit a more 'migratory' phenotype than the population recruited to CNV lesions which are most likely to be 'inflammatory' DCs. A more detailed phenotypic characterisation would be necessary to confirm this but these two DC subsets probably have very different pro-angiogenic capacities. Having demonstrated the infiltration of DCs into laser-induced CNV lesions in $CX3CR1^{GFP/+}$, Eter et al. concluded that these were of a 'conventional' (cDC) phenotype based on their expression of CD11b, however a high level of CD11b expression is also a feature of inflammatory DCs and consequently the marker cannot be used to distinguish the two populations[164, 186].

Finally, the possibility that the 3-fold increase in CNV lesion size with age in both genotypes might be explained by similar 3-fold increases in Gr-1⁻ monocyte/macrophage and DC populations in the spleens of $CCL2^{-/-}$ and wild-type mice was considered (*Figure 31*). The finding that DC populations in the spleens of $CCL2^{-/-}$ mice were smaller by a factor of 2 and those of Gr-1⁻ macrophages smaller by a factor of 3 compared with age-matched wild-types, correlated with the consistently smaller CNV lesion sizes observed in CCL2-deficient animals. It has also recently been established that post-ischaemic neovascularisation is highly dependent on monocyte levels in the bloodstream

and that CCL2/CCR2 signalling is important in regulating circulating levels of both CCR2$^+$ and CCR2$^-$ monocytes (it is postulated that the impact of disrupted CCL2/CCR2 signalling on CCR2$^-$ cells is a downstream consequence of a primary effect on CCR2$^+$ cells) [187, 188]. However, the age-related changes in systemic innate immune cell populations were not reflected in changes to the same populations recruited to CNV lesions post-laser. DC recruitment to lasered choroid, if anything, declined with age in wild-type and CCL2 deficient mice and Gr-1$^-$ macrophage recruitment appeared largely unchanged. So whilst changes in innate immune cell populations in the spleens of wild-type and *CCL2$^{-/-}$* mice underwent consistent changes with age it was not possible to infer a causative effect where increases in CNV lesion size were concerned. Interestingly, whilst granulocyte recruitment to lasered choroids was increased with age, no significant increase in granulocyte populations in spleens was seen.

In summary, granulocytes and DCs were identified as the main innate immune cell populations associated with laser-induced choroidal neovascularisation at the 3 day timepoint in mice. The almost 3-fold increase in CNV size with age observed in wild-type and *CCL2$^{-/-}$* mice might be explained by an increased propensity to recruit granulocytes to RPE-choroidal tissue with age, but these two factors could not be claimed to correlate closely. A 3-fold increase in Gr-1$^-$ macrophage and DC populations with age in unprocedured wild-type and *CCL2$^{-/-}$* mice spleens did correlate closely with increased CNV size but this was not reflected in changes in populations recruited to CNV lesions. Increased severity of CNV with age may therefore be a function of local anatomical changes (or a combination of factors including cytokine expression). CCL2 deficiency in young mice resulted in a significantly reduced proportion of Gr-1$^-$ monocyte/macrophages in retina in the acute phase following rupture of Bruch's membrane and this correlated with smaller CNV. CCL2 deficiency also results in the build-up of a Gr-1$^-$ resident macrophage population with age - were this population to exert a protective effect it might explain the slower increase in CNV size with age in *CCL2$^{-/-}$* mice. Finally, analysis of innate immune cell populations in the JR5558 model of spontaneous CNV indicates a particular role for CCR2$^+$ monocytes in pathological neovascularisation in association with

DCs in this model and provides further evidence to support the hypothesis that shifts in innate immune populations in the periphery are capable of influencing the pattern of innate immune cell distribution in the eye.

Chapter 5: Manipulation of innate immune cell populations as a means of attenuating pathological neovascularisation

The work in this chapter explores the effects of inhibition of tyrosine kinase receptors on innate immune cell populations in the context of experimental treatments for CNV. It also explores the effects of direct manipulation of innate immune cell activation on CNV growth through activation of the CD200R signalling pathway and the relationship to cell phenotype.

VEGF-A antagonists such as ranibizumab and bevacizumab improve vision in wet AMD by reducing the excessive vascular permeability of choroidal neovascular membranes. They do not, however, cause existing CNV to regress and the reduction of treatment below a critical level results in resumption of CNV growth and leakage[17]. It is possible that other VEGF family members and growth factors, such as platelet-derived growth factor B (PDGF-B) – known to promote pericyte survival - have a role in sustaining neovascular membranes. Manipulation of these other pathways may therefore prove useful in the development of more effective therapies for both wet AMD and neovascularisation in tumours. Consequently, a number of compounds have been developed which target the kinase activity of tyrosine kinase-containing receptors – of which VEGF receptors (VEGFR) and PDGF receptor (PDGFR) are closely related examples. Members of the VEGF family bind to three tyrosine kinase receptors: VEGFR-1, VEGFR-2 and VEGFR-3. Both VEGFR-1 and VEGFR-2 are expressed on vascular endothelial cells, monocytes, macrophages and haemopoietic stem cells. Receptor tyrosine kinase inhibitors (RTKIs) may therefore have intended or unintended effects on innate immune cell populations when employed in the treatment of wet AMD or other conditions where neovascularisation plays a prominent role[189].

The potential for receptor kinase inhibition in the treatment of CNV was explored using pazopanib, a small-molecule kinase inhibitor that blocks VEGFR1, VEGFR2 and VEGFR3 with 50% inhibitory concentration of 10nM, 30nM and 47nM respectively. It is also active, at higher concentrations, against PDGFR-B and c-Kit (a cytokine receptor expressed on the surface of haemopoietic stem cells), fibroblast growth factor receptor 1 (FGFR1), FGFR3 and c-fms (another tyrosine kinase receptor the ligand for which is macrophage colony stimulating factor, also known as M-CSF or CSF-1)[190].

Pazopanib has been demonstrated previously to be effective in inhibiting the development of CNV, causing the regression of established neovascular membranes following oral delivery and suppressing the development of CNV by as much as 93%[190]. An initial experiment was therefore performed to confirm the suppressive effect of pazopanib delivered by oral gavage in the mouse model of laser-induced CNV. Flow cytometric analysis of retinal and RPE-choroidal tissue harvested at 3 days post-laser induction of CNV in pazopanib-treated mice was undertaken in order to determine whether local innate immune cell populations might be affected by tyrosine kinase receptor inhibition and whether any changes might correlate with the effect of the drug on lesion size. Evidence is emerging to support a role for myeloid-derived innate immune cells in the regulation of tumour angiogenesis, growth and metastasis – in particular, research has focused on M1- and M2-polarised macrophages, Tie-2 expressing monocytes, myeloid-derived suppressor cells (defined as CD11b$^+$ Gr-1$^+$) and tumour-associated neutrophils. Other research has indicated the potential for RTKIs to promote tumour metastasis through their inhibition of pericyte recruitment to tumour vasculature. Further work was therefore undertaken to determine the effects of pazopanib on peripheral innate immune cell populations and provide information regarding its mechanism of action. Therapeutic doses of pazopanib were administered by oral gavage over a 17 day period to determine the response to laser-induced CNV and spleens from these animals were then harvested for flow cytometric analysis[189].

Pazopanib has been observed to remain associated with the uveal tract in rodents after quantitative whole body autoradiography experiments which may

be due to melanin binding (*Figure 49;* personal communication: Peter Adamson, GlaxoSmithKline). Experiments were therefore conducted to determine whether bound pazopanib in the uveal tract might have biological activity in the absence of detectable concentrations in the plasma. Were pazopanib bound within the uveal tract demonstrated to have therapeutic effects on CNV, this might allow for the development of reduced dosing regimens of the drug.

The potential to treat choroidal neovascularisation through the induction of specific regulatory pathways was investigated. Given the effect of CCL2-deficiency on lesion size in *CCL2$^{-/-}$* mice subjected to laser-induction of CNV, it was hypothesised that therapeutic manipulation of monocyte/macrophage activation might have a beneficial effect on the neovascular response. The membrane glycoprotein CD200 receptor (CD200R) is expressed on myeloid cells and T and B cell subsets, its ligand CD200 is a also a membrane glycoprotein that is expressed on a wide variety of cell types including lymphoid cells, neurones (such as those in the CNS and retina) and endothelial cells. Ligation of CD200R by CD200 has been demonstrated to inhibit classical monocyte/macrophage activation and suppress inflammation in a number of models (such as the experimental autoimmune uveitis and experimental autoimmune encephalomyelitis models) and CD200R signalling is down-regulated in lesions associated with multiple sclerosis, Parkinson's and Alzheimer's disease[110, 191-194]. Use of a rat monoclonal antibody that was agonistic for mouse CD200R allowed the effects of myeloid cell manipulation on CNV to be studied without the potentially confounding effects associated with use of more broad spectrum drugs such as pazopanib (especially given that monocyte/macrophages express VEGF receptors). The effect of an agonist for CD200R on CNV lesion size, following both intraperitoneal and intravitreal delivery of CD200R agonist was established. Changes in the proportions of innate immune cell populations in the retina and choroid were then determined using flow cytometry and immunohistochemistry.
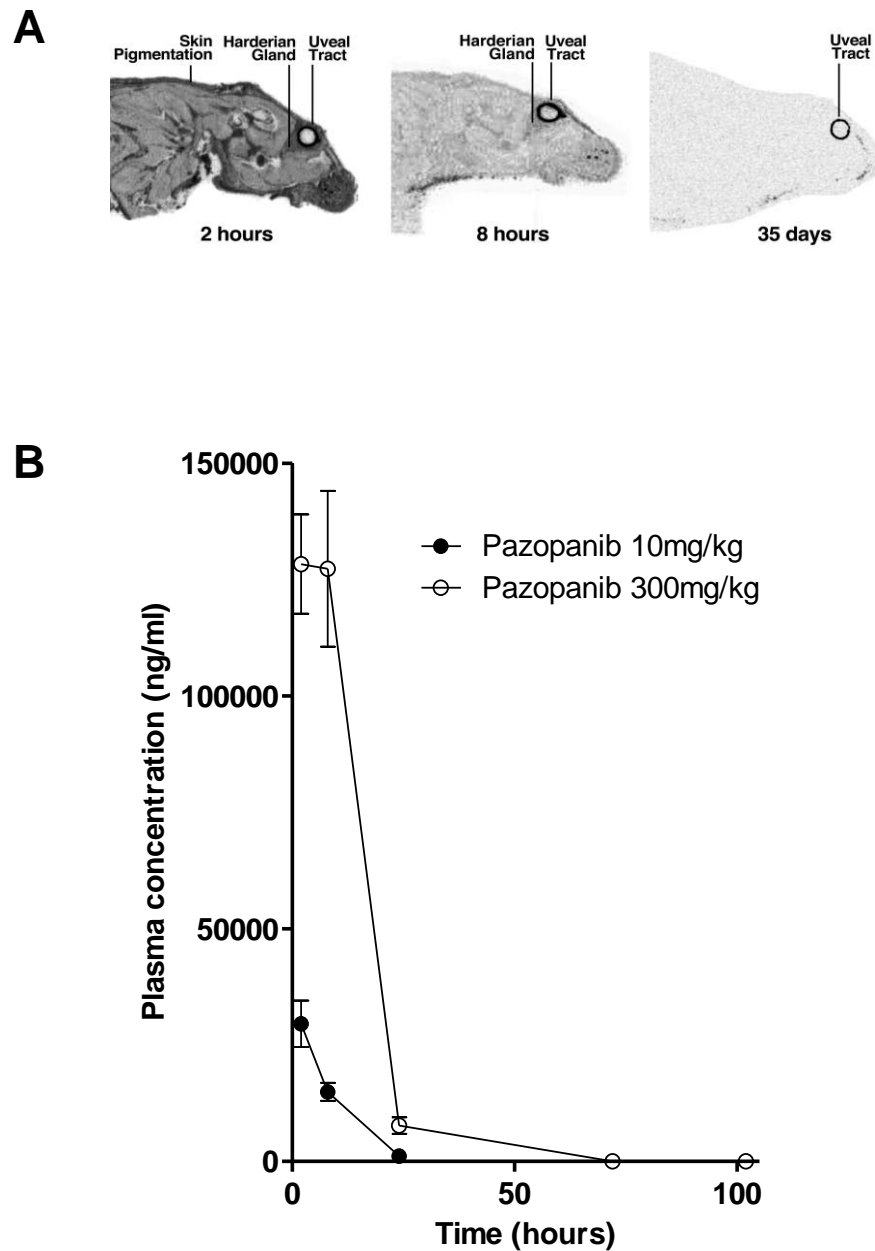
Figure 40 Pazopanib is retained in the uveal tract of rodents in the absence of detectable concentrations in the plasma

Whole body radiography of a rat following a single dose (100mg/kg) of pazopanib by oral gavage. Pazopanib radioactivity was observed in melanin-containing tissues including the uveal tract up to 35 days after delivery (A). Plasma concentrations following a single oral administration of pazopanib (10mg/kg or 300mg/kg) to 10wk old C57Bl/6NCrl mice (n=15/dose group). Levels of drug in the 300mg dose group approached limits of detection at 102 hours and were undetectable in the 10mg dose group at >72 hours post-delivery (B). Data reproduced by kind permission GSK Plc.

In summary, confirmation of the effect of receptor tyrosine kinase inhibition on laser-induced CNV was sought – therapeutics targeting multiple pathways simultaneously may prove the most effective way of controlling CNV in patients not only via their direct effects on endothelial cell proliferation but also on the recruitment and activation of innate immune cells. Such an approach may come with an increased risk of unwanted side effects, particularly on innate immune cell populations. Experiments were therefore designed to identify the effects of receptor tyrosine kinase inhibition on innate immune cell populations both in the eye and in the periphery. The possibility of using pazopanib's property of retention in the uveal tract to minimise dose was also explored. Finally, the potential for modulating monocyte/macrophage activation directly as a means of suppressing CNV was explored using an agonist for the CD200 receptor delivered both systemically and locally. The effect of such an approach on the local innate immunophenotype was also determined.

5.1 The effect of multi-target kinase inhibition in the laser-induced CNV model

Based on published data on the pharmacokinetics of orally administered pazopanib[190], young adult wild-type mice were divided into two cohorts with one group receiving vehicle only and the other a dose of 10mg/kg pazopanib twice daily by oral gavage for a total of 22 days, beginning 5 days before induction of CNV. Fundus fluorescein angiography was performed at 1 week and 2 weeks post-induction of CNV by diode laser and the results of the early phase of the angiograms analysed to determine the mean CNV lesion size in each cohort.

The results of early phase angiographic analysis revealed significant reductions in mean lesion size of 54% at 1 week post-induction of CNV in animals receiving pazopanib compared to vehicle only, and 60% at 2 weeks post-induction of CNV (t-test; p<0.01 at both timepoints; *Figure 41*). This effect compared favourably with published data indicating a 93% reduction in mean area of CNV at 2 weeks post-laser in wild-type mice receiving a dose of 10

A

B
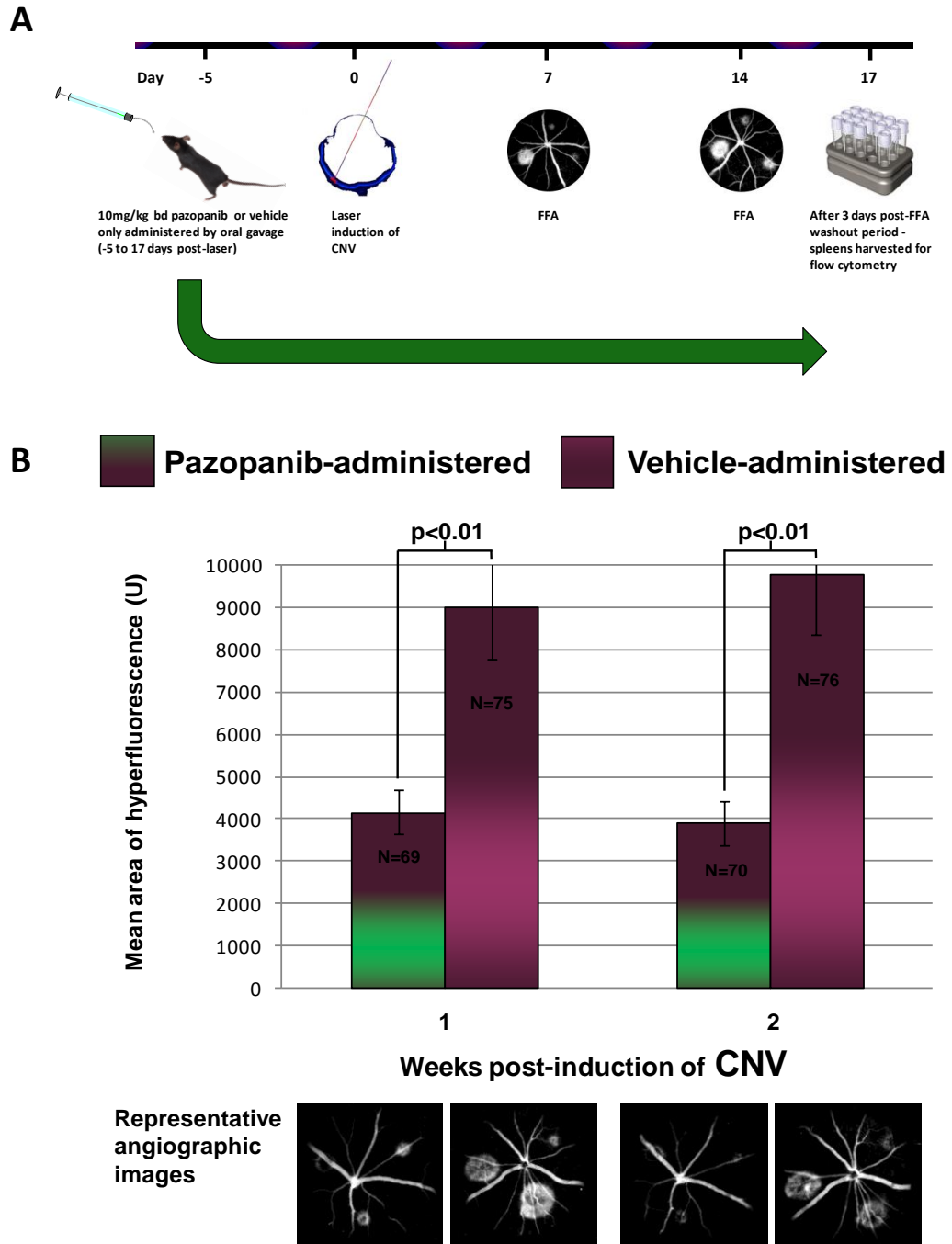
Figure 41 Pazopanib delivered by oral gavage results in a significant reduction in mean lesion size at 1 and 2 weeks post-induction of CNV by diode laser

Results of early phase angiographic analysis in animals receiving either pazopanib (20mg/kg) or vehicle only by oral gavage for a period before and after induction of CNV by diode laser. Figure shows experimental timeline (A) and mean lesion size in each experimental group at 1 week and 2 weeks post-induction of CNV with representative angiographic images below (B). Significant reductions in mean lesion size of 54% at 1 week post-induction of CNV and 60% at 2 weeks post-induction of CNV were observed in animals receiving pazopanib compared to vehicle only, (t-test; p<0.01 at both timepoints; error bars=SEM).

times higher (100mg/kg twice daily by oral gavage). The experimental protocol also differed from published work in that lesion size was determined by fundus fluorescein angiography as opposed to the analysis of choroidal flat-mounts obtained from fluorescein-labelled dextran-perfused animals[190].

5.2 Systemic delivery of pazopanib results in altered proportions of peripheral innate immune cell populations

To determine the effect of pazopanib on peripheral innate immune cell populations, spleens were harvested from young adult mice that had received either vehicle only or 10mg/kg pazopanib twice daily for a total period of 22 days. These mice underwent laser induction of CNV at three locations in each fundus at 5 days and fundus fluorescein angiography at 1 and 2 weeks post-laser. A washout period of three days following the last set of angiograms was included in the protocol to allow time for residual fluorescein (which is highly water soluble) to make its way out of system so that this did not interfere with flow cytometric analysis.

Splenocyte suspensions were stained for dead cells, CD11b, F4/80, Gr-1, Ly6C and CD11c as previously described. A significant reduction in the proportion of CD11b$^+$ Gr-1$^+$ cells was noted in the spleens of animals receiving pazopanib (t-test; vehicle only vs. pazopanib; $p < 0.05$), based on their lack of F4/80 expression these cells appeared to be granulocytes. No significant differences were observed in any other populations though trends towards reductions in levels of Gr-1$^+$ macrophages and Ly6C^{Low} monocytes were seen.

The reduction in Cd11b$^+$ Gr-1$^+$ cells in the spleens of pazopanib-treated animals is suggestive of an effect on myeloid-derived suppressor cells (MDSCs). MDSCs may be isolated from spleen, bone marrow and tumour infiltrate and are of interest in tumour biology because of their ability to promote tumour progression by rendering tumours refractive to anti-VEGF treatments[176].
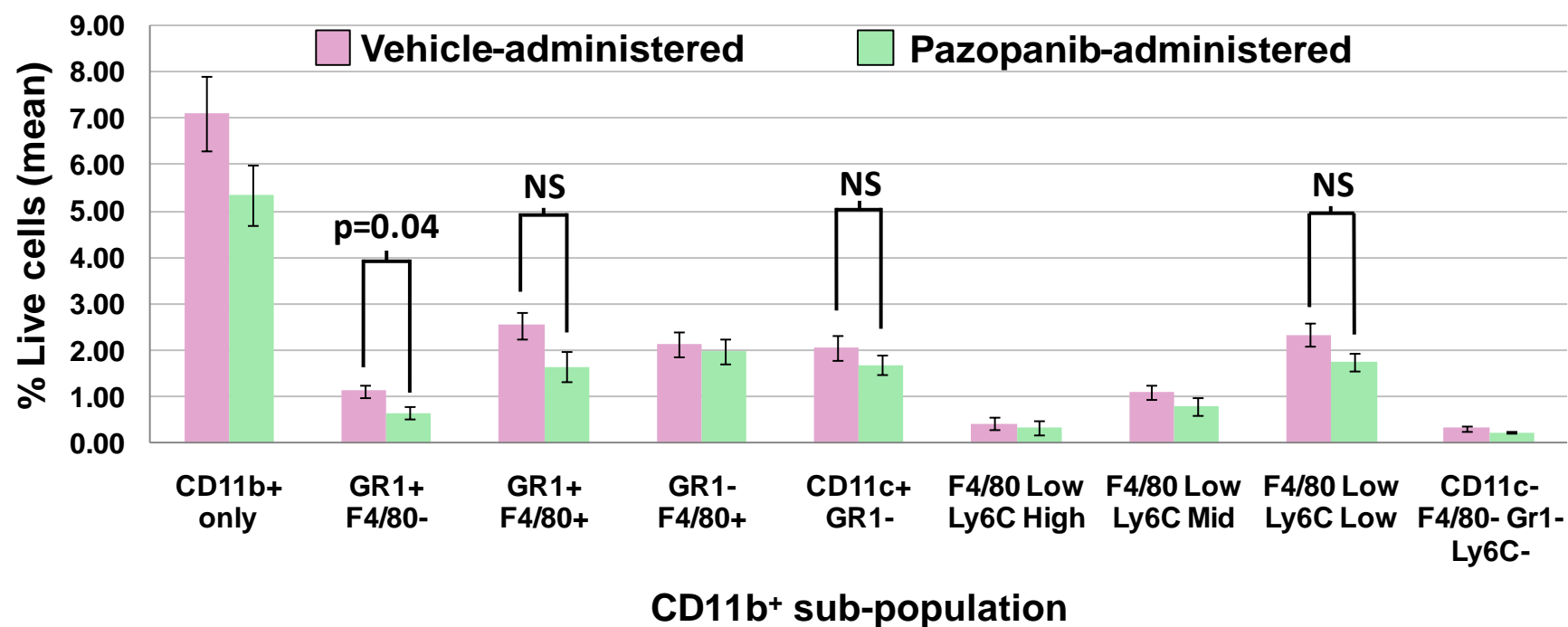
Figure 42 Prolonged systemic delivery of pazopanib is associated with a significant reduction in the proportion of granulocytes in the spleen

The proportions of innate immune cell subpopulations were determined in splenocyte suspensions obtained from young adult wild-type mice receiving either 10mg/kg pazopanib bd or vehicle only by oral gavage for a total of 22 days; mice were subjected to laser induction of CNV in three locations in the fundus after 5 days of oral gavage and underwent fundus fluorescein angiography subsequently (see Figure 41A). No significant differences were observed between any of the key populations except granulocytes which were significantly lower in animals receiving pazopanib (mean % live cells +/- SEM). N=5 for pazopanib-administered animals and N=5 for vehicle-administered animals.

5.3 The effect of multi-target kinase inhibition on innate immune cell populations in the retina and choroid

Previous work had demonstrated that all key innate immune populations were increased post-induction of CNV in wild-type mouse retina with similar increases observed in RPE-choroid (Gr-1$^-$ macrophages excepted in the case of lasered RPE-choroid). Laser-induction of CNV in the *CCL2$^{-/-}$* mouse had revealed that a failure of DC and Gr-1$^-$ monocyte/macrophage recruitment might be an important factor in the reduced levels of CNV in this model (*Figure 37* and *Figure 38*). To determine the effect of pazopanib on innate immune cell populations in retina and RPE-choroid post-induction of CNV, young wild-type mice were divided into two cohorts with one group receiving 10mg/kg pazopanib bd from 1 day pre-laser and the other receiving vehicle only. Tissue was harvested 3 days post-induction of CNV by diode laser, when macrophage infiltration is at its peak, and cell suspensions were subjected to flow cytometric analysis. CNV was induced at 10 separate locations in each fundus.

Analysis of cell populations derived from pazopanib-treated animals revealed that the proportion of Gr-1$^+$ monocyte/macrophages in the retinae of these mice was more than double that observed in those receiving vehicle only (t-test; p<0.05). There was also a trend towards an increase in the fraction of granulocytes and a more subtle reduction in the proportion of Gr-1$^-$ monocyte/macrophages in the retinae of pazopanib-treated animals. Analysis of RPE-choroidal cell suspensions revealed no significant differences between pazopanib and vehicle-treated animals although there was a trend towards increased levels of Gr-1$^+$ monocyte/macrophages and a reduction in levels of DCs in the pazopanib-treated group (*Figure 43*).

These results suggest a role for pazopanib in modulating monocyte/macrophage responses to laser-induced CNV, particularly in the retina. These data also provide additional evidence in support of a pro-angiogenic role for Gr-1$^-$ (CCR2$^-$) monocytes in the acute phase of pathological

neovascularisation in the eye that may be countered by measures favouring recruitment of Gr-1$^+$ (CCR2$^+$) monocytes.

5.4 Retention of pazopanib in the uveal tract may be exploited to minimise systemic exposure to drug

Pazopanib, administered by oral gavage or by periocular injection, accumulates in the uveal tract which is hypothesised to occur through an ability to bind ocular melanin (personal communication; Peter Adamson, GSK). Flow cytometric analysis of innate immune cell populations derived from the pazopanib-treated animals indicated that the drug appeared to have an effect on the proportions of innate immune cells in the retina and RPE-choroid following induction of CNV and also on myeloid-derived cell populations in the spleen following a protracted course of administration. It was hypothesised that melanosomes in the retinal pigment epithelium might act as a slow-release depot for pazopanib. An experiment was designed with the aim of establishing the longevity of action of retained pazopanib in the uveal tract. Were retained pazopanib demonstrated to be biologically active this would have implications for the optimisation of therapeutic dosing regimens (potentially limiting systemic exposure to the drug). It would also suggest that pazopanib's effect is derived from modulation of cell behaviour at a local rather than peripheral level provided no other tissues in the body exhibit a depot effect (this does not appear to be the case based on whole body quantitative autoradiography in rodents – personal communication; Peter Adamson, GSK).

Previous work had indicated that pazopanib has a predicted half-life in the mouse of <4 hours[190]. It was calculated that dosing 3 days prior to induction of CNV would result in only 0.0001% of the original oral dose remaining at the time of the lasering. Young adult wild-type mice were administered single doses of pazopanib, ranging from 3 – 300mg/kg, or vehicle only and then subjected to induction of CNV by diode laser at three separate fundus locations 3 days later. Peripheral blood samples were collected from three animals receiving the highest dose of pazopanib at the day 3 timepoint to confirm undetectable

A

B Retina

C RPE-choroid
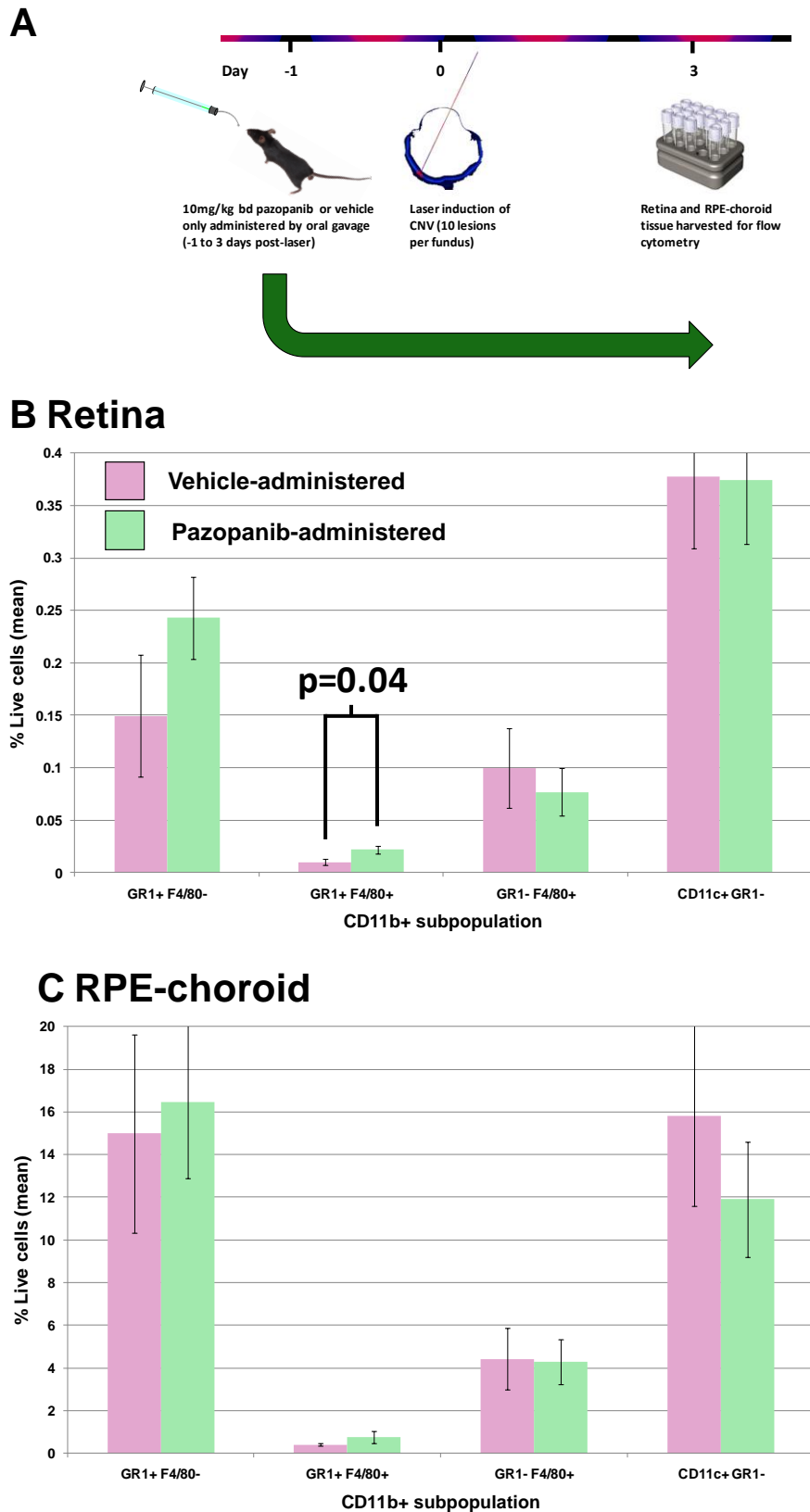
Figure 43 Pazopanib increases levels of Gr-1⁺ monocyte/macrophages in the retina at the 3 day post-laser timepoint

Timeline summarising the experiment is shown (A). The proportions of key innate immune cell populations in the retinae (B) and RPE-choroids (C) of young adult wild-type mice 3 days post-induction of CNV following administration of pazopanib 10mg/kg twice daily by oral gavage (-1 to 3 days post-laser). The proportion of Gr-1$^+$ monocyte/macrophages in the retinae of pazopanib-treated mice was more than double that observed in animals receiving vehicle only with a trend towards a reduction in the Gr-1$^-$ fraction. Trends towards an increase in the fraction of Gr-1$^+$ monocyte/macrophages in RPE-choroids of pazopanib-treated animals and a decrease in the fraction of DCs were also observed. Mean % live cells calculated from retinal cell suspensions obtained by pooling tissue from both eyes of each animal. CNV induced at 10 separate locations per fundus. N=7 for pazopanib-treated mice and n=5 for vehicle-treated mice.

levels of pazopanib in the plasma at the time of CNV induction. Fluorescein angiography was then performed at 7 and 14 days post-laser.

Initial results indicated that pazopanib delivered at a dose of 10mg/kg and above 3 days prior to induction of CNV was capable of significantly reducing CNV lesion size two weeks post-induction of CNV (*Figure 44*) – that is with the exception of the group receiving a dose of 30mg/kg in which a reduction was observed that did not achieve significance (p=0.09), the reasons for this were unclear. However, analysis of plasma samples revealed detectable levels of pazopanib well above those expected (GSK; data not shown) and therefore the possibility that circulating pazopanib may have had an effect on CNV development could not be excluded.

The experiment was repeated with a 5 day lag time after dosage of animals with 30mg/kg pazopanib, 3mg/kg pazopanib or vehicle only (*Figure 45*). Levels of pazopanib were found to be undetectable (analysis by GSK – data not shown) at the day 0 timepoint, when CNV was induced. Since oral pazopanib had been demonstrated to have an effect on peripheral innate immune cell populations following multiple administrations over a prolonged period (*Figure 42*), splenocyte suspensions derived from animals dosed either with pazopanib or vehicle 5 days previously were analysed for changes to proportions of innate immune cell sub-populations – no changes were observed. Results indicated that a 30mg/kg dose of pazopanib was sufficient to have an effect on CNV induced 5 days later when fundus fluorescein angiography was performed at the 1 week post-laser timepoint but not at 2 weeks (t-test vehicle vs. pazopanib-dosed groups; p=0.05 for group receiving pazopanib 30mg/kg and p=0.08 for 3mg/kg group). Results for animals receiving 3 mg/kg pazopanib suggested a non-significant intermediate effect supportive of a dose-dependent response. These data indicate that retained pazopanib is pharmacologically active and has a potential therapeutic effect in CNV for up to a week after induction, with lesion size remaining reduced (if not quite significantly) at 2 weeks post-induction when levels of the drug are presumably insufficient to prevent the further increase in lesion size that is observed in vehicle-administered animals.
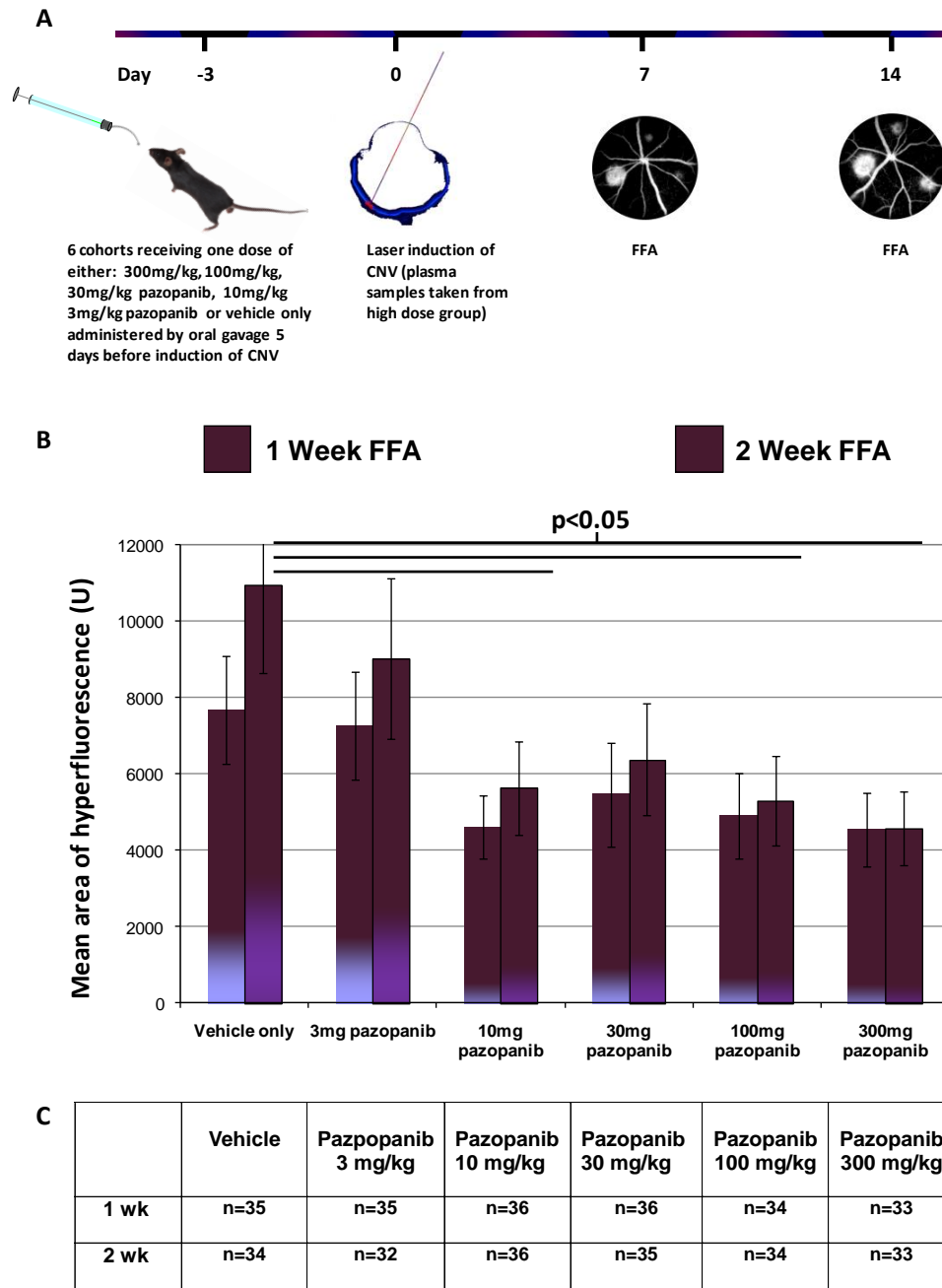
Figure 44 The effect on lesion size of pazopanib delivered by oral gavage 3 days prior to induction of CNV by laser

Multiple dosages of pazopanib or vehicle delivered by oral gavage 3 days prior to induction of CNV. Timeline for experiment shown (A). Mean lesion size in each group following fundus fluorescein angiography at 1 and 2 weeks (B) and N numbers (C). Initial results indicated that pazopanib delivered at a dose of 10mg/kg and above, 3 days prior to induction of CNV, was capable of significantly reducing CNV lesion size two weeks post-induction of CNV. However, analysis of plasma samples revealed detectable levels of pazopanib well above those expected (GSK; data not shown) it could therefore not be concluded that melanosome-bound pazopanib was responsible for the observed effects on CNV. Error bars = SEM.

A

Day -5   0   7   14

Wild-type mice dosed with pazopanib or vechicle only by oral gavage at -5 days

Induction of CNV by diode laser

FFA

FFA

B

Vehicle-administered

Pazopanib-administered (3mg/kg)

Pazopanib-administered (30mg/kg)

p=0.05

p=0.08

Mean area of hyperfluorescence (U)

N=75   N=80   N=83   N=76   N=76   N=82

Weeks post-induction of CNV

Representative angiographic images
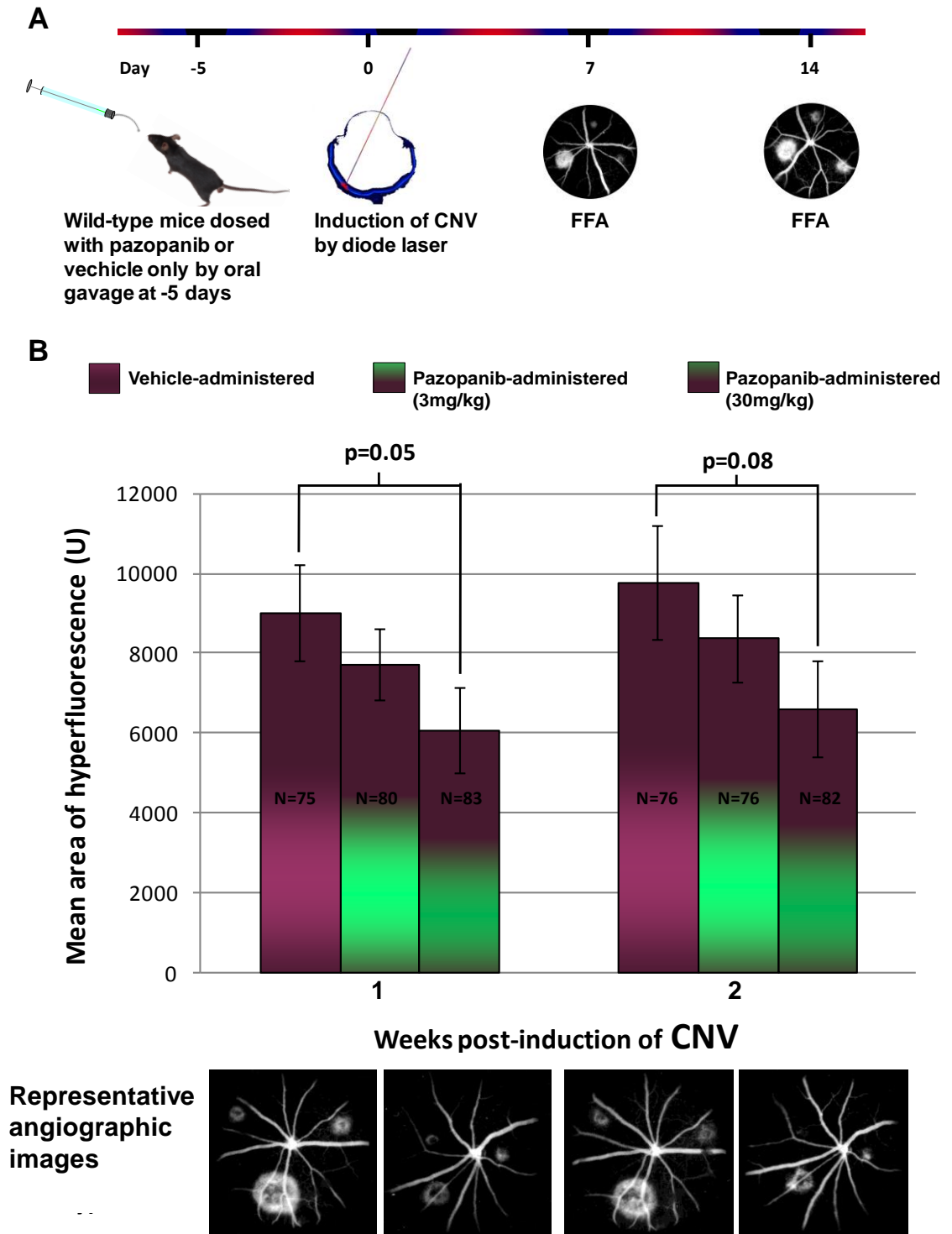
Figure 45 Pazopanib retained in the uvea exhibits a depot-effect and is biologically active

Young adult wild-type mice were administered a single dose of either 30mg/kg pazopanib, 3mg/kg pazopanib or vehicle only by oral gavage 5 days prior to induction of CNV by diode laser. Timeline for experiment is shown (A). Levels of pazopanib in the 30mg/kg group were found to be undetectable at the day 0 timepoint, when CNV was induced (n=4; plasma concentrations as determined by GSK using HPLC/MS). A 30mg/kg dose of pazopanib resulted

in sufficient levels of bioavailable, melanosome-bound drug to significantly reduce lesion size by a third at 1 week post-induction of CNV and possibly beyond, though results did not quite achieve significance at 2 weeks (B; t-test vehicle vs pazopanib 30mg/kg; p=0.05 at 1 week and p=0.08 at 2 weeks). Representative images taken from vehicle-administered and 30mg/kg pazopanib-dosed animals.
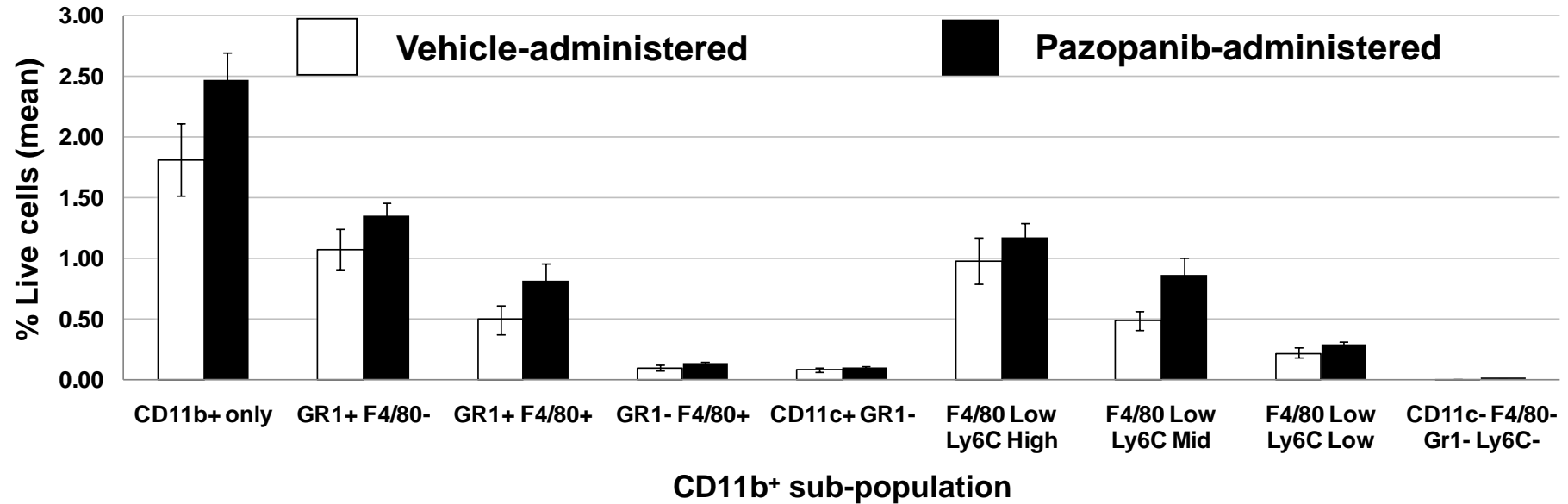
Figure 46 Pazopanib delivered by oral gavage (30mg/kg) has no effect on peripheral innate immune cell populations at 5 days post-delivery

Pazopanib had previously been demonstrated to have an effect on innate immune cell populations in the spleen following prolonged administration by oral gavage. Innate immune cell populations in spleens harvested from young adult wild-type mice 5 days after delivery of either 30mg/kg pazopanib or vehicle were analysed to exclude the possibility that changes in peripheral innate immune cell populations might account for the depot-effect observed with pazopanib retained in the uvea. Results demonstrated no significant effect on any peripheral innate immune cell populations that might account for the effect on CNV lesion size observed in pazopanib-treated animals at this timepoint.

5.5 The effect of CD200R agonist on laser-induced choroidal neovascularisation

Induction of CD200R signalling on monocyte/macrophages has been demonstrated to significantly attenuate inflammatory responses in models of autoimmune uveitis and autoimmune encephalitis and down-regulation of signalling has been linked with multiple sclerosis, Parkinson's and Alzheimer's disease[107, 109, 110, 191, 192]. Evidence suggests that CD200-CD200R interactions exert their effect through alternative macrophage activation[193].

To establish whether alternative activation of monocyte/macrophages has an effect on the development of CNV, young adult mice were subjected to induction of CNV by diode laser and injected intravitreally with either 10µg of an agonist rat IgG1-anti-mouse CD200R mAb (courtesy of Andrew Dick/DNAX Schering-Plough) or isotype control 3 days later[109]. Animals were injected at the 3 day timepoint because this was known to be the peak time for macrophage recruitment to CNV lesions[153, 155]. Lesion sizes were assessed by fundus fluorescein angiography at 7 and 14 days post-laser.

Results indicated that induction of CD200R signalling by intravitreal injection of an agonist antibody 3 days post-laser significantly reduced mean lesion size in young adult wild-type mice at the 2 week timepoint by as much as 43% (*Figure 47*; t-test isotype control vs. CD200R agonist-injected eyes). This suggests that innate immune cell controlled CNV remodelling takes place over a relatively prolonged period even though lesion size is almost maximal at 1 week post-induction. Consequently, there may be a wide window of opportunity for intervention by way of driving alternative macrophage activation. The effects of a once-only injection of the more specific CD200R agonist into the eye also compared favourably with those of daily delivery of pazopanib by oral gavage (*Figure 41*).
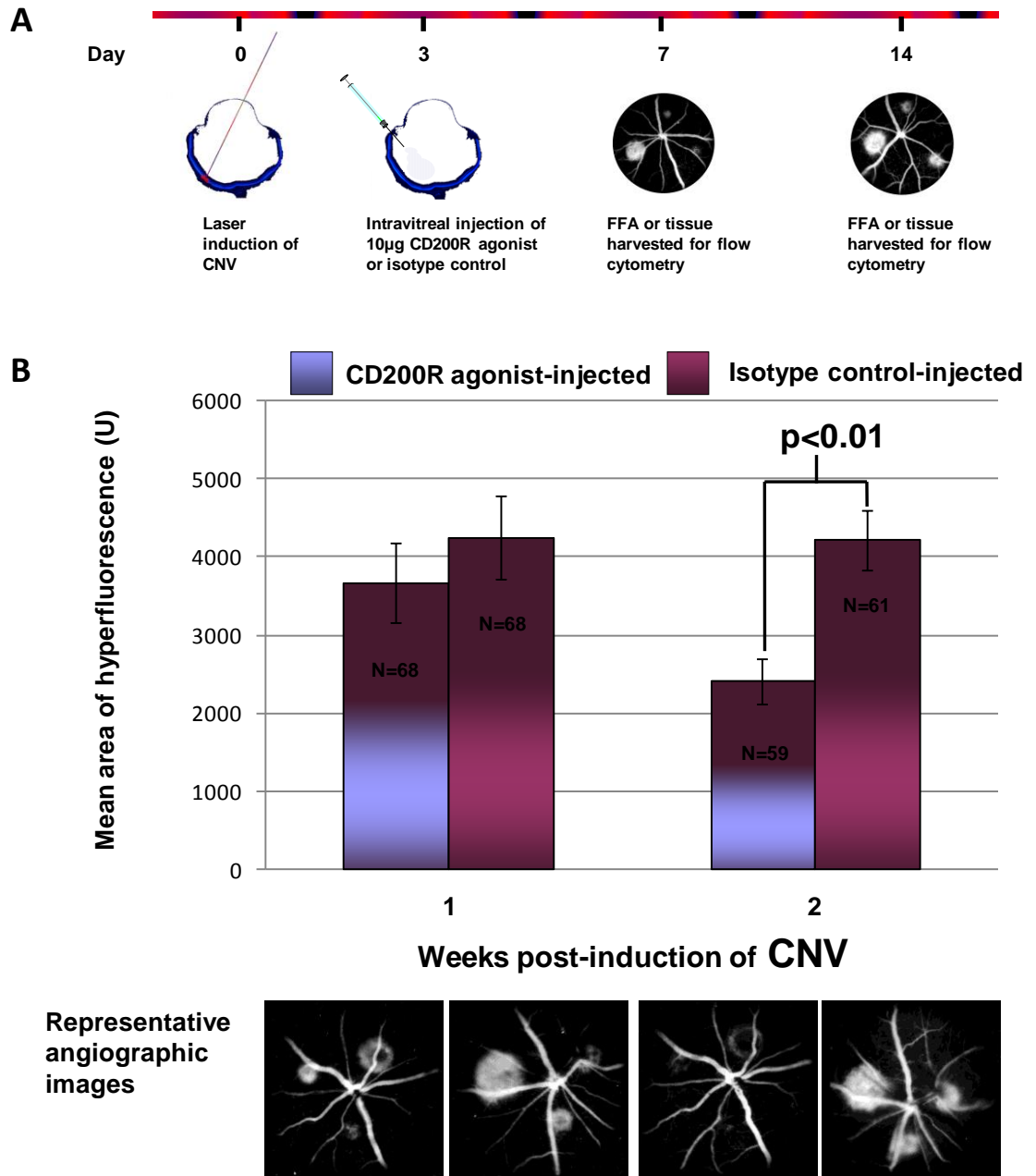
Figure 47 CD200R agonist delivered at the time of peak monocyte/macrophage recruitment results in significantly reduced mean lesion size on fundus fluorescein angiography performed 2 weeks after laser-induction of choroidal neovascularisation

Mean lesion size following laser-induced CNV in young adult WT mice following injection of either CD200R agonist or isotype control antibody at 3 days post-laser (timeline of experiment - A). Results are shown from the early phase of fluorescein angiograms at 1 and 2 weeks post-laser (B - mean area of hyperfluorescence +/- SEM; N refers to number of lesions) with representative images from angiograms shown below. Mean lesion size in mice receiving 10µg CD200R agonist compared with isotype control antibody was significantly reduced by 43% at the 2 week post-laser timepoint (t-test; p<0.01).

5.6 Effect of CD200R agonist on CNV correlates with changes in innate immune cell populations in the retina and choroid

Having established that delivery of a CD200R agonist 3 days post-induction of CNV resulted in a significant reduction in lesion size, confirmation of an effect on innate immune cell populations was sought by assessing the phenotype of myeloid-derived cells present in the retinae and RPE-choroids of CD200R agonist- or isotype control-injected young adult wild-type mice at the 1 and 2 week post-laser timepoints (*Figure 48*).

To drive detectable levels of cell recruitment/proliferation, CNV was induced at 10 separate locations in each fundus. Intravitreal delivery of 10µg CD200R agonist at 3 days post-laser resulted in a significant increase in the proportion of Gr-1$^-$ monocyte/macrophages in the retina at 1 week and granulocytes in the RPE-choroid at the 2 week timepoint (*Figure 48A and Figure 49B*; t-tests of pooled tissue from CD200R-injected eyes vs. isotype control-injected eyes; $p<0.05$ for Gr-1$^-$ macrophages in retina at 1 week and $p<0.05$ for granulocytes in RPE-choroid at 2 weeks). No significant differences were observed in any other innate immune cell populations.

Induction of CD200R signalling therefore resulted in an increase in the proportion of Gr-1$^-$ monocyte/macrophages in the retina that preceded breakdown of the neovascular complex, with a subsequent increase in the recruitment of granulocytes (most likely neutrophils) to the RPE-choroid. The recruitment of neutrophils to the RPE-choroid at two weeks may be explained by an increase in CNV-derived cellular debris requiring clearance.

Immunohistochemical confirmation of the innate immune cell phenotypes present in the CNV lesions of CD200R agonist-injected or isotype control-injected eyes at the 1 week timepoint was sought. A total of 3 CD200R-injected eyes and 3 isotype control-injected eyes were harvested for

immunohistochemistry at 1 week post-induction of CNV. Saggital sections were stained for F4/80 and Ly6C (the Ly6C$^-$ macrophage population was found to behave identically to the Gr-1$^-$ macrophage population on flow cytometric analysis – data not shown). In keeping with the results of flow cytometric analysis smaller lesion size was associated with higher numbers of Ly6C$^-$ F4/80$^+$ cells in the retina (*Figure 50*). Accurate quantification of macrophage numbers in sections was not possible given the close proximity of cells to one another in the retina, CNV lesions and RPE-choroid. Consequently only representative images are shown.

Ly6C and Gr-1 were found to be expressed in a similar pattern to that obtained from immunostaining of the retinal vasculature and choroid. Confirmation of co-localisation of Gr-1 expression with the vascular marker collagen IV was therefore obtained (*Figure 51*). Constitutive expression of Ly6C on a subpopulation of small vessel endothelium has been described previously, though not in the retina/choroid[195-197]. Gr-1 has not been described as being expressed on vascular endothelium before. Confirmation that monocyte/macrophages expressing the CD200R were present in the periphery and in the eye was also sought. Immunostaining for the markers F4/80, Ly6C and CD200R revealed the presence of large numbers of CD200R positive, Ly6C$^-$ monocyte/macrophages clustered around large, multinucleated F4/80$^-$ Ly6C^{High} cells in young adult wild-type spleen follicles (*Figure 52A*).

Immunostaining of saggital sections taken from young adult wild-type mouse eyes 1 week after induction of CNV in 10 locations revealed the presence of Ly6C$^-$ CD200R$^+$ macrophages in close proximity to retina overlying CNV. CD200R is known to be expressed on a range of myeloid cell types, whether it is preferentially expressed on Ly6C^{High} (CCR2$^+$) or Ly6C^{Low} (CCR2$^-$) monocytes is not known though these results would suggest that levels are higher on Ly6C^{Low} populations. The possibility that those cells staining positive for CD200R in the spleen might be DCs could not be excluded – CD200R has been demonstrated to be most highly expressed on DCs[194]. In keeping with
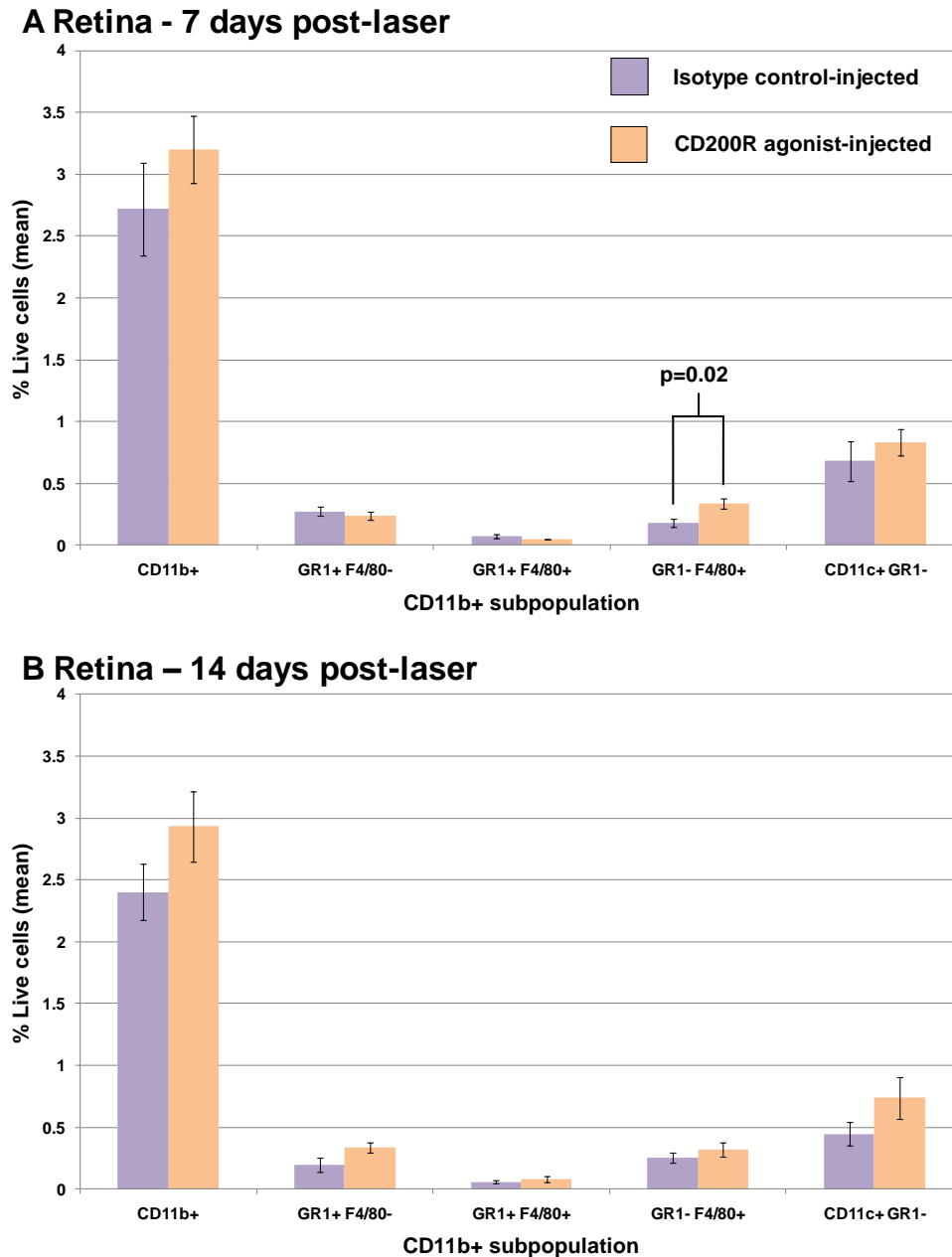
Figure 48. CD200R agonist delivered at the time of peak monocyte/macrophage recruitment following laser-induction of CNV results in a significant increase in the proportion of Gr-1$^-$ macrophages at 1 week post-laser in the retina

The proportion Gr-1$^-$ (and Ly6C$^-$ macrophages – data not shown) in the retinae of young adult wild-type mice following intravitreal delivery of CD200R agonist 3 days post-induction of CNV was found to be significantly increased compared with isotype antibody injected controls at 1 week post-laser (A). The difference was not maintained at 2 weeks post-laser (B). Mean % live cells calculated from retinal cell suspensions obtained by pooling tissue from both eyes of each animal. CNV induced at 10 separate locations per fundus. For isotype control-injected mice, n=5 and 9 for the 1 week and 2 week timepoints respectively; for CD200R agonist-injected mice, n=6 and 8 for 1 week and 2 week timepoints respectively; error bars=SEM.

A RPE-choroid - 7 days post-laser
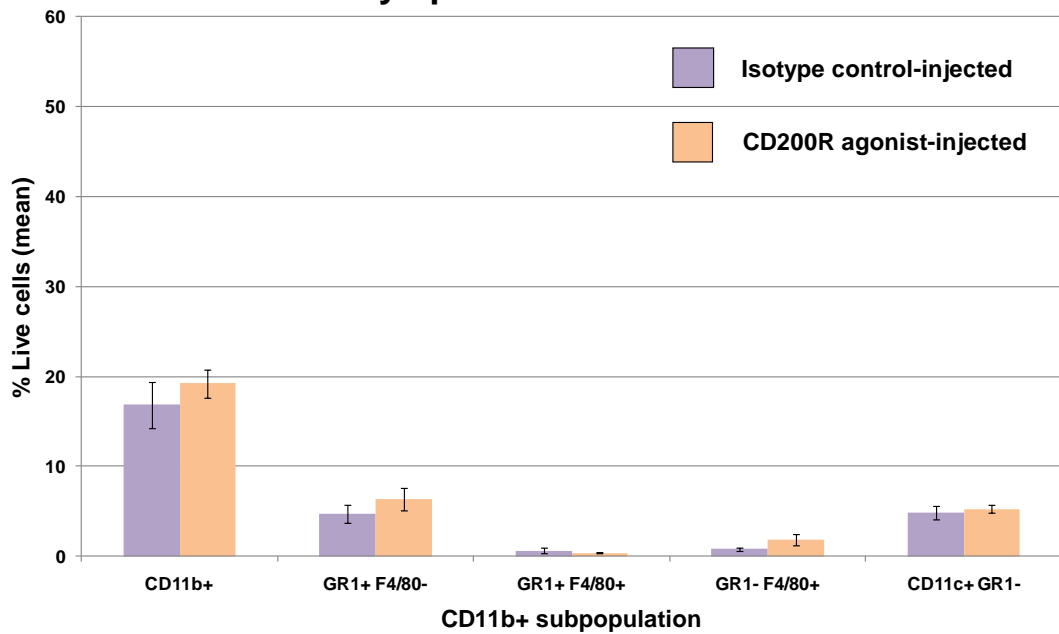
B RPE-choroid - 14 days post-laser
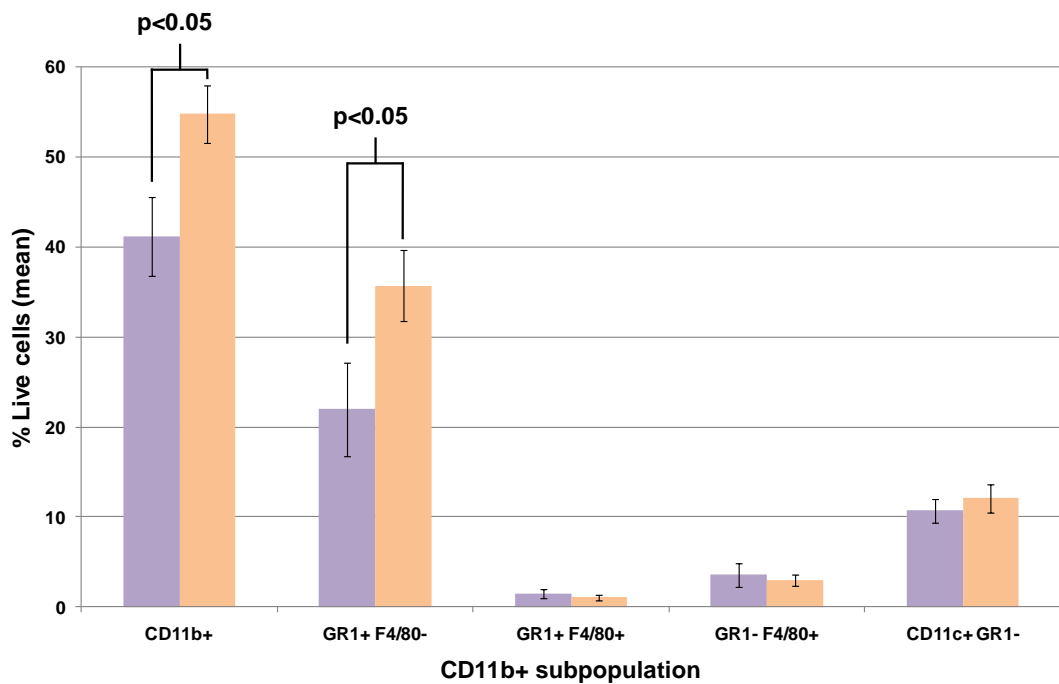
Figure 49 CD200R agonist delivered at the time of peak monocyte/macrophage recruitment following laser-induction of CNV results in a significant increase in the proportion of granulocytes at 2 weeks post-laser in the RPE-choroid

The proportion granulocytes (CD11b^{+} Gr-1^{+} F4/80^{-}) cells in the choroids of young adult wild-type mice following intravitreal delivery of CD200R agonist 3 days post-induction of CNV was found to be unchanged at 1 week post-laser (A) but increased compared with isotype antibody injected controls at the 2 week timepoint (B). Mean % live cells calculated from RPE-choroidal

cell suspensions obtained by pooling tissue from both eyes of each animal. CNV induced at 10 separate locations per fundus. For isotype control-injected mice, n=5 and 8 for the 1 week and 2 week timepoints respectively; for CD200R agonist-injected mice, n=6 and 12 for 1 week and 2 week timepoints respectively; error bars=SEM.

Manipulating innate immune cells

A. Isotype control-injected eye (1 week post-induction of CNV)
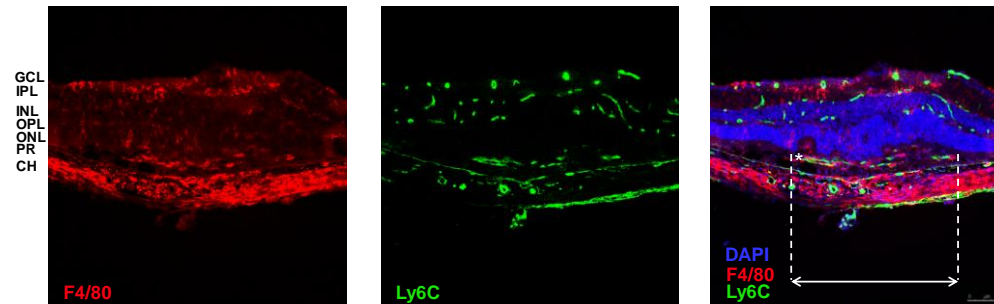
B. CD200R agonist-injected eye (1 week post-induction of CNV)
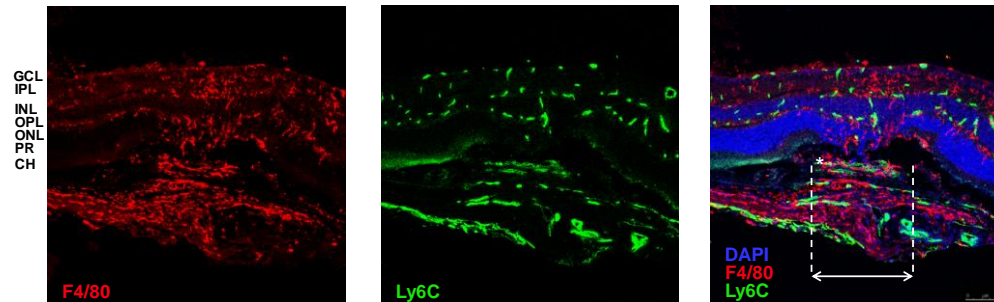
Figure 50 Immunohistochemistry demonstrating smaller lesions and more Ly6C⁻ F4/80⁺ cells in CD200R agonist-injected eyes at 1 week

Representative confocal photomicrograph projections (x20) of sections taken from the centre of CNV lesions in isotype control- and CD200R agonist-injected eyes (A and B respectively). 10µg of either isotype control or CD200R agonist were injected intravitreally at 3 days post-induction of CNV by laser. Increased numbers of Ly6C⁻ F4/80⁺ macrophages with a ramified microglial appearance are clearly visible in CD200R agonist-injected eyes in

association with smaller lesion size (as indicated by arrows). Retinal and choroidal vascular endothelium was Ly6C⁺ (confirmed by collagen IV staining -). Site of CNV is marked by asterisks.
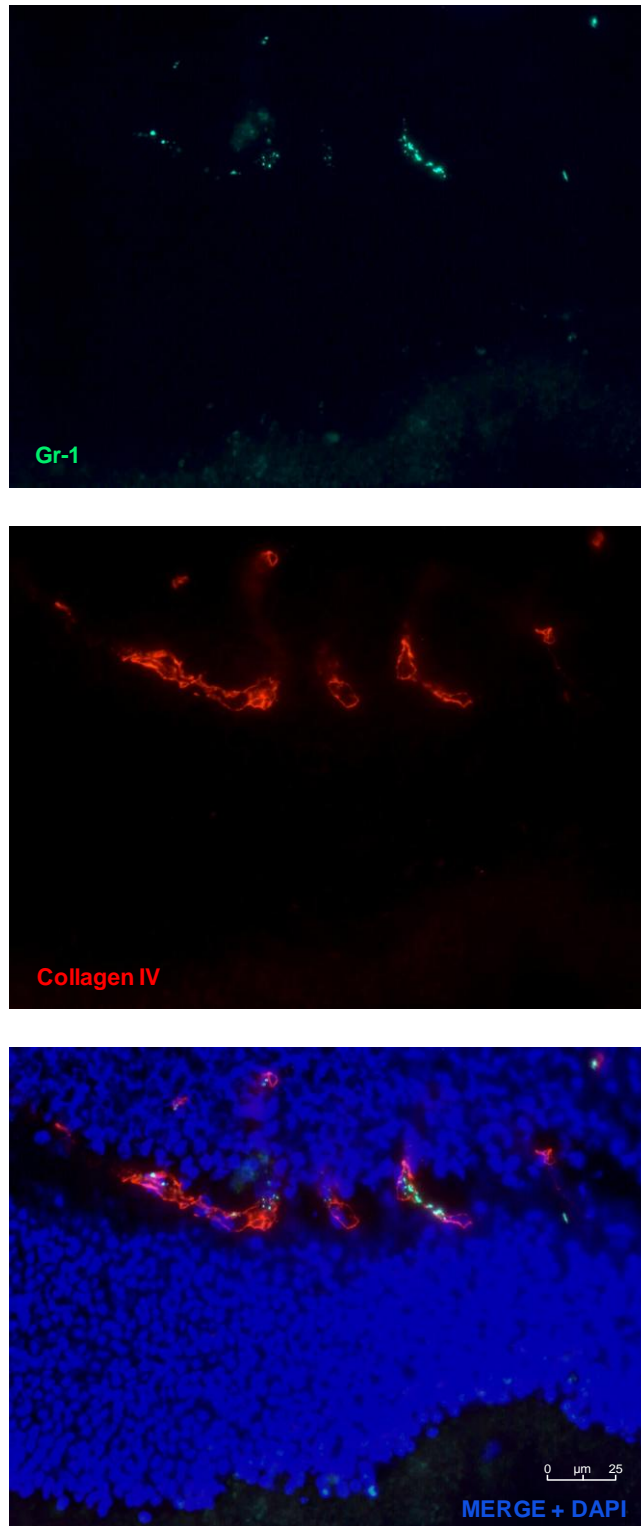
Figure 51 Gr-1 is expressed in the retinal vasculature

Immunohistochemistry staining demonstrating co-localisation of the vascular marker collagen IV (red) with Gr-1 (green) in a section taken from a young adult wild-type mouse 3 days post-induction of CNV by diode laser. A similar pattern was seen using the Ly6C marker (Figure 50). Fluorescence micrographs at x60 magnification.

A Spleen
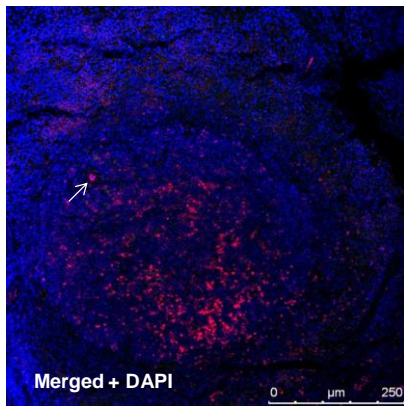
20x
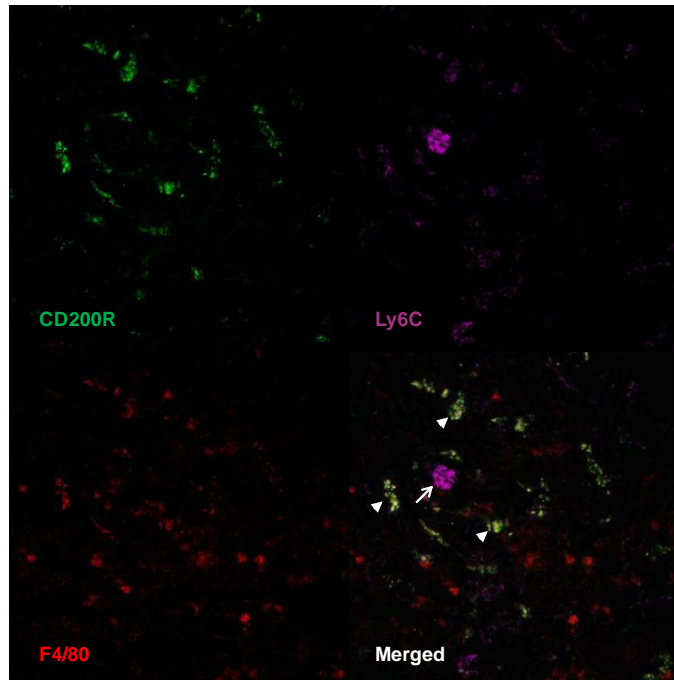
40x

B Retina
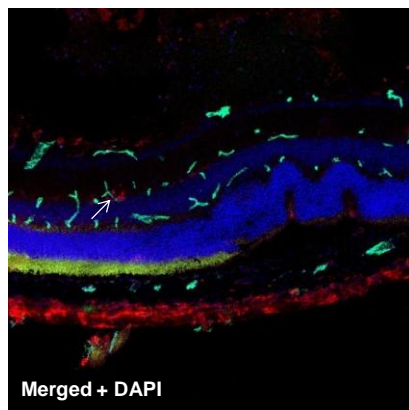
20x
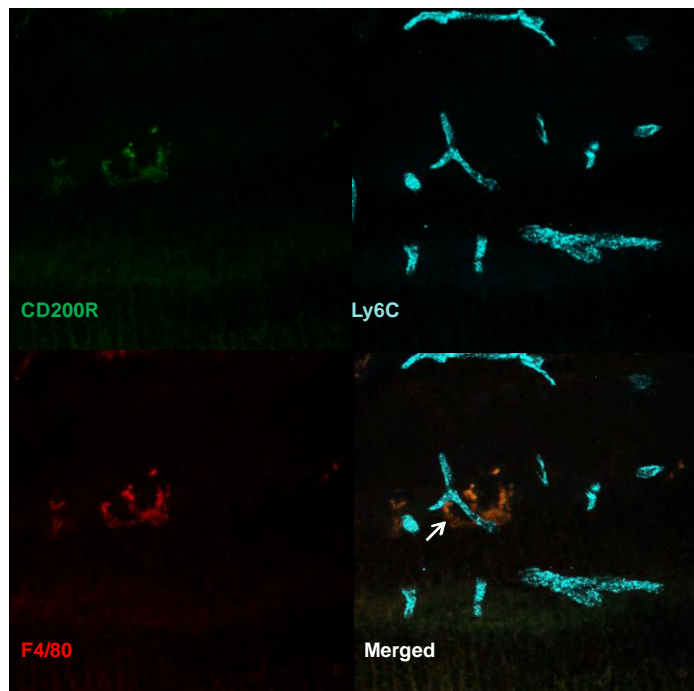
40x

Figure 52 Ly6C^{Low} monocyte/macrophages in the spleen and Ly6C$^-$ macrophages in the retina express CD200R

Representative confocal micrograph projections showing small numbers of CD200R positive (Ly6C^{Low}) monocyte/macrophages clustered around a large, multinucleated F4/80$^-$ Ly6C$^+$ cell

(arrow) in young wild-type spleen. Arrowheads indicate the position of cells where F4/80 and CD200R staining colocalise (A). Confocal microscopy images demonstrating the presence of weakly CD200R$^+$ Ly6C$^-$ microglia in the retina 1 week after laser-induction of CNV; vessels in retinal tissue and choroid stain positive for Ly6C (B). 20x merged images (left); 40x panels (right).

the immunohistochemistry data indicating lower levels of expression of CD200R on retinal macrophages compared with those in the spleen, other work has confirmed that microglia in human brain express lower levels of CD200R than peripheral blood-derived macrophages[110].

5.7 Anti-angiogenic effect of CD200R agonist is accelerated when administered prior to induction of CNV

The potential for early delivery of CD200R agonist antibody to attenuate the neovascular response in the laser-induced CNV model was explored. This would have implications for manipulation of the CD200R-CD200 pathway in acute cases of wet AMD and also further understanding of the importance of CD200R signalling in the initial stages of the neovascular response.

The possibility of injecting CD200R agonist antibody intravitreally immediately pre- or post-laser induction of CNV was considered. This would reduce the number of anaesthetic treatments to which animals were subjected from two to one. The advantages of this would be to minimise harm to the mice and also to reduce the risk of keratopathy associated with general anaesthesia that otherwise reduces the quality of angiographic imaging. A pilot experiment, however, revealed that injection immediately prior to lasering resulted in a temporary cataract that significantly reduced levels of energy delivered to Bruch's membrane in attempts to rupture it. Injection immediately after lasering precipitated haemorrhage at sites of CNV induction. Consequently, two cohorts of young adult mice were injected intravitreally with either 10µg CD200R agonist antibody or 10µg isotype control 1 day pre-induction of CNV at three locations in each fundus and subjected to fundus fluorescein angiography at 1 and 2 weeks post-laser (*Figure 53A*).

Results indicated that delivery of CD200R agonist antibody 1 day prior to induction of CNV by diode laser resulted in reduced lesion size at 2 weeks (t-test; $p<0.05$). Levels were comparable with those achieved following injection at 3 days post-laser (39% compared with 43% in animals injected at 3 days post-laser. However, injection 1 day prior to laser had the additional effect of

significantly reducing lesion size at 1 week post-laser, by 30% compared with isotype control-injected eyes, suggesting an effect on cells recruited before maximal infiltration of monocyte/macrophages at 3 days – most likely neutrophils (*Figure 53B*).

5.8 Systemic delivery of CD200R agonist 3 days post-induction of CNV does not reduce lesion size in the laser model

Systemic delivery of CD200R agonist antibody has been demonstrated to attenuate the inflammatory response in the experimental autoimmune uveitis model[109]. An experiment was undertaken to determine whether intraperitoneal delivery of CD200R antibody agonist results in significant suppression of the neovascular response in the laser-induced CNV model. If systemic delivery of CD200R agonist antibody were found to reduce CNV lesion size, this would have implications for the role of the CD200R-CD200 axis in modulating the behaviour of peripheral innate immune cells in pathological neovascularisation and give some indication as to the potential for systemic toxicity, or even benefit, in other tissues. It would also permit greater flexibility in terms of when the drug might be delivered in relation to the timing of CNV induction and avoid the increased variability associated with undertaking intravitreal injections.

CD200R agonist antibody, at a dose found to be effective in the EAU model (120µg), or isotype control antibody were delivered by intraperitoneal injection in young adult wild-type mice 3 days post-induction of CNV by diode laser (at 3 locations in each fundus). Animals were subjected to fundus fluorescein angiography at 1 and 2 weeks post-laser. No significant effect on lesion size was observed in the CD200R agonist-treated group at either the 1 or 2 week timepoints. These data suggest that either insufficient quantities of therapeutically active antibody were available to the intravascular compartment or that concentrations achieved had no significant effect on either peripheral or local innate immune cell populations (*Figure 54*).

A

B

Weeks post-induction of CNV
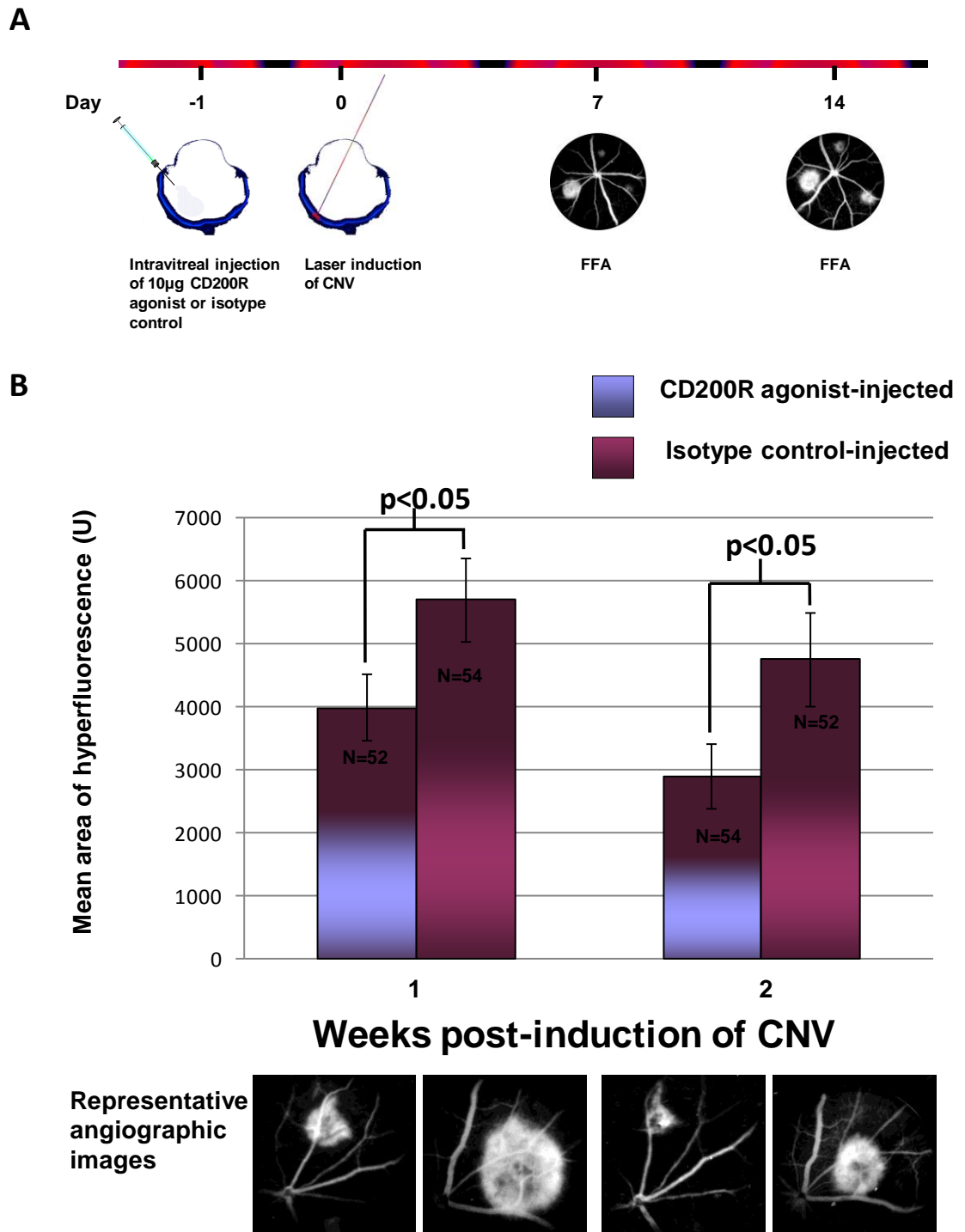
Figure 53. Delivery of CD200R agonist before induction of CNV results in an earlier effect on the neovascular response.

10µg CD200R agonist delivered by intravitreal injection 1 day pre-induction of CNV results in significantly reduced mean lesion size on fundus fluorescein angiography performed 1 and 2 weeks after laser-induction of choroidal neovascularisation. Summary of experimental timeline shown (A).Chart shows mean lesion sizes following laser-induced CNV in young adult WT mice after injection of either CD200R agonist or isotype control antibody at 1 day pre-laser (B).

Results are shown from the early phase of fluorescein angiograms at 1 and 2 weeks post-laser (mean area of hyperfluorescence +/- SEM; N refers to number of lesions) with representative images from angiograms shown below. Mean lesion size in mice receiving 10µg CD200R agonist compared with isotype control antibody was significantly reduced by 30% at the 1 week and 39% at the 2 week post-laser timepoints (t-test; p<0.05).

A
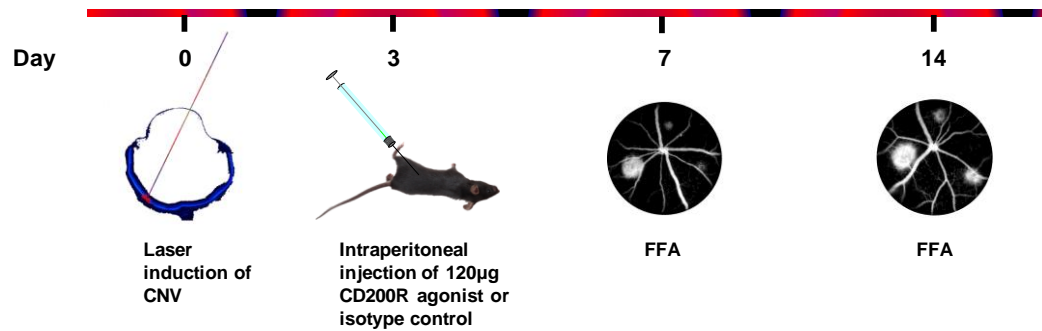
B
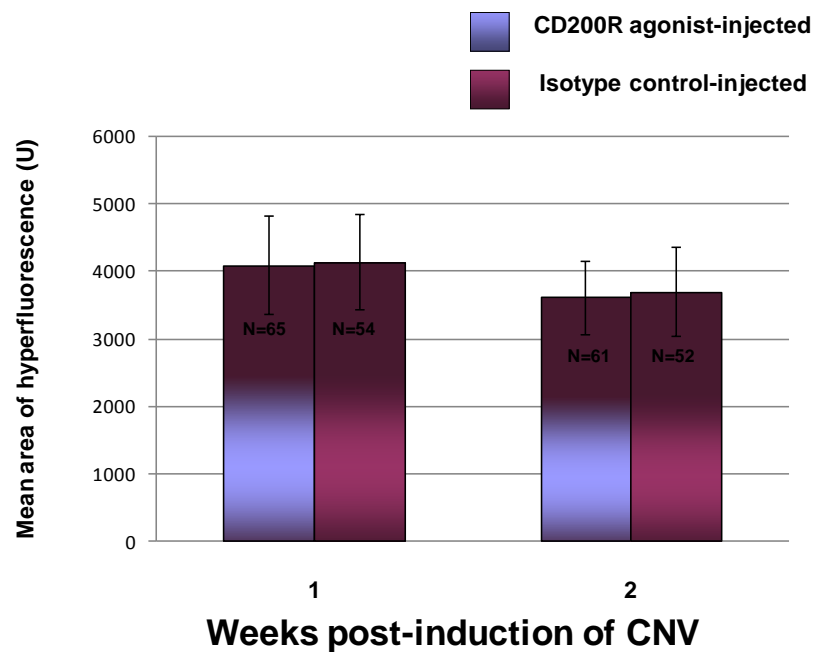
Figure 54 120µg CD200R agonist delivered by intraperitoneal injection 3 days post-induction of CNV has no effect on neovascular response

Mean lesion size as assessed by fundus fluorescein angiography performed 1 and 2 weeks after laser-induction of choroidal neovascularisation in young adult wild-type mice. Mice received either 120µg isotype control antibody or CD200R agonist intraperitoneally at 3 days post-induction of CNV. Timeline summarising experiment shown (A). Results are shown from the early phase of fluorescein angiograms at 1 and 2 weeks post-laser (B) - mean area of hyperfluorescence +/- SEM; N refers to number of lesions.

5.9 Discussion

This chapter documents two approaches to the treatment of CNV: one where a more conventional treatment directed at inhibition of tyrosine kinase receptors, such as VEGF receptors, was demonstrated to have an effect on both local and systemic innate immune cell populations; and one in which innate immune cells were targeted directly using an agonist for the CD200 receptor. The purpose of the work on tyrosine kinase receptor inhibition was to establish whether an approach primarily targeting the VEGFR signalling pathway, hitherto the most successful method of treating wet AMD, might have effects on innate immune cell populations also known to express VEGF receptors. The purpose of the work focusing on CD200R signalling was to explore the effect of targeting innate immune cell alternative activation pathways directly – such an approach might have additional benefits beyond those derived from VEGFR inhibition which, on their own, appear only to reduce leakage in established CNV[23].

VEGFR-1 and VEGFR-2 are expressed in vascular endothelial cells, monocytes, macrophages and hematopoietic stem cells. These cells have been demonstrated to modulate tumour growth and angiogenesis in a VEGF-dependent manner and the effect of anti-VEGF treatment on myeloid cells has therefore been widely studied. It is noteworthy that VEGFR-1 blocking antibodies inhibit the formation of bone marrow –derived progenitor cells that form pre-metastatic clusters in tumour models. VEGF has been implicated in the defective maturation of DCs from immature precursors and blocking this effect improves the efficacy of anti-tumour immunotherapy in cancer patients. Decreases in levels of VEGF following anti-VEGF treatment have been demonstrated to enhance the antigen-presenting capacity of DCs by reducing numbers of immature myeloid cells, such as MDSCs, that are known to inhibit DC function. For example, the delivery of the anti-VEGF antibody bevacizumab in metatstatic renal cancer has been shown to reduce the size of the CD11b^{+} VEGFR^{+} population of MDSCs in peripheral blood. Studies aimed at identifying VEGF-independent mediators of tumour angiogenesis have identified the G-CSF-mediated upregulation of a protein known as Bv8 in CD11b^{+} Gr-1^{+} cells associated with tumours that are resistant to treatment – blocking these

pathways has been demonstrated reduce the growth of refractory tumours. The results of these studies suggest a possible role for such cell types in the propagation of CNV in the aged eye and new avenues to explore in the delivery of more effective treatments for CNV, both responsive and unresponsive to current therapies[189].

The multi-target tyrosine kinase inhibitor pazopanib has been demonstrated to be capable of both suppressing the development of CNV and inducing the regression of established neovascular membranes in the laser model[190]. In causing the regression of established CNV, pazopanib exerts additional effects beyond those expected from blockade of VEGFR signalling alone. The mechanism for these effects remains a source of speculation but candidates include the blockade of PDGF-B signalling (known to promote the recruitment, proliferation and survival of pericytes) and blockade of c-Kit (a receptor for stem cell factor that contributes to angiogenesis by increasing nuclear localisation of hypoxia inducible factor 1α). However, pazopanib is also active to a lesser extent on a number of other tyrosine kinase receptors including FGFR1, FGFR3 and c-fms (also known as CSF-1 receptor). CSF-1 regulates macrophage differentiation, survival and function – making it an attractive therapeutic target in a number of chronic inflammatory and neoplastic diseases[198].

In a series of experiments, the antiangiogenic effect of pazopanib was confirmed and it was determined that multi-target tyrosine kinase inhibition is associated with changes in innate immune cell phenotypes both in the spleen and the eye. Specifically, it was established that prolonged administration (over a 3 week period) of therapeutic doses of pazopanib resulted in a significant reduction in the proportion of granulocytes (or even the more loosely defined $CD11b^+$ $Gr-1^+$ 'myeloid-derived suppressor cell' population of cancer biology), in the wild-type mouse spleen (*Figure 42*). It was also established that delivery of pazopanib in the context of laser-induced CNV resulted in a significant increase in the proportion of $Gr-1^+$ ($CCR2^+$) monocyte/macrophages in the retinae of treated mice at the 3 day post-laser timepoint, when levels of monocyte/macrophage recruitment to CNV are at their highest (*Figure 43*). Preferential recruitment of $Gr-1^+$ ($CCR2^+$) monocyte/macrophages to the retina

at 3 days post-induction of CNV would be in keeping with evidence suggesting that Gr-1$^-$ (CCR2$^-$) monocyte/macrophages constitute the key pro-angiogenic subpopulation at this timepoint. Therapies designed to affect the balance of monocyte subpopulations at critical points in the neovascular process may therefore have beneficial effects in the context of CNV. Such effects may partly explain the additional anti-angiogenic effects of pazopanib.

The possibility that pazopanib exerted some of its anti-angiogenic effects through suppression of circulating granulocytes or myeloid-derived suppressor cells (effects found to be in evidence following prolonged administration of the drug) could not be excluded entirely. The heterogeneous myeloid-derived suppressor cell populations of the spleen, bone marrow and tumour infiltrate are thought to exert pro-angiogenic effects that render tumours refractive to anti-VEGF therapies[189]. Granulocytes, which are also CD11b$^+$ Gr-1$^+$ (but F4/80$^-$), remain the largest innate immune cell population in retina and RPE-choroid at the 3 day post-laser time point, they are most likely the principal effectors of angiogenesis in the context of CCL2 deficiency where normal monocyte/macrophage recruitment is inhibited (*Figure 37*) and their role in pathological neovascularisation has been described previously[153]. It is certainly conceivable that suppression of granulocytes in the periphery might have beneficial effects for CNV but the potential side effects, particularly in leaving a subject open to acute infection, are highly significant. Consequently an experiment was designed to determine whether the uveal tract retention properties of pazopanib might be exploited in such a way that exposure of the drug was limited to its site of action in the eye. Such an approach would minimise systemic exposure to pazopanib (whether delivered orally or topically), reduce the therapeutically effective dose in the eye and give some indication as to whether pazopanib retains significant biological activity in the absence of any systemic effects. Initial work identified that the pharmacokinetics of pazopanib were such that 3 days after a single dose by oral gavage, significant amounts of the drug were still present in plasma samples obtained from young adult wild-type mice. A further experiment was conducted where pazopanib was delivered in a single dose 5 days prior to induction of CNV by diode laser. In this experiment no significant levels of pazopanib were detectable in plasma

samples obtained at the time of lasering. Lesion size at 1 week post-laser was significantly reduced by as much as 33% in animals pre-treated with pazopanib and it was therefore concluded that pazopanib retained in the uveal tract is therapeutically active. The absence of a significant effect on lesion size at the 2 week timepoint indicated that levels of retained drug were either insufficient or not in a pharmacologically active form for an effect on neovascularisation much beyond 11 days after delivery. Further work would be needed to determine the long-term effects of bound and non-bound pazopanib on the innate immune cell populations of the eye. Potentially toxic effects on the neuroretina and choroidal vaculature have been attributed to VEGFR blockade and the additional effects of targeting other tyrosine kinase receptors in the eye cannot be underestimated: it has been demonstrated, for example, that CSF-1 is important for migratory DC development and the effects of prolonged CSF-1 receptor blockade are therefore of particular importance given the striking effects that chemokine deficiencies appear to have on DC trafficking in the retina and choroid[20, 21, 164].

To determine whether targeting innate immune cell activation pathways directly might be of benefit in CNV, the effect of intravitreal delivery of a CD200R agonist on lesion size was investigated. To maximise any potential therapeutic effect, CD200R agonist antibody was delivered at the peak time of monocyte/macrophage recruitment, 3 days after induction of CNV by diode laser. CD200R agonist-injected eyes exhibited significantly reduced CNV, compared with those injected with isotype control antibody, by as much as 43% at the 2 week timepoint. Interestingly, CD200R induction appeared to result in the breakdown of CNV that was otherwise almost fully formed at the 1 week time point. The precipitation of CNV regression was preceded by a significant increase in the proportion of Gr-1$^-$ (CCR2$^-$) monocyte/macrophages in the retinae of CD200R agonist-injected mice at 1 week post-laser and an increase in granulocytes in the RPE-choroid (presumably triggered by the release of material from the degenerating neovascular membrane) at 2 weeks post-laser.

The finding that an in increase in the proportion of Gr-1$^-$ monocyte/macrophages in the retinae of CD200R agonist-injected eyes was

associated with a subsequent reduction in CNV lesion size in some ways runs contrary to evidence obtained following use of pazopanib suggesting that these cells constitute a more pro-angiogenic subset. However, a direct comparison of the data is not possible since tissue was harvested at the 3 day post-laser timepoint in the case of pazopanib-treated animals and at the 1 and 2 week post laser time points in the case of CD200R agonist-treated animals. Differences between these datasets most likely reflect the sequential recruitment of monocyte/macrophages described in other disorders[159]. That is to say that whilst a balance favouring recruitment or proliferation of Gr-1$^+$ monocyte/macrophages at 3 days post-laser results in a suppression of CNV, a similar effect may potentially result from the recruitment/proliferation of the Gr-1$^-$ subset at 1 week post-laser. Since differentiation between microglia and Gr-1$^-$ monocytes was not possible, any changes in the proportion of retinal CD11b$^+$ Gr-1$^-$ F4/80$^+$ cells may be due to either proliferation of the microglial population or recruitment of the monocytic subset – further work would be needed to establish this. The process of pathological neovascularisation, at least in the early stages, is highly dynamic with cells exhibiting the same surface markers appearing to have different functions at different time points. Therapies targeting a specific population of innate immune cells may therefore be extremely effective if delivered in the first week of onset but achieve little, or even be counterproductive, at other time points. There is at least circumstantial evidence to support this given that a significant increase in the proportion of granulocytes in the RPE-choroid precedes a rapid increase in lesion size at 3 days post-laser but a further increase (compared to isotype control-injected eyes) is also associated with a reduction in lesion size at 2 weeks post-laser in CD200R agonist-injected eyes.

Intravitreal injection of CD200R agonist or isotype control antibody immediately after induction of CNV resulted in significant subretinal and intravitreal haemorrhage at the site of Bruch's membrane rupture and this precluded flow cytometric analysis of innate immune cell populations post-treatment at the 3 day post-laser timepoints. However, intravitreal delivery of CD200R agonist 1 day prior to induction of CNV was found to be effective in suppressing the neovascular response at both 1 and 2 weeks post-laser and consequently it

may be possible to examine the effect of CD200R signalling on innate immune cell populations at the 3 day timepoint using this approach (*Figure 53*).

Systemic delivery of CD200R agonist by intraperitoneal injection was found not to be effective in suppressing laser-induced CNV, although intravenous delivery of the same antibody has previously been shown to significantly reduce CD45^{+} inflammatory infiltrate and structural damage in the EAU model[109]. These results suggest that the induction of CD200R signalling on cells in the periphery fails to significantly alter the progression of CNV in the eye. Fundamental differences between the EAU and laser-induced CNV models may explain why systemic delivery is effective in the former but not the latter. The EAU model relies on the systemic delivery of an antigen (interphotoreceptor retinoid binding protein in wild-type animals) in combination with an adjuvant that is taken up by antigen presenting cells which drive a T cell-mediated immune response in the eye. The process of systemic antigen uptake and presentation is very likely to be attenuated following systemic delivery of CD200R agonist, resulting in less uveitis. In contrast, the laser-induced CNV model relies on the combined activity of recruited myeloid cells and resident microglia to generate pathology that is heavily dependent on the nature of the local inflammatory microenvironment. Consequently the effects of systemically delivered CD200R agonist in the context of laser-induced CNV are more limited.

In summary, two experimental approaches to the treatment of CNV were investigated using the laser model of CNV induction. In both cases it was possible to associate effects on innate immune cell populations in the eye with an effect on the degree of neovascularisation. Systemic delivery of the multi-target tyrosine kinase inhibitor pazopanib was demonstrated to suppress the development of CNV in association with an increase in the proportion of Gr-1^{+} monocyte/macrophages in the retina at 3 days post-laser. Prolonged systemic exposure to pazopanib was also associated with a significant reduction in the proportion of granulocytes in the spleens of treated animals. It was hypothesised that pazopanib retained in the uveal tract might confer a depot effect and the drug was found to be active in suppressing CNV in the absence

of detectable levels in the plasma of treated animals. Certain innate immune cell populations, such as macrophages, express VEGF receptors but it is also possible that pazopanib exerts its effect on innate immune cells by acting on the CSF-1 receptor.

Induction of CD200R signalling was also found to suppress CNV development (when administered intravitreally before CNV induction). In addition, CD200R agonist antibody delivered intravitreally 3 days after CNV induction appeared to accelerate the breakdown of neovascular membrane in association with raised levels of Gr-1$^-$ monocyte/macrophages in the retina at 1 week and granulocytes in the RPE-choroid at 2 weeks. A rise in Gr-1$^-$ macrophages in the retinae of aged $CCL2^{-/-}$ was also associated with a reduction in the neovascular response in these animals and, overall, these results in combination with those obtained from therapeutic intervention suggest that manipulation of macrophage populations in the retina, rather than the choroid or periphery, may have greatest impact on the development and/or regression of CNV. Further work would be required to confirm that peripheral innate immune cell populations are unaffected following a once-only delivery of pazopanib and to identify the functional changes associated with particular patterns of surface marker expression in the relevant populations.

Chapter 6: Discussion

6.1 Analysis of the innate immune system of the retina and RPE-choroid

This thesis describes a body of work aimed at developing a greater understanding of the role played by innate immune cells in ageing of the retina and RPE-choroid. It explores how changes in the various innate immune cell sub-populations might contribute to the pathogenesis of age-related macular degeneration and how they might be manipulated to improve its management.

The first chapter documents experiments designed to determine the phenotypes of innate immune cells in the retina and RPE-choroid of wild-type mice and the changes in these populations with age, before going on to identify how a deficiency of the chemokine CCL2 in $CCL2^{-/-}$ mice affects the proportions of the various populations in young and aged animals. The second chapter details the effects of age and CCL2 deficiency on laser-induced CNV lesion size and investigates the role played by innate immune cells in this process. The innate immune cell populations recruited following laser-induction of CNV are compared with those found in a model of spontaneous CNV with the aim of identifying common pro-angiogenic cell types. The final chapter explores the effects of tyrosine kinase receptor inhibition on local and peripheral innate immune cell populations in the context of laser-induced CNV and the potential for inducing alternative activation, through CD200R signalling, as a means of inhibiting the neovascular response.

There has been a revival of interest in the role played by innate immune cells in the pathology of AMD (and many other age-related disorders) in recent years following the discovery that polymorphisms in complement genes, such as those for CFH and C3 are associated with the condition[30-32, 41, 64]. This thesis demonstrates that it is possible to detect small but significant changes in innate immune cell populations, as defined by their levels of surface marker

expression in response to ageing, chemokine deficiency, induction of CNV and therapeutic intervention. Given the difficulties of identifying individual myeloid cells in the retina and RPE-choroid for the purpose of cell counts (particularly in eyes subjected to laser induction of CNV), the inherent variability associated with immunohistochemical staining of fixed tissue and the variability associated with the laser model and intravitreal injections, it might not have been possible to detect these changes using any method other than flow cytometry. The initial attempts of others to identify DCs in the retina using immunohistochemical staining were negative for example[111]. Having said that, immunohistochemistry does have one important advantage over flow cytometry in providing more information about the location of cell types and their morphology. A considerable amount of data, based largely on immunohistochemistrical analysis, already exists in the literature regarding the trafficking and behaviour of innate immune cells in the retina and RPE-choroid (as defined by their expression of CD11b, F4/80, the microglial marker Iba-1 or expression of CX3CR1^{GFP}), however comparatively little was known about the specific phenotypes of these broadly defined populations and hence this became a focus for further investigation[102, 111, 112, 153, 171].

There exists a degree of variation in the literature relating to how innate immune cell populations may be defined using surface markers. CCR2$^+$ monocytes in particular are various described as being F4/80^{Low} cells that are Gr-1$^+$, Ly6C$^+$ or Ly6C^{High} – in some cases these markers are referred to interchangeably, despite evidence that they are epitopically distinct[93]. In the case of DCs there is some debate as to whether they exist as a separate population from the mononuclear phagocyte system at all, though most authors would agree that these cells, regarded as highly important in bridging the innate and adaptive immune responses, may be defined by their high levels of expression of the integrin CD11c[111, 174]. F4/80, a marker thought to have a role in the induction of regulatory T cell responses[89], has been consistently used to identify monocyte/macrophages since its discovery over 25 years ago, however recent evidence suggests that even neutrophils are capable of acquiring this marker and transdifferentiating to macrophages under certain conditions[88, 173]. These

points are made by way of stressing the plasticity of the immune system and not with the intention of undermining the approach taken to defining cell populations in this thesis or any other work. By analysing changes in cell populations, as defined using surface markers, it was the aim of this study to establish, even if only in snapshot, an association between specific cell populations and the changes observed with age or pathological neovascularisation in the eye. Similar approaches have yielded extremely valuable data in other areas of immunology and permitted a more focused exploration of associated functional changes[166, 170, 199].

The role played by innate immune cells, in particular microglia, in ocular ageing and choroidal neovascularisation is unclear – perhaps because macrophages in the retina and RPE-choroid have been defined very broadly in the past. Using antibodies against innate immune cell surface markers in combination with flow cytometry it was possible to determine that innate immune cells constitute approximately 1.2% of live cells in the retinae and 16.6% of live cells in the choroids of young adult wild-type mice. Interestingly, of the definable sub-populations, CD11b$^+$ Gr-1$^+$ F4/80$^-$ cells (most likely granulocytes) appear to comprise the largest fraction both in the retina and RPE-choroid at a young age. The possibility that such a high proportion of granulocytes might simply reflect the composition of the intravascular compartment was considered. However, the effect of perfusing animals with a buffered salt solution prior to harvesting tissue - thereby removing cells from the lumens of the retinal and choroidal vasculature - has been found to be insignificant[186]. This leaves open the possibility that CD11b$^+$ Gr-1$^+$ F4/80$^-$ cells, in this context, are in fact pericytes. Pericytes have been demonstrated to express the myeloid lineage marker CD11b and macrophage marker ED-2 in culture and microvessels isolated from rat brain. Future work that makes use of other markers for pericytes, such as the chondroitin sulphate proteoglycan NG2, in conjunction with immunohistopathological techniques may enable the exact nature of this population to be determined.

As wild-type mice age the DC populations in both retina and RPE-choroid rapidly overtake granulocytes to become the predominant innate immune cell

population in these tissues. The increase in DCs appears greatest in the first year of life in both tissues and is the only feature of ageing, at least where the relative proportions of innate immune cells are concerned, in the RPE-choroid. In the retina, rapid expansion of the DC population in the first year of life is followed by an equally rapid expansion in the Gr-1⁻ macrophage population after 12 months of age.

How do these results square with what is known about innate immune cells in the retina and RPE-choroid and the way they change with age? In the retina, microglial cells are generally thought of as the main resident immune cells in young adult wild-type mice, and DCs and resident macrophages as the key populations in the choroid. These findings do contrast slightly with those described in Chapter 3 where granulocytes appeared the main innate immune cell population in young adult wild-type retina. Xu et al. have described an increase in the number of MHC-II^{Low} TLR3^{+} TLR4^{+} 33D1^{+} cells derived from the CD11b^{+} CD45^{Low} population in aged mouse retinae and concluded that this change arose from an age-dependent activation of retinal microglia (*Figure 55*). They also described an accumulation of CD11c^{+} cells with age although, interestingly, additional work has identified *subretinal* microglia as expressing both the microglial marker Iba-1 and the phagocytic marker CD68, but not MHCII or CD11c antigens[9].

Xu et al. arrived at their conclusions regarding subretinal microglia through the immunohistochemical analysis of RPE-choroidal flat mounts, however a flow cytometric analysis of the CD11b^{+} F4/80^{+} subpopulations described in this thesis revealed no significant difference in their levels in the RPE-choroid with age. The reasons for this are unclear: one possibility is that autofluorescent cells such as lipofuscin-laden subretinal microglia were excluded from the analysis as a by-product of exercising the standard controls, another is that large bloated subretinal macrophages are incapable of withstanding the rigours of the flow cytometric protocol and rupture easily. A further possibility is that the flow cytometric protocol, whilst allowing enormous flexibility in terms of the cell populations analysed, was simply not sensitive enough to detect a population of cells that probably numbers no more than 100 in an aged wild-type RPE-
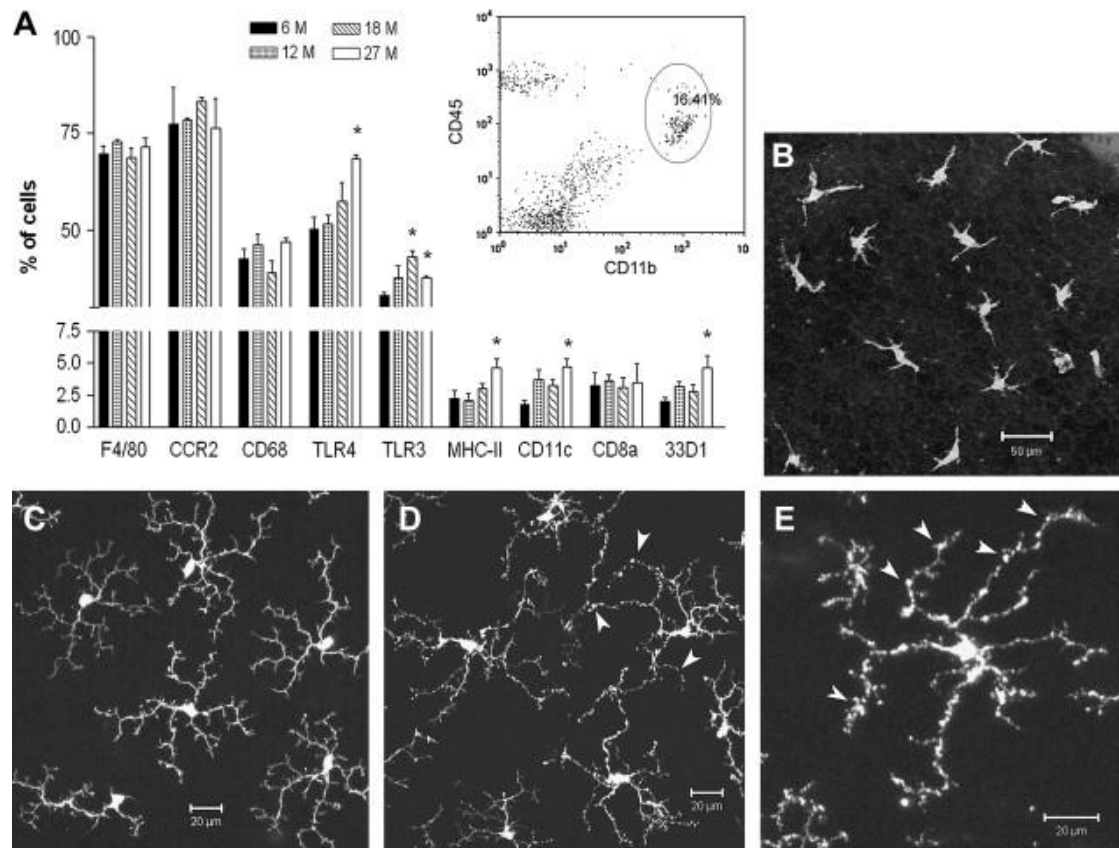
Figure 55 Microglial changes in the aged mouse retina.

(A) Phenotype of CD11b$^+$CD45^{low} (insert) retinal microglia in different ages of mice. *, p<0.05 compared to 6-month old mice (n = 4; student t test). (B), Subretinal Iba-1$^+$ microglia in a 22-month old mouse. (C), Normal CX3CR1$^{gfp/gfp}$ retinal microglia in the inner plexiform layer of a 3-month old mouse. (D, E), Atrophic Cx3cr1$^{gfp/gfp}$ retinal microglia in the inner plexiform of a 22-month old mouse. Atrophic cells have fragmented, tortuous processes with bulbous swellings (arrowheads). From Xu et al. 2008

choroidal flatmount (this may explain why it was possible to detect an increase in Gr-1⁻ macrophages with age in the RPE-choroids of $CCL2^{-/-}$ mice but not wild-types). In any case, it is not possible to conclude with any certainty which of the two populations seen to increase in the retina with age (DCs and Gr-1⁻ macrophages), if either, equates to the subretinal microglial population. The timing of the responses and the markers identified on subretinal microglia suggest that these are (or are derived from) the Gr-1⁻ macrophages and that the increase in DCs, though very likely to be related to the accumulation of subretinal microglia, occurs independently. This is important because the timing of these responses suggests that a failure of DC trafficking/maturation precedes active or reactive changes in the microglial population.

Ageing is thought to affect every innate immune cell in the body, whether by changes in numbers or function or both. Such changes may be related to intrinsic or extrinsic factors – that is altered function may either occur independently of a cell's microenvironment or as a direct result of age-related cues from the tissues. The effect of ageing on innate immune cell function also varies according to the method of study (*in vitro* or *in vivo*), the species studied and the subpopulation. Some subpopulations are more heavily studied than others in this context - there are almost no studies on morphological and functional changes in neutrophil granulocytes, for example, and those in mice date back more than two decades. In mice the evidence available suggests that the concentration of neutrophils in the peripheral blood increases with age but that their functional capacity remains unchanged. In contrast, neutrophils in humans exhibit impaired function and altered signal transduction that may serve to explain the susceptibility of the elderly to bacterial and fungal sepsis – these differences have led some to conclude that mice may not be ideal models for studying neutrophil immunosenescence[200].

The evidence for immunosenescence in the mononuclear phagocyte system is more consistent: macrophages isolated from aged subjects have been demonstrated to have decreased chemotactic activity and defective phagocytosis (*Table 5*)[201]. An impaired ability either to phagocytose or process phagocytosed debris may account for the lipofuscin-laden appearance of

dystrophic microglia in the subretinal space and brains of aged mice[129]. Cytokine production also appears to be reduced in aged mice compared with young *in vitro* though the importance of the microenvironment is underlined by a more pro-inflammatory cytokine output of the same cells *in vivo* following LPS exposure. In the brain, aged microglia are thought to be 'primed' to produce higher levels of pro-inflammatory cytokines. This increase has been noted to be in proportion to higher basal levels of cytokine secretion, and therefore suggests intact acute inflammatory mechanisms. Nevertheless, exposure to high levels of pro-inflammatory cytokines may directly enhance neurodegeneration regardless of whether the response is 'proportional' and therefore contribute to the death of photoreceptors and supporting cells in a condition such as AMD[129].

An age-related increase in circulating levels of inflammatory cytokines such as TNF-α and Il-6 has been attributed to both cells of the monocytic lineage and aged stromal cells such as fibroblasts. The observed *in vivo* effects of ageing on macrophage function also correlate with reduced efficiency of TLR-dependent pathways which may be of particular relevance in AMD given a putative association between geographic atrophy and TLR3 signalling[202]. Dendritic cell populations also undergo age-related changes with descriptions of a decline in cell numbers, impaired antigen presentation and reduced migration to peripheral lymph nodes all featuring in the literature. It appears that the migration of mature antigen-carrying DCs from the peripheries to secondary lymphoid organs is highly dependent on chemokine signalling. Levels of the chemokine receptor CCR7 on DCs and chemokines in the tissues, such as CCL19 and CCL21 are similar in young and aged mice but the capacity for their upregulation is impaired in the latter. These features of ageing are thought to account for the reduced accumulation of DCs in the draining lymph nodes of aged mice[200]. Subretinal macrophages have previously been shown to originate from the retinal microglial population[9]. The work in this thesis suggests that a failure of DC maturation/migration or saturation of this pathway may precede the accumulation of subretinal macrophages with age and that normal functioning of the DC population is CCL2-dependent. Levels of the cytokine

	Effect
NK cells	↑ **Numbers**
	↓ **Cytotoxicity**
	Intact antibody-dependent cell cytotoxicity
	Il-2-dependent IFN-γ and Il-2 and Il-12-induced chemokine production (MIP-1α, RANTES and Il-8)
Monocytes	↑, ↓ **or unchanged LPS-induced cytokine production**
	↓ **TLR1/2-induced Il-6 and TNF-α production**
	↓ **TLR1 and TLR4 surface expression**
	↓ **TLR-induced CD80 upregulation**
	↓ **DC-SIGN signalling in macrophages (to West Nile virus)**
	↓ **Phagocytosis**
	↓ **Percentage of CD68-positive macrophages in the bone marrow**
Dendritic cells	↑ **Or unchanged number or percentage of mDCs**
	↓ **Or unchanged number or percentage of pDCs**
	↓ **Langerhans cell density in skin**
	Unchanged transendothelial migration, preserved ability of antigen-pulsed DCs to stimulate T-cell proliferation
	↓ **Pinocytosis or endocytosis and impaired chemokine-induced migration**
	↓ **LPS-induced Il-12 production in mDCs**
	↓ **IFN-α production in PBMCs**
	↑ **TLR4- and TLR-8-induced Il-6 and TNF-α production in MDDCs**
	↑ **Self-DNA-induced production of IFN-α and Il-6 in MDCCs**
	↓ **Akt-phosphorylation, ↑ p38 phosphorylation (MDCCs)**

NK cells, natural killer; Il, interleukin; IFN, interferon; MIP, macrophage inflammatory protein; RANTES, regulated upon activation, normal T-cell expressed and lipopolysaccharide; TLR, Toll-like receptor; TNF, tumour necrosis factor; DC-SIGN, dendritic cell-specific ICAM-3 grabbing non-lectin; mDC, myeloid dendritic cell; pDC, plasmacytoid dendritic cell; PBMC, peripheral blood mononuclear cell; MDDC, monocyte-derived dendritic cell

Table 5 Age-related changes in the human innate immune system

Macrophages isolated from aged subjects have been demonstrated to have decreased chemotactic activity and defective phagocytosis. An impaired ability either to phagocytose or process phagocytosed debris may account for the lipofuscin-laden appearance of dystrophic microglia in the subretinal space and brains of aged mice. Immunosenescence affecting dendritic cells, NK cells and neutrophils may also have role in the pathogenesis of AMD. Adapted from Panda et al. 2009.

TNF-α and chemokines CCL2, CCL3, CCL8 and CCL12 have been found to be increased in the retinae of aged mice[114, 124]. Similarly chemokines and signalling pathways involved in leukocyte migration and extravasation, such as CCL2, have been found to be upregulated in the aged RPE-choroid. This would appear to be a part of the parainflammatory response associated with ageing - the question is: what role do DCs and subretinal macrophages play in the pathogenesis or prevention of AMD?

Given that an increase in CCL2 is a feature of normal ageing, it was hypothesised that failure of its expression might result in an exaggerated ageing phenotype detectable before the appearance of subretinal macrophages. The relative proportions of innate immune cells in the retinae and RPE-choroids of *CCL2*^{-/-} mice were therefore established, as in wild-type mice, in three different age groups. The proportion of DCs in the retinae of *CCL2*^{-/-} mice was found to be four times higher in <4 month old mice than in age-matched wild-types with levels appearing to plateau after 12 months of age, after which time a much greater rise in the proportion of Gr-1^{-} macrophages (most likely subretinal) was noted. These findings suggest that a failure of DCs to traffic out of the retina, or saturation of this pathway, results in the activation of microglia and their migration to the subretinal space. It was thought that such an effect might not be confined to the retina and that a system-wide failure of DC maturation might result in depleted numbers in the lymph nodes and spleen to which they would normally traffic to. To confirm this, proportions of innate immune cells in the spleens of wild-type and *CCL2*^{-/-} mice were analysed. Age-related increases in DCs and Gr-1^{-} monocyte/macrophages were identified in both genotypes; however CCL2-deficient animals exhibited consistently lower levels of these subpopulations compared to wild-types suggesting that it might be possible to detect the effects of defective DC trafficking in peripheral tissues other than the eye. In support of this, studies on Langerhans' cells (the DC population in the skin) have revealed that cells lacking the receptor for CCL2 (CCR2) exhibit defective trafficking from the dermis to draining lymph nodes and have lower numbers of DCs in their spleens[203]. A role for CCR2 ligands in local DC activation has also been in established in the lung with *CCR2*^{-/-} mouse DCs exhibiting an intrinsic activation/maturation defect and an associated diminution

of Th1 responses[204]. A system-wide failure of DC trafficking raises the intriguing possibility that lipofuscin-laden macrophages may be a feature of other tissues with age in the $CCL2^{-/-}$ mouse – increased skin autofluorescence, for example, is a feature of normal ageing in both humans and mice and has also been associated with wet AMD[205].

Another possible explanation for the findings in $CCL2^{-/-}$ mice is that a failure of monocyte recruitment to the retina in some way resulted in the 'exhaustion' of resident macrophage populations that were not replenished, resulting in a compensatory increase in DCs – however the increase in the proportion of DCs in the retina precedes the time taken for microglia to turn over (6 months), so this is unlikely[206]. Furthermore, the absence of either CCL2 or CCR2 individually has not been found to affect the turnover of monocyte-derived microglia in the mouse brain although double knockout of both ligand and receptor does result in a significant reduction in turnover[137]. Of particular interest where monocyte recruitment is concerned is the increase in the Gr-1$^-$ monocyte/macrophage population of the spleen that was observed with ageing in both wild-type and $CCL2^{-/-}$ mice. An increase in the equivalent CCR2$^-$ population in humans (CD14$^+$ CD16$^+$ monocytes) has also been found. CD14$^+$ CD16$^+$ monocytes from aged humans display reduced levels of the activation molecule HLA-DR and the chemokine receptor CX$_3$CR1 which may have functional relevance given the potential effect on their migratory capacity, most especially in AMD where polymorphisms of the CX$_3$CR1 receptor have already been linked with an increased risk of developing the disease[169, 207].

6.2 The role of the innate immune system in choroidal neovascularisation

Having established a role for CCL2 in modulating the retinal response to ageing, further work was undertaken to determine the effect of CCL2 deficiency on choroidal neovascularisation following laser-induced rupture of Bruch's membrane. Three principle questions were addressed, the first being which innate immune cell populations were involved in the neovascular response at 3 days post-induction of CNV when monocyte/macrophage recruitment is at its

peak, the second being the extent to which CCL2 deficiency affects lesion size and the recruitment of particular cell populations, and the third being whether the increases in CNV lesion size with age might be explained either by increased numbers of subretinal macrophages.or by changes in innate immune cell recruitment.

The development of CNV and pathological neovascularisation in general depends largely on patterns of cell recruitment and cytokine expression typically associated with acute inflammation (as opposed to the chronic inflammation associated with ageing). The laser-induced model of CNV was used to determine whether recently identified, monocyte subpopulations – classified as Gr-1$^+$ Ly6C^{High} CCR2$^+$ and Gr-1$^-$ Ly6C^{Low} CCR2$^-$ - might have particular roles to play in choroidal neovascularisation. It was hypothesised that changes in CNV lesion size with age might be explained by differences in the level of recruitment of these populations and that their manipulation might prove therapeutically beneficial. The phenotypes of the two principal monocyte populations have been characterised in disease models as diverse as those for myocardial infarction (**Error! Reference source not found.**), urinary tract infection and foreign body responses in the peritoneum[165, 166, 173]. CCR2$^+$ monocytes have been broadly defined as having 'pro-inflammatory' properties and CCR2$^-$ monocytes 'wound healing' properties that include pro-angiogenic potential. In addition CCR2$^-$ monocytes are thought to be the principal population involved in the replenishment of resident macrophage populations and, in keeping with the analysis of innate immune cell populations in murine spleen described previously, a significant age-related shift in monocyte populations from CCR2$^+$ to CCR2$^-$ has been established in humans [7].

Analysis of retinal and RPE-choroidal cell suspensions from young adult wild-type mice revealed an increase in the proportions of all of the key innate immune cell populations at 3 days post-induction of CNV by diode laser in the retina (in particular DCs and granulocytes) and increases in the proportion of DCs and granulocytes only in the RPE-choroid. These findings are largely in keeping with those of Nakai et al. who identified recruitment of VEGR2-expressing DCs to newly formed blood vessels following induction of CNV, with

levels peaking between 2 and 4 days post-laser[160]. It is also in keeping with the results of others, including Tsutsumi et al. and Eter et al. whose work, using *CCR2^{-/-}* and *CX3CR1^{GFP/+}* mice respectively, suggests roles for macrophages (both recruited and resident), granulocytes and DCs in the propagation of CNV at similar timepoints in its pathogenesis[153, 186]. However, the results do run contrary to the findings of Apte et al. who advocate a role for macrophages in the inhibition of laser-induced CNV after demonstrating that increased macrophage recruitment is associated with smaller CNV size in *Il-10^{-/-}* mice and that anti-CD11b and anti-F4/80 antibody-mediated depletion of systemic monocyte/macrophage populations is associated with increased lesion size. The findings of Apte et al. are in direct contradiction, in fact, to those of Espinosa-Heidmann et al. who, using clodronate liposomes to deplete circulating and choroidal monocyte/macrophage populations, demonstrated a correlation with reduced lesion size[96, 152].

It was hypothesised that conflicting reports of the effects of monocyte/macrophage depletion (or inhibition) on CNV lesion size in the literature might be explained by the preferential effects of the various experimental techniques on particular monocyte subpopulations – interventions favouring a reduction in CCR2^- Gr-1^- monocyte populations might result in reduced CNV whereas a reduction in CCR2^+ Gr-1^+ monocyte populations might have the opposite effect. *CCL2^{-/-}* mice were used to determine whether absence of the ligand for CCR2^+ cells might result in an increase in lesion size. In fact, a reduction in laser-induced CNV lesion size, as well as lesion size in a model of alkali-induced corneal neovascularisation, has previously been demonstrated in *CCR2^{-/-}* mice - suggesting that, in these models at least, CCR2^+ cells might be important effectors in the neovascular process[150, 189]. The validity of the observations in *CCR2^{-/-}* mice is open to question, however, since absence of CCR2, though not CCL2, has been shown to inhibit the emigration of monocytes from the bone marrow[136, 156, 208]. Equally, the results of experiments employing chimeric GFP^+ animals to distinguish resident from recruited cells are in dispute since the total body irradiation required in the development of

chimeric mice triggers enhanced recruitment of blood monocytes to the retina[209].

Comparison of innate immune cells isolated from the eyes of young adult $CCL2^{-/-}$ mice at 3 days post-laser with both unlasered $CCL2^{-/-}$ tissue and lasered wild-type tissue revealed a significant reduction in the proportions of all innate immune cell populations, except granulocytes, in both the retina and RPE-choroid. This was associated with a significant reduction in lesion size (*Figure 34*). The effect of CCL2 knockout suggested an important role for recruited cells in the development of CNV. It also suggested that granulocytes might be capable of making a limited, though significant, contribution to pathological neovascularisation in the absence of other innate immune cell populations – something also found in the $CCR2^{-/-}$ mouse[153].

The percentage of Gr-1$^+$ monocytes in the retina and RPE-choroid, even post-laser, was found to be much lower than expected (a finding supported by immunohistochemistry analysis) and recruitment of both monocyte subpopulations appeared to be suppressed in $CCL2^{-/-}$ mice. It was perhaps surprising to observe such a marked effect of CCL2 deficiency on the recruitment of Gr-1$^-$ monocytes given they do not express CCR2. This effect was attributed to the sequential recruitment of monocyte subsets observed elsewhere in the body – failure to recruit even small numbers of CCR2$^+$ monocytes in the initial stages of a response may have knock-on effects on the recruitment of the CCR2$^-$ subset[159]. One reason why levels of Gr-1$^+$ monocytes appeared so low – even in wild-types post-laser – might be that their recruitment peaks a lot earlier than 3 days post-laser and therefore any effect of CCL2 deficiency on their recruitment may have been missed. The division of monocyte phenotypes into distinct 'inflammatory' and 'healing' subsets may be slightly misleading in this context – the retinal and RPE-choroidal environments are highly dynamic and interruption of recruitment of one cell type very likely has effects on the recruitment of others. This may have implications for the treatment of patients with wet AMD because if the inhibition of chemokine pathways is to prove successful in the management of CNV, consideration will have to be given to the timing of drug delivery relative to the onset of

neovascularisation. The results of work on mice, for example, suggest that targeting of CCR2 signalling in humans would be most effective in the first 48 hours of onset of CNV.

The effect of CCL2 deficiency on CNV was to significantly reduce lesion size compared with age-matched wild-types – an effect observed even in $CCL2^{-/-}$ mice >18 months old (*Figure 34*). Even so, significant increases in lesion sizes were observed in both $CCL2^{-/-}$ and wild-type animals with age although the increase appeared to be attenuated with age in CCL2-deficient animals. It was not possible to identify consistent changes in samples of lasered tissue taken from the eyes of these animals that might account for the effects of ageing on lesion size (*Figure 37* and *Figure 38*). The relative proportions of innate immune cell populations in retina at 3 days post-laser remained relatively consistent in both $CCL2^{-/-}$ and wild-type mice with age. In the choroid, DC recruitment to CNV appeared to decline with age in wild-type mice and remained low in $CCL2^{-/-}$ animals. In contrast, granulocyte recruitment to the choroid post-laser more than doubled with age in both wild-type and $CCL2^{-/-}$ mice. This observation might serve to explain the linear increase in lesion size observed with age in both genotypes were it not for the non-linear increase in granulocyte recruitment observed in wild-type mice (a 3-fold increase in granulocytes was observed in 12m animals compared with a 4-fold increase in <4m animals). Even so the results were strongly suggestive of a link between enhanced granulocyte recruitment to CNV lesions and increased lesion size with age.

One conclusion that could be drawn from the analysis of lasered tissue was that the accelerated accumulation in $CCL2^{-/-}$ mice of subretinal macrophages appeared not to be associated with a pro-angiogenic effect (otherwise the effect of CCL2 deletion on lesion size would have been attenuated with age - this was not found to be the case). This finding is in keeping with evidence, derived from mice expressing eGFP under the promoter for the *c-fms* gene, suggesting that brain microglia in fact increase expression of both *pro-* (TNFα, Il-1β, IL-6) *and* anti-inflammatory (Il-10, TGFβ1) cytokines with age and that age-related changes in the response to LPS remain in proportion to basal levels of cytokine production[129]. However, the notion that subretinal microglia exert little pro-

angiogenic effect runs contrary to the findings of Ma et al. who, having established that subretinal microglia induce structural and functional changes in the RPE, proceeded to isolate retinal microglia from CX3CR1$^{+/GFP}$ mice, activate them with LPS and inject them subretinally using a Matrigel model of CNV induction. Their results suggested that subretinal microglia exert a 'strong' pro-angiogenic effect on CNV. However the expression profile of microglia cultured from young CX3CR1$^{+/GFP}$ mice and LPS-activated before being transplanted into genetically different wild-type animals is likely to be very different to that of the dystrophic, lipofuscin-laden cells observed in aged animals and it is worth noting in this context that spontaneous CNV has not been conclusively demonstrated in any of the chemokine knockout models for AMD where accelerated accumulation of subretinal microglia is a feature[210].

The possibility that changes in innate immune cell populations in the periphery might explain the change in CNV size with age was considered. The effects of these changes remain unclear however – approximately 3–fold increases in Gr-1$^-$ monocyte/macrophage and DC populations were observed in the spleens of both wild-type and *CCL2$^{-/-}$* mice with age yet this was not reflected in the proportion of cell types recruited locally following CNV-induction despite similar increases in lesion size with age. This suggests that whilst changes in the proportion of innate immune cells in the periphery do correlate with the *chronic* inflammatory changes observed with age in the eye, the acute inflammatory response that follows an event such as induction of CNV by diode laser remains largely unchanged. Age-related changes in the cytokine profiles of the various recruited cell types that might explain the increase in lesion size cannot be excluded but it is more likely - increased granulocyte recruitment to CNV aside - that anatomical changes in the RPE and Bruch's membrane render the aged eye more susceptible to larger CNV lesions. Having said this, it has recently been established that post-ischaemic neovascularisation is highly dependent on monocyte levels in the bloodstream and CCL2/CCR2 signalling is thought to be important in regulating circulating levels of both CCR2$^+$ and CCR2$^-$ monocytes (it is postulated that the impact of disrupted CCL2/CCR2 signalling on CCR2$^-$ cells is a downstream consequence of a primary effect on CCR2$^+$ cells)[187, 188]. Consequently, the reduced CNV lesion size observed in *CCL2$^{-/-}$* mice compared

with wild-types may be explained by reduced levels of circulating monocytes as inferred from levels observed in the spleen. Similarly, the age-related increase in lesion size in both *CCL2*$^{-/-}$ and wild-type mice may be explained by an increase in circulating levels of monocytes with age. If these hypotheses are correct, how is a failure to demonstrate increased levels of CCR2^{-} monocytes in lasered tissue with age to be explained? This may in fact be due to the highly variable nature of the laser CNV model, a feature compounded by the variation in resident innate immune cell populations with age in retina and RPE-choroidal tissues.

6.3 Targeting innate immune cells in choroidal neovascularisation

In the final results chapter of this thesis the potential for tyrosine kinase inhibitors and CD200R agonists to modulate the neovascular response following laser-induction of CNV was explored.

The capacity for the multi-target tyrosine kinase inhibitor pazopanib (delivered by oral gavage) to reduce CNV lesion size was confirmed and a biological mechanism suggested by an increase in the proportion of Gr-1^{+} monocyte/macrophages in the retinae of young adult mice receiving the compound 3 days post-laser. A reduction in the proportion of granulocytes in the spleen following prolonged systemic administration of pazopanib was also observed, raising the possibility that changes in the peripheral innate immune system might contribute to the inhibition of pathological neovascularisation through inhibition of tyrosine kinase receptors other than VEGF receptors – colony stimulating factor 1 receptors (CSF-1R) for example. CSF-1 regulates macrophage Inhibition of CSF-1R appears to be a feature of other small molecules primarily designed as PDGFR or VEGFR inhibitors such as sunitinib and axitinib – any therapeutic advantage conferred by this, in the context of tumour biology at least, remains undetermined[189]. Further work identified a role for pazopanib retained in the uveal tract in inhibiting choroidal neovascularisation, thus demonstrating a novel approach to achieving

therapeutic levels of drug in the RPE-choroid whilst minimising effects on other tissues both systemically and in the eye.

Previous work had suggested that macrophages remain activated in the retina and the RPE-choroid for a prolonged period (at least 5 weeks) following induction of CNV; it was hypothesised that driving alternative macrophage activation by exploiting the CD200R-CD200 axis might result in reduced lesion size. Intravitreal delivery of CD200R agonist at the time of peak monocyte/macrophage recruitment was found to significantly reduce CNV lesion size 2 weeks after induction, a finding associated with a significant increase in the proportion of Gr-1$^-$ monocyte/macrophages in the retina at 1 week and granulocytes in the RPE-choroid at 2 weeks. These data indicated that it was possible to have an effect on pathological neovascularisation by the direct induction of alternative macrophage activation and without VEGFR inhibition. Whether the rise in the Gr-1$^-$ population observed at 1 week reflected changes in the levels of CCR2$^-$ monocytes or microglia is unclear. However, using immunohistochemistry it was possible to identify Gr-1$^-$ F4/80$^+$ CD200R$^+$ cells in the retina at this timepoint that were consistent with a microglial phenotype. Further work would be necessary to confirm whether induction of the CD200R pathway affected the balance of monocyte recruitment at the 3 day post-laser timepoint and the functional changes associated with the observed shift in cell populations.

Both the proliferation of microglia and the recruitment of monocytes from the periphery have been observed following laser-induction of CNV[186]. Distinguishing newly recruited monocytes from the microglial population in the retina and RPE-choroid was not a central aim of the work in this thesis but passing comment on the relative effects of CCL2 deficiency and the use of potential therapeutics on monocyte subsets is very difficult unless this is given some consideration. It was not possible to distinguish CCR2$^-$ monocytes in lasered tissue from proliferating microglia that shared the same surface markers. Consequently, confirmation of whether CCR2$^-$ monocytes constitute the more pro-angiogenic subset in CNV was not possible. Conflicting opinions exist in the literature regarding the relative roles of CCR2$^+$ and CCR2$^-$

monocytes where pathological neovascularisation is concerned. Models of myocardial infarction (essentially ischaemia-reperfusion models) suggest that CCR2⁻ monocytes, recruited from day 4 post-injury onwards, constitute the more pro-angiogenic subset[175]. In contrast, work undertaken using the alkali-induced corneal neovascularisation model suggests that elimination of the same CCR2⁻ subset in *CX3CR1⁻/⁻* mice is actually associated with *increased* lesion size and reduced macrophage infiltration[208]. Recent work in models of hind limb ischaemia using *CCL2⁻/⁻,* *CCR2⁻/⁻* and *CX3CR1⁻/⁻* mice, in combination with adoptive transfer experiments, suggests that vessel growth correlates most strongly with levels of circulating monocytes and that of these cells the CCR2⁺ population is that most involved in angiogensis[187, 188].

When one considers the effects of CCR2 deletion on monocyte emigration from the bone marrow (*CCR2⁻/⁻* mice being a commonly used model in this context), the apparent biphasic nature of monocyte recruitment and the effects of CX3CR1 deletion on CCR2⁺ monocytes – cells which nevertheless express some CX3CR1 albeit at low levels - the picture that emerges is one of extraordinary complexity. To some extent this was reflected in the observed changes in innate immune cell populations following delivery of pazopanib and CD200R agonist and in the high proportion of Gr-1⁺ monocyte/macrophages in the spleens and RPE-choroids of JR5558 mice. It is nevertheless interesting to note that changes in the proportions of innate immune cells in the retina were often associated with an effect on lesion size and this suggests that the immune system of the retina plays a role in modulating the development of CNV.

6.4 Conclusions

This thesis established at its outset the innate immune cell populations of the retina and RPE-choroid in young, adult wild-type mice. The retina in particular was demonstrated to accumulate Gr-1⁻ macrophages and dendritic cells with age. The chemokine CCL2 is expressed by the RPE and upregulated with age in the retina and RPE-choroid and from an early age dendritic cell trafficking out of the retina appeared to be defective in *CCL2⁻/⁻* mice[124]. Levels of DCs rapidly reached a plateau after which the accumulation of Gr-1⁻ macrophages was

observed. The timing of these changes suggests that DCs have an important role to play in maintaining the homeostasis of the ageing retina and that saturation of this pathway (which may be accelerated in subjects at high risk of AMD) results in activation of retinal microglia that are perhaps less able to meet the challenge of age-related parainflammation. It was not possible to determine whether the macrophages observed to accumulate in the retina with age were those identified subretinally using immunohistochemistry but the numbers of cells in the subretinal space are few and consequently unlikely to feature prominently in the flow cytometric analysis. Changes in innate immune cell populations observed in the eye were associated with an increase in the proportion of dendritic cells and Gr-1$^-$ macrophages in the spleen with age. The proportion of DCs in *CCL2*$^{-/-}$ spleen was significantly reduced and this provided further evidence of a role for CCL2 in DC trafficking. Cell tracking studies where the cells responsible for clearing subretinally injected Q-dots are identified and then traced on their migration to the spleen (in wild-type and CCL2-deficient animals) may be helpful in clarifying the role of DCs in maintaining retinal and choroidal homeostasis.

DCs and granulocytes were identified as the principle effectors of laser-induced CNV at the 3 day timepoint. CCL2 was identified as critical for the recruitment of monocyte/macrophage and DC populations - but not granulocytes - following laser-induction of CNV. A failure to recruit all innate immune cell populations, granulocytes excepted, correlated with smaller lesion sizes in *CCL2*$^{-/-}$ mice. An age-related increase in lesion size in CCL2-deficient mice was still observed though lesions were consistently smaller than age-matched wild-types. Increased lesion size with age was associated with enhanced granulocyte recruitment to the choroid in both wild-type and CCL2-deficient mice. Lower numbers of DCs and Gr-1$^-$ macrophages were observed in the spleens of *CCL2*$^{-/-}$ mice and these populations increased in size with age in both CCL2-deficient animals and wild-types. That age-related changes to peripheral innate immune cell populations might be responsible for the increase in lesion size observed with ageing could not be excluded, however enhanced recruitment of DCs and Gr-1$^-$ macrophages to CNV with age was not seen. The accelerated accumulation of subretinal microglia in *CCL2*$^{-/-}$ mice was not associated with a

tendency to increased lesion size suggesting that subretinal microglia do not exert a pro-angiogenic effect. Finally, with regard to identifying a role for a particular monocyyte population in CNV development, it was not possible to determine whether a failure to recruit the Gr-1$^+$ CCR2$^+$ monocyte subset was a feature of CCL2 deficiency. However, changes in the proportions of Gr-1$^+$ and Gr-1$^-$ monocyte/macrophage populations were observed in the retina following the delivery of the RTKI pazopanib and a CD200R agonist, as well as in JR5558 mice, suggesting an important role for these cells in the development of choroidal neovascularisation.

The use of surface markers to define changes in innate immune cell populations has been established for many decades but has its limitations, as the difficulties of distinguishing monocyte subpopulations from microglia illustrate. In part this reflects the challenge of dissecting populations of cells from a rapidly changing and highly plastic milieu - a challenge which, if anything, grows with our understanding of the complexity of the immune system and the tools available for its investigation. It also derives from the different approaches adopted by investigators from seemingly unrelated areas of research in tackling what are often very similar pathways. The markers CD11b and Gr-1 are actually used to define the heterogeneous myeloid-derived suppressor cell population in tumour biology, for example, and the striking parallels between the various monocyte populations and those established in tumour biology – the tumour-associated and tie-2 expressing macrophage subsets - add a further layer of complexity to the immunobiology[176]. Nevertheless, current therapies for CNV – the VEGFR antagonists ranibizumab and bevacizumab - were born out of research into therapies for colorectal carcinoma and other tumours; so, at a clinical level at least, disparate scientific strategies would appear to have a tendency to converge. In reality, cell surface markers not only serve to define cell populations but have functional effects of their own that are often not fully understood. Of those markers employed in this thesis the surface integrins CD11b and CD11c are probably the best characterised, but the others - F4/80 (thought to be involved in the induction of antigen-specific efferent regulatory T cells and peripheral tolerance), Ly6C and Gr-1 - remain something of an enigma where their functional roles are concerned. It is interesting to speculate on the

purpose of Gr-1 and Ly6C expression in the innate immune system, especially given their association with the vasculature of the retina and CNS. Of more immediate functional relevance, perhaps, are the patterns of cytokine expression associated with particular innate immune cell populations and shifts in the proportions of these cells in the retina and RPE-choroid.

Future work will take three directions (in line with the areas explored in this thesis): the first will be to further test the hypothesis that DCs are responsible for maintaining tissue homeostasis in the sub-RPE and choroidal microenvironment and that defective DC trafficking is integral to the accumulation of subretinal microglia in ageing wild-type and $CCL2^{-/-}$ mice. The phenotype of cells responsible for phagocytosing Q-dot markers injected subretinally in mice will be identified. The presence (or absence) of these cells in tissues such as the spleen will then be established at specific timepoints post-injection. Secondly, the hypothesis that enhanced neutrophil recruitment contributes to increased CNV lesion size in aged mice will be tested. Neutrophils have been demonstrated to upregulate CCR2 in the context of a number of inflammatory conditions and models and the attenuation of increased lesion size with age observed in CCL2-deficient animals may be a consequence of this[76, 85, 211]. Neutrophils will be isolated from the bone marrow of young and aged mice and their capacity to migrate to CCL2 investigated using a chemotaxis assay. Levels of expression of CCR2 on neutrophils derived from young and aged mice will be established using flow cytometry. Results may inform translational approaches to determining the risk of developing CNV in AMD – peripheral blood neutrophils isolated from human subjects with CNV or aged individuals may be demonstrated to have increased expression of CCR2 and enhanced chemotaxis to CCL2 for example. Thirdly the functional changes associated with changes in innate immune cell populations following delivery of pazopanib and CD200R agonist will be identified using flow cytometry to analyse cell populations and intracellular cytokines such as TNF-alpha, IL-10, IL-6, IL-4 and IFN-gamma in combination.

It is generally accepted that progress towards answering the key questions in AMD research has been hindered by the limitations of experimental models

available for study (the absence of maculae in mice for example). More patient-focused translational approaches to AMD may ultimately prove more successful in bridging the gaps in our knowledge. The role of the systemic immune system and immunosenscence in AMD has been discussed in this thesis. Over several decades the concept of immune privilege has evolved from one based on immunological ignorance (maintained by blood-tissue barriers and an absence of a lymphatic drainage system) to one based on the complex and dynamic interaction of the immune system with specialised tissues such as those of the eye. Exploring the role of the wider immune system in AMD and other age-related pathologies remains a huge challenge that must be met if these conditions are to be prevented. This thesis, in identifying a potential role for local and peripheral innate immunosenescence in driving the pathology of AMD, serves as a platform on which to build further experimental work and clinical studies. Key questions that might be answered with the involvement of patients and the acquisition of post-mortem tissue include: Is the accumulation of subretinal microglia a feature of normal ageing in humans? Is the accumulation of subretinal microglia accelerated in those at risk of AMD and might the presence of these cells be associated with a particular phenotype? Are numbers of peripheral blood innate immune cells altered in AMD subjects compared to age-matched controls and is this associated with detectable changes in their function? What is the role of dendritic cells in the development or prevention of chronic inflammation in the retina and RPE-choroid? It is hoped that by answering at least some of these questions it will be possible to design more focused approaches to the study of how patients might best be treated and ultimately determine how this debilitating disease might be prevented.

Reference List

1.   Hutchinson J & Tay W Symmetrical central choroido-retinal disease occurring in senile persons. *R Lond Ophthalmic Hosp Rep J Ophthalmic Med Surg* **8**, 231-244 (1874).

2.   Bressler,N.M. *et al.* Potential public health impact of Age-Related Eye Disease Study results: AREDS report no. 11. *Arch. Ophthalmol.* **121**, 1621-1624 (2003).

3.   Schmier,J.K., Jones,M.L., & Halpern,M.T. The burden of age-related macular degeneration. *Pharmacoeconomics.* **24**, 319-334 (2006).

4.   Gupta,O.P., Brown,G.C., & Brown,M.M. Age-related macular degeneration: the costs to society and the patient. *Curr. Opin. Ophthalmol.* **18**, 201-205 (2007).

5.   Friedman,D.S. *et al.* Prevalence of age-related macular degeneration in the United States. *Arch. Ophthalmol.* **122**, 564-572 (2004).

6.   Strauss,O. The retinal pigment epithelium in visual function. *Physiol Rev.* **85**, 845-881 (2005).

7.   Gordon,S. & Taylor,P.R. Monocyte and macrophage heterogeneity. *Nat. Rev. Immunol.* **5**, 953-964 (2005).

8.   Wihlmark,U., Wrigstad,A., Roberg,K., Brunk,U.T., & Nilsson,S.E. Lipofuscin formation in cultured retinal pigment epithelial cells exposed to photoreceptor outer segment material under different oxygen concentrations. *APMIS* **104**, 265-271 (1996).

9.   Xu,H., Chen,M., Manivannan,A., Lois,N., & Forrester,J.V. Age-dependent accumulation of lipofuscin in perivascular and subretinal microglia in experimental mice. *Aging Cell* **7**, 58-68 (2008).

10.   Katz,M.L. Potential reversibility of lipofuscin accumulation. *Arch. Gerontol. Geriatr.* **34**, 311-317 (2002).

11.   Wang,J.J., Foran,S., Smith,W., & Mitchell,P. Risk of age-related macular degeneration in eyes with macular drusen or hyperpigmentation: the Blue Mountains Eye Study cohort. *Arch. Ophthalmol.* **121**, 658-663 (2003).

12.   Ferris,F.L. *et al.* A simplified severity scale for age-related macular degeneration: AREDS Report No. 18. *Arch. Ophthalmol.* **123**, 1570-1574 (2005).

13.   Lengyel,I. *et al.* Association of drusen deposition with choroidal intercapillary pillars in the aging human eye. *Invest Ophthalmol. Vis. Sci.* **45**, 2886-2892 (2004).

14.   Killingsworth,M.C., Sarks,J.P., & Sarks,S.H. Macrophages related to Bruch's membrane in age-related macular degeneration. *Eye (Lond)* **4 (Pt 4)**, 613-621 (1990).

15.   Edwards,R.B. & Szamier,R.B. Defective phagocytosis of isolated rod outer segments by RCS rat retinal pigment epithelium in culture. *Science* **197**, 1001-1003 (1977).

16.   A randomized, placebo-controlled, clinical trial of high-dose supplementation with vitamins C and E, beta carotene, and zinc for age-related macular degeneration and vision loss: AREDS report no. 8. *Arch. Ophthalmol.* **119**, 1417-1436 (2001).

17.   Rosenfeld,P.J. *et al.* Ranibizumab for neovascular age-related macular degeneration. *N. Engl. J Med* **355**, 1419-1431 (2006).

18.   Blaauwgeers,H.G. *et al.* Polarized vascular endothelial growth factor secretion by human retinal pigment epithelium and localization of vascular endothelial growth factor receptors on the inner choriocapillaris. Evidence for a trophic paracrine relation. *Am. J. Pathol.* **155**, 421-428 (1999).

19.   Gillies,M.C. What we don't know about avastin might hurt us. *Arch. Ophthalmol.* **124**, 1478-1479 (2006).

20.   Lee,S. *et al.* Autocrine VEGF signaling is required for vascular homeostasis. *Cell* **130**, 691-703 (2007).

21.   Lambrechts,D. *et al.* VEGF is a modifier of amyotrophic lateral sclerosis in mice and humans and protects motoneurons against ischemic death. *Nat. Genet.* **34**, 383-394 (2003).

22.   Harper,S.J. & Bates,D.O. VEGF-A splicing: the key to anti-angiogenic therapeutics? *Nat. Rev. Cancer* **8**, 880-887 (2008).

23.   Rosenfeld,P.J. *et al.* Characteristics of Patients Losing Vision after 2 Years of Monthly Dosing in the Phase III Ranibizumab Clinical Trials. *Ophthalmology*(2010).

24.   Thornton,J. *et al.* Smoking and age-related macular degeneration: a review of association. *Eye (Lond)* **19**, 935-944 (2005).

25.   Evans,J.R., Fletcher,A.E., & Wormald,R.P. 28,000 Cases of age related macular degeneration causing visual loss in people aged 75 years and above in the United Kingdom may be attributable to smoking. *Br. J Ophthalmol.* **89**, 550-553 (2005).

26.	Mitchell,P., Smith,W., & Wang,J.J. Iris color, skin sun sensitivity, and age-related maculopathy. The Blue Mountains Eye Study. *Ophthalmology* **105**, 1359-1363 (1998).

27.	Taylor,H.R. *et al.* The long-term effects of visible light on the eye. *Arch. Ophthalmol.* **110**, 99-104 (1992).

28.	van der Schaft,T.L., Mooy,C.M., de Bruijn,W.C., & de Jong,P.T. Early stages of age-related macular degeneration: an immunofluorescence and electron microscopy study. *Br. J. Ophthalmol.* **77**, 657-661 (1993).

29.	Anderson,D.H., Mullins,R.F., Hageman,G.S., & Johnson,L.V. A role for local inflammation in the formation of drusen in the aging eye. *Am. J. Ophthalmol.* **134**, 411-431 (2002).

30.	Edwards,A.O. *et al.* Complement factor H polymorphism and age-related macular degeneration. *Science* **308**, 421-424 (2005).

31.	Hageman,G.S. *et al.* A common haplotype in the complement regulatory gene factor H (HF1/CFH) predisposes individuals to age-related macular degeneration. *Proc. Natl. Acad. Sci. U. S. A* **102**, 7227-7232 (2005).

32.	Haines,J.L. *et al.* Complement factor H variant increases the risk of age-related macular degeneration. *Science* **308**, 419-421 (2005).

33.	Klein,R.J. *et al.* Complement factor H polymorphism in age-related macular degeneration. *Science* **308**, 385-389 (2005).

34.	Hughes,A.E. *et al.* A common CFH haplotype, with deletion of CFHR1 and CFHR3, is associated with lower risk of age-related macular degeneration. *Nat. Genet.* **38**, 1173-1177 (2006).

35.	Hageman,G.S. *et al.* Extended haplotypes in the complement factor H (CFH) and CFH-related (CFHR) family of genes protect against age-related macular degeneration: characterization, ethnic distribution and evolutionary implications. *Ann. Med* **38**, 592-604 (2006).

36.	Gold,B. *et al.* Variation in factor B (BF) and complement component 2 (C2) genes is associated with age-related macular degeneration. *Nat. Genet.* **38**, 458-462 (2006).

37.	Jakobsdottir,J., Conley,Y.P., Weeks,D.E., Ferrell,R.E., & Gorin,M.B. C2 and CFB genes in age-related maculopathy and joint action with CFH and LOC387715 genes. *PLoS. One.* **3**, e2199 (2008).

38.	Despriet,D.D. *et al.* Complement component C3 and risk of age-related macular degeneration. *Ophthalmology* **116**, 474-480 (2009).

39.   Maller,J.B. *et al.* Variation in complement factor 3 is associated with risk of age-related macular degeneration. *Nat. Genet.* **39**, 1200-1201 (2007).

40.   Park,K.H., Fridley,B.L., Ryu,E., Tosakulwong,N., & Edwards,A.O. Complement component 3 (C3) haplotypes and risk of advanced age-related macular degeneration. *Invest Ophthalmol. Vis. Sci.* **50**, 3386-3393 (2009).

41.   Yates,J.R. *et al.* Complement C3 variant and the risk of age-related macular degeneration. *N. Engl. J Med* **357**, 553-561 (2007).

42.   Markiewski,M.M. & Lambris,J.D. The role of complement in inflammatory diseases from behind the scenes into the spotlight. *Am. J Pathol.* **171**, 715-727 (2007).

43.   Zhu,Y., Thangamani,S., Ho,B., & Ding,J.L. The ancient origin of the complement system. *EMBO J* **24**, 382-394 (2005).

44.   Nozaki,M. *et al.* Drusen complement components C3a and C5a promote choroidal neovascularization. *Proc. Natl. Acad. Sci. U. S. A* **103**, 2328-2333 (2006).

45.   Laine,M. *et al.* Y402H polymorphism of complement factor H affects binding affinity to C-reactive protein. *J Immunol.* **178**, 3831-3836 (2007).

46.   Ormsby,R.J. *et al.* Functional and structural implications of the complement factor H Y402H polymorphism associated with age-related macular degeneration. *Invest Ophthalmol. Vis. Sci.* **49**, 1763-1770 (2008).

47.   Skerka,C. *et al.* Defective complement control of factor H (Y402H) and FHL-1 in age-related macular degeneration. *Mol. Immunol.* **44**, 3398-3406 (2007).

48.   Sjoberg,A.P. *et al.* The factor H variant associated with age-related macular degeneration (His-384) and the non-disease-associated form bind differentially to C-reactive protein, fibromodulin, DNA, and necrotic cells. *J Biol. Chem.* **282**, 10894-10900 (2007).

49.   Yu,J. *et al.* Biochemical analysis of a common human polymorphism associated with age-related macular degeneration. *Biochemistry* **46**, 8451-8461 (2007).

50.   Johnson,P.T. *et al.* Individuals homozygous for the age-related macular degeneration risk-conferring variant of complement factor H have elevated levels of CRP in the choroid. *Proc. Natl. Acad. Sci. U. S. A* **103**, 17456-17461 (2006).

51.	Seddon,J.M., Gensler,G., Milton,R.C., Klein,M.L., & Rifai,N. Association between C-reactive protein and age-related macular degeneration. *JAMA* **291**, 704-710 (2004).

52.	Anderson,D.H. *et al.* The pivotal role of the complement system in aging and age-related macular degeneration: Hypothesis re-visited. *Prog. Retin. Eye Res.*(2009).

53.	Johnson,L.V., Leitner,W.P., Staples,M.K., & Anderson,D.H. Complement activation and inflammatory processes in Drusen formation and age related macular degeneration. *Exp. Eye Res.* **73**, 887-896 (2001).

54.	McLaughlin,B.J. *et al.* Novel role for a complement regulatory protein (CD46) in retinal pigment epithelial adhesion. *Invest Ophthalmol. Vis. Sci.* **44**, 3669-3674 (2003).

55.	Vogt,S.D., Barnum,S.R., Curcio,C.A., & Read,R.W. Distribution of complement anaphylatoxin receptors and membrane-bound regulators in normal human retina. *Exp. Eye Res.* **83**, 834-840 (2006).

56.	Reynolds,R. *et al.* Plasma complement components and activation fragments: associations with age-related macular degeneration genotypes and phenotypes. *Invest Ophthalmol. Vis. Sci.* **50**, 5818-5827 (2009).

57.	Scholl,H.P. *et al.* Systemic complement activation in age-related macular degeneration. *PLoS. One.* **3**, e2593 (2008).

58.	Mullins,R.F., Aptsiauri,N., & Hageman,G.S. Structure and composition of drusen associated with glomerulonephritis: implications for the role of complement activation in drusen biogenesis. *Eye* **15**, 390-395 (2001).

59.	Gupta,N., Brown,K.E., & Milam,A.H. Activated microglia in human retinitis pigmentosa, late-onset retinal degeneration, and age-related macular degeneration. *Exp. Eye Res.* **76**, 463-471 (2003).

60.	Mullins,R.F., Russell,S.R., Anderson,D.H., & Hageman,G.S. Drusen associated with aging and age-related macular degeneration contain proteins common to extracellular deposits associated with atherosclerosis, elastosis, amyloidosis, and dense deposit disease. *FASEB J* **14**, 835-846 (2000).

61.	Rescigno,M. *et al.* Dendritic cells express tight junction proteins and penetrate gut epithelial monolayers to sample bacteria. *Nat. Immunol.* **2**, 361-367 (2001).

62.	Cherepanoff,S., McMenamin,P.G., Gillies,M.C., Kettle,E., & Sarks,S.H. Bruch's membrane and choroidal macrophages in early and advanced age-related macular degeneration. *Br. J Ophthalmol.*(2009).

63.   Cousins,S.W., Espinosa-Heidmann,D.G., & Csaky,K.G. Monocyte activation in patients with age-related macular degeneration: a biomarker of risk for choroidal neovascularization? *Arch. Ophthalmol.* **122**, 1013-1018 (2004).

64.   Tuo,J. *et al.* The involvement of sequence variation and expression of CX3CR1 in the pathogenesis of age-related macular degeneration. *FASEB J* **18**, 1297-1299 (2004).

65.   Combadiere,C. *et al.* CX3CR1-dependent subretinal microglia cell accumulation is associated with cardinal features of age-related macular degeneration. *J Clin. Invest* **117**, 2920-2928 (2007).

66.   Mrak,R.E. & Griffin,W.S. Glia and their cytokines in progression of neurodegeneration. *Neurobiol. Aging* **26**, 349-354 (2005).

67.   Streit,W.J. & Xue,Q.S. Life and death of microglia. *J. Neuroimmune. Pharmacol.* **4**, 371-379 (2009).

68.   Ley,K., Laudanna,C., Cybulsky,M.I., & Nourshargh,S. Getting to the site of inflammation: the leukocyte adhesion cascade updated. *Nat. Rev. Immunol.* **7**, 678-689 (2007).

69.   Middleton,J. *et al.* Transcytosis and surface presentation of IL-8 by venular endothelial cells. *Cell* **91**, 385-395 (1997).

70.   Boring,L. *et al.* Impaired monocyte migration and reduced type 1 (Th1) cytokine responses in C-C chemokine receptor 2 knockout mice. *J. Clin. Invest* **100**, 2552-2561 (1997).

71.   Zhou,Y., Yang,Y., Warr,G., & Bravo,R. LPS down-regulates the expression of chemokine receptor CCR2 in mice and abolishes macrophage infiltration in acute inflammation. *J. Leukoc. Biol.* **65**, 265-269 (1999).

72.   Kuziel,W.A. *et al.* Severe reduction in leukocyte adhesion and monocyte extravasation in mice deficient in CC chemokine receptor 2. *Proc. Natl. Acad. Sci. U. S. A* **94**, 12053-12058 (1997).

73.   Geissmann,F., Jung,S., & Littman,D.R. Blood monocytes consist of two principal subsets with distinct migratory properties. *Immunity.* **19**, 71-82 (2003).

74.   Sallusto,F. *et al.* Rapid and coordinated switch in chemokine receptor expression during dendritic cell maturation. *Eur. J. Immunol.* **28**, 2760-2769 (1998).

75.   Speyer,C.L. *et al.* Novel chemokine responsiveness and mobilization of neutrophils during sepsis. *Am. J. Pathol.* **165**, 2187-2196 (2004).

76.   Reichel,C.A. *et al.* Chemokine receptors Ccr1, Ccr2, and Ccr5 mediate neutrophil migration to postischemic tissue. *J. Leukoc. Biol.* **79**, 114-122 (2006).

77.   Kivisakk,P. *et al.* T-cells in the cerebrospinal fluid express a similar repertoire of inflammatory chemokine receptors in the absence or presence of CNS inflammation: implications for CNS trafficking. *Clin. Exp. Immunol.* **129**, 510-518 (2002).

78.   Dzenko,K.A., Song,L., Ge,S., Kuziel,W.A., & Pachter,J.S. CCR2 expression by brain microvascular endothelial cells is critical for macrophage transendothelial migration in response to CCL2. *Microvasc. Res.* **70**, 53-64 (2005).

79.   Dagkalis,A. *et al.* Development of experimental autoimmune uveitis: efficient recruitment of monocytes is independent of CCR2. *Invest Ophthalmol. Vis. Sci.* **50**, 4288-4294 (2009).

80.   Lee,F.H., Haskell,C., Charo,I.F., & Boettiger,D. Receptor-ligand binding in the cell-substrate contact zone: a quantitative analysis using CX3CR1 and CXCR1 chemokine receptors. *Biochemistry* **43**, 7179-7186 (2004).

81.   Horuk,R. Chemokine receptor antagonists: overcoming developmental hurdles. *Nat. Rev. Drug Discov.* **8**, 23-33 (2009).

82.   Streilein,J.W. Ocular immune privilege: therapeutic opportunities from an experiment of nature. *Nat. Rev. Immunol.* **3**, 879-889 (2003).

83.   Hoechst,B., Gamrekelashvili,J., Manns,M.P., Greten,T.F., & Korangy,F. Plasticity of human Th17 cells and iTregs is orchestrated by different subsets of myeloid cells. *Blood* **117**, 6532-6541 (2011).

84.   Johnston,B. *et al.* Chronic inflammation upregulates chemokine receptors and induces neutrophil migration to monocyte chemoattractant protein-1. *J. Clin. Invest* **103**, 1269-1276 (1999).

85.   Hartl,D. *et al.* Infiltrated neutrophils acquire novel chemokine receptor expression and chemokine responsiveness in chronic inflammatory lung diseases. *J. Immunol.* **181**, 8053-8067 (2008).

86.   Takeda,A. *et al.* CCR3 is a target for age-related macular degeneration diagnosis and therapy. *Nature* **460**, 225-230 (2009).

87.   Swirski,F.K. *et al.* Identification of splenic reservoir monocytes and their deployment to inflammatory sites. *Science* **325**, 612-616 (2009).

88.   Hume,D.A., Perry,V.H., & Gordon,S. Immunohistochemical localization of a macrophage-specific antigen in developing mouse retina: phagocytosis of dying neurons and differentiation of microglial cells to form a regular array in the plexiform layers. *J. Cell Biol.* **97**, 253-257 (1983).

89.   Lin,H.H. *et al.* The macrophage F4/80 receptor is required for the induction of antigen-specific efferent regulatory T cells in peripheral tolerance. *J. Exp. Med.* **201**, 1615-1625 (2005).

90.   Auffray,C., Sieweke,M.H., & Geissmann,F. Blood monocytes: development, heterogeneity, and relationship with dendritic cells. *Annu. Rev. Immunol.* **27**, 669-692 (2009).

91.   Van,C.E., Van,D.J., & Opdenakker,G. The MCP/eotaxin subfamily of CC chemokines. *Cytokine Growth Factor Rev.* **10**, 61-86 (1999).

92.   Xu,H. *et al.* Differentiation to the CCR2+ inflammatory phenotype in vivo is a constitutive, time-limited property of blood monocytes and is independent of local inflammatory mediators. *J. Immunol.* **175**, 6915-6923 (2005).

93.   Nagendra,S. & Schlueter,A.J. Absence of cross-reactivity between murine Ly-6C and Ly-6G. *Cytometry A* **58**, 195-200 (2004).

94.   Auffray,C. *et al.* Monitoring of blood vessels and tissues by a population of monocytes with patrolling behavior. *Science* **317**, 666-670 (2007).

95.   Nahrendorf,M. *et al.* The healing myocardium sequentially mobilizes two monocyte subsets with divergent and complementary functions. *J. Exp. Med.* **204**, 3037-3047 (2007).

96.   Apte,R.S., Richter,J., Herndon,J., & Ferguson,T.A. Macrophages inhibit neovascularization in a murine model of age-related macular degeneration. *PLoS. Med.* **3**, e310 (2006).

97.   Bobryshev,Y.V. Dendritic cells and their role in atherogenesis. *Lab Invest*(2010).

98.   Sporri,R., Joller,N., Hilbi,H., & Oxenius,A. A novel role for neutrophils as critical activators of NK cells. *J. Immunol.* **181**, 7121-7130 (2008).

99.   Checchin,D., Sennlaub,F., Levavasseur,E., Leduc,M., & Chemtob,S. Potential role of microglia in retinal blood vessel formation. *Invest Ophthalmol. Vis. Sci.* **47**, 3595-3602 (2006).

100.   Nakajima,K., Tohyama,Y., Maeda,S., Kohsaka,S., & Kurihara,T. Neuronal regulation by which microglia enhance the production of neurotrophic factors for GABAergic, catecholaminergic, and cholinergic neurons. *Neurochem. Int.* **50**, 807-820 (2007).

101.   Lee,J.E., Liang,K.J., Fariss,R.N., & Wong,W.T. Ex vivo dynamic imaging of retinal microglia using time-lapse confocal microscopy. *Invest Ophthalmol. Vis. Sci.* **49**, 4169-4176 (2008).

102. Xu,H., Chen,M., Mayer,E.J., Forrester,J.V., & Dick,A.D. Turnover of resident retinal microglia in the normal adult mouse. *Glia* **55**, 1189-1198 (2007).

103. Kezic,J., Xu,H., Chinnery,H.R., Murphy,C.C., & McMenamin,P.G. Retinal microglia and uveal tract dendritic cells and macrophages are not CX3CR1 dependent in their recruitment and distribution in the young mouse eye. *Invest Ophthalmol. Vis. Sci.* **49**, 1599-1608 (2008).

104. Perry,V.H., Nicoll,J.A., & Holmes,C. Microglia in neurodegenerative disease. *Nat. Rev. Neurol.* **6**, 193-201 (2010).

105. Langmann,T. Microglia activation in retinal degeneration. *J. Leukoc. Biol.* **81**, 1345-1351 (2007).

106. Barclay,A.N. & Ward,H.A. Purification and chemical characterisation of membrane glycoproteins from rat thymocytes and brain, recognised by monoclonal antibody MRC OX 2. *Eur. J. Biochem.* **129**, 447-458 (1982).

107. Hoek,R.M. *et al.* Down-regulation of the macrophage lineage through interaction with OX2 (CD200). *Science* **290**, 1768-1771 (2000).

108. Wright,G.J. *et al.* Lymphoid/neuronal cell surface OX2 glycoprotein recognizes a novel receptor on macrophages implicated in the control of their function. *Immunity.* **13**, 233-242 (2000).

109. Copland,D.A. *et al.* Monoclonal antibody-mediated CD200 receptor signaling suppresses macrophage activation and tissue damage in experimental autoimmune uveoretinitis. *Am. J. Pathol.* **171**, 580-588 (2007).

110. Walker,D.G., sing-Hernandez,J.E., Campbell,N.A., & Lue,L.F. Decreased expression of CD200 and CD200 receptor in Alzheimer's disease: a potential mechanism leading to chronic inflammation. *Exp. Neurol.* **215**, 5-19 (2009).

111. Forrester,J.V., Xu,H., Kuffova,L., Dick,A.D., & McMenamin,P.G. Dendritic cell physiology and function in the eye. *Immunol. Rev.* **234**, 282-304 (2010).

112. McMenamin,P.G. Dendritic cells and macrophages in the uveal tract of the normal mouse eye. *Br. J. Ophthalmol.* **83**, 598-604 (1999).

113. Forrester,J.V., McMenamin,P.G., Holthouse,I., Lumsden,L., & Liversidge,J. Localization and characterization of major histocompatibility complex class II-positive cells in the posterior segment of the eye: implications for induction of autoimmune uveoretinitis. *Invest Ophthalmol. Vis. Sci.* **35**, 64-77 (1994).

114. Xu,H., Chen,M., & Forrester,J.V. Para-inflammation in the aging retina. *Prog. Retin. Eye Res.* **28**, 348-368 (2009).

115.   Gao,H. & Hollyfield,J.G. Aging of the human retina. Differential loss of neurons and retinal pigment epithelial cells. *Invest Ophthalmol. Vis. Sci.* **33**, 1-17 (1992).

116.   Cherra,S.J., III, Dagda,R.K., & Chu,C.T. Review: autophagy and neurodegeneration: survival at a cost? *Neuropathol. Appl. Neurobiol.* **36**, 125-132 (2010).

117.   Bird,A.C. Bruch's membrane change with age. *Br. J Ophthalmol.* **76**, 166-168 (1992).

118.   Han,M. *et al.* Age-related structural abnormalities in the human retina-choroid complex revealed by two-photon excited autofluorescence imaging. *J. Biomed. Opt.* **12**, 024012 (2007).

119.   Chan-Ling,T. *et al.* Inflammation and breakdown of the blood-retinal barrier during "physiological aging" in the rat retina: a model for CNS aging. *Microcirculation.* **14**, 63-76 (2007).

120.   Luhmann,U.F. *et al.* The drusenlike phenotype in aging Ccl2-knockout mice is caused by an accelerated accumulation of swollen autofluorescent subretinal macrophages. *Invest Ophthalmol. Vis. Sci.* **50**, 5934-5943 (2009).

121.   Rudolf,M. *et al.* Sub-retinal drusenoid deposits in human retina: organization and composition. *Exp. Eye Res.* **87**, 402-408 (2008).

122.   Sarks,S., Cherepanoff,S., Killingsworth,M., & Sarks,J. Relationship of Basal laminar deposit and membranous debris to the clinical presentation of early age-related macular degeneration. *Invest Ophthalmol. Vis. Sci.* **48**, 968-977 (2007).

123.   Glabinski,A., Jalosinski,M., & Ransohoff,R.M. Chemokines and chemokine receptors in inflammation of the CNS. *Expert. Rev. Clin. Immunol.* **1**, 293-301 (2005).

124.   Chen,H., Liu,B., Lukas,T.J., & Neufeld,A.H. The aged retinal pigment epithelium/choroid: a potential substratum for the pathogenesis of age-related macular degeneration. *PLoS. One.* **3**, e2339 (2008).

125.   Pawelec,G. & Larbi,A. Immunity and ageing in man: Annual Review 2006/2007. *Exp. Gerontol.* **43**, 34-38 (2008).

126.   Fortin,C.F., McDonald,P.P., Lesur,O., & Fulop,T., Jr. Aging and neutrophils: there is still much to do. *Rejuvenation. Res.* **11**, 873-882 (2008).

127.   Plowden,J., Renshaw-Hoelscher,M., Engleman,C., Katz,J., & Sambhara,S. Innate immunity in aging: impact on macrophage function. *Aging Cell* **3**, 161-167 (2004).

128.   Streit,W.J., Braak,H., Xue,Q.S., & Bechmann,I. Dystrophic (senescent) rather than activated microglial cells are associated with tau pathology and likely precede neurodegeneration in Alzheimer's disease. *Acta Neuropathol.* **118**, 475-485 (2009).

129.   Sierra,A., Gottfried-Blackmore,A.C., McEwen,B.S., & Bulloch,K. Microglia derived from aging mice exhibit an altered inflammatory profile. *Glia* **55**, 412-424 (2007).

130.   Rink,L. & Haase,H. Zinc homeostasis and immunity. *Trends Immunol.* **28**, 1-4 (2007).

131.   Tate,D.J., Jr., Newsome,D.A., & Oliver,P.D. Metallothionein shows an age-related decrease in human macular retinal pigment epithelium. *Invest Ophthalmol. Vis. Sci.* **34**, 2348-2351 (1993).

132.   Mocchegiani,E. & Malavolta,M. NK and NKT cell functions in immunosenescence. *Aging Cell* **3**, 177-184 (2004).

133.   Kile,B.T., Mason-Garrison,C.L., & Justice,M.J. Sex and strain-related differences in the peripheral blood cell values of inbred mouse strains. *Mamm. Genome* **14**, 81-85 (2003).

134.   Hollyfield,J.G., Perez,V.L., & Salomon,R.G. A hapten generated from an oxidation fragment of docosahexaenoic acid is sufficient to initiate age-related macular degeneration. *Mol. Neurobiol.* **41**, 290-298 (2010).

135.   Ambati,J. *et al.* An animal model of age-related macular degeneration in senescent Ccl-2- or Ccr-2-deficient mice. *Nat. Med.* **9**, 1390-1397 (2003).

136.   Serbina,N.V. & Pamer,E.G. Monocyte emigration from bone marrow during bacterial infection requires signals mediated by chemokine receptor CCR2. *Nat. Immunol.* **7**, 311-317 (2006).

137.   Schilling,M., Strecker,J.K., Ringelstein,E.B., Kiefer,R., & Schabitz,W.R. Turn-over of meningeal and perivascular macrophages in the brain of MCP-1-, CCR-2- or double knockout mice. *Exp. Neurol.* **219**, 583-585 (2009).

138.   Mildner,A. *et al.* Microglia in the adult brain arise from Ly-6ChiCCR2+ monocytes only under defined host conditions. *Nat. Neurosci.* **10**, 1544-1553 (2007).

139.   Silverman,M.D. *et al.* Constitutive and inflammatory mediator-regulated fractalkine expression in human ocular tissues and cultured cells. *Invest Ophthalmol. Vis. Sci.* **44**, 1608-1615 (2003).

140.   Saederup,N., Chan,L., Lira,S.A., & Charo,I.F. Fractalkine deficiency markedly reduces macrophage accumulation and atherosclerotic lesion formation in CCR2-/- mice: evidence for

independent chemokine functions in atherogenesis. *Circulation* **117**, 1642-1648 (2008).

141.   Zerbib,J. *et al.* No association between the T280M polymorphism of the CX3CR1 gene and exudative AMD. *Exp. Eye Res.* **93**, 382-386 (2011).

142.   Huang,D. *et al.* The neuronal chemokine CX3CL1/fractalkine selectively recruits NK cells that modify experimental autoimmune encephalomyelitis within the central nervous system. *FASEB J.* **20**, 896-905 (2006).

143.   Tuo,J. *et al.* Murine ccl2/cx3cr1 deficiency results in retinal lesions mimicking human age-related macular degeneration. *Invest Ophthalmol. Vis. Sci.* **48**, 3827-3836 (2007).

144.   Ross,R.J. *et al.* Immunological protein expression profile in Ccl2/Cx3cr1 deficient mice with lesions similar to age-related macular degeneration. *Exp. Eye Res.* **86**, 675-683 (2008).

145.   Ng,T.F. & Streilein,J.W. Light-induced migration of retinal microglia into the subretinal space. *Invest Ophthalmol. Vis. Sci.* **42**, 3301-3310 (2001).

146.   Qiu,G. *et al.* A new model of experimental subretinal neovascularization in the rabbit. *Exp. Eye Res.* **83**, 141-152 (2006).

147.   Ambati,J., Ambati,B.K., Yoo,S.H., Ianchulev,S., & Adamis,A.P. Age-related macular degeneration: etiology, pathogenesis, and therapeutic strategies. *Surv. Ophthalmol.* **48**, 257-293 (2003).

148.   Balaggan,K.S. *et al.* EIAV vector-mediated delivery of endostatin or angiostatin inhibits angiogenesis and vascular hyperpermeability in experimental CNV. *Gene Ther.* **13**, 1153-1165 (2006).

149.   Edelman,J.L. & Castro,M.R. Quantitative image analysis of laser-induced choroidal neovascularization in rat. *Exp. Eye Res.* **71**, 523-533 (2000).

150.   Ohno-Matsui,K. & Yoshida,T. Myopic choroidal neovascularization: natural course and treatment. *Curr. Opin. Ophthalmol.* **15**, 197-202 (2004).

151.   Khandhadia,S., Cipriani,V., Yates,J.R., & Lotery,A.J. Age-related macular degeneration and the complement system. *Immunobiology* **217**, 127-146 (2012).

152.   Espinosa-Heidmann,D.G. *et al.* Macrophage depletion diminishes lesion size and severity in experimental choroidal neovascularization. *Invest Ophthalmol. Vis. Sci.* **44**, 3586-3592 (2003).

153.   Tsutsumi-Miyahara,C. *et al.* The relative contributions of each subset of ocular infiltrated cells in experimental choroidal neovascularisation. *Br. J. Ophthalmol.* **88**, 1217-1222 (2004).

154.   Caicedo,A., Espinosa-Heidmann,D.G., Pina,Y., Hernandez,E.P., & Cousins,S.W. Blood-derived macrophages infiltrate the retina and activate Muller glial cells under experimental choroidal neovascularization. *Exp. Eye Res.* **81**, 38-47 (2005).

155.   Campos,M., Amaral,J., Becerra,S.P., & Fariss,R.N. A novel imaging technique for experimental choroidal neovascularization. *Invest Ophthalmol. Vis. Sci.* **47**, 5163-5170 (2006).

156.   Tsutsumi,C. *et al.* The critical role of ocular-infiltrating macrophages in the development of choroidal neovascularization. *J. Leukoc. Biol.* **74**, 25-32 (2003).

157.   De,P.M. & Naldini,L. Tie2-expressing monocytes (TEMs): novel targets and vehicles of anticancer therapy? *Biochim. Biophys. Acta* **1796**, 5-10 (2009).

158.   Pucci,F. *et al.* A distinguishing gene signature shared by tumor-infiltrating Tie2-expressing monocytes, blood "resident" monocytes, and embryonic macrophages suggests common functions and developmental relationships. *Blood* **114**, 901-914 (2009).

159.   Nahrendorf,M., Pittet,M.J., & Swirski,F.K. Monocytes: protagonists of infarct inflammation and repair after myocardial infarction. *Circulation* **121**, 2437-2445 (2010).

160.   Nakai,K. *et al.* Dendritic cells augment choroidal neovascularization. *Invest Ophthalmol. Vis. Sci.* **49**, 3666-3670 (2008).

161.   Fainaru,O. *et al.* Tumor growth and angiogenesis are dependent on the presence of immature dendritic cells. *FASEB J.* **24**, 1411-1418 (2010).

162.   Espinosa-Heidmann,D.G. *et al.* Age as an independent risk factor for severity of experimental choroidal neovascularization. *Invest Ophthalmol. Vis. Sci.* **43**, 1567-1573 (2002).

163.   Lu,B. *et al.* Abnormalities in monocyte recruitment and cytokine expression in monocyte chemoattractant protein 1-deficient mice. *J. Exp. Med.* **187**, 601-608 (1998).

164.   Shortman,K. & Naik,S.H. Steady-state and inflammatory dendritic-cell development. *Nat. Rev. Immunol.* **7**, 19-30 (2007).

165.   Engel,D.R. *et al.* CCR2 mediates homeostatic and inflammatory release of Gr1(high) monocytes from the bone marrow, but is dispensable for bladder infiltration in bacterial urinary tract infection. *J. Immunol.* **181**, 5579-5586 (2008).

166.   Panizzi,P. *et al.* Impaired infarct healing in atherosclerotic mice with Ly-6C(hi) monocytosis. *J. Am. Coll. Cardiol.* **55**, 1629-1638 (2010).

167.   Lee,J.A. *et al.* MIFlowCyt: the minimum information about a Flow Cytometry Experiment. *Cytometry A* **73**, 926-930 (2008).

168.   Kerr,E.C., Raveney,B.J., Copland,D.A., Dick,A.D., & Nicholson,L.B. Analysis of retinal cellular infiltrate in experimental autoimmune uveoretinitis reveals multiple regulatory cell populations. *J. Autoimmun.* **31**, 354-361 (2008).

169.   Raoul,W. *et al.* Lipid-bloated subretinal microglial cells are at the origin of drusen appearance in CX3CR1-deficient mice. *Ophthalmic Res.* **40**, 115-119 (2008).

170.   Combadiere,C. *et al.* Combined inhibition of CCL2, CX3CR1, and CCR5 abrogates Ly6C(hi) and Ly6C(lo) monocytosis and almost abolishes atherosclerosis in hypercholesterolemic mice. *Circulation* **117**, 1649-1657 (2008).

171.   Dick,A.D., Ford,A.L., Forrester,J.V., & Sedgwick,J.D. Flow cytometric identification of a minority population of MHC class II positive cells in the normal rat retina distinct from CD45lowCD11b/c+CD4low parenchymal microglia. *Br. J. Ophthalmol.* **79**, 834-840 (1995).

172.   Bouma,G. *et al.* NOD mice have a severely impaired ability to recruit leukocytes into sites of inflammation. *Eur. J. Immunol.* **35**, 225-235 (2005).

173.   Mooney,J.E. *et al.* Cellular plasticity of inflammatory myeloid cells in the peritoneal foreign body response. *Am. J. Pathol.* **176**, 369-380 (2010).

174.   Hume,D.A. Macrophages as APC and the dendritic cell myth. *J. Immunol.* **181**, 5829-5835 (2008).

175.   Swirski,F.K., Weissleder,R., & Pittet,M.J. Heterogeneous in vivo behavior of monocyte subsets in atherosclerosis. *Arterioscler. Thromb. Vasc. Biol.* **29**, 1424-1432 (2009).

176.   Serafini,P. *et al.* Derangement of immune responses by myeloid suppressor cells. *Cancer Immunol. Immunother.* **53**, 64-72 (2004).

177.   Sunderkotter,C. *et al.* Subpopulations of mouse blood monocytes differ in maturation stage and inflammatory response. *J. Immunol.* **172**, 4410-4417 (2004).

178.   Ingersoll,M.A. *et al.* Comparison of gene expression profiles between human and mouse monocyte subsets. *Blood* **115**, e10-e19 (2010).

179.   Mildner,A. *et al.* CCR2+Ly-6Chi monocytes are crucial for the effector phase of autoimmunity in the central nervous system. *Brain* **132**, 2487-2500 (2009).

180.   Laoui,D. *et al.* Mononuclear phagocyte heterogeneity in cancer: different subsets and activation states reaching out at the tumor site. *Immunobiology* **216**, 1192-1202 (2011).

181.   Dick,A.D. Influence of microglia on retinal progenitor cell turnover and cell replacement. *Eye (Lond)* **23**, 1939-1945 (2009).

182.   Rivard,A. *et al.* Age-dependent impairment of angiogenesis. *Circulation* **99**, 111-120 (1999).

183.   Ryan,S.J. The development of an experimental model of subretinal neovascularization in disciform macular degeneration. *Trans. Am. Ophthalmol. Soc.* **77**, 707-745 (1979).

184.   Nagai,N. Spontaneous Cnv In A Novel Mutant Mouse Is Associated With Early Chorio-retinal Para-inflammation And Vegf Driven Angiogenesis. ed. Kanako Izumi-Nagai, S. R. J. W. B. B. C. R. H. Y. N. D. T. S. ARVO 1015/A387.
Ref Type: Generic

185.   Salinas-Alaman,A., Rifon-Roca,J., & Garcia-Layana,A. Retinal neovascularization and vitreous haemorrhage in a patient with acute myeloid leukaemia and haematopoietic stem cell transplantation. *Acta Ophthalmol. Scand.* **81**, 418-419 (2003).

186.   Eter,N. *et al.* In vivo visualization of dendritic cells, macrophages, and microglial cells responding to laser-induced damage in the fundus of the eye. *Invest Ophthalmol. Vis. Sci.* **49**, 3649-3658 (2008).

187.   Heil,M. *et al.* Blood monocyte concentration is critical for enhancement of collateral artery growth. *Am. J. Physiol Heart Circ. Physiol* **283**, H2411-H2419 (2002).

188.   Cochain,C. *et al.* Regulation of monocyte subset systemic levels by distinct chemokine receptors controls post-ischaemic neovascularization. *Cardiovasc. Res.* **88**, 186-195 (2010).

189.   Ferrara,N. Role of myeloid cells in vascular endothelial growth factor-independent tumor angiogenesis. *Curr. Opin. Hematol.* **17**, 219-224 (2010).

190.   Takahashi,K. *et al.* Suppression and regression of choroidal neovascularization by the multitargeted kinase inhibitor pazopanib. *Arch. Ophthalmol.* **127**, 494-499 (2009).

191.   Koning,N., Swaab,D.F., Hoek,R.M., & Huitinga,I. Distribution of the immune inhibitory molecules CD200 and CD200R in the normal central nervous system and multiple sclerosis lesions suggests neuron-

glia and glia-glia interactions. *J. Neuropathol. Exp. Neurol.* **68**, 159-167 (2009).

192.   Wang,X.J., Ye,M., Zhang,Y.H., & Chen,S.D. CD200-CD200R regulation of microglia activation in the pathogenesis of Parkinson's disease. *J. Neuroimmune. Pharmacol.* **2**, 259-264 (2007).

193.   Koning,N. *et al.* Expression of the inhibitory CD200 receptor is associated with alternative macrophage activation. *J. Innate. Immun.* **2**, 195-200 (2010).

194.   Jenmalm,M.C., Cherwinski,H., Bowman,E.P., Phillips,J.H., & Sedgwick,J.D. Regulation of myeloid cell function through the CD200 receptor. *J. Immunol.* **176**, 191-199 (2006).

195.   Jutila,M.A. *et al.* In vivo distribution and characterization of two novel mononuclear phagocyte differentiation antigens in mice. *J. Leukoc. Biol.* **54**, 30-39 (1993).

196.   D'Mello,C., Le,T., & Swain,M.G. Cerebral microglia recruit monocytes into the brain in response to tumor necrosis factoralpha signaling during peripheral organ inflammation. *J. Neurosci.* **29**, 2089-2102 (2009).

197.   Alliot,F., Rutin,J., & Pessac,B. Ly-6C is expressed in brain vessels endothelial cells but not in microglia of the mouse. *Neurosci. Lett.* **251**, 37-40 (1998).

198.   Irvine,K.M. *et al.* Colony-stimulating factor-1 (CSF-1) delivers a proatherogenic signal to human macrophages. *J. Leukoc. Biol.* **85**, 278-288 (2009).

199.   Peng,Y., Latchman,Y., & Elkon,K.B. Ly6C(low) monocytes differentiate into dendritic cells and cross-tolerize T cells through PDL-1. *J. Immunol.* **182**, 2777-2785 (2009).

200.   Kovacs,E.J. *et al.* Aging and innate immunity in the mouse: impact of intrinsic and extrinsic factors. *Trends Immunol.* **30**, 319-324 (2009).

201.   Panda,A. *et al.* Human innate immunosenescence: causes and consequences for immunity in old age. *Trends Immunol.* **30**, 325-333 (2009).

202.   Yang,Z. *et al.* Toll-like receptor 3 and geographic atrophy in age-related macular degeneration. *N. Engl. J. Med.* **359**, 1456-1463 (2008).

203.   Sato,N. *et al.* CC chemokine receptor (CCR)2 is required for langerhans cell migration and localization of T helper cell type 1 (Th1)-inducing dendritic cells. Absence of CCR2 shifts the Leishmania major-resistant phenotype to a susceptible state dominated by Th2 cytokines, b cell outgrowth, and sustained neutrophilic inflammation. *J. Exp. Med.* **192**, 205-218 (2000).

204.   Chiu,B.C. *et al.* Impaired lung dendritic cell activation in CCR2 knockout mice. *Am. J. Pathol.* **165**, 1199-1209 (2004).

205.   Mulder,D.J., Bieze,M., Graaff,R., Smit,A.J., & Hooymans,J.M. Skin autofluorescence is elevated in neovascular age-related macular degeneration. *Br. J. Ophthalmol.* **94**, 622-625 (2010).

206.   Kezic,J. & McMenamin,P.G. Differential turnover rates of monocyte-derived cells in varied ocular tissue microenvironments. *J. Leukoc. Biol.* **84**, 721-729 (2008).

207.   Seidler,S., Zimmermann,H.W., Bartneck,M., Trautwein,C., & Tacke,F. Age-dependent alterations of monocyte subsets and monocyte-related chemokine pathways in healthy adults. *BMC. Immunol.* **11**, 30 (2010).

208.   Lu,P. *et al.* Opposite roles of CCR2 and CX3CR1 macrophages in alkali-induced corneal neovascularization. *Cornea* **28**, 562-569 (2009).

209.   Muther,P.S. *et al.* Conditions of retinal glial and inflammatory cell activation after irradiation in a GFP-chimeric mouse model. *Invest Ophthalmol. Vis. Sci.* **51**, 4831-4839 (2010).

210.   Ma,W., Zhao,L., Fontainhas,A.M., Fariss,R.N., & Wong,W.T. Microglia in the mouse retina alter the structure and function of retinal pigmented epithelial cells: a potential cellular interaction relevant to AMD. *PLoS. One.* **4**, e7945 (2009).

211.   Souto,F.O. *et al.* Essential role of CCR2 in neutrophil tissue infiltration and multiple organ dysfunction in sepsis. *Am. J. Respir. Crit Care Med.* **183**, 234-242 (2011).